Investigating the role of the platelet receptor C-type lectin-like receptor 2 in models of thrombosis

…

Untersuchungen zur Rolle des Thrombozytenrezeptors CLEC-2 (*C-type lectin-like receptor 2*) in Thrombosemodellen

Doctoral thesis for a doctoral degree
at the Graduate School of Life Sciences,
Julius-Maximilians-Universität Würzburg,
Section Biomedicine

submitted by

Helena Charlotte Brown

From Stevenage

Würzburg, 2022

Submitted on:

Members of the Thesis Committee:

Chairperson: Prof. Dr. Thomas Dandekar

Primary Supervisor: Prof. Dr. David Stegner

Supervisor (Second): Prof. Steve Watson

Supervisor (Third): Dr Steven Thomas

Supervisor (Fourth): Prof. Dr. Katrin Heinze

Date of Public Defence:

Date of Receipt of Certificates:

Summary

Platelets have a key physiological role in haemostasis however, inappropriate thrombus formation can lead to cardiovascular diseases such as myocardial infarction or stroke. Although, such diseases are common worldwide there are comparatively few anti-platelet drugs, and these are associated with an increased risk of bleeding. Platelets also have roles in thrombo-inflammation, immuno-thrombosis and cancer, in part via C-type lectin-like receptor 2 (CLEC-2) and its ligand podoplanin. Although CLEC-2 contributes to these diseases in mice, as well as to thrombus stability, it is unclear whether CLEC-2 has similar roles in humans, particularly as human CLEC-2 (hCLEC-2) cannot be investigated experimentally *in vivo*.

To investigate hCLEC-2 *in vivo*, we generated a humanised CLEC-2 mouse (hCLEC-2^{KI}) model, as well as a novel monoclonal antibody, HEL1, that binds to a different site than an existing antibody, AYP1. Using these antibodies, we have provided proof of principle for the use of hCLEC-2^{KI} mice to test potential therapeutics targeting hCLEC-2, and shown for the first time that hCLEC-2 can be immunodepleted, with little effect on haemostasis. However, our results have also suggested that there are species differences in the role of CLEC-2 in arterial thrombosis. We further confirmed this using human blood where blocking CLEC-2 ligand binding had no effect on thrombosis, whereas we confirmed a minor role for mouse CLEC-2 in thrombus stability. We also investigated the effect of blocking CLEC-2 signalling using the Bruton's tyrosine kinase inhibitor PRN473 on CLEC-2 mediated immuno-thrombosis in a *Salmonella typhimurium* infection model. However, no effect on thrombosis was observed suggesting that CLEC-2 signalling is not involved.

Overall, our results suggest that there may be differences in the role of human and mouse CLEC-2, at least in arterial thrombosis, which could limit the potential of CLEC-2 as an anti-thrombotic target. However, it appears that the interaction between CLEC-2 and podoplanin is conserved and therefore CLEC-2 could still be a therapeutic target in immuno-thrombosis,

thrombo-inflammation and cancer. Furthermore, any potential human specific therapeutics could be investigated *in vivo* using hCLEC-2^{KI} mice.

Zusammenfassung

Thrombozyten sind ein wichtiger Bestandteil der Hämostase, können allerdings durch die Bildung eines Blutgerinnsels auch kardiovaskuläre Krankheitsbilder wie Myokardinfarkte oder Schlaganfälle hervorrufen. Obwohl diese Erkrankungen weltweit zu den führenden Todesursachen zählen, gibt es vergleichsweise wenig Thrombozyteninhibitoren und die bislang verfügbaren Wirkstoffe gehen mit einem erhöhten Blutungsrisiko einher. Darüber hinaus spielen Thrombozyten auch bei thrombo-inflammatorischen oder malignen Erkrankungen eine Rolle und sind maßgeblich an Entzündungs-vermittelten Thrombosen (Immunothrombosen) beteiligt. Daten aus Mausmodellen legen nahe, dass die Interaktion zwischen dem Thrombozytenrezeptor CLEC-2 (*C-type lectin-like receptor 2)* und seinem Liganden Podoplanin von Bedeutung für diese Krankheitsbilder, und die Thrombusstabilität ist. Allerdings ist bislang unklar, ob CLEC-2 im Menschen eine ähnliche Rolle spielt, da die Rolle des menschlichen CLEC-2 (hCLEC-2) in diesen Prozessen bislang nicht experimentell *in vivo* erforscht werden kann.

Um hCLEC-2 *in vivo* zu erforschen, haben wir Mäuse generiert, die humanes CLEC-2 exprimieren (hCLEC-2^{KI}), sowie einen neuen, monoklonalen Antikörper (HEL1) entwickelt, der an eine andere Bindungsstelle als der zuvor generierter Antikörper (AYP1) bindet. Mit Hilfe dieser Antikörper haben wir erstmalig gezeigt, dass hCLEC-2^{KI} Mäuse geeignet sind, um potenzielle Therapeutika zu testen, die auf hCLEC-2 abzielen. Des Weiteren konnten wir erstmalig zeigen, dass auch hCLEC-2 immunodepletiert werden kann und dass der Verlust des Rezeptors in zirkulierenden Thrombozyten die Hämostase nur minimal beeinträchtigt. Allerdings deuten unsere Ergebnisse auch darauf hin, dass es hinsichtlich der Bedeutung CLEC-2 für die arterielle Thrombose artspezifische Unterschiede gibt: Während Maus CLEC-2 zur Stabilität der Thromben beiträgt, hatte die Blockade der Ligandenbindungsstelle von hCLEC-2 keinen Einfluss auf Thrombose. Des Weiteren wurde mit Hilfe des Bruton's tyrosine kinase Inhibitors PRN473 der Effekt einer Blockierung des CLEC-2 Signalwegs auf die durch

CLEC-2 hervorgerufene Immuno-Thrombose in einem *Salmonella typhimurium* Infektionsmodel erforscht. Da jedoch keine Effekte nachgewiesen werde konnten, schlussfolgern wir, dass der CLEC-2 Signalweg nicht in diesen Prozess involviert ist.

Insgesamt deuten unsere Ergebnisse darauf hin, dass es Unterschiede in der Rolle von CLEC-2 zwischen Mensch und Maus gibt, zumindest im Kontext der arteriellen Thrombose, was das Potenzial von CLEC-2 als antithrombotisches Ziel einschränken könnte. Da allem Anschein nach die Interaktion zwischen CLEC-2 und Podoplanin konserviert ist, könnte CLEC-2 dennoch als Therapeutikum für Thrombo-Inflammation, Immunothrombose und Krebsbildungen genutzt werden. Des Weiteren könnten für den Menschen entwickelte Therapieansätze mit Hilfe von hCLEC-2^{KI} Mäusen *in vivo* untersucht werden.

Table of contents

1. Introduction

1.1 Platelets

Platelets are the smallest cells in the haematopoietic system with a diameter of just 1-2 μm in humans and 0.5 μm in mice and circulate in very high numbers; 150,000 to 400,000/μl and 1,000,000 to 1,500,000/μl in humans and mice respectively.[1] Platelets are anucleate and are produced by megakaryocytes predominately residing in the bone marrow, they circulate for 7-10 days in humans and around 4 days in mice and are constantly cleared by the reticulo-endothelial system in the spleen and liver.[1,2]

As they circulate, platelets monitor vascular integrity and have a crucial physiological role in haemostasis, in which they aggregate and form a platelet plug following vessel injury, thereby preventing excessive blood loss. However, this process is also a key component of the pathology of cardiovascular disease, for example, thrombus formation following atherosclerotic plaque rupture and formation of blood clots resulting in myocardial infarction or stroke. Globally, cardiovascular disease has one of the highest disease burdens and is one of the leading causes of death.[3] Therefore, platelets are a major therapeutic target for both prophylaxis and treatment of such diseases.[4] Nevertheless, such drugs are often associated with an increased risk of bleeding due to disruption of the tightly controlled interactions of many platelet receptors, ligands and their respective signalling pathways that contribute to haemostasis.

In addition to their roles in haemostasis and thrombosis, platelets also have crucial roles in development,[5-7] wound healing,[8] inflammation,[9] including thrombo-inflammation,[10] infection (immuno-thrombosis)[11] and cancer.[12]

1.1.1 Signalling in platelet activation

There are two main signalling pathways involved in initial platelet activation: soluble agonists binding G protein-coupled platelet receptors (GPCRs) and (hemi-)immunoreceptor tyrosine-

based activation motif (hemITAM) receptor induced activation via glycoprotein (GP) VI and C-type lectin-like receptor 2 (CLEC-2). These pathways result in the activation of phospholipase C (PLC) β and γ2 respectively leading to increased intracellular Ca^{2+} and integrin activation via hydrolysis of phosphatidylinositol-4,5-bisphosphate (PIP_2) to inositol-1.4.5-trisphosphate (IP_3) and diacylglycerol (DAG). PIP_2 is also converted to phosphatidylinositol-3,4,5-trisphosphate (PIP_3) via phosphoinositide-3-kinase (PI3K) which also contributes to integrin activation (Figure 1.1). In addition to integrin activation, increased intracellular Ca^{2+} concentration is also key for platelet granule release and procoagulant activity.[13]

Platelets secrete three types of granule: α-granules, dense granules and lysosomes. α-granules contain adhesion molecules such as von Willebrand factor (vWF) and fibrinogen, as well as growth factors, chemokines and coagulation factors. Their secretion also results in P-selectin expression which is considered a key marker of degranulation and platelet activation when expressed on the platelet surface. Dense granules secrete secondary mediators such as adenosine diphosphate (ADP), adenosine triphosphate (ATP), thromboxane A_2 (TxA_2) and serotonin creating a positive feedback loop on platelet activation.[13,14] Furthermore, signalling via GPCR receptors results in platelet shape change which is key for granule centralisation and therefore secretion.[14]

The soluble platelet agonists ADP and TxA_2, as well as locally produced thrombin and weaker agonists such as serotonin, epinephrine and prostaglandin E_2, signal via GPCRs coupled to G_q, G_{12}/G_{13} or G_i. This induces signalling via Rho-GTPases, PI3K and PLCβ resulting in platelet shape change and spreading via cytoskeletal re-arrangement (Figure 1.1).[14] GPCRs are also the targets of key anti-platelet drugs. For example, one of the ADP receptors, $P2Y_{12}$, is the target of clopidogrel, ticagrelor and cangrelor and the production of TxA_2 form arachidonic acid by cyclo-oxygenase-1 (COX-1) is inhibited by aspirin, which remains the gold standard in anti-platelet therapy and prevention of cardiovascular disease.[4,15]

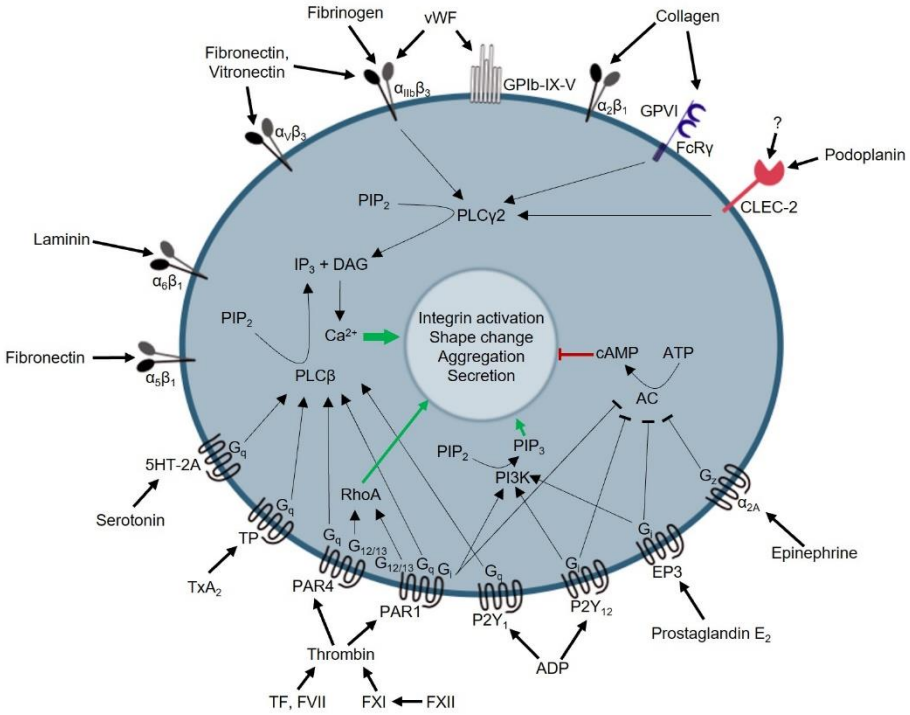

Figure 1.1 Primary signalling pathways in platelet activation.
GPCRs are activated by soluble agonists and signal via Gq, G12/G13 and Gi leading to PLCβ and PI3K activation. Ligand binding of the (hem)ITAM receptors GPVI and CLEC-2 results in PLCγ2 activation. Both pathways then culminate in PIP_2 hydrolysis to IP_3 and DAG resulting in increased intracellular Ca^{2+} and therefore integrin activation, shape change, aggregation and granule secretion. Adapted from Stegner and Nieswandt, (2011).[13]

Platelet activation via (hem)ITAM receptor is mediated by the GPVI-Fc receptor γ-chain (FcRγ) complex and CLEC-2. Activation via GPVI is initiated by ligand binding which crosslinks receptors allowing contact between FcRγ and the Src family tyrosine kinases (SFKs) Fyn and Lyn. This begins a tyrosine phosphorylation cascade via spleen tyrosine kinase (Syk) and multiple adaptor and effector proteins resulting in activation of PLCγ2 and Ca^{2+} release.[13,16] This results in platelet aggregation as well as degranulation and integrin activation as previously discussed. CLEC-2 has a similar signalling pathway to GPVI with the exception that it is via a single (hem)ITAM. This will be discussed in more detail in the next chapter.

1.1.2 Platelet activation and thrombus formation

Platelet activation, and therefore thrombus formation, is triggered by exposure of the extracellular matrix (ECM) due to vascular injury. The ECM contains or binds platelet receptor ligands such as collagen, vWF and laminin that cause initial platelet adhesion and aid

subsequent activation and aggregation. The process of thrombus formation can be divided into three stages: (1) platelet tethering, (2) platelet activation and (3) firm platelet adhesion and thrombus growth (Figure 1.2).[17]

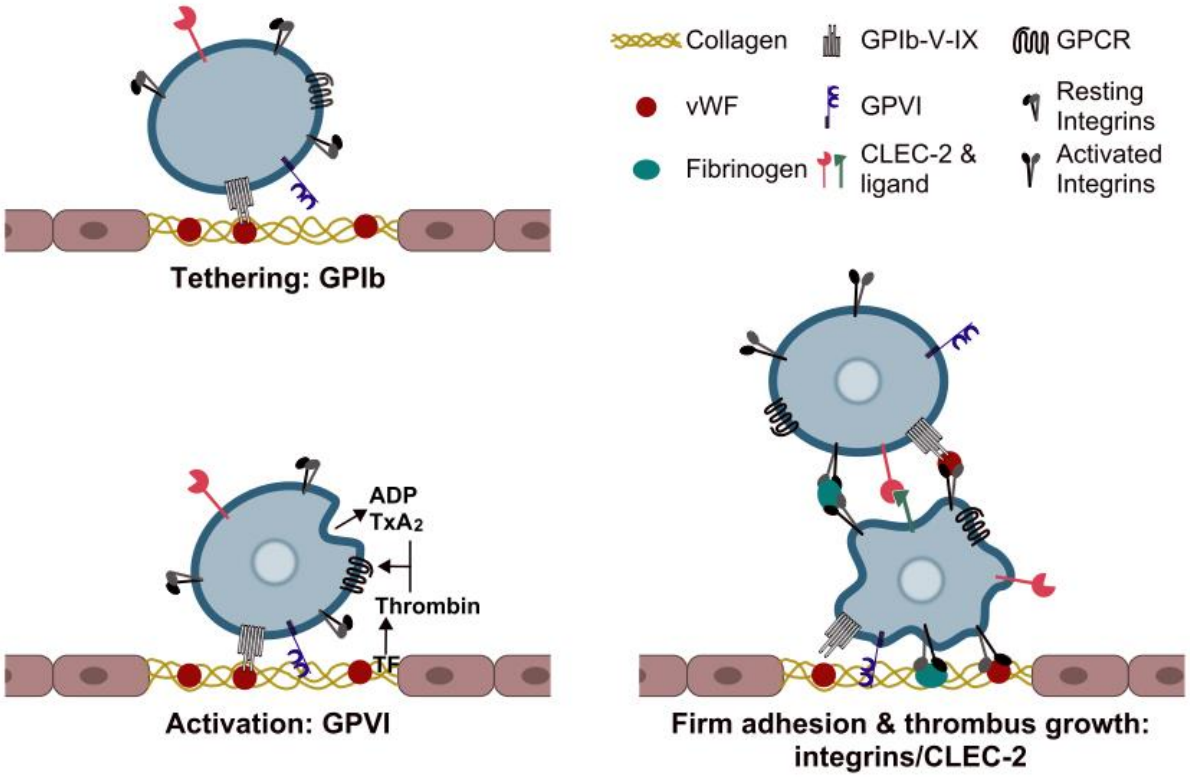

Figure 1.2 Platelet adhesion and thrombus formation at sites of arterial injury. Thrombus formation occurs in three stages. 1) Platelet tethering; this is mediated by GPIb in the GPIb-V-IX complex interacting with vWF immobilised on the exposed ECM. 2) Platelet activation; tethering allows the interaction of GPVI with collagen resulting in platelet activation. This is reinforced by the release of the secondary mediators ADP and TxA_2 as well as locally formed thrombin that further activates platelets via GPCR receptors. 3) Firm adhesion and thrombus growth. Platelet activation causes integrins to transition from a low to a high affinity or activated state, this mediates firm platelet adhesion to the ECM as well as other platelets via interactions with vWF and fibrinogen. CLEC-2 has also been shown to have a role in this final stage via an interaction with an unknown ligand that contributes to thrombus stability. Adapted from Nieswandt, Pleines and Bender (2011) and Stegner and Nieswandt (2011).[13,18]

In the initial stage, the platelet GPIb-V-IX complex interacts with vWF immobilised on collagen in the exposed ECM. This leads to platelet tethering which slows down circulating platelets, particularly at high shear rates.[19] The GPIb-vWF interaction is not stable and leads to platelet rolling rather than firm adhesion however, this allows the principle platelet collagen receptor GPVI to interact with its ligand.[19,20] This then results in platelet activation,[21] the transition of

integrins from a low (inactive) to a high affinity (active) state and release of secondary mediators such as ADP and TxA_2.[17] These bind to the GPCRs, $P2Y_1$ and $P2Y_{12}$ and thromboxane-prostanoid (TP) receptors respectively (Figure 1.1 and 1.2).[13,14]

Following initial platelet activation transduction of signals within the platelet results in integrin activation by a process known as “inside-out” signalling. Platelet integrin “inside out” signalling leads to ligand binding and results in firm platelet adhesion and thrombus growth. The major platelet integrin αIIbβ3 (GPIIb/IIIa) binds to both vWF and fibrinogen facilitating platelet bridging and allowing firm platelet adhesion to the ECM; interactions with fibronectin and vitronectin also play a role.[17,22] The interaction between α2β1 with collagen, α5β1 with fibronectin and α6β1 with laminin also contribute to platelet adhesion to the ECM, although these are not essential for thrombus growth.[19,21,22] Secondary mediators, on the other hand, reinforce initial platelet activation, as well as activation of new platelets, leading to aggregation via integrin-vWF binding and plasma fibrinogen, which are released from platelet α-granules upon activation.[13] In addition, plasmatic coagulation occurs as a result of thrombin formation. This is triggered by tissue factor (TF) and reinforced by phosphatidylserine (PS) exposure which further contributes to platelet activation via protease activation receptor (PAR) 3 and 4 in mice and PAR1 and 4 in humans.[14] Thrombin also cleaves fibrinogen to fibrin thereby stabilising the thrombus and anchoring it to the vessel. [23,24] This process is also supported by activated Factor (F)XIII-mediated cross-linking of fibrin.[24]

The hemITAM receptor CLEC-2 has also been proposed to have a role in thrombus aggregation and stabilisation but its exact role in thrombus formation and the ligand it interacts with remain unknown.[7,25,26]

1.1.3 Thrombus structure and stability

Thrombi forming in the venous and arterial vasculature have very different structures and cell contributions. Venous thrombi are formed under a low flow rate allowing accumulation of

coagulation factors and thrombin with little platelet contribution and are instead rich in erythrocytes.[27] However, the focus of this section will be on platelet rich arterial thrombi.

Arterial thrombi have a heterogeneous structure and are often depicted as a core and a shell, with differences in composition, platelet activation, signalling and density having been described.[23] As shown in Figure 1.3, the core of the thrombus is closest to the site of injury, fibrin rich and contains densely packed, fully activated platelets. The shell surrounds the core and is characterised by lower levels of platelet activation and has a lower density.[28] The differences in thrombus density or porosity (space between platelets) and platelet activation between the two areas are key to their function. Platelet adhesion in the core is increased due to shape change and integrin-mediated interactions making it denser. This allows the accumulation of soluble platelet agonists such as ADP and TxA_2, as well as thrombin, and results in further platelet activation, fibrin production and coagulation.[23,28] At high thrombin concentrations thin fibrin networks are formed that stabilise the thrombus, a process limited to the inner core.[23,29] The density of the core also means that plasma-borne molecules are unable to penetrate it. This prevents endogenous thrombin inhibitors or fibrinolytic molecules, such as tissue plasminogen activator (tPA), entering the core and therefore prevents premature thrombus resolution. However, it also prevents the accumulation of plasma coagulation factors that would further increase thrombin generation and therefore fibrin formation, thereby limiting the size of the core.[23,28,29]

As the shell of the thrombus is less dense there is more space between platelets allowing for a greater movement of molecules. This means that secondary mediators of platelet activation are more diluted and can be washed away by the blood flow. As a result, platelets are less activated and therefore the shell is less stable than the core which limits the size of the thrombus. Evidence for this comes from Stalker *et al*. (2013) who have shown that P-selectin positive platelets are only found within the thrombus core whereas only P-selectin negative platelets embolise.[23]

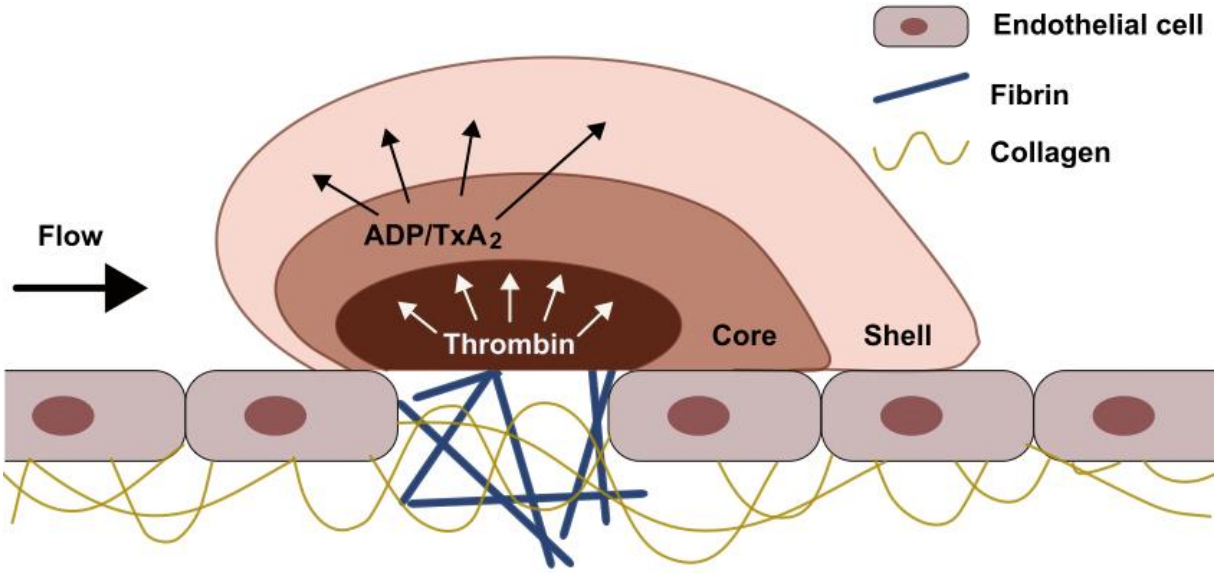

Figure 1.3 Thrombus structure and its influence on stability.
A thrombus is comprised of distinct regions characterised by platelet activation and density. The inner core of the thrombus is closest to the site of injury and consists of the first platelets to be activated. These platelets are fully activated and become densely packed due to contact-dependent signalling as well as high levels of thrombin, ADP and TxA_2 which are able to accumulate. This leads to coagulation and fibrin deposition. The outer shell surrounds the core and contains less activated platelets that have a lower density. As a result, ADP and TxA_2 are more dispersed and can be washed away in the blood flow. Therefore, the shell is less stable and limits the overall size of the thrombus. Adapted from Stalker *et al*. (2013).[23]

As previously mentioned, ADP has a key role in thrombus stability and is released from activated platelets in the thrombus core where it contributes to further activation. However, it also contributes to platelet recruitment and adherence in the shell through $P2Y_{12}$ mediated signalling. A G_{i2} gain of function mutation, $G_{i2}\alpha$(G184S), that results in increased signalling by ADP downstream of $P2Y_{12}$, increases shell size (P-selectin negative platelets) with no effect on the core, thereby increasing platelet adherence without full activation.[23,30] Furthermore, the $P2Y_{12}$ inhibitors cangrelor and ticagrelor respectively decrease shell size with no effect on core thrombus size and decrease thrombus size while increasing blood flow, when administered after ferric chloride ($FeCl_3$) induced vessel injury.[23,31]

Integrin αIIbβ3 also has a role in thrombus stabilisation via crosslinking of platelets with fibrinogen. αIIbβ3 antagonists reduce the size of preformed thrombi and cause the detachment of both single platelets and small aggregates until only a single layer of platelets remains.[32,33]

This suggest that αIIbβ3 has a role in the stability of both the thrombus core and shell although it has been suggested that αIIbβ3 antagonists can only successfully dissolve non-occlusive thrombi.[33] Furthermore, the GPIb-vWF interaction has been suggested as mediating platelet-platelet adhesion in the shell, particularly of occlusive thrombi, with antagonists restoring blood flow following occlusive thrombus formation.[33]

More recently a role for GPVI has been proposed in thrombus stability with the anti-human GPVI antibody fragments ACT017 or 1G5 being used to disaggregate thrombi.[34,35] Although GPVI has a role in initial platelet adhesion to collagen in the thrombus core, its main role in stability has been suggested to be via its interaction with fibrinogen in the thrombus shell.[36] This is a result of ACT017, which blocks the interaction of GPVI and fibrinogen, having little effect on disaggregation of thrombi from patients lacking fibrinogen but causing disaggregation of thrombi from healthy donor blood.[34] Furthermore, platelets from GPVI deficient mice adhere to preformed thrombi to the same extent as wildtype (WT) platelets whereas platelets from human blood treated with the anti-human GPVI antibody 9O12 did not adhere to preformed thrombi to the same extent as control treated samples.[36,37] This further supports a role of the GPVI-fibrinogen interaction in thrombus stability as mouse GPVI does not interact with fibrinogen.[36,37] It was also reported that mouse thrombi appeared less stable than human in general, further suggesting a species differences in the regulation of thrombus stability between humans and mice.[37]

A role for CLEC-2 in mouse thrombus stability has been proposed due to both *in vivo* and *in vitro* experiments using CLEC-2 deficient mice[7,25] however, the exact nature and mechanism of its contribution remain unknown.

1.2 The C-type lectin-like receptor 2 (CLEC-2)

CLEC-2 is a unique platelet activation receptor that signals through a hemITAM.[38] It is a type II transmembrane receptor consisting of 229 amino acids with a molecular mass of

approximately 27 kDa, but an apparent molecular mass of 32 - 40 kDa due to differential glycosylation.[38,39] Furthermore, human CLEC-2 is apparent as a doublet of 32 and 40 kDa and mouse CLEC-2 as a single band of approximately 32 kDa by Western Blotting.[25,38,40] It is encoded by the *Clec1b* gene which is located on chromosome 6 and 12 in mice and humans respectively.[39] CLEC-2 belongs to the C-type lectin receptor superfamily which were originally characterised by Ca^{2+}-dependent carbohydrate binding, however, this is not the case for all C-type lectins, including CLEC-2.[39,41,42] Although CLEC-2 is structurally similar to other C-type lectins, its differences, namely the helix in the long loop region, which is key to ligand binding, account for its function. This region is also the only one likely to undergo a conformational change upon ligand binding and therefore alters the angle of the helix.[42] There is a high sequence homology of 62% between human and mouse CLEC-2 with key sequences being conserved. These include the ligand binding domain as well as the cytoplasmic tail, including the YXXL hemITAM motif. Furthermore, there are also two conserved glycosylation sites (N120 and N134) that are necessary for translocation to the cell surface.[43]

CLEC-2 was only identified on platelets in 2006,[38] and although it has also been suggested to be expressed on immune cells such as monocytes, dendritic cells and granulocytes as well as liver sinusoidal endothelial cells (LSECs) and Kupffer cells,[39,44,45] its highest expression is on platelets and megakaryocytes.[38,46] The copy number of CLEC-2 on mouse and human platelets is reported to have an up to 20-fold difference with 2000-4000 copies having been reported on human platelets[40,47] and 40,000 on mouse.[48,49]

CLEC-2 was first identified as the receptor for the snake venom toxin rhodocytin isolated from the Malayan pit viper, *Calloselasma rhodostoma*.[38,50,51] Rhodocytin stimulation of platelets results in activation and aggregation following a dose-dependent lag phase that is characteristic of CLEC-2 mediated activation.[38] An endogenous ligand, podoplanin, has since been identified. It is expressed on kidney podocytes, lymphatic endothelial cells (LECs), lung alveolar cells, inflammatory macrophages and by some cancer cells, but is not expressed in

the vasculature.[52-55] Podoplanin stimulation of platelets results in aggregation and its interaction with CLEC-2 is crucial during development, but also has a role in tumour metastasis.[6,52,56] Rhodocytin and podoplanin both bind to three sites on CLEC-2; one site is shared whereas the other two are ligand specific.[57] More recently heme has also been suggested as an endogenous CLEC-2 ligand, suggesting a role in haemolysis.[58] In addition to roles in development and tumour metastasis via its interaction with podoplanin, CLEC-2 also has a role in thrombosis, particularly in thrombus stability and infection/inflammation-induced thrombosis.[25,59,60]

1.2.1 CLEC-2 signalling

CLEC-2 has a hemITAM motif in its cytoplasmic tail with a single tyrosine residue. Upon ligand binding, this residue is phosphorylated by SFK leading to recruitment and activation of Syk via its two Src homology 2 (SH2) domains (Figure 1.4).[38,61] The following signalling cascade is similar to that downstream of the ITAM receptor GPVI, although this is initiated by binding of Syk to two ITAM motifs rather than a hemITAM. The adaptor protein linker of activated T cells (LAT) is recruited and phosphorylated resulting in further phosphorylation of effector proteins such as Bruton's tyrosine kinase (Btk), SH2 domain containing leukocyte protein of 76 kDa (SLP-76) and VAV1/3 (Figure 1.4). Further differences to GPVI include only a partial dependence on SLP-76 and VAV1/3 for CLEC-2 signalling.[38,61] Phosphorylation of effector proteins culminates in the activation of PLCγ2 leading to platelet activation, aggregation and secretion via IP_3 and DAG, as previously described. It has also been shown that CLEC-2 phosphorylation following ligand binding is dependent on lipid rafts as well as on actin polymerisation.[62] Furthermore, secondary mediators, such as ADP, as well as the small GTPase Rac1 are required to amplify CLEC-2 signalling.[62,63] Secondary mediators are particularly important for human CLEC-2 where they are required for positive feedback signalling but are less critical in signalling by mouse CLEC-2.[62,64,65] Unwanted signalling via

CLEC-2 is prevented by the G6b-B receptor which contains two immunoreceptor tyrosine-based inhibitory motifs (ITIMs) (Figure 1.4).[66]

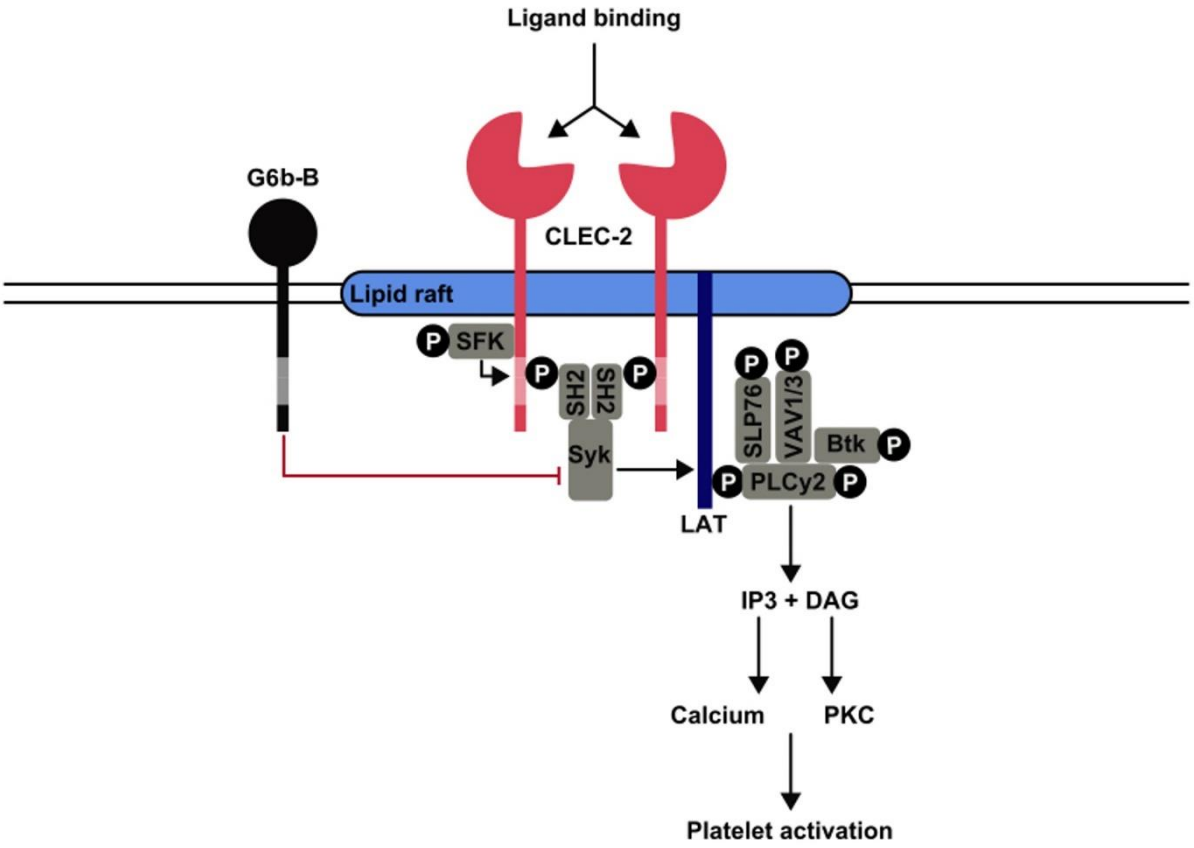

Figure 1.4 CLEC-2 hemITAM signalling cascade.
Ligand binding to CLEC-2 induces hemITAM phosphorylation via SFK and consequently recruitment of Syk. Phosphorylation of Syk leads to the recruitment and phosphorylation of LAT and subsequent recruitment of effector proteins including SLP-76, VAV1/3 and Btk. The signalling cascade results in the phosphorylation and activation of PLCγ2 and the generation of IP_3 and DAG resulting in release of intracellular Ca^{2+} and PKC activation. This results in platelet activation, aggregation and granule secretion. The ITIM receptor G6b-B prevents unwanted signalling via CLEC-2.

It has been suggested that CLEC-2 can be either a monomer or a dimer under basal conditions.[7,67] However, Hughes *et al.* have shown that two CLEC-2 receptors are needed for every one Syk molecule for downstream signalling and activation, suggesting that a single hemITAM is not sufficient for Syk activation.[67] Although, it is also possible that multiple hemITAM receptors are brought into close proximity upon ligand binding as rhodocytin can

bind to multiple CLEC-2 receptors and podoplanin co-clusters with CLEC-2.[67-69] This could lead to multimerisation of either monomers or dimers of CLEC-2.

1.2.2 CLEC-2 in development

The interaction between CLEC-2 and podoplanin is critical for the separation of blood and lymphatic vessels during development. The importance of this interaction is evident in either CLEC-2 or podoplanin constitutive knockout mice in which death occurs shortly after birth. In these mice, there is a separation defect between the blood and lymphatic vessels that results in blood-filling of the latter, as well as a disorganised and twisted appearance.[7,70] Furthermore, oedema can also be clearly seen embryonically and at birth suggesting defective lymphatic drainage.[5-7] Respiratory defects at birth are also seen in CLEC-2 deficient mice as their lungs have a reduced airspace and contain fluid, resulting in dyspnoea (shortness of breath). Brain haemorrhage can also be observed in these mice.[5] Mice deficient in the CLEC-2 downstream signalling mediators Syk,[5] SLP-76,[6] or PLCγ2[71] have also highlighted the importance of this pathway in blood-lymph separation as they have similar phenotypes to CLEC-2 deficient mice. The specific importance of platelet CLEC-2 in lymphatic development has been shown in conditional PF4-Cre (*Clec1b*$^{fl/flPF4Cre+}$) as well as in novel GPIbα-Cre (*Clec1b*$^{fl/fl}$*GPIbα-Cre*) induced CLEC-2 deficiency in which only platelets and megakaryocytes lack CLEC-2.[5,72,73] Although perinatal lethality is reduced in these mice, they still exhibit blood-filled lymphatic vessels, although to a lesser extent than constitutive CLEC-2 knockouts. Furthermore, they have reduced platelet counts, most likely due to the presence of blood in the lymphatic vessels.[5,72,73]

As LECs express podoplanin, platelets can be activated by, and adhere to them, but this does not occur in platelets deficient in either CLEC-2 or its downstream signalling mediators.[5,6] In addition, lethal blood-lymphatic defects have been observed in the CLEC-2 signalling null Y7A knockin mouse, where the CLEC-2 receptor is present but unable to signal (as the hemITAM cannot become phosphorylated), further suggesting that it is platelet activation via CLEC-2 that

is necessary for blood and lymphatic vessel separation.[74] Platelet activation by LECs has no effect on their viability but reduces their ability to migrate and form networks. However, these are only partially reduced in *Clec1b*$^{fl/flPF4Cre+}$ conditional CLEC-2 deficient mice, potentially due to residual expression, particularly in early development.[5] In lymphatic vascular development LEC progenitors in the cardinal vein form the primary lymph sacs that will then form the lymphatic vasculature by sprouting, proliferation and migration.[75] Platelet aggregates have been observed on these LECs in the separation zone between the lymph sacs and the cardinal vein in wildtype but not SLP-76 or podoplanin knockout mice.[6,70] It has therefore been suggested that podoplanin on LECs activates platelets, resulting in aggregate formation, which breaks the connection between blood vessels and the developing lymphatic vasculature.[70] It has also been suggested that platelet CLEC-2 has a role in preventing blood entering lymphatic vessels during development when the valves of the lymphovenous junctions are not yet fully formed. At these junctions, platelets come into contact with podoplanin on LECs and form aggregates that prevent blood flow into the lymphatic vessels.[76]

A role for CLEC-2 in the maintenance of lymphatic vessel integrity in adulthood has also been suggested through experiments using irradiated mice reconstituted with foetal liver cells from knockout and wildtype mice or by depleting CLEC-2 in neonates.[5,76] However, as mice that are only deficient in platelet CLEC-2 survive to adulthood, albeit with a mild lymphatic phenotype, and as lethal irradiation results in vascular remodelling, which could confound the results of experiments using chimeras, whether or not CLEC-2 has a role in lymphatic integrity in adulthood has been brought into question.[5,72] Furthermore, the lymphatic system could still be developing in neonatal mice which could explain why CLEC-2 depletion during this time period results in lymphatic defects.[72,76] Indeed, double depletion of both CLEC-2 and GPVI in adult mice has been shown not to cause lymphatic vessel separation defects, whereas genetic knockout of both receptors results in a more severe lymphatic defect than observed in single CLEC-2 knockout mice.[73] In addition, in a recent study by Haining *et al*. the role of CLEC-2 in

adult mice was investigated without the confounding effects of irradiation.[72] It was concluded that the interaction between CLEC-2 and podoplanin is not required after development to maintain lymphatic integrity in otherwise healthy mice.[72]

1.2.3 CLEC-2 in cancer

CLEC-2 is known to have a role in tumour metastasis via its interaction with podoplanin which activates platelets resulting in aggregation around cancer cells in the circulation thereby increasing their survival and facilitating metastasis.[52,56,77] This occurs as the platelets can protect the tumour from shear stress, as well as from the immune system; they can also aid with adhesion to the vessel wall.[78,79] It has further been suggested that podoplanin induced activation of CLEC-2 contributes to cancer-associated thrombosis within tumours and therefore reduces their oxygen and nutrient supply.[78,80] Furthermore, depleting or blocking CLEC-2 and podoplanin respectively using monoclonal antibodies (mAb) results in reduced metastasis and thrombosis and could therefore increase survival.[56,78,80] As a result, blocking the interaction between CLEC-2 and podoplanin could provide a novel therapeutic approach in treating certain types of cancer.[78]

1.2.4 CLEC-2 in thrombosis and haemostasis

As previously mentioned, CLEC-2 also plays a role in thrombosis, particularly in thrombus stability. The lymphatic phenotype of CLEC-2 knockout mice limited investigation into the role of CLEC-2 in thrombosis and haemostasis and therefore antibody-induced immunodepletion and irradiated/foetal liver chimeras were initially used to study the function of mouse CLEC-2. Generation of platelet/megakaryocyte specific CLEC-2 knockout mice then allowed further investigation.

Initial evidence for the role of CLEC-2 in thrombosis was shown using the anti-mouse CLEC-2 mAb INU1. Intravenous injection of the IgG form results in a transient thrombocytopenia lasting 3 to 4 days and dose-dependent depletion of CLEC-2 from the platelet surface for up to 6 days with no effect on other platelet surface receptors.[25] CLEC-2 deficient platelets were

unresponsive to rhodocytin stimulation for 5 days but responded normally to other platelet agonists.[25] Investigation into the mechanism of INU1-induced depletion suggests that CLEC-2 is internalised and then degraded in a SFK-dependent manner whereas Syk is required for the accompanying thrombocytopenia.[81] Furthermore, the ability of the antibody to bind to megakaryocytes and proplatelets could explain why CLEC-2 depletion lasts longer than the platelet lifespan.[25,81]

Immunodepletion of CLEC-2 by INU1 first showed its role in mouse thrombus stability. CLEC-2-deficient platelets adhere normally to a collagen coated surface under flow, but three-dimensional thrombus formation is impaired. Although new platelets are recruited throughout blood perfusion, they do not form stable attachments and are therefore washed away in the flowing blood.[25] This was also observed with blood from CLEC-2 knockout chimeras and in both cases the surface area coverage of the thrombi was reduced.[7,25] Furthermore, co-infusion of secondary mediators or their mimetics (ADP or U46619) rescued the phenotype, as did perfusion of non-anticoagulated blood which allows thrombin generation. This suggests that CLEC-2 acts as an activation receptor to stabilise the growing thrombus.[7,25] A similar effect of CLEC-2 deficiency on thrombus stability had been shown in several *in vivo* models of thrombosis. This includes laser induced injury to the mesenteric capillaries in CLEC-2 constitutive knockout chimeras,[7] $FeCl_3$-induced injury of the mesenteric arterioles in immunodepleted[25] and *Clec1b*$^{fl/flPF4Cre+}$ knockout mice[73,74] as well as mechanical injury of the abdominal aorta in *Clec1b*$^{fl/flPF4Cre+}$ knockouts.[74] In all cases, vessel occlusion time was increased, without an effect on initial platelet adhesion to the injured vessel wall (where recorded), as a result of embolisation of platelets and small aggregates from the initial thrombi, making full vessel occlusion less likely.[7,25,73,74] Interestingly, thrombus formation and stability were unaltered in constitutive CLEC-2 Y7A knockin mice suggesting that it is the presence of CLEC-2 itself, rather than CLEC-2-induced platelet activation via its hemITAM signalling cascade, that has a role in thrombus stability.[74] However, the mechanism of this role of CLEC-

2 is unknown as its endogenous ligand podoplanin is not present in the vasculature. It has therefore been suggested there is an as yet unknown CLEC-2 ligand, either within the plasma or on the surface of activated platelets.[7,25]

In contrast to its role in thrombosis, CLEC-2 deficiency has shown only minor effects on haemostasis in mice. INU1 induced CLEC-2 depletion had a minor effect on haemostasis with around a third of mice bleeding for more than 20 min, whereas no control mice failed to stop bleeding.[25] This was a greater effect than seen in CLEC-2 knockout chimeras which was initially attributed to additional effects of immunodepletion.[7,26] However, two different assays were used (filter paper and saline tail bleeding assay respectively) and it was later shown that variable bleeding times are observed for both INU1 depleted and *Clec1b*$^{fl/flPF4Cre+}$ knockout mice using both assays.[73] Therefore, CLEC-2 has been shown to have only a minor role in haemostasis. However, deficiency of both CLEC-2 and GPVI, either genetic knockout (*Gp6*$^{-/-}$*/Clec-2*$^{fl/f;\ Pf4\text{-}Cre}$) or by immunodepletion, has shown redundancy between the two (hem)ITAM receptors. In these mice tail bleeding times are significantly increased compared to single immunodepleted or *Gp6*$^{-/-}$ or *Clec-2*$^{fl/f;\ Pf4\text{-}Cre}$ knockout mice.[73]

Overall, research using CLEC-2 deficient mice had shown its major role is in thrombus stability with few effects on haemostasis. CLEC-2 has therefore been suggested as a potential anti-thrombotic target with a reduced bleeding risk compared to current anti-platelet drugs.[4,25,73] However, the role of human CLEC-2 in thrombosis has not been well studied as research is limited to *in vitro* experiments and no patients with defects in CLEC-2 have been identified to date.[16]

1.2.5 CLEC-2 in infection and inflammation

Thrombo-inflammation describes the interaction of platelets and immune cells, particularly in sterile inflammation, and is usually associated with ischaemia-reperfusion injury.[18] However, it should be noted that the term has also been (mis-)used to describe the relationship between inflammation and thrombosis more generally in the pathology of both arterial and venous

thrombosis.[16] The CLEC-2-podoplanin axis has been suggested to play a role in ischaemia-reperfusion injury following ischaemic stroke, with blockade of podoplanin reducing neurological defects and infarct volume as well as inflammatory cytokines.[82] On the other hand CLEC-2 has been shown to have a neuroprotective effect by regulating inflammation following traumatic brain injury as well as improving the integrity of the blood brain barrier with knockout mice having worse outcomes.[83] However, in humans plasma CLEC-2 upregulation has recently been suggested as a marker of poor prognosis and increased mortality following both acute ischaemic stroke and traumatic brain injury.[84,85] CLEC-2 and podoplanin also have a role in deep vein thrombosis (DVT) that occurs following sterile inflammation resulting from irregular blood flow, stasis and hypoxia. In mice deficient in platelet CLEC-2 or following podoplanin inhibition, thrombosis was prevented or reduced respectively.[60,86] Furthermore, podoplanin upregulation has been observed in a venous valve associated with a thrombus in a patient who died from DVT, whereas there was no podoplanin upregulation in unaffected valves which also suggests a role for CLEC-2 and podoplanin in human DVT.[87]

Immuno-thrombosis refers to the innate immune response to a pathogen that is accompanied by a thrombotic event. Its function has been suggested as recognising, containing and destroying pathogens,[88] although the thrombotic response can become uncontrolled, such as in sepsis. The term has also been used more generally to describe immune-driven thrombosis occurring in the presence, or absence, of infection.[11,88] CLEC-2 can have a role in both bacterial and viral infection. It has been suggested to have a role in viral dissemination of HIV-1 although further evidence for this is lacking.[44] Furthermore, platelet activation via CLEC-2 by dengue virus can increase neutrophil extracellular trap (NET) formation and release of pro-inflammatory cytokines through the release of platelet extracellular vesicles.[89] CLEC-2 also has a role in bacterial infections including those leading to sepsis and acute respiratory distress syndrome (ARDS). Platelet CLEC-2, as well as podoplanin, are protective in sepsis as mice deficient in either have increased organ damage and sepsis severity. This effect is independent

of thrombosis and is instead a result of CLEC-2 regulating inflammation and immune cell recruitment potentially by reducing the inflammatory phenotype of macrophages, as well as their accumulation, and thereby reducing inflammation.[90,91] Furthermore, CLEC-2 and podoplanin can also regulate lung inflammation severity in a LPS induced model of ARDS by limiting neutrophil recruitment.[92] It has also been shown to have a major role in experimental *Salmonella* infection in particular,[59] which will be discussed in more detail in the next chapter.

A role for CLEC-2 has also been described in vascular integrity during inflammation. In two models of inflammation (reverse passive Arthus reaction and LPS-induced lung inflammation) CLEC-2 deficiency reduced vascular integrity resulting in haemorrhage. However, it appears that GPVI and CLEC-2 again have redundant roles as a greater effect on vascular integrity was observed in double deficient mice.[93] It has also been found however, that loss of vascular integrity in GPVI and CLEC-2 double deficient mice can lead to accelerated wound healing..[94]

1.3 *Salmonella* infection as a model of bacteria-induced thrombosis

Salmonella enterica are gram-negative bacteria with over 2500 distinct variants (serovars) that can infect many species.[11] *Salmonella* infections, particularly with *Salmonella typhi*, have been linked to thrombosis in humans, although this is a rare complication of infection, particularly since the introduction of antibiotics.[59,95-97] Thrombosis has also been associated with *Salmonella* infection in other mammals including rodents and livestock, with *Salmonella typhimurium* (STm) infection of mice being used as a model of human typhoid, as well as of immuno-thrombosis.[11,59] However, the susceptibly of mice to *Salmonella* infection is dependent on the expression of natural resistance-associated macrophage protein 1 (NRAMP1) of which there are two variants differing by one amino acid.[98] This point mutation is present in susceptible mice, including the common laboratory strains C57BL/6J and BALB/c, which often survive less than 7 days after STm infection due to uncontrolled increases in bacteria number, whereas in resistant strains (e.g. Sv129S6 mice) the infection is resolved.[11,59,98] As many

genetically modified mice are on susceptible backgrounds, an attenuated strain of STm is often used that reproduces most features of the infection and allows both its progression and resolution to be investigated over several months, although there is a reduced severity of the infection.[11,59,99] This also allows investigation of immuno-thrombosis from initial thrombus formation to resolution.[11,59,100]

Intraperitoneal administration of attenuated STm in susceptible mice results in bacterial colonisation of the bone marrow, brain, kidney and lungs but is highest in the spleen and liver.[11,59] Bacterial load peaks after 7 days and decreases over the first month of infection in both the spleen and liver.[59,101] This is accompanied by immune and inflammatory responses resulting in increasing leukocyte numbers, thrombosis and thrombocytopenia.[59] It is a process dependent on toll-like receptor 4 (TLR4), which recognises LPS on gram-negative bacteria, initiating the innate immune response, and interferon gamma (IFN-γ) which is key to the inflammatory response following infection.[102,103] Both TLR4 and IFN-γ are vital for a full immune response to infection and respective knockout mice have increased bacterial load and mortality in comparison to WT controls following STm infection, as well as no evidence of thrombosis or thrombocytopenia.[59,104,105]

In the liver, leukocytes, mainly myeloid cells and monocytes, accumulate within inflammatory foci. Their presence continues past day 21, when bacterial numbers decline, suggesting that the inflammatory response continues even after bacterial clearance.[59] An increase in macrophages is also observed in the spleen 24 h after infection, as well as the presence of platelet rich thrombi containing neutrophils and with macrophages around the edges of the thrombi.[100] However, in the liver, thrombosis occurs around day 5 and peaks between days 7 and 21 after infection, when bacterial numbers are low, suggesting that continued bacterial presence is not required for the maintenance of thrombosis. Thrombi are also platelet rich and are mainly observed in branches of the portal vein accompanied by inflammatory infiltrates and surrounded by leukocytes. However, despite this, there are few signs of permanent liver injury.

The kinetics of liver thrombosis are parallel to those of inflammatory foci suggesting these processes are co-regulated, likely by the innate immune system.[59]

Platelet activation via GPVI, ADP, TxA_2 or thrombin is not required for thrombus formation in the liver which instead appears to be mediated via the interaction of CLEC-2 and podoplanin.[59] Expression of podoplanin increases in the liver from 24 h after infection and by day 7 it is expressed on leukocytes in inflammatory foci as well as on macrophages and on sub-endothelial cells such as pericytes or fibroblasts. However, it is not expressed by the vascular endothelium, instead it is suggested that endothelial damage exposes platelets to podoplanin thereby activating them and initiating thrombus formation. Platelets are then able to anchor thrombi by forming protrusions into the parenchyma via the site of endothelial damage.[59] This process is dependent on TLR4 and IFN-γ which contribute to podoplanin upregulation in the liver suggesting podoplanin as the link between inflammation (TLR4 and IFN-γ) and thrombosis (CLEC-2).[59] Further evidence is provided by a reduction in thrombosis in CLEC-2 deficient mice (*Clec1b*$^{fl/f;lPF4Cre+}$) as well as in mice with reduced podoplanin expression (*pdpn*$^{fl/fl;VAV1Cre+}$) and as a result of macrophage depletion using clodronate which also reduced podoplanin expression.[59] Consequently, it could be possible to target CLEC-2 and podoplanin therapeutically in patients with pathological immuno-thrombosis, either with monoclonal antibodies or using inhibitors of the tyrosine kinases Syk or Btk.[11]

The purpose of thrombosis following infection has been proposed as trapping and clearing bacteria.[88] However, although this can be observed *in vitro*, with STm activating platelets and the resulting aggregates containing bacteria, it is unlikely to be the case *in vivo*, at least for STm infection.[100] At the peak of thrombosis in either the spleen or liver few bacteria were observed in thrombi despite higher numbers in the surrounding tissue.[100] Furthermore, thrombosis in the spleen peaks before bacterial load and in the liver, thrombosis is at its peak when bacterial number is declining.[59,100,101] Therefore, no direct relationship appears to exist

between bacterial number and thrombosis following initiation by STm.[100] Instead it has been suggested that thrombi help to maintain vascular integrity during infection.[11]

1.4 Targeting CLEC-2

The most commonly used anti-platelet drug, aspirin, targets TxA_2 and is often administered in combination with $P2Y_{12}$ inhibitors, such as clopidogrel and ticagrelor. These drugs inhibit secondary mediators of platelet activation, although they also have effects on the amplification of other platelet activation pathways such as via (hem)ITAM signalling. However, they are associated with an increased risk of bleeding and in some patients further thrombotic events or resistance occur.[4,106,107] Therefore, targeting (hem)ITAM signalling, by either GPVI or CLEC-2, directly could reduce the risk of bleeding associated with anti-platelet therapy. The main benefits would include the minimal role these receptors, individually, play in haemostasis and that their expression is mainly restricted to platelets and megakaryocytes, reducing the likelihood of off-target effects.[73,106]

As a result of its role in thrombosis, cancer, infection and thrombo-inflammation CLEC-2 has been suggested as a potential therapeutic target for many diseases.[11,16,60,77] However, so far, no therapeutic intervention specific to CLEC-2 has been trialled, although several compounds used in basic research could guide the development, or potentially form the basis, of future therapeutics. These include antibodies against hCLEC-2 as well as inhibitors of its downstream signalling such as those of Btk.[106] These will be discussed in more detail in the following sections.

1.4.1 Antibodies

Since the approval of the first monoclonal antibody in 1986, the number of antibodies approved and in clinical trials has increased dramatically.[108] In 2018, 79 antibodies had been approved by the United States Food and Drug Agency (US FDA) and 570 were in clinical trials.[108,109] The most common therapeutic area which antibodies are developed for is oncology, followed by

inflammatory and autoimmune diseases. However, they are also being developed for cardiovascular and metabolic diseases, with 5 approved and 23 in clinical trials, and bleeding diseases, with 4 approved and 17 in clinical trials in 2017.[110] The notable approved antibody based therapies with regards to platelets and thrombosis are abciximab and caplacizumab which target αIIbβ3 and vWF respectively.

1.4.1.1 Types of antibody used as therapeutics and their production

The majority of approved antibodies are full immunoglobulin G (IgG) antibodies, these consist of two heavy and two light chains, with the antigen binding domain comprising of a variable heavy (V_H) and a variable light (V_L) domain, and have a molecular weight of 150 kDa (Figure 1.5A).[111,112] Smaller fragments of these can also be generated, including fragment antigen binding (Fab) and the single chain fragment variable (scFv) which consist of the V_H and V_L domains joined by a linker, examples of both of these fragments have been approved for clinical use (Figure 1.5A).[108,113-115] Advantages of antibody fragments include their small size, with Fab and scFv fragments having a molecular weight of around 50 and 27 kDa respectively, that can allow better tissue penetration.[112,113] Furthermore, without the Fc domain the likelihood of immune cell activation is reduced however, this can lead to rapid clearance and therefore a short half-life.[113,115] Antibodies from camelids have also been generated and are smaller than conventional IgG antibodies as they lack the light chains.[116] Fragments of the variable domain of these heavy chain antibodies (VHH), also termed nanobodies, have been produced and have a molecular weight of just 13-15 kDa (Figure 1.5B).[108,112,117] Benefits of nanobodies, aside from their small size, include increased solubility in water, increased shelf-life and resistance to proteolytic degradation however, as with Fab fragments they are rapidly cleared and have a short half-life.[118]

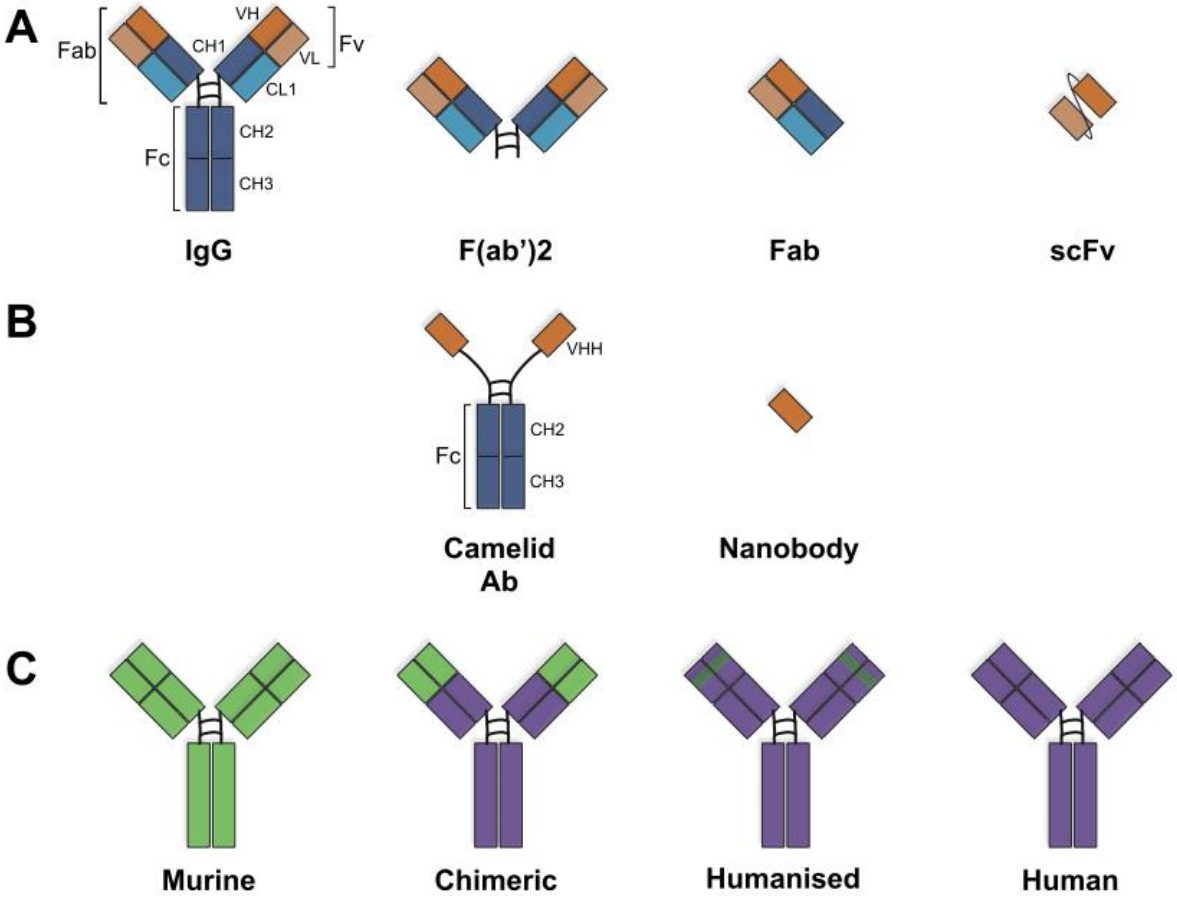

Figure 1.5 Antibodies and antibody fragments.
(**A**) IgG antibodies are comprised of two heavy chains and two light chains with each consisting of a constant and a variable region. IgG antibody fragments include F(ab')$_2$, Fab and scFv. (**B**) Camelid antibodies are comprised of two heavy chains consisting of a constant and a variable region. The variable region forms the antibody fragment termed a nanobody. (**C**) For clinical use in humans, murine antibodies can be modified to increase their efficacy and reduce their immunogenicity. This can be achieved by chimerisation of murine variable regions and human constant regions or by humanisation. Here the hypervariable region of a murine antibody is grafted in a human antibody. Alternatively, fully human antibodies can be produced using transgenic mice. CH, constant heavy chain; CL, constant light chain; V_H, variable heavy chain; V_L, variable light chain; IgG, immunoglobulin G; Fab, fragment antigen binding; scFv, single chain fragment variable; Ab, antibody; VHH, heavy chain variable domain. Adapted from Lu *et al*. (2020).[108]

Several types of antibody exist and have been approved. These include murine, chimeric, humanised and human antibodies (Figure 1.5C). As antibodies are often raised in animals, particularly mice, by immunisation followed by hybridisation of splenocytes with myeloma cells, techniques were needed to improve their efficacy in humans as well as to lower their immunogenicity, allowing their use over longer time periods.[108] Initially this was achieved by

forming chimeric antibodies where the original variable region remained but the constant region of the antibody was human (Figure 1.5C).[108] A further advance led to the generation of humanised antibodies by grafting the hypervariable or complementarity-determining regions (CDRs), that form the antigen binding site, of the original antibody into a human antibody (Figure 1.5C).[119] These techniques allow retention of antibody specificity but reduce immunogenicity, particularly with humanised antibodies.[108] It is also possible to generate human mAbs from transgenic mouse lines that have been genetically modified to express human immunoglobulin genes.[120] The process of immunisation and hybridoma formation is then the same as for a WT mouse however, the antibodies produced are fully human.[108,120]

A further method to generate human mAbs and antibody fragments is through phage display libraries.[108,121-123] These consist of bacteriophages that display antibody genes on their surface, through a selection process known as biopanning, antibodies for a target antigen or antigens can then be identified and isolated.[108,121] The variable region of these antibodies can be inserted into expression vectors with the constant regions and various cell systems can be used for large scale production.[121] Antibody production via phage display has several advantages including that it is an entirely *in vitro* process, there is increased selectivity of antibodies with high specificity and the potential to isolate antibodies against toxic targets.[108,121] However, most approved antibodies have been produced by immunisation as they tend to have better biophysical properties.[121]

1.4.1.2 Approved antibodies that target platelets

Two antibodies have been approved that target platelets, abciximab and caplacizumab. Abciximab, which targets GPIIb/IIIa (integrin αIIbβ3), was approved in 1994 as both the first chimeric antibody and the first Fab fragment.[108] In phase I trials in patients with unstable angina abciximab dose-dependently inhibited platelet aggregation and partially blocked GPIIb/IIIa for 72 h, furthermore, angina was not observed for at least 12 h. However, prolonged bleeding time at the highest concentration and a decrease in platelet count were observed. In addition,

2 of the 15 patients developed antibodies against abciximab suggesting it could be immunogenic.[124] Abciximab was later found to be safe in patients with myocardial infarction in combination with rt-Pa, aspirin and heparin administration during angioplasty,[125] but was not beneficial in patients with acute coronary syndrome who were not undergoing revascularisation or in the treatment of ischaemic stroke.[126,127] Furthermore, targeting GPIIb/IIIa in general has been associated with the highest risk of bleeding of all approved anti-platelet therapies.[128] Current guidelines now suggest GPIIb/IIIa inhibitors, including abciximab, should only be using during percutaneous coronary intervention (angioplasty) and only when there are thrombotic complications and not for long term prevention of thrombosis.[129]

Caplacizumab (ALX-0681) is a humanised bivalent nanobody that targets the vWF A1 domain for the treatment of acquired thrombotic thrombocytopenic purpura (TTP) and was first approved in 2018.[108,130] It is currently the only approved nanobody.[108] vWF is produced as ultra-large multimers that can cause platelet aggregation, however, normally the protease ADAMTS13 cleaves these multimers and as a result the A1 binding domain is only exposed at high shear rates, preventing unwanted platelet aggregation.[131,132] In TTP patients, ADAMTS13 is dysfunctional and therefore ultra-large vWF causes platelet aggregation and as a result thrombosis and thrombocytopenia.[132] In a baboon model of TTP caplacizumab restored platelet counts and was not linked with a risk of bleeding.[133] In clinical trials caplacizumab treatment lead to faster platelet count normalisation as well as reduced mortality, recurrence or thromboembolism with only mild bleeding adverse effects.[134-136]

1.4.1.3 The anti-GPVI Fab fragment ACT017

This section will focus on the development of the anti-GPVI fab fragment ACT017 (glenzocimab), particularly the use of a humanised mouse model to aid pre-clinical *in vivo* studies and key considerations for developing antibodies against platelet activation receptors.

ACT017 is the humanised form of the murine antibody 9012, which was originally described in 2003.[137] 9012 is specific to primate GPVI and does not bind to rodent platelets. Both the IgG

and F(ab')$_2$ fragment of 9012 can activate human platelets, although IgG-induced activation can be inhibited by the FcγRIIA blocking Fab fragment, IV.3.[137] This is an important consideration when using antibodies that target platelets as the Fc portion of an antibody can itself activate human platelets, although this is not the case with mouse platelets which do not have an FcγRIIA receptor.[138] Furthermore, the dimeric nature of F(ab')$_2$ fragments could also lead to platelet activation by receptor dimerisation. As a result, Fab fragments of 9012 were produced which did not activate platelets and instead exhibited a dose-dependent inhibition of collagen and collagen-related peptide (CRP) induced platelet activation and aggregation as well as collagen-induced procoagulant activity. Furthermore, the Fab fragment reduces both platelet adhesion and aggregation on collagen under both static and flow conditions.[137]

Due to the high specificity of antibodies, those raised against human antigens often cannot be tested in common laboratory animals such as rodents. As a result, *in vivo* experiments are initially carried out in higher order organisms such as non-human primates. As 9012 only binds to primate GPVI its *in vivo* function was investigated in cynomolgus monkeys.[139] *In vitro* results were similar to those with human platelets.[137,139] Administration of 4 mg/kg did not cause thrombocytopenia and had no effect on GPVI expression whereas collagen-induced platelet aggregation was inhibited and thrombus formation on collagen under flow was reduced.[139]

An alternative to initial *in vivo* experiments in non-human primates could be through the use of humanised mice in which the human antigen of the antibody being tested is expressed. A humanised GPVI mouse was developed in which the human cDNA was inserted into the *mgp6* gene and this vector was then electroporated into embryonic stem cells and positive clones were injected into blastocysts resulting in a hGPVI expressing mouse line.[140] These mice had normal platelet function and *in vitro* results with 9012 Fab were similar to those in human and monkey platelets.[137,139,140] *Ex vivo* results after administration of 4 mg/kg were similar to those in monkeys: collagen-induced platelet aggregation was delayed and thrombus formation on collagen under flow was reduced.[139,140] In addition, there was no thrombocytopenia, although

GPVI expression was slightly reduced at 30 min but normalised by 6 h after 9012 Fab administration.[139,140] Neither 4 or 8 mg/kg had an effect on bleeding time and reduced and prevented mortality respectively in a lethal thromboembolism model. Furthermore, thrombus formation and size were reduced after superficial laser and mechanical injury respectively.[140] These results suggest humanised GPVI mice are a suitable tool to test the role of hGPVI in *in vivo* thrombosis models as well as to test anti-GPVI compounds. Furthermore, they could be used to test bleeding tendencies of such compounds alone, or in combination with other anti-platelet drugs and could help with dosing strategies for clinical trials.[140] Humanised mice have also been used to test a pre-clinical anti-human podoplanin antibody, further supporting their use as models to test human specific antibodies.[141]

As 9012 Fab is from a murine antibody, its use in humans could lead to immunogenicity, therefore it was humanised with 18 versions generated. Of these ACT017 had the best humanness, as well as affinity, and inhibited collagen-induced platelet aggregation.[142] *Ex vivo* analysis in cynomolgus monkeys showed ACT017 inhibited collagen-induced platelet aggregation which returned to normal after 24 h with the highest dose tested, it had no effect on platelet count, GPVI expression or haematological parameters and little or no effect on bleeding time.[142] Results from phase I clinical trials have shown that ACT017 is well tolerated and caused no serious adverse effects including no clinically significant changes in bleeding time. It also had no effect on platelet count or GPVI expression and did not induce anti-drug antibodies.[143] ACT017 inhibited collagen induced aggregation up to 90% at the highest concentrations tested, an effect that lasted up to 18 h.[143] It is now undergoing phase I/II trials in acute ischaemic stroke patients in combination with rt-Pa with or without thrombectomy.[144]

1.4.1.4 Potential of CLEC-2 antibodies

The development of ACT017 provides a framework for the development of further antibodies targeting platelet (hem)ITAM receptors, namely that antibodies should be humanised to reduce immunogenicity and that Fab fragments will avoid unwanted Fc-mediated platelet activation.[142]

It also shows the potential of these drug targets for anti-platelet drugs with a reduced risk of bleeding.[140,143] Furthermore, it shows the potential of using humanised mice to test human antibodies *in vivo* particularly in terms of bleeding risk and dose determination.[140]

Although antibodies against both human and mouse CLEC-2 have been generated and the mCLEC-2 antibody INU1 has anti-thrombotic effects *in vivo*, as well as only a mild bleeding risk, these antibodies have not been further developed for potential clinical use.[25,40] Only INU1 IgG has been tested *in vivo* as the Fab fragment causes widespread thrombosis via an unknown mechanism (Nieswandt *et al*., unpublished). Furthermore, the anti-hCLEC-2 antibody AYP1 has only been tested *in vitro* in platelet aggregation and activation assays using rhodocytin or podoplanin to stimulate platelets and has not been tested in *in vitro* thrombosis assays prior to this thesis.[40] Despite this there is still a potential for CLEC-2 antibodies to be used clinically either in thrombosis, infection or cancer.

1.4.2 Btk inhibitors

Bruton's tyrosine kinase (Btk) is a non-receptor signalling kinase. It is expressed by haematopoietic cells including B cells, platelets and macrophages but notably not by T cells. Btk is involved in B cell development, differentiation and signalling but also in platelet signalling via (hem)ITAM receptors.[145] Furthermore, Btk is crucial for both the adaptive and innate immune response. It is involved in the signalling of toll-like receptors and antibody signalling via Fc receptors as well as in sterile inflammation, such as in autoimmune or ischaemic diseases, due to its role in neutrophil recruitment and function.[146-149]

Btk was first identified due to congenital mutations leading to Btk deficiency in patients with X-linked agammaglobulinemia (XLA).[150] These patients have an almost complete lack of mature B cells and therefore cannot produce antibodies or, as a result, mount a humoral immune response and suffer from recurrent infections.[150,151] A similar mutation has also occurred spontaneously in mice resulting in X-linked immunodeficiency.[152] However, the effects of the

mutation in mice are less severe than those in humans suggesting there is a species difference in the function of Btk.[151]

1.4.2.1 First and second generation Btk inhibitors

Inhibitors of Btk are used clinically for the treatment of B cell malignancies but some are also undergoing clinical trials for autoimmune diseases.[106] There are two main groups of Btk inhibitor: irreversible and reversible. Irreversible inhibitors covalently bind to cysteine residue 481 within the ATP-binding site thereby preventing kinase activity, whereas reversible inhibitors bind to Btk in its inactive form thereby preventing conformational change and subsequent activation. The first-in-class Btk inhibitor ibrutinib is an irreversible inhibitor used for the treatment of B cell malignancies. However, its use is associated with off-target effects including bleeding and atrial fibrillation.[153,154] The second-generation irreversible inhibitors, such as acalabrutinib and zanabrutinib, were designed to have better selectivity for Btk, although selectivity for Tec has been reported to be similar to Btk for both inhibitors.[155-157] Both acalabrutinib and zanabrutinib are undergoing clinical trials for use in chronic lymphocytic leukaemia and mantel cell lymphoma.[106,157,158] However, they have also been associated with bleeding,[157-160] although this could have been over reported as a result of the off-target effects of ibrutinib.[106]

1.4.2.2 Third generation Btk inhibitors

Third generation Btk inhibitors, such as rilzabrutinib (PRN1008), remibrutinib (LOU64) and PRN473, have higher selectivity for Btk compared to other kinases and potentially better pharmacokinetic and pharmacodynamic profiles.[106,146,161,162] Although rilzabrutinib and PRN473 have similar EC_{50} values for both Btk and Tec.[162,163] Rilzabrutinib is currently undergoing clinical trials for immune thrombocytopenia (ITP) and the autoimmune skin condition pemphigus vulgaris, whereas remibrutinib is undergoing trials for chronic spontaneous urticaria, asthma and Sjögren's Syndrome and PRN473 has recently entered clinical trials for atopic dermatitis.[106,164-170] These inhibitors have novel mechanisms of action

with the potential to increase their safety and selectivity. Rilzabrutinib and PRN473 are slowly reversible covalent inhibitors with the covalent bond allowing greater efficacy over a longer time combined with a unique binding mechanism that allows the residence time to be tailored.[146,162,171] However, rilzabrutinib is an ATP competitive Btk inhibitor and therefore its potency decreases with increasing ATP concentration.[146] Remibrutinib, on the other hand, is an irreversible inhibitor but binds selectively to the inactive conformation of Btk making its mechanism of action unique.[161] Both rilzabrutinib and remibrutinib have been shown to be safe in clinical trials with no reported bleeding, including in patients with ITP where bleeding risk is higher due to their reduced platelet count.[145,164,169,172,173]

1.4.2.3 Effect of Btk inhibition on platelet activation by GPVI and CLEC-2

The (hem)ITAM platelet receptors GPVI and CLEC-2 use Btk in their downstream signalling cascade.[16] It has therefore been suggested that Btk inhibitors could also be used to block platelet activation. The effects of ibrutinib and acalabrutinib on platelet activation and aggregation by the GPVI agonists collagen and CRP as well as the CLEC-2 agonist rhodocytin have been investigated.[65,155,174]

Ibrutinib was found to have two effects on CRP-induced platelet aggregation: at low concentrations in washed platelets (70 nM) it delays, but does not inhibit platelet activation, whereas at higher concentrations (700 nM) it reversibly inhibits platelet activation.[155] Similar results were also found for acalabrutinib, albeit at higher concentrations due to the inhibitors lower potency.[155,159] Similar results have also been shown for ibrutinib using collagen to induce platelet aggregation.[175] As this effect is reversible it is not mediated by the covalent binding of ibrutinib to Btk or another Tec kinase. This was shown as an off-target effect of ibrutinib using blood from XLA patients in which CRP-induced aggregation was further inhibited compared to healthy donors.[155] Furthermore, low concentrations (70 nM) of ibrutinib had no effect on platelet adhesion or thrombus formation on collagen under flow.[155] On the other hand, high concentrations (1 µM) of ibrutinib led to unstable thrombus formation whereas with

acalabrutinib thrombus formation was comparable to that of vehicle treated blood. Similar dysfunction was also seen with blood from patients taking ibrutinib.[174] In patients taking either ibrutinib or acalabrutinib *ex vivo* platelet aggregation induced by CRP was only blocked in those taking ibrutinib[155] It has been suggested that this is due to the difference in dosing of ibrutinib and acalabrutinib and suggests the increased risk of bleeding seen following ibrutinib use could be due to the off-target effects observed at higher concentrations.[155] However, Bye *et al.* (2017) reported that both ibrutinib and acalabrutinib blocked CRP and collagen induced platelet aggregation, although this discrepancy has been attributed to differences in how the aggregation experiments were carried out.[155,174]

In contrast to their effect on GPVI, ibrutinib and acalabrutinib inhibit CLEC-2 mediated human platelet activation and aggregation at a 20-fold lower concentration. Furthermore, platelets from patients taking either inhibitor did not aggregate following CLEC-2 stimulation.[65,155] A reduction in platelet adhesion and aggregate size on recombinant podoplanin under flow was also observed using blood from patients treated with ibrutinib or acalabrutinib or XLA patients.[65] The specificity of low dose Btk inhibition to CLEC-2 was further shown by its ability to block tyrosine phosphorylation of Syk, LAT, Btk and PLCγ2 following rhodocytin stimulation but not following GPVI-mediated platelet activation.[65,155] In XLA patients rhodocytin-induced platelet aggregation was abolished as was PLCγ2 phosphorylation therefore, the effects of Btk inhibitors on CLEC-2 are via Btk and not due to off-target effects as with GPVI.[65,155]

In human platelets, activation by CLEC-2 is dependent on positive feedback from the secondary mediators ADP and TxA_2.[62] However, standard human platelet preparations can lead to desensitisation to ADP. Therefore, the effect of ibrutinib on CLEC-2 mediated platelet activation in the presence of ADP has also been investigated. Platelet aggregation was still inhibited as was Btk autophosphorylation at Y233 and PLCγ2 phosphorylation however, phosphorylation of the upstream signalling proteins Syk and LAT or Btk at its Src kinase phosphorylation site, Y551, were no longer blocked.[65] On the other hand, these positive

feedback pathways are less crucial in CLEC-2 signalling in mouse platelets.[64] Therefore, a higher concentration of ibrutinib was required to block CLEC-2 mediated aggregation of mouse platelets and, consistent with the human results in the presence of ADP, Syk and LAT phosphorylation were maintained and only Btk and PLCγ2 phosphorylation were blocked.[65]

As previously described, CLEC-2 deficiency has a beneficial effect in mouse models of DVT and STm infection induced thrombosis and has therefore been suggested as a therapeutic target in inflammation and immune-mediated thrombosis.[11,59,86] It has further been proposed that Btk inhibitors could be used to target CLEC-2 in such conditions. However, as Btk is also involved in the immune response a balance would need to be struck between platelet inhibition and maintaining an appropriate immune response.[11] In a mouse DVT model, in which the inferior vena cava is ligated to induce thrombus formation, intraperitoneal ibrutinib administration failed to significantly reduce thrombosis. There was however, a trend for decreased thrombus prevalence following ibrutinib treatment, although the size of the remaining thrombi did not differ between control and ibrutinib treated groups. It was suggested that the limited effect of ibrutinib could be due to a lack of CLEC-2 inhibition across the entire 48 h experiment or due to the differences in the role of Btk in humans and mice.[65]

Both remibrutinib and rilzabrutinib have been shown to inhibit GPVI but not GPCR-mediated platelet aggregation in whole blood.[163] However, at the concentrations necessary to inhibit GPVI-mediated platelet aggregation both inhibitors increased closure time in an *in vitro* bleeding time model. Although this was to a lesser extent with remibrutinib than rilzabrutinib which likely reflects the lower dose needed to inhibit platelet aggregation by GPVI.[163] Furthermore, similar results have not been observed in clinical trials for either inhibitor.[145,164,169,172,173] On the other hand, a different study found that rilzabrutinib had no effect on collagen-induced platelet aggregation which is mediated by GPVI.[146] It is possible this discrepancy is due to the pre-incubation time of rilzabrutinib before platelet stimulation, as for the experiments where no inhibition was observed this was shorter whereas platelet inhibition

has been show to increase with the length of Btk inhibitor incubation.[146,155,163] Furthermore, it has been suggested that clinically relevant concentrations of remibrutinib will inhibit platelet activation mediated by GPVI in patients but that relevant concentrations of rilzabrutinib will only partially block activation.[163] However, whether or not these inhibitors have an effect on CLEC-2 induced platelet aggregation remains to be determined.

1.4.2.4 Potential of Btk inhibitors as anti-platelet drugs

Due to their ability to block platelet aggregation in response to GPVI and particularly CLEC-2 mediated platelet aggregation Btk inhibitors have been suggested as potential anti-platelet drugs.[65,106,155] Their selectivity for CLEC-2 at low concentrations also adds to their potential, as this is likely to result in fewer off target effects.[65] Furthermore, due to the role of CLEC-2 in thrombo-inflammation and immuno-thrombosis, as previously described, as well as the potential for reducing inflammation, Btk inhibitors could be an ideal intervention in such diseases.[11,87]

Additional benefits of using Btk inhibitors as anti-platelet drugs include the limited expression of Btk to certain haematopoietic cells, reducing the likelihood of off-target effects, particularly with the newer generation inhibitors that are more selective for Btk.[106,146,161] This also means that newer generation Btk inhibitors have a limited bleeding risk and could therefore be safe to use in thrombosis patients.[145] Indeed, their safety has already been shown in clinical trials and even in patients with immune thrombocytopenia, who have a high risk of bleeding, for remibrutinib.[169] There is also the potential for long-term treatment as they can be administered orally unlike other potential therapeutics such as antibody fragments.[106]

1.5 Aims

A role for CLEC-2 in thrombus stability has been proposed several times however, the exact nature of this role is unknown. In the first part of this thesis relative contributions of CLEC-2 and GPVI in mouse thrombus stability are investigated using blocking antibody fragments and

Syk inhibitors in order to further elucidate the proposed role of CLEC-2 compared to the known role of GPVI.

Although CLEC-2 has been proposed as a therapeutic target in an array of disease areas including thrombosis, infection, thrombo-inflammation and cancer, no potential therapeutics have been developed further than basic research. A key reason for this could be due to the difficulties associated with testing human-specific drugs in *in vivo* disease models, particularly that common laboratory animals cannot be used. Therefore, in the second part of this thesis a humanised CLEC-2 mouse model was characterised for its potential to test anti-platelet CLEC-2 agents *in vivo*, particularly for their effects on CLEC-2 receptor surface expression and haemostasis. A second aim was to generate a novel anti-hCLEC-2 antibody and characterise it using the humanised mouse model as a proof of concept of its potential to test future CLEC-2 therapeutics.

In the third part of this thesis, third generation Btk inhibitors were investigated for their ability to inhibit platelet CLEC-2, both *in vitro* and in a *Salmonella*-induced immuno-thrombosis model. First and second generation Btk inhibitors have previously been shown to selectively inhibit CLEC-2 at low concentrations although their use in the clinic for B cell malignancies has been associated with an increased risk of bleeding that could limit their use as anti-platelet drugs. Therefore, safer, third generation inhibitors, were used in a model where thrombosis is known to be mediated by CLEC-2.

The underlying aim of this thesis was to investigate the role of CLEC-2 in different models of thrombosis including in thrombus stability and infection-induced thrombosis using anti-CLEC-2 agents such as antibodies and tyrosine kinase inhibitors.

2. Materials and Methods

2.1 Materials

2.1.1 Reagents and chemicals

Acetic acid	Roth (Karlsruhe, Germany)
Ammonium peroxodisulphate (APS)	Roth (Karlsruhe, Germany)
Atipamezole	Pfizer (Karlsruhe, Germany)
Beta-mercaptoethanol	Roth (Karlsruhe, Germany) Gibco (UK)
BlueBlock PF	SERVA (Heidelberg, Germany)
BlueStar prestained protein marker	NIPPON Genetics (Düren, Germany)
Bovine serum albumin (BSA)	Sigma-Aldrich (Steinheim, Germany) Sigma-Aldrich (Poole, UK)
Calcium chloride	Roth (Karlsruhe, Germany) Sigma-Aldrich (Poole, UK)
Colour prestained protein standard, broad range (10-150 kDa)	New England Biolabs (Hitchin, UK)
$DIOC_6$	ThermoFisher (USA)
DPX mountant	Sigma-Aldrich (Poole, UK)
DyLight-488	Pierce (Rockford,USA)
Ethylenediaminetetraacetic acid (EDTA)	AppliChem (Darmstadt, Germany)
Enhanced chemiluminescence (ECL) detection substrate	MoBiTec (Göttingen, Germany) ThermoFisher (Waltham, MA)
Eosin	Roth (Karlsruhe, Germany)
Eukitt mounting medium	Sigma-Aldrich (Steinheim, Germany)
Fentanyl	Janssen-Cilag GmbH (Neuss, Germany)
Flumazenil	Delta Select GmbH (Dreieich, Germany)
Fluorescein-isothiocyanate (FITC)	Molecular Probes (Oregon, USA)
Fluoroshield™ with DAPI	Sigma-Aldrich (Steinheim, Germany)
Freund's Adjuvant	Sigma-Aldrich (Steinheim, Germany)
Haematoxylin	Sigma-Aldrich (Steinheim, Germany)
Haematoxylin & Eosin Stain Kit (Harris 1900)	Atom Scientific (Hyde, UK)
Histoclear	National Diagnostics (Nottingham, UK)
Hoechst 33342	Invitrogen (Paisley, UK)
Igepal CA-630	Sigma-Aldrich (Steinheim, Germany)
Isoflurane CP®	CP-pharma (Burgdorf, Germany)
Isopropanol	Roth (Karlsruhe, Germany)

Magnesium chloride	Roth (Karlsruhe, Germany) Sigma-Aldrich (Poole, UK)
Medetomidine (Dormitor)	Pfizer (Karlsruhe, Germany)
Methanol	Roth (Karlsruhe, Germany) VWR (Poole, UK)
Midazolam (Dormicum)	Roche Pharma AG (Grenzach-Wyhlen, Germany)
MOPS SDS running buffer	Life Technologies (Paisley, UK)
Naloxon	Delta Select GmbH (Dreieich, Germany)
Neutral buffered formalin	CellPath Ltd (Newtown, UK)
4-12% NuPage Bis-Tris gradient gels	Invitrogen (Paisley, UK)
Parafromaldehyde (PFA)	Roth (Karlsruhe, Germany)
Phycoerythrin (PE)	EUROPA (Cambridge, UK)
Protein G-Sepharose	GE Healthcare (Uppsala, Sweden)
ProLong^{TM} Diamond Antifade Mountant	Invitrogen (Paisley, UK)
Protease Inhibitor Cocktail	Sigma-Aldrich (Steinheim, Germany)
Polyvinylidene difluoride (PVDF) membranes	Merck Millipore (Darmstadt, Germany) Bio-Rad (Hemel Hempstead, UK)
Rotiphorese Gel 30% (PAA)	Roth (Karlsruhe, Germany)
Sodium dodecyl sulphate (SDS)	Sigma-Aldrich (Steinheim, Germany)
Sodium chloride	AppliChem (Darmstadt, Germany) Sigma-Aldrich (Poole, UK)
Tetramethylethylenediamine (TEMED)	Roth (Karlsruhe, Germany)
TissueTek OCT compound	Sakura Finetec (Staufen, Germany)
Tris(hydroxymethyl)aminomethane (TRIS)	Roth (Karlsruhe, Germany)

All other chemicals were obtained from Sigma (Sigma-Aldrich Steinheim, Germany or Poole, UK) or Roth (Karlsruhe, Germany).

2.1.2 Cell culture materials

Cell strainer, 100 µm	Falcon (Bedford, USA)
Foetal Bovine Serum (FCS)	Gibco (Karlsruhe, Germany)
HAT (hypoxanthine-aminopterin-thymidine, 50x)	Roche Diagnostics (Mannheim, Germany)
Polyethylene glycol 1500 (PEG 1500)	Roche Diagnostics (Mannheim, Germany)
RPMI 1640	Gibco (Karlsruhe, Germany)
Tissue culture flasks	Greiner (Frickenhausen, Germany)
Well plates	Greiner (Frickenhausen, Germany)

2.1.3 Antibodies

Purchased primary antibodies are shown in Table 2.1 and directly couples and secondary antibodies in Table 2.2. Antibodies generated in-house are shown in Table 2.3.

Table 2.1 Purchased primary antibodies

Antibody	Clone	Host	Manufacturer
Anti-human vWF Ig	Polyclonal	Rabbit	DAKO (Hamburg, Germany)
Anti-phosphotyrosine	4G10	Mouse	Sigma-Aldrich (Poole, UK)
Btk pY223	EP420Y	Rabbit	Abcam (Cambridge, UK)
CD31	Polyclonal	Rabbit	Invitrogen (Paisley, UK)
CD31	MEC13.3	Rat	BD Pharmigen (Wokingham, UK)
GAPDH	Polyclonal	Rabbit	Sigma-Aldrich (Steinheim, Germany)
LAT	Polyclonal	Rabbit	Sigma-Aldrich (Poole, UK)
PLCγ2 pY1217	3871	Rabbit	Cell Signalling Technology (Hitchin, UK)
Podoplanin	eBio8.1.1	Hamster	Invitrogen (Paisley, UK)
P-selectin	CTB201	Mouse	Santa Cruz (Heidelberg, Germany)

Table 2.2 Purchased directly coupled and secondary antibodies

Antibody conjugates	Clone	Host	Manufacturer
Anti-hamster IgG A647	Polyclonal	Goat	Invitrogen (Paisley, UK)
Anti-mouse CD41-PE	MWReg30	Rat	Biolegend (UK)
Anti-mouse IgG-FITC	Polyclonal	Rabbit	DAKO (Hamburg, Germany)
Anti-mouse IgG-HRP	Polyclonal	Rat	(Sigma-Aldrich Steinheim, Germany)
	Polyclonal	Sheep	Amersham (UK)
Anti-mouse P-selectin-FITC	WUG.E9	Rat	Emfret Analytics (Eibelstadt, Germany)
Anti-rabbit IgG A488	Polyclonal	Goat	Invitrogen (Paisley, UK)
Anti-rabbit IgG-HRP	Polyclonal	Donkey	Jackson Immuno (Suffolk, UK)
	NA934	Donkey	Sigma-Aldrich (Poole, UK)
Anti-rat IgG-FITC	Polyclonal	Rabbit	DAKO (Hamburg, Germany)
Anti-rat IgG-HRP	Polyclonal	Goat	Dianova (Hamburg, Germany)
hCLEC-2-FITC	AYP1	Mouse	Biolegend (Germany)
CD105-A647	MJ7/18	Rat	Biolegend (Germany)
αIIbβ3-PE	JON/A	Rat	Emfret Analytics (Eibelstadt, Germany)

Table 2.3 Antibodies generated in-house

Antibody	Antigen	Clone	Isotype	Reference
25B11	α5	25B11	Not determined	Unpublished
AYP1	Human CLEC-2	-	IgG1κ	[40]
AYP2	Human CLEC-2	-	IgG1	[40]
DOM1	GPV	89H11	IgG2a	[176]
EDL-1	β3	57B10	IgG2a	[176]
HEL1	Human CLEC-2	22H12	Not determined	Unpublished
INU1	Mouse CLEC-2	11E9	IgG1κ	[25]
INU2	Mouse CLEC-2	8C7	Not determined	Unpublished
JAQ1	GPVI	98A3	IgG2a	[177]
JON/A	αIIbβ3	4H5	IgG2b	[178]
JON6	αIIbβ3	14A3	IgG2b	Unpublished
LEN1	α2	12C6	IgG2b	[177]
p0p1	GPIbβ	3G6	IgG2a	[176,179]
p0p4	GP1bα	15E2	IgG2b	[176,179]
p0p6	GPIX	56F8	IgG1	[176]
WUG1.9	P-selectin	5C8	IgG1	Unpublished

2.1.4 Platelet agonists and inhibitors

Platelet agonists are shown in Table 2.4 and inhibitors in Table 2.5.

Table 2.4 Platelet agonists

Agonist	Receptor target	Source
ADP	P2Y12, P2Y1	Sigma-Aldrich (Steinheim, Germany)
AYP1	Human CLEC-2	Generated in house[40]
Collagen Horm® suspension	GPVI, α2β1	Takeda (Linz, Austria)
Collagen-related peptide-cross-linked	GPVI	CambCol Laboratories (Ely, UK) or a gift from Paul Bray (Baylor College, USA)
Fibrinogen from human plasma	αIIbβ3	Sigma-Aldrich (Steinheim, Germany)
INU1	Mouse CLEC-2	Generated in house[25]
PAR4 peptide	PAR4	Alta Biosciences (custom order) (Redditch, UK)
Thrombin	PAR1, PAR4	Roche Diagnostics (Mannheim, Germany)
Rhodocytin	CLEC-2	Gift from Johannes Eble (WWU Münster, Germany)
U46619	TP (TxA_2)	Alexis Biochemicals (San Diego, USA)

Table 2.5 Platelet inhibitors

Inhibitor	Target	Source
Apyrase (grade III)	ATP	Sigma-Aldrich (Steinheim, Germany)
BI1002494	Syk	Boehringer Ingelheim (Germany)
Cangrelor	$P2Y_{12}$	Sigma-Aldrich (Poole, UK)
Eptifibatide	αIIbβ3	GSK (Brentford, UK)
Heparin	Potentiates anti-thrombin III	Ratiopharm GmbH (Ulm, Germany) Iduron (Alderley Edge, UK)
Indomethacin	Cyclo-oxygenase	Sigma-Aldrich (Poole, UK)
PPACK	Thrombin	Cambridge Biosciences (Cambridge, UK)
PRN1008 (Rilzabrutinib)	Btk	Principia
PRN473	Btk	Principia
Prostacyclin (PGI_2)	Potentiates cAMP production	Calbiochem (Bad Soden, Germany) Cambridge Biosciences (Cambridge, UK)

2.1.5 Buffers and media

All buffers were prepared in double distilled water (ddH_2O) and the pH was adjusted with HCl or NaOH.

Acid citrate dextrose (ACD), pH 4.5

Trisodium citrate dehydrate	85 mM
Citric acid anhydrous	65 mM
Glucose anhydrous	110 mM

Blocking solution (Western blot)

BSA in PBS or washing buffer	5%

n-dodecyl-β-D-maltoside (DDM) Lysis buffer (immunoprecipitation for rat immunisation)

NaCl	150 mM
HEPES	50 mM
DDM	1%
Protease inhibitor mix	1%

Decalcification buffer, pH 7.4

EDTA in PBS	10%

HEPES buffer, pH 7.45

NaCl	136 mM
KCl	2.7 mM
HEPES	10 mM
$MgCl_2$	2 mM
$CaCl_2$	2 mM
Glucose	0.1%
BSA	0.1%

Hypoxanthine aminopterin thymidine (HAT) medium

RPMI	
FCS	10%
HAT	2%

Igepal lysis buffer, pH 7.5

NaCl	300 mM
TRIS	20 mM
EGTA	2 mM
EDTA	2 mM
Na_3VO_4	2 mM
Igepal CA-630	1%
Protease inhibitor mix	1%

Laemmli buffer (SDS-PAGE)

TRIS	40 mM
Glycine	0.95 M
SDS	0.5%

Lysine buffer

Lysine	125 mM
0.1 M NaH_2PO_4	37.5%
0.1 M Na_2HPO_4	12.5%

Periodate-lysine-paraformaldehyde (PLP)

Lysin buffer	75%
4% PFA	25%
Sodium periodate ($NaIO_4$)	12 mM

Phosphate buffered saline (PBS), pH 7.14

NaCl	137 mM
KCl	2.7 mM
KH_2PO_4	1.5 mM
Na_2HPO_4	8 mM

PBS-Tween washing buffer (immunofluorescence)

Tween-20	0.1%

Red blood cell (RBC) washing buffer

NaCl	140 mM
HEPES	10 mM
Glucose	5 mM

RPMI medium

RPMI 1640	
FCS	10%

SDS sample buffer 4x

β-mercaptoethanol (for reducing conditions)	20%
TRIS buffer (1.25 M) pH 6.8	20%
Glycerine	40%
SDS	8%
Bromophenolblue	0.02%

SDS sample buffer 5x (tyrosine phosphorylation)

SDS	10%
β-mercaptoethanol	25%
Glycerol	50%
TRIS/HCl stacking buffer	25%
Bromophenolblue	0.02%

Separating gel buffer (SDS-PAGE), pH 8.8

TRIS/HCl	1.5 M

Stacking gel buffer (SDS-PAGE), pH 6.8

TRIS/HCl	0.5 M

Stripping buffer (Western blot), pH 6.8

TRIS/HCl	62.5 mM
SDS	2%
β-mercaptoethanol	100 mM

Transfer buffer (Western blot)

TRIS Ultra	48 mM
Glycine	39 mM
Methanol	20%

TRIS-buffered saline (TBS), pH 7.3

NaCl	137 mM
TRIS/HCl	20 mM

Tyrode-HEPES buffer, pH 7.3

NaCl	137 mM
KCl	2.7 mM
$NaHCO_3$	12 mM
NaH_2PO_4	0.43 mM
$CaCl_2$	1 mM
$MgCl_2$	1 mM
HEPES	5 mM
BSA	0.35%
Glucose	0.1%

Washing buffer (Western blot)

Tween 20 in TBS	0.1%

2.1.6 Animals

Female Wistar rats aged 6 weeks were purchased from Janvier and WT C57BL/6 mice and female, ex-breeder NMRI mice were purchased from Charles River Laboratories.

Humanised CLEC-2 (hCLEC-2^{KI}) mice were generated by Biocytogen on a C57Bl/6N background using CRISPR Cas9 to replace the mouse *Clec1b* gene with the human variant. They were subsequently bred in Würzburg and WT mice resulting from heterozygous matings were used as controls for the experiments. Mice were genotyped by PCR using the following primers by Ewa Stepien-Bötsch:

Forward: 5'-GCAAAACAAACCCCAAGTGTCCTGG-3'

WT-rev: 5'- ATGCCCAAATTGCTGAATGAGCCTT-3'

KI-rev: 5'-CCGTTATCCCCTTGACTTCTATGCCC-3'

Animal studies were either approved by the district government of Lower Franconia or were performed in accordance with the Animal (Scientific Procedures) Act 1986 with approval of the UK Home Office under PPL PP9677279 and P06779746 granted to the University of Birmingham.

2.1.7 Blood donors

Blood samples were obtained from drug free, healthy volunteers after obtaining written informed consent in accordance with the Declaration of Helsinki and with approval from the Institutional Review Boards of the University of Würzburg or the University of Birmingham Research Ethics Committee (Ref: UHSP/22/BTVR/07).

2.1.8 Cell lines

The mouse myeloma cell line Sp2/0-Ag14 was kindly provided by D. Männel, University Hospital Regensburg, Germany.

2.2. Methods

2.2.1 Production of monoclonal antibodies

2.2.1.1 Immunisation of rats

In order to generate rat anti-hCLEC-2 antibodies, 3 6-week-old female Wistar rats were repeatedly immunised with hCLEC-2. hCLEC-2 was obtained from human platelet lysates, made using DDM lysis buffer, by immunoprecipitation using 5 µg of the anti-hCLEC-2 antibody AYP1 coupled to 100 µl protein G sepharose beads per rat. Immunisations were subcutaneous and took place every 14 to 21 days for a minimum of 7 times. The hCLEC-2 pulldown was resolved in Freund's complete adjuvant for the initial immunisation and Freund's incomplete adjuvant for all subsequent immunisations.

2.2.1.2 Generation of hybridoma cells

Following immunisation, the spleens were removed under sterile conditions and a single cell suspension was obtained by homogenisation using a 100 µm cell strainer. For the fusion the

cell suspension and mouse myeloma cells (Ag14 at 10^8 per fusion) were washed twice in RPMI medium (160 *g*, 5 min, RT), combined and washed a further two times. The supernatant was then removed and 1 ml of polyethylene glycol 1500 (37°C) was added drop-by-drop over a period of 2 min. 10 ml of RPMI medium (37°C) were then added over a period of 10 min to allow the cells to fuse. Cells were seeded in 15 96-well plates and fed with hypoxanthine-aminopterin-thymidine (HAT) selection medium so that only fused hybridoma cells survived. This was carried out by Steffi Hartmann.

2.2.1.3 Clone screening by flow cytometry

Hybridoma clones were screened by flow cytometry to detect those producing antibodies against hCLEC-2. Once the clones were large enough 50 µl of supernatant was removed and mixed with diluted human or hCLEC-2^{KI} mouse whole blood and incubated for 15 min at RT. Samples were then washed in 1 ml PBS (300 *g*, 5 min, RT) and incubated with an anti-rat IgG FITC conjugate for a further 15 min. Samples were analysed on a FACS Calibur (Becton Dickinson, Heidelberg, Germany). Positive clones were sub-cloned and re-screened and any clones that remained positive were expanded and the antibody purified.

2.2.2 Biochemistry

2.2.2.1 Western blotting

For Western blotting platelet rich plasma (PRP) was centrifuged at 800 *g* for 5 min and the resulting platelet pellet was resuspended and washed twice in PBS containing 5 mM EDTA. Platelets were resuspended at 1 x 10^6 platelets/µl in 1% IGEPAL lysis buffer containing protease inhibitors for 20 min on ice then centrifuged at 20,000 *g* for 10 min at 4°C to remove cell membranes. Platelet lysates were then mixed with either reducing or non-reducing Laemmli buffer before boiling at 95°C for 5 min. Samples were separated by sodium dodecyl sulphate polyacrylamide gel electrophoresis (SDS-PAGE; 12%) and transferred onto PVDF membranes. Membranes were blocked for either 30 min in BlueBlock or 1 h in 5% BSA at RT and then incubated with primary antibody overnight at 4°C on a rotor. They were then washed 3 times in TBS-T and incubated with secondary, HRP-conjugated antibody for 1 h at RT before being washed a further 3 times. The antibodies were then detected using ECL and an Amersham Imager.

2.2.2.2 Immunoprecipitation

For immunoprecipitation of CLEC-2 Protein G Sepharose beads were washed and coupled to 5 µg anti-CLEC-2 mAb for 1h at 4°C under rotating conditions then washed to remove excess

antibody (800 *g*, 5 min, 4°C). platelet lysates were pre-cleared with Protein G Sepharose for 1 h at 4°C and combined with the antibody-coupled Sepharose beads overnight at 4°C under rotating conditions. Samples were then centrifuged and washed three times at 800 *g* at 4°C for 5 min using TBS-T. Precipitated proteins used for immunisation of rats were then flash frozen in liquid nitrogen and stored at -80°C until use. Precipitated proteins for Western blot analysis were mixed with Laemmli sample buffer and boiled at 95°C for 5 min before centrifugation at 20,000 *g* to separate the supernatant from the Protein G Sepharose beads.

2.2.2.3 Tyrosine phosphorylation

To study tyrosine phosphorylation following Btk inhibition $5x10^5$ platelets/µl were incubated with Btk inhibitors for 1h at RT. Samples were then warmed for 5 min at 37°C and 9 µM eptifibatide was added to prevent aggregation induced by integrin αIIbβ3. Platelets were then activated with 300 nM rhodocytin under stirring conditions (1200 rpm) at 37°C for 3 min using a ChronoLog Model 700 aggregometer. Activation was stopped with 5x reducing sample buffer and samples were stored at -20°C until use. Samples were incubated at 95°C for 5 min and separated by SDS-PAGE on 4-12% NuPage Bis-Tris gels followed by transfer on to PVDF membranes. Membranes were block in 5% BSA for 1h at RT and then incubated with either the anti-phosphotyrosine antibody 4G10 (1:1000) or anti-Btk Y223 (1:500), anti-PLCγ2 Y1217 (1:250) or pan-LAT (1:500) antibodies overnight at 4°C. Membranes were then washed 3 times and incubated with secondary anti-mouse HRP conjugate for 4G10 and anti-rabbit HRP conjugate for PLCγ2, Btk and LAT diluted 1:10,000 for 1h at RT before being washed a further 3 times. The phosphorylated proteins were then visualised using ECL and autoradiograph exposure.

2.2.3 *In vitro* analysis of platelet function

2.2.3.1 Mouse platelet preparation

Humanised CLEC-2^{KI} mouse experiments

Mice were bled from the retro-orbital plexus into 300 µl 20 U/ml heparin using a heparinised glass capillary under isoflurane anaesthesia. The blood was then centrifuged twice at 300 *g* for 6 min to obtain the platelet-rich plasma (PRP), after the first centrifugation PRP as well as some red blood cells were transferred into 300 µl heparin before being re-centrifuged. 0.02 µg/ml apyrase and 0.1 µg/ml prostacyclin were added to the resulting PRP which was further centrifuged at 800 *g* for 5 min to pellet the platelets. Platelets were resuspended in Tyrode's

buffer supplemented with apyrase and prostacyclin, counted and centrifuged again before being resuspended in Tyrode's buffer at 5 x 10^5 for aggregation or 3 x 10^5 platelet/µl for spreading assays and left to rest at 37°C for 30 min prior to use.

Btk inhibitor experiments

Mice were CO_2 asphyxiated and blood was collected from the inferior vena cava up to 1 ml into 100 µl ACD. Blood was then combined with 200 µl Tyrode's buffer and centrifuged at 2000 rpm for 5 min to obtain PRP. This, as well as some red blood cells, were further centrifuged at 200 *g* for 6 min, PRP was then transferred to a new tube while 200 µl Tyrode's buffer was added to the remaining red blood cells and centrifuged again at 200 *g* for 6 min. PRP was then pooled with that from the previous centrifuge and Tyrode's buffer was added to bring the total volume to 1 ml. 0.01 µg/ml prostacyclin was added and the PRP was then centrifuged at 1000 *g* for 6 min and the platelet pellet was resuspended in 400 µl of Tyrode's buffer. The platelet count was then determined and adjusted to 4 x 10^5 platelets/µl for aggregation of 5 x 10^5 platelet/µl for stimulation and Western blotting experiments.

2.2.3.2 Human platelet preparation

Citrated blood was taken from healthy volunteers and further anticoagulated with ACD. PRP was obtained by centrifugation at 300 *g* for 20 min. 0.02 µg/ml apyrase, 0.1 µg/ml prostacyclin and 100 µl/ml ACD were added to the PRP before centrifugation at 500 *g* for 10 min. The resulting platelets were resuspended in 2 ml Tyrode's buffer supplemented with 0.02 µg/ml apyrase, 0.1 µg/ml prostacyclin and 150 µl/ml ACD and further centrifuged at 500 *g* for 10 min. Platelets were counted and resuspended in Tyrode's buffer at 5 x 10^5 platelet/µl and left to rest at 37°C for 30 min prior to use.

2.2.3.3 Blood cell counts

10 µl of blood was collected from the retro-orbital plexus in EDTA coated tubes and inverted multiple times to ensure proper mixing. Blood cell counts were then measured using a scil Vet analyser.

2.2.3.4 Flow cytometry

Glycoprotein expression

50 µl of whole mouse blood was collected in 300 µl heparin and further diluted in 700 µl PBS. Blood was incubated with saturating amounts of FITC conjugated antibodies for 15 min at RT. 500 µl of PBS were added prior to measuring surface expression on a BD FACS Celesta. For

expression of CLEC-2 on human platelets whole blood was diluted 1:20 in PBS and incubated with 2 µl AYP1-FITC.

Platelet count

Whole blood was collected and diluted as described above and saturating amounts of p0p6-FITC and JON6-PE conjugated antibodies were incubated for 15 min before addition of 500 µl PBS. Double positive platelets were then counted for 30 s.

Platelet activation

50 µl of whole mouse blood was collected in 300 µl heparin and further diluted with 1 ml of Tyrode's buffer without Ca^{2+} and centrifuged twice at 800 *g* for 5 min, the washed blood was resuspended in 1 ml Tyrode's buffer without Ca^{2+} after the first centrifugation and 750 µl of Tyrode's supplemented with 2 mM Ca^{2+} after the second centrifugation. Saturating amounts of JON/A-PE and anti-P-selectin-FITC antibodies were added to the blood as well as 10 µM ADP, 3 µM U4662, 0.001 – 0.1 U/ml thrombin, 0.1 – 10 µg/ml CRP, 1.2 µg/ml rhodocytin or 10 µg/ml of INu1 or AYP1 and incubated for 15 min after which 500 µl PBS were added and platelet activation was measured on a BD FACS Celesta.

Platelet activation following Btk inhibition

Blood was collected as described above from WT mice fed with a PRN473 or control diet. Per sample, 5 µl blood was diluted in 30 µl PBS and incubated with 5 µl each of JON/A-PE and anti-mouse P-selectin-FITC antibodies as well as 300 or 500 nM rhodocytin or 500 nM PAR4 for 20 min. 200 µl of 4% formalin were then added to each sample and platelet activation was measured using a BD Accuri C6 Plus flow cytometer.

2.2.3.5 Aggregometry

50 µl of washed platelets were further diluted with 110 µl of Tyrode's buffer supplemented with 2 mM Ca^{2+} and 100 µg/ml fibrinogen for all agonists except thrombin where Tyrode's buffer without fibrinogen was used. Platelet aggregation was then measured using a 4-channel aggregometer (APACT) under stirring conditions for 10 min after the addition of 5 µg/ml collagen, 0.01 U/ml thrombin, 0.24 µg/ml rhodocytin, 5 µg/ml HEL1 or 10 µg/ml of either INU1 or AYP1 antibodies. Tyrode's buffer was used to represent 100% light transmission.

For aggregation using ADP PRP was used. Blood was obtained from mice as described above and centrifuged twice at 300 *g* for 6 min without the addition of extra heparin. 50 µl of PRP was then diluted in 110 µl of Tyrode's buffer supplemented with 2 mM Ca^{2+} and aggregation was

measured for 10 min after the addition of 5µM ADP with platelet poor plasma being used to represent 100% light transmission.

Btk inhibition experiments

287 µl of washed mouse platelets were incubated for 1 h with 50, 200, 500 or 2000 nM of inhibitor or DMSO at a final concentration of 0.1%. Platelets were also incubated with 10 µM of the secondary mediator inhibitors cangrelor and indomethacin for 10 min or with DMSO (final concentration 0.1%). Platelets were warmed to 37°C for 5 min prior to addition on 100 nM rhodocytin and aggregation was measured for 5 min under stirring conditions (1200 rpm) using a ChronoLog Model 700 aggregometer.

2.2.3.6 Platelet spreading

Glass coverslips were coated over night at 4°C with either 100 µg/ml human fibrinogen or 10 µg/ml CRP or mouse podoplanin before being blocked with 1% BSA for 1 h at room temperature and rinsed with PBS. Platelets were allowed to spread at 37°C for 30 min for fibrinogen and CRP and 60 min for mouse podoplanin before being fixed in 4% PFA. For spreading on fibrinogen 0.01 U/ml thrombin were added to the platelet suspension immediately prior to spreading. Coverslips were mounted and then imaged using a Zeiss Axiovert 200 microscope in differential interference contrast (DIC) mode fitted with a 100x objective. 5 fields of view per coverslip were imaged and the platelets were categorised into 4 categories: 1) unspread platelets, 2) platelets forming filopodia, 3) platelets with lamellipodia and 4) fully spread platelets.

2.2.4 *In vitro* thrombus formation

2.2.4.1 Flow adhesion on collagen

Coverslips were coated with 200 µg/ml HORM collagen overnight at 37°C then blocked in 1% BSA for 30 min at RT. 800 µl of whole heparinised blood was diluted with 400 µl of Tyrode's buffer supplemented with 2 mM Ca^{2+} and platelets were labelled with a Dylight 488 conjugated p0p6 for 5 min at 37°C. The blood was then perfused over the collagen coated coverslip at shear rates of 150, 1000, 1200 and 1700 s^{-1} for 4 min and washed for a further 4 min with Tyrode's buffer supplemented with Ca^{2+}. 8 representative fields of view were imaged in both brightfield and fluorescence using a Leica DMI6000B microscope with a 63x objective. Images were then analysed in terms of platelet surface coverage and volume (fluorescent integrated density) using ImageJ.[180]

2.2.4.2 Thrombus stability flow adhesion on collagen

To assess the effect of (hem)ITAM inhibition on thrombus stability diluted whole mouse blood was perfused over collagen coated coverslips at a shear rate of 1000 and 1700 s^{-1} as described above. Flow was kept constant through the use of y-tubing and two pumps to prevent the build-up of secondary mediators that could occur when the flow stopped, for example, when changing syringe. After blood perfusion 8 representative fields of view were imaged. The thrombi were perfused with either Tyrode's buffer supplemented with 2 mM Ca^{2+} containing either the Syk inhibitor BI-1002494 (500 nM), the GPVI blocking Fab fragment JAQ1 (10 µg/ml) or the CLEC-2 blocking Fab fragment INU1 (10 µg/ml) for 5 min followed by 10 min perfusion of Tyrode's buffer supplemented with 2 mM Ca^{2+}. Controls were perfused with only Tyrode's buffer supplemented with 2 mM Ca^{2+} and in the case of BI1002494 an equal volume of DMSO. A further 8 representative fields of view were imaged and the change in platelet surface coverage and volume (fluorescent integrated density) were assessed using ImageJ.

2.2.4.3 Flow adhesion on vWF

To study whether hCLEC-2^{KI} platelets showed normal binding to vWF under flow conditions glass coverslips were coated with rabbit anti-human vWF antibody diluted 1:500 in carbonate buffer overnight at 4°C. Coverslips were then rinsed in PBS and blocked with 1% BSA for 1h at RT followed by coating with 200 µl of normal mouse plasma at 37°C. Plasma was obtained by centrifuging heparinised whole blood at 800 *g* for 10 min and then the resulting supernatant at 20,000 *g* for a further 10 min. Mouse blood was obtained and diluted as described previously and perfused at 1700 s^{-1} for 4 min followed by 4 min perfusion of Tyrode's buffer supplemented with 2 mM Ca^{2+}. 10 representative brightfield images were then taken using a Zeiss Axiovert 200 microscope fitted with a 40x objective and the number of adherent platelets were analysed.

2.2.4.4 Reconstituted flow adhesion

Coverslips were coated with collagen and blocked as previously described. Platelets were washed and resuspended at 5 x 10^5 platelets/µl in Tyrode's buffer. Red blood cells were also washed 5 times in red blood cell buffer. 700 µl washed platelets were combined with 500 µl RBCs, 250 µg/ml human fibrinogen, 1.7 mM $CaCl_2$ and 2 µl of p0p6 up to a volume of 1400 µl and perfused at 1000 s^{-1} for 4 min. The thrombi were then washed and imaged as previously described using a Zeiss Axiovert 200 microscope with a 40x objective.

2.2.4.5 Flow adhesion on collagen with human blood

Coverslips were coated with 100 µg/ml HORM collagen overnight at 37°C and blocked with 1% BSA for 30 min at RT. Whole citrated human blood from healthy donors was incubated for

5 min with 10 µg/ml AYP1 F(ab')$_2$ or Fab fragments or 52 µg/ml hFC-hCLEC-2 recombinant protein and 20 µM PPACK. Prior to flow at 1000 s^{-1} a further 20 µM PPACK, 3.75 mM Mg^{2+} and 7.5 mM Ca^{2+} were added to the blood. Blood was the perfused at 1000 s^{-1} for 4 min and washed for a further 4 min with HEPES buffer supplemented with 1 U/ml heparin and 2 mM Ca^{2+}. 8 representative fields of view were imaged in brightfield using an EVOS microscope with a 63x objective. Images were then analysed in terms of platelet surface coverage using ImageJ.

2.2.5 CLEC-2 depletion

100 µg of either AYP1, HEL1 or INU1 were injected intraperitoneally and platelet count and CLEC-2 surface expression was measured for up to 25 days as described above. Antibody binding to platelets was determined by incubating blood with anti-mouse IgG-FITC (AYP1) or anti-rat IgG-FITC (HEL1 and INU1) for 15 min. Prior to incubation, blood was further diluted in 1 ml PBS and centrifuged at 300 *g* for 5 min to remove unbound AYP1, HEL1 or INU1 antibodies. Mice were depleted between 5 and 10 days before *in vivo* experiments.

2.2.6 *In vivo* analysis of platelet function

2.2.6.1 Tail bleeding time

Mice were anaesthetised using a combination of medetomidine, midazolam and fentanyl (1 mg/ml, 5 mg/ml and 0.05 mg/ml respectively) injected intraperitoneally at 10 µl/g. 1.5 mm of the tail was cut with a scalpel and using filter paper the resulting blood was collected every 20 s until bleeding ceased, classed as the time when no further blood could be collected. This was done without touching the wound directly with the filter paper and for a maximum of 20 min.

2.2.6.2 $FeCl_3$ injury of mesenteric arterioles

4-5 week old mice were anaesthetised as for the tail bleeding time assay and injected retro-orbitally with 2 µg/g of p0p6 Dylight-488 conjugate to label platelets. The mesentery was exposed and the arterioles were visualised using a Zeiss Axiovert 200 microscope fitted with a 10x objective. Injury was induced by topical application of $FeCl_3$ using 3 mm^2 filter paper. Platelet adhesion and thrombus formation were visualised in the arterioles for 40 min or until vessel occlusion which was classified by the blood flow stopping for more than 1 min. Images

were analysed using Metavue software (Molecular Devices). These experiments were conducted by Sarah Beck.

2.2.6.3 Mechanical injury of abdominal aorta

6-12 week old mice were anaesthetised as previously described and the abdominal aorta was exposed following a longitudinal midline excision. A Doppler ultrasonic flow probe (Transonic Systems, New York, USA) was placed around the aorta and thrombosis was induced by mechanical injury resulting from a 15 sec compression upstream of the flow probe using forceps. Blood flow was monitored until either it ceased (complete vessel occlusion) or 30 min had elapsed. These experiments were conducted by Sarah Beck.

2.2.7 Blood pressure and heart rate

Blood pressure and heart rate were measured using a Non-invasive Blood Pressure System for Rodents (Harvard Apparatus). Mice were anaesthetised using isoflurane and blood pressure and heart rate were measured using a cuff placed around the tail.

2.2.8 *Salmonella* infection immuno-thrombosis model

Mice were injected intraperitoneally with 5 x 10^5 attenuated *Salmonella Typhimurium* SL3261 7 days after starting a diet containing the Btk inhibitor PRN473 or a control diet. After 7 days mice were culled and their livers removed and flash frozen in liquid nitrogen.

2.2.9 Histology for hCLEC-2^{KI} organs

2.2.9.1 Preparation of paraffin sections

Organs were removed, washed in PBS and fixed in 4% paraformaldehyde (PFA) overnight at 4°C followed by dehydration and embedding in paraffin. Prior to dehydration and embedding femurs were decalcified in PBS containing 10% EDTA for 4 days with the buffer being changed daily. Organs were cut into 5 µm sections using a Microm Cool Cut microtome (Thermo Scientific, Braunschweig, Germany).

2.2.9.2 Preparation of cryosections

Organs were removed and washed in PBS and then embedded in Tissue-Tek OCT compound and frozen on dry ice. They were cut into 7 µm sections using a Cryostat (Leica, Wetzlar, Germany).

2.2.9.3 Haematoxylin and eosin (H&E) staining

Sections were deparaffinated in xylol for 2 incubations of 5 min, rehydrated in decreasing concentrations of ethanol (100, 96, 90, 80 and 70%) and finally in deionised water each for 2 min. Sections were stained in haematoxylin for 5 min followed by 10 min of annealing in running tap water and stained with acidified eosin for a further 3 min before being washed in deionised water. Sections were then dehydrated in ethanol as described above but in reverse order, followed by two 5 min incubations in xylol. Sectioned were then mounted using Eukitt, left to dry overnight and imaged using a Leica DHI 4000B microscope. H&E staining of cryosections followed the same procedure excluding deparaffination. Megakaryocytes in the spleen and bone marrow were counted in 8 fields of view per mouse using a 20x objective.

2.2.9.4 Immunofluorescence staining of lung cryosections

Cryosections were fixed in PLP for 30 min at RT and washed 3 times in PBS. Each section was circled using a lipid pen and blocked with PBS-Tween containing 3% rat serum and 3% BSA for 1 h at RT. Sections were washed in PBS-Tween for 5 min and incubated with 10 µg/ml each of CD105-A647 and p0p6-A488 in blocking buffer for 1 h at RT then washed a further 3 times in PBS-Tween and once in PBS. Sectioned were mounted using Fluoroshield mounting medium with DAPI and imaged using a Leica DMI6000B microscope.

2.2.10 Histology following *Salmonella* infection

2.2.10.1 Preparation of liver cryosections

Livers were flash frozen in liquid nitrogen and sectioned into 5 µm thick sections using a Clinicut cryostat (Bright Instruments, Huntingdon, UK). Sections were allowed to dry for 1 h and were then fixed in ice cold acetone for 20 min. They were stored at -20°C until needed.

2.2.10.2 Haematoxylin and eosin staining

Liver sections were brought to room temperature for 30 min, circled using a lipid pen and then fixed in 10% formalin for a further 20 min. They were then rehydrated in decreasing concentrations of ethanol (100, 96, 90, 80 and 70%) and finally in deionised water each for 2 min. For H&E staining an Atom Scientific H&E kit was used following the manufacturer's instructions. In brief, sections were incubated with haematoxylin for 5 min, washed in running tap water and then differentiated in 0.5% acid alcohol for 20 s before a further wash in running tap water. The haematoxylin was then blued in Scotts tap water for 5 min followed by a 2 min wash in deionised water. Sections were incubated with eosin for 12 min, washed briefly and

then dehydrated in ethanol as described above but with increasing ethanol concentration. This was followed by two 2 min incubations in Histoclear. Sections were then mounted and coverslipped using DPX. Sections were imaged using a Zeiss Axioscan.Z1 slide scanner using a 20x objective. The percentage area of the portal vein branches containing thrombi were then calculated using Zen 3.1 (blue addition) software.

2.2.10.3 Immunofluorescence staining

Liver sections were brought to room temperature for 30 min, circled with a lipid pen and washed in PBS containing 0.1% Tween-20 (PBS-T) for 5 min. Sections were then incubated with 20 mM ammonium chloride for 15 min to quench autofluorescence and washed for a further 5 min in PBS-T. Sections were then blocked in PBS-T containing 1% BSA and either 5% goat or donkey serum for 1 h and incubated with the combinations of primary antibodies shown in Table 2.6 diluted in blocking solution overnight at 4°C. Sections were washed in PBS-T three times, each for 10 min and incubated with the secondary antibodies shown in Table 2.6 diluted 1:500 in PBS for 45 min and washed a further three times. Nuclei were stained using Hoechst diluted 1:1000 for 5 min and sections were washed a further three times before being coverslipped using ProLong Diamond Antifade Mountant. Sections were imaged using a Zeiss Axioscan.Z1 slide scanner using a 20x objective. The total number of thrombi as well as the percentage area of the portal vein branches containing thrombi were then calculated using Zen 3.1 (blue edition) software. As was thrombus P-selectin intensity. Large vessels were considered as those with an area greater than 200,000 AU. P-selectin and podoplanin expression was calculated in ImageJ[180] as the average surface area coverage from 5 representative fields of view per section.

Table 2.6 Antibodies used for immunofluorescence staining of liver sections following *Salmonella* infection

Primary antibodies	Dilution	Blocking	Secondary antibodies
CD41-PE	1:250		-
CD31	1:100	Goat serum	Goat α-rabbit A488
Podoplanin	1:200		Goat α-hamster A647
CD41-PE	1:250		-
CD31	1:100	Donkey serum	Goat α-rabbit A488
P-selectin	1:200		Goat α-mouse A647

2.2.11 Intestine imaging

Wildtype, hCLEC-2^{KI} and *Clec1b*$^{fl/flPF4Cre+}$ mice were sacrificed and their intestines exposed using cotton buds following a midline excision. Mice were placed in a Petri dish on a light box and images of the intestine were taken on a Lumix DMC-G3 digital camera (Panasonic).

2.2.12 Power calculations

To determine the number of mice needed for experiments power calculations were carried out using a power of 0.8 and an alpha of 0.05 using G*power 3.1 software[181]. Example for both *in vitro* and *in vivo* experiments are shown below.

For *in vitro* experiments reference values from Thielmann *et al*. (2012) were used.[182] Values of 332.2 ± 65.8 for WT mice and 196.0 ± 29.0 for knockout mice for GPIIb/IIIa activation and 131.4 ± 35.9 for WT and 81.8 ± 18.8 for knockout mice for P-selectin exposure following thrombin stimulation were used.

The effect size (d) was calculated as follows:

$$d = \frac{\delta}{\sigma} = \frac{196.0 - 332.2}{\sqrt{\frac{1}{2}(65.8^2 + 29.0^2)}} = 2.68 \qquad d = \frac{\delta}{\sigma} = \frac{81.8 - 131.4}{\sqrt{\frac{1}{2}(35.9^2 + 18.8^2)}} = 1.73$$

Based on the effect sizes of 1.73 to 2.68, the number of mice needed per group for *in vitro* experiments was calculated as n = 4 to n = 7 respectively.

For *in vivo* experiments reference values from Stegner *et al.* (2013) for occlusion time following $FeCl_3$-induced injury to the mesenteric arterioles of 14.2 ± 3.8 min for WT mice and 19.8 ± 6.4 min for knockout mice were used.[183]

The effect size (d) was calculated as follows:

$$d = \frac{\delta}{\sigma} = \frac{19.8 - 14.2}{\sqrt{\frac{1}{2}(3.8^2 + 6.4^2)}} = 1.06$$

Based on this, the number of mice needed per group for *in vivo* experiments was calculated as n = 15.

2.2.13 Data analysis

Data was first tested for normality using the Shapiro-Wilk test with normally distributed data then being shown as mean ± standard deviation and being analysed by either an unpaired t-test or ANOVA followed by multiple comparison correction where appropriate, unless otherwise stated. Data that did not follow a normal distribution is shown as the median and interquartile range and was analysed by Mann-Whitney tests, unless otherwise stated. P-values < 0.05 were considered to be statistically significant with * $P < 0.05$, ** $P < 0.01$, *** $P < 0.001$ and **** $P < 0.0001$.

3. Results

3.1 CLEC-2 contributes to stability of the thrombus shell in mice

CLEC-2 has been proposed to have a role in thrombus stability but the mechanism through which it acts has not been identified.[7,25] Here we formed thrombi on collagen using anti-coagulated blood to model the thrombus shell where there is a lower contribution of coagulation factors to stability than in the core.[23,28] Furthermore, previous experiments identifying a role for CLEC-2 in thrombus stability have used blood from mice deficient in CLEC-2,[25] meaning CLEC-2 is absent through the entire process of thrombus formation therefore, here we used blocking agents against CLEC-2 after thrombus formation instead. This allowed us to investigate the role of CLEC-2 specifically in the stability of the outer layers of a thrombus and compare it to the role of the ITAM receptor GPVI.

3.1.1 Inhibition of Syk reduces thrombus stability

The Syk inhibitor BI-1002494 has been shown to block both CLEC-2 and GPVI-induced platelet aggregation.[184] Here we used it in an *in vitro* thrombosis model at a concentration of 500 nM to investigate the role of CLEC-2 and GPVI in thrombus stability. At arterial shear rates of both 1000 (Figure 3.1 A-C) and 1700 s^{-1} (Figure 3.1 D-F) inhibition of Syk increased the thrombus surface coverage of preformed thrombi relative to control treated thrombi. Increased surface coverage was the result of thrombus disaggregation with platelets or small aggregates dispersing from the thrombi in the direction of flow (Figure 3.1 C and F). Although some platelets were washed away in the flow, many remained attached to the collagen. It should be noted that disaggregation of the control treated thrombi was also observed, although to a lesser extent than those treated with BI-1002494.

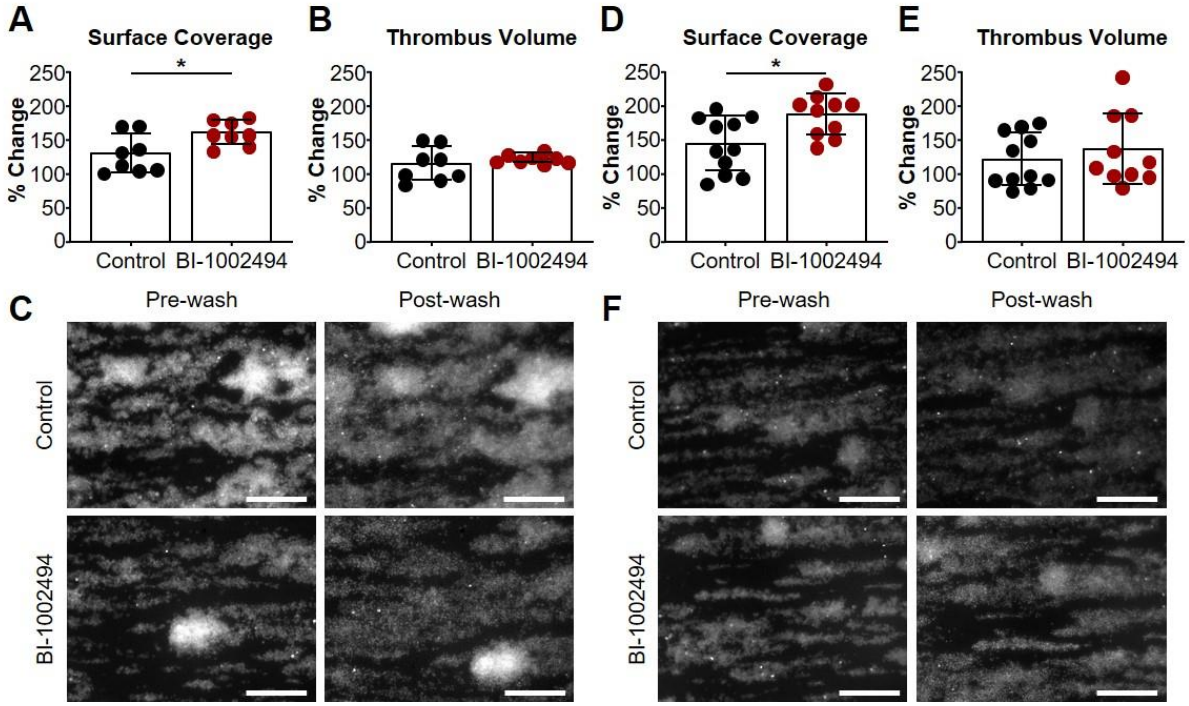

Figure 3.1 Inhibition of Syk by BI-1002494 reduces thrombus stability.
Thrombi were formed by perfusing anti-coagulated mouse blood over collagen at either 1000 or 1700 s^{-1} for 4 min followed by perfusion of 500 nM BI-1002494 or DMSO control for 5 min and 10 min of washing with Tyrode's buffer. The changes in thrombus surface coverage and thrombus volume (measured by integrated fluorescent density) were then determined between images taken before and after inhibitor perfusion. (A) Change in thrombus surface coverage after perfusion of BI-1002494 at 1000 s^{-1}. Unpaired t-test P = 0.021. (B) Change in thrombus volume after perfusion of BI-1002494 at 1000 s^{-1}. Unpaired t-test P = 0.40. (C) Representative images before and after perfusion of BI-1002494 or DMSO control at 1000 s^{-1}. (D) Change in surface coverage after perfusion of BI-1002494 at 1700 s^{-1}. Unpaired t-test P = 0.012. (E) Change in thrombus volume after perfusion of BI-1002494 at 1700 s^{-1}. Unpaired t-test P = 0.46. (F) Representative images before and after perfusion of BI-1002494 or control at 1700 s^{-1}. Data are shown as percentage change before and after perfusion of BI-1002494 or DMSO control and each symbol represents one individual with n = 8 to 11 mice. Scale bars represent 50 µm and * P < 0.05.

3.1.2 GPVI contributes to thrombus stability at high, and CLEC-2 at low, arterial shear

As inhibition of Syk affects signalling by GPVI and CLEC-2 the contribution of each receptor was investigated individually using 10 µg/ml blocking antibody fragments. At a shear rate of 1000 s^{-1} blockade of GPVI by JAQ1-Fab had no effect on thrombus stability (Figure 3.2 A-C). However, at a higher shear rate of 1700 s^{-1} thrombus surface coverage was increased following JAQ1-Fab perfusion (Figure 3.2 D and F). No effect on thrombus volume was observed at either shear rate (Figure 3.2 B and E). JAQ1-Fab had a similar effect to that of BI-1002494 in

terms of thrombus disaggregation which caused the increased change in surface coverage. On the other hand, blockade of CLEC-2 by INU1-Fab reduced thrombus stability at 1000 s^{-1} (Figure 3.3 A-C) but not 1700 s^{-1} (Figure 3.3 D-F). As with Syk inhibition and GPVI blockade the reduction in thrombus stability caused by INU1-Fab was due to thrombus disaggregation and the resulting increase in surface coverage following perfusion.

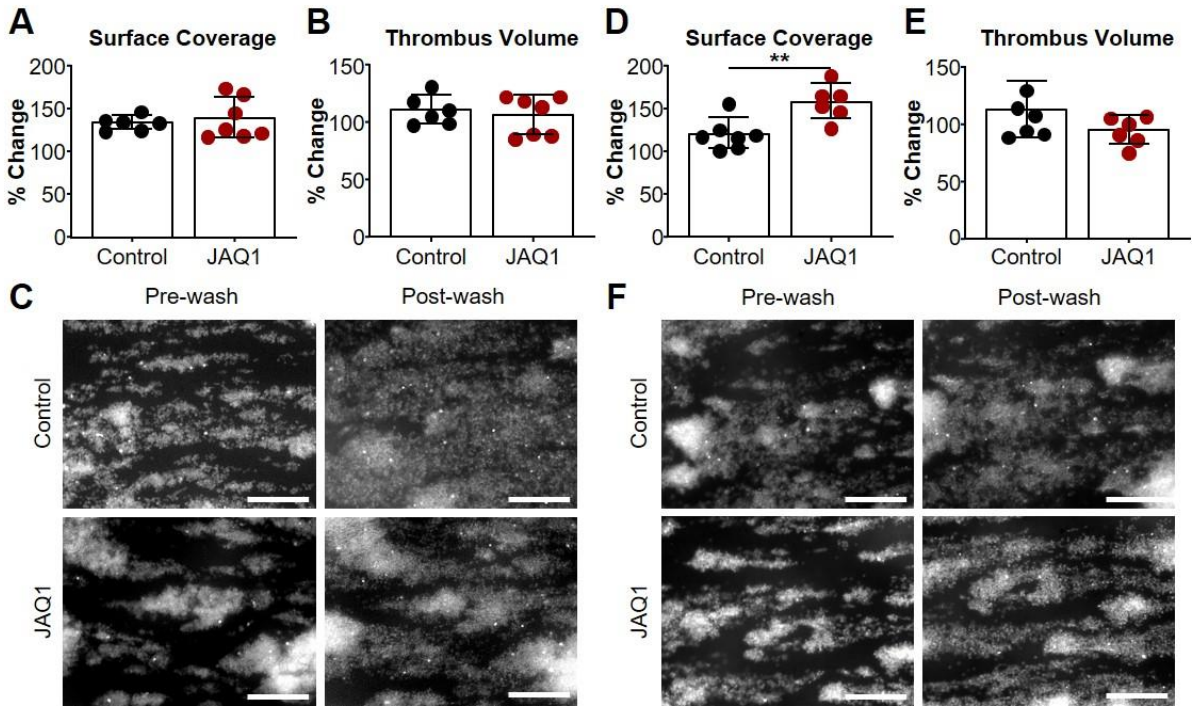

Figure 3.2 Blockade of GPVI reduces thrombus stability at high shear.
Thrombi were formed by perfusing anti-coagulated mouse blood over collagen at either 1000 or 1700 s^{-1} for 4 min followed by perfusion of 10 µg/ml JAQ1-Fab for 5 min and 10 min of washing with Tyrode's buffer. The changes in thrombus surface coverage and thrombus volume (measured by integrated fluorescent density) were then determined between images taken before and after JAQ1-Fab perfusion. (A) Change in thrombus surface coverage after perfusion of JAQ1-Fab at 1000 s^{-1} Unpaired t-test P = 0.62. (B) Change in thrombus volume after perfusion of JAQ1-Fab at 1000 s^{-1}. Unpaired t-test P = 0.60. (C) Representative images before and after perfusion of JAQ1-Fab or PBS control at 1000 s^{-1}. (D) Change in surface coverage after perfusion of JAQ1-Fab at 1700 s^{-1}. Unpaired t-test P = 0.0048. (E) Change in thrombus volume after perfusion of JAQ1-Fab at 1700 s^{-1}. Unpaired t-test P = 0.14. (F) Representative images before and after perfusion of JAQ1-Fab or PBS control at 1700 s^{-1}. Data are shown as percentage change before and after perfusion of JAQ1-Fab or control and each symbol represent one individual with n = 6-7 mice per group. Scale bars represent 50 µm and ** P < 0.01.

In summary, CLEC-2 has a minor role in the stability of the thrombus shell at low, but not high, arterial shear rates, which could instead be mediated by GPVI. Inhibition of Syk reduces

thrombus stability at either shear rate most likely due to its role in the downstream signalling cascades of both CLEC-2 and GPVI.

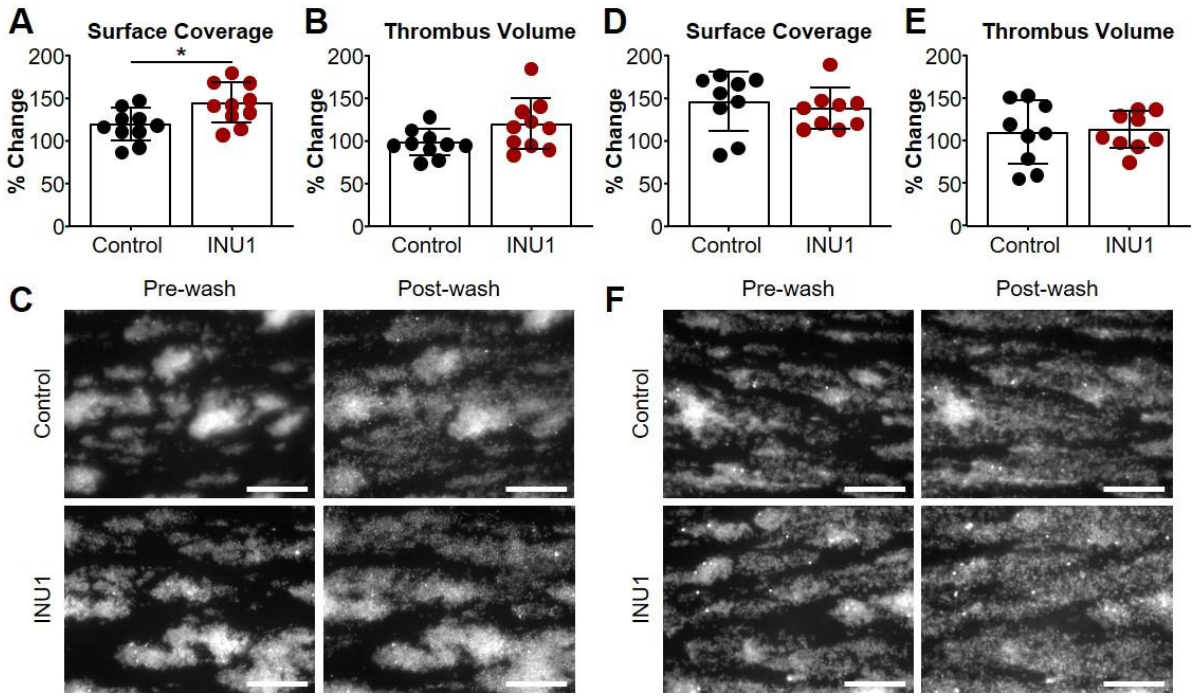

Figure 3.3 Blockade of CLEC-2 reduces thrombus stability at low arterial shear.
Thrombi were formed by perfusing anti-coagulated mouse blood over collagen at either 1000 or 1700 s^{-1} for 4 min followed by perfusion of 10 µg/ml INU1-Fab for 5 min and 10 min of washing with Tyrode's buffer. The changes in thrombus surface coverage and thrombus volume (measured by integrated fluorescent density) were then determined between images taken before and after INU1-Fab perfusion. (A) Change in thrombus surface coverage after perfusion of INU1-Fab at 1000 s^{-1}. Unpaired t-test P = 0.016. (B) Change in thrombus volume after perfusion of INU1-Fab at 1000 s^{-1}. Unpaired t-test P = 0.063. (C) Representative images before and after perfusion of INU1-Fab or PBS control at 1000 s^{-1}. (D) Change in surface coverage after perfusion of INU1-Fab at 1700 s^{-1}. Unpaired t-test P = 0.57. (E) Change in thrombus volume after perfusion of INU1-Fab at 1700 s^{-1}. Unpaired t-test P = 0.83. (F) Representative images before and after perfusion of INU1-Fab or PBS control at 1700 s^{-1}. Data are shown as percentage change before and after perfusion of INU1-Fab or control and each symbol represent one individual with n = 9-10 mice per group. Scale bars represent 50 µm and * P < 0.05.

3.2 Characterisation of humanised CLEC-2 (hCLEC-2^{KI}) mice

3.2.1 Generation of hCLEC-2^{KI} mice

To investigate the role of hCLEC-2 *in vivo*, particularly in response to anti-hCLEC-2 agents, a novel humanised CLEC-2 knockin (hCLEC-2^{KI}) mouse was generated using CRISPR/Cas9 technology (Biocytogen, Wakefield, MA, USA). The targeting strategy for the generation of

hCLEC-2^{KI} is shown in Figure 3.4. A single guide RNA was designed to remove the mouse *Clec1b* gene which was then replaced with the human gene. Mice were genotyped by PCR resulting in a PCR product of 247 bp for the WT and a 479 bp for the KI (hCLEC-2) allele.

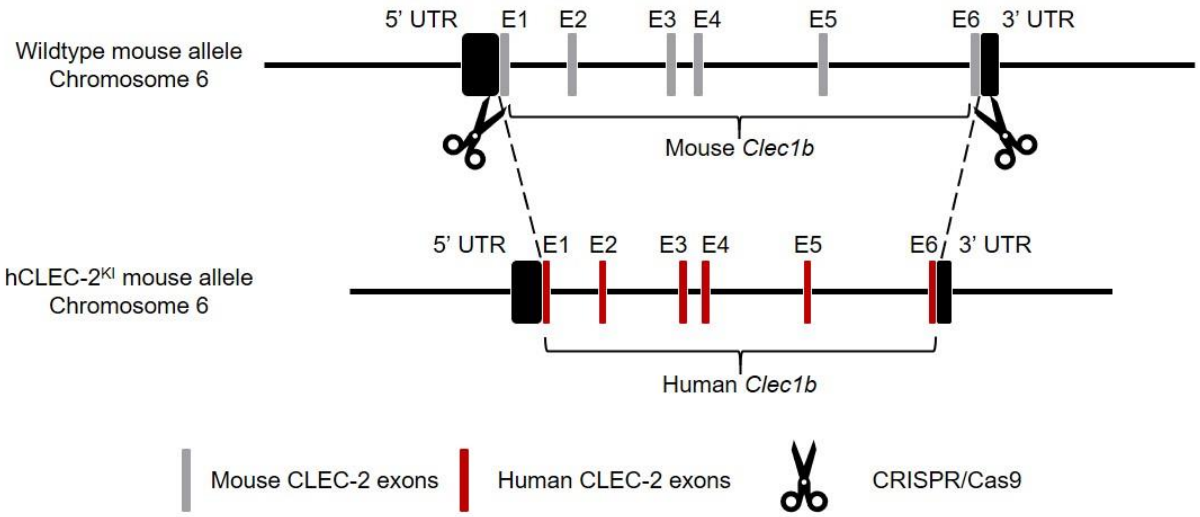

Figure 3.4 Targeting strategy for generation of hCLEC-2^{KI} mice.
CRISPR/Cas9 technology was used to replace the mouse *Clec1b* gene on chromosome 6 with the human gene. A single guide RNA was designed so that Cas9 cleaved the DNA between the 5' untranslated region (UTR) and exon (E) 1 and E6 and the 3' UTR to remove the mouse *Clec1b* gene. This was then replaced with E1 to E6 of the human *Clec1b* gene whilst the UTRs from the mouse DNA remained.

3.2.2 hCLEC-2^{KI} mice show no signs of developmental or lymphatic defects

Other mouse lines in which CLEC-2 has been knocked out or genetically modified have resulted in embryonic and neonatal lethality due to the role of CLEC-2 and its ligand podoplanin in the separation of blood and lymphatic vessels during development.[7,70] Therefore, we examined the ratio of pups born to ensure it was Mendelian as well as examining blood parameters and intestine morphology that could give an indication of a blood-lymphatic vessel separation defect.

We determined the Mendelian ratio of pups born to heterozygous parents at the time of weaning. Of the 206 pups 30.6% were wildtype, 44.7% were heterozygous and 24.8% were homozygous for hCLEC-2 (Table 3.1). Using a Chi-squared test we showed that this was not statistically different from the expected ratio (25, 50 and 25% respectively) and therefore the

pups were born at Mendelian ratio. Furthermore, there was no difference in platelet count such as can be observed in CLEC-2 conditional knockout mice (Figure 3.5),[5,72] or other blood parameters, such as haemoglobin levels, that would be decreased if blood were leaking into the lymphatic system (Table 3.2). There was also no difference in either blood pressure or heart rate in hCLEC-2^{KI} mice compared to WT littermate controls (Figure 3.6).

Table 3.1 Genotype analysis at weaning of pups born to heterozygous hCLEC-2^{KI} parents

	Expected	Observed
Wildtype	52	63
Heterozygous	102	92
hCLEC-2^{KI}	52	51
Total	206	206
Chi^2		1.58 (P = 0.45)

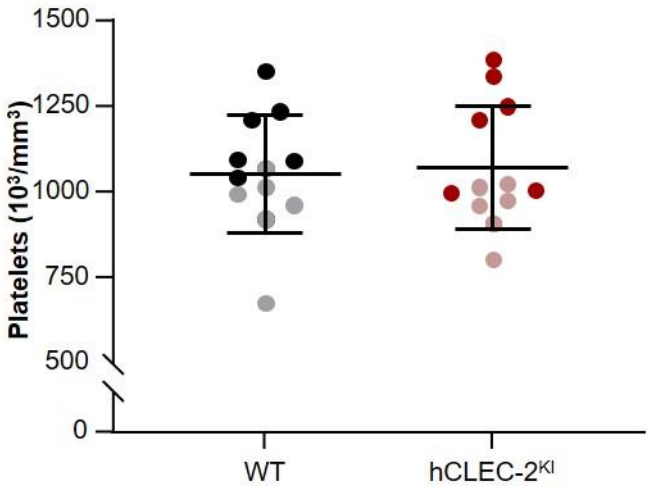

Figure 3.5 hCLEC-2^{KI} mice have comparable platelet counts to WT.
Platelet counts determined in whole blood by a ScilVet analyser showed no significant difference between WT and hCLEC-2^{KI} mice, unpaired t-test, P = 0.81. 6 female (light symbols) and 6 male (dark symbols) mice of each genotype were analysed. Data is shown as mean ± standard deviation.

Table 3.2 No differences in blood parameters were observed in hCLEC-2^{KI} mice compared to WT.

	WT	hCLEC-2^{KI}	Mann-Whitney
WBC 10^3/mm^3	4.45 (2.13)	4.25 (1.25)	P > 0.05
LYM 10^3/mm^3	3.50 (1.58)	3.55 (0.83)	P > 0.05
MON 10^3/mm^3	0.10 (0.08)	0.10 (0)	P > 0.05
GRA 10^3/mm^3	0.70 (0.28)	0.60 (0.35)	P > 0.05
EOS 10^3/mm^3	0.03 (0.02)	0.05 (0.01)	P > 0.05
RBC 10^6/mm^3	9.91 (0.66)	9.73 (0.48)	P > 0.05
MPV µm^3	5.55 (0.3)	5.65 (0.10)	P > 0.05
HGB g/dl	14.60 (0.95)	14.80 (0.75)	P > 0.05
HCT%	47.10 (3.23)	47.10 (2.10)	P > 0.05
MCV µm^3	48.00 (2.75)	48.50 (2.75)	P > 0.05
MCH pg	14.75 (0.75)	15.25 (0.82)	P > 0.05
MCHC g/dl	30.95 (0.57)	31.10 (0.75)	P > 0.05
RDW%	15.10 (0.65)	15.25 (1)	P > 0.05

Blood parameters were determined in whole blood by a ScilVet analyser. Data is show as median with the interquartile range in brackets, n = 12. WBC, white blood cell; LYM, lymphocyte; MON, monocyte; GRA, granulocyte; EOS, eosinophil; RBC, red blood cell; MPV, mean platelet volume; HGB, haemoglobin; HCT, haematocrit; MCV, mean corpuscular volume; MCH, mean corpuscular haemoglobin; MCHC, mean corpuscular haemoglobin concentration; RDW, red cell distribution width.

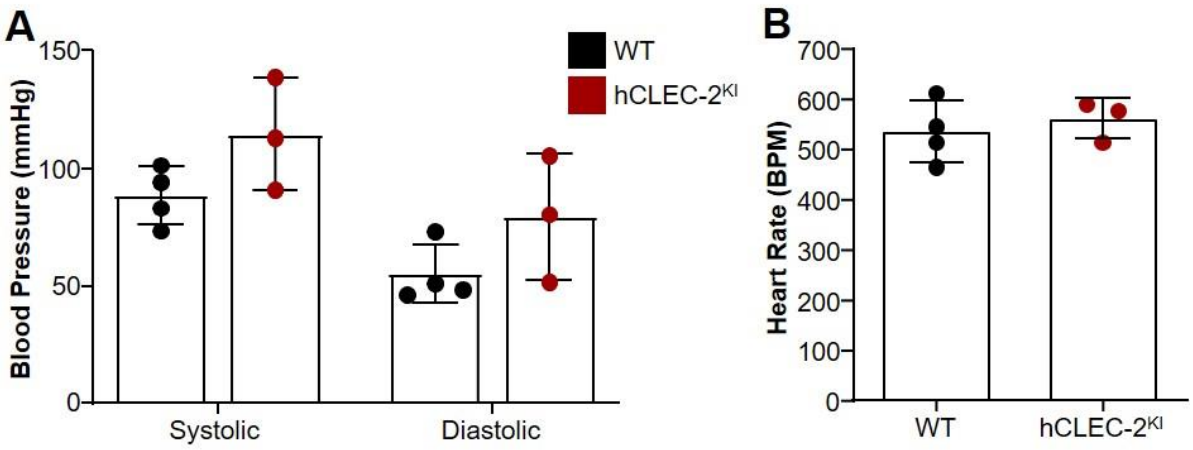

Figure 3.6 Blood pressure and heart rate are normal in hCLEC-2^{KI} mice.
Blood pressure and heart rate were measured using a tail cuff and Non-invasive Blood Pressure System in anaesthetised mice. (A) Blood pressure is not statistically different between WT and hCLEC-2^{KI} mice, two-way ANOVA, P = 0.92. (B) Heart rate is comparable between WT and hCLEC-2^{KI} mice, unpaired t-test, P = 0.55. Each symbol represents one animal with n = 4 WT and 3 hCLEC-2^{KI}. mmHg, millimetres of mercury; BPM, beats per minute.

The blood-lymphatic separation defect of CLEC-2 knockout or genetically modified mice can be clearly seen in the intestine due to the disorganised nature of the vasculature as well as blood being visible in lymphatic as well as blood vessels.[5,72-74] We therefore imaged the intestines of adult hCLEC-2^{KI} mice and compared them to WT and *Clec1b*$^{fl/flPF4Cre+}$ knockout mice (Figure 3.7). In addition, we stained sections of the intestine, as well as the lymph nodes, brains and livers, by H&E to compare organ morphology between WT and hCLEC-2^{KI} mice. Unlike in knockout mice, lymph nodes did not have a bloody appearance in hCLEC-2^{KI} mice (data not shown) and all organs appeared normal in comparison to WT controls (Figure 3.8A). Bone and spleen morphology were also comparable between hCLEC-2^{KI} and WT mice as were the megakaryocyte counts in both organs (Figure 3.8 B-C).

Figure 3.7 Vessels in the intestine had a normal appearance.
Intestines of WT, hCLEC-2^{KI} and *Clec1b*$^{fl/flPF4Cre+}$ were exposed and photographed, vessel appearance and visible blood were then compared. hCLEC-2^{KI} vessels had a similar appearance to those of WT mice and did not exhibit the disorganised appearance of those from *Clec1b*$^{fl/flPF4Cre+}$ mice. There was also no evidence of blood in the lymphatic vessels as indicated by the increase in blood visible in lymphatic vessels in intestines from *Clec1b*$^{fl/flPF4Cre+}$ mice. n = 3.

Figure 3.8 (below) Organ morphology and megakaryocyte counts are comparable between hCLEC-2^{KI} and WT mice.
Intestines, lymph nodes, brains, livers, spleens and femoral bones were removed, paraffin embedded and sectioned before staining with haematoxylin and eosin. (A) Haematoxylin and eosin staining of intestines, lymph nodes, brains and livers from WT and hCLEC-2^{KI} mice show no differences in morphology. (B) Megakaryocyte counts in haematoxylin and eosin stained bone sections were comparable between WT and hCLEC-2^{KI} mice, unpaired t-test P = 0.71. (C) Megakaryocyte counts in haematoxylin and eosin stained spleen sections were comparable between WT and hCLEC-2^{KI} mice, unpaired t-test P = 0.19. Megakaryocytes were

counted in 8 fields of view per mouse. Scale bars represent 100 µM. For each organ the right-hand images are a zoom-in of the area marked in the left-hand images. Yellow arrowheads indicate megakaryocytes. Images are representative of n = 3.

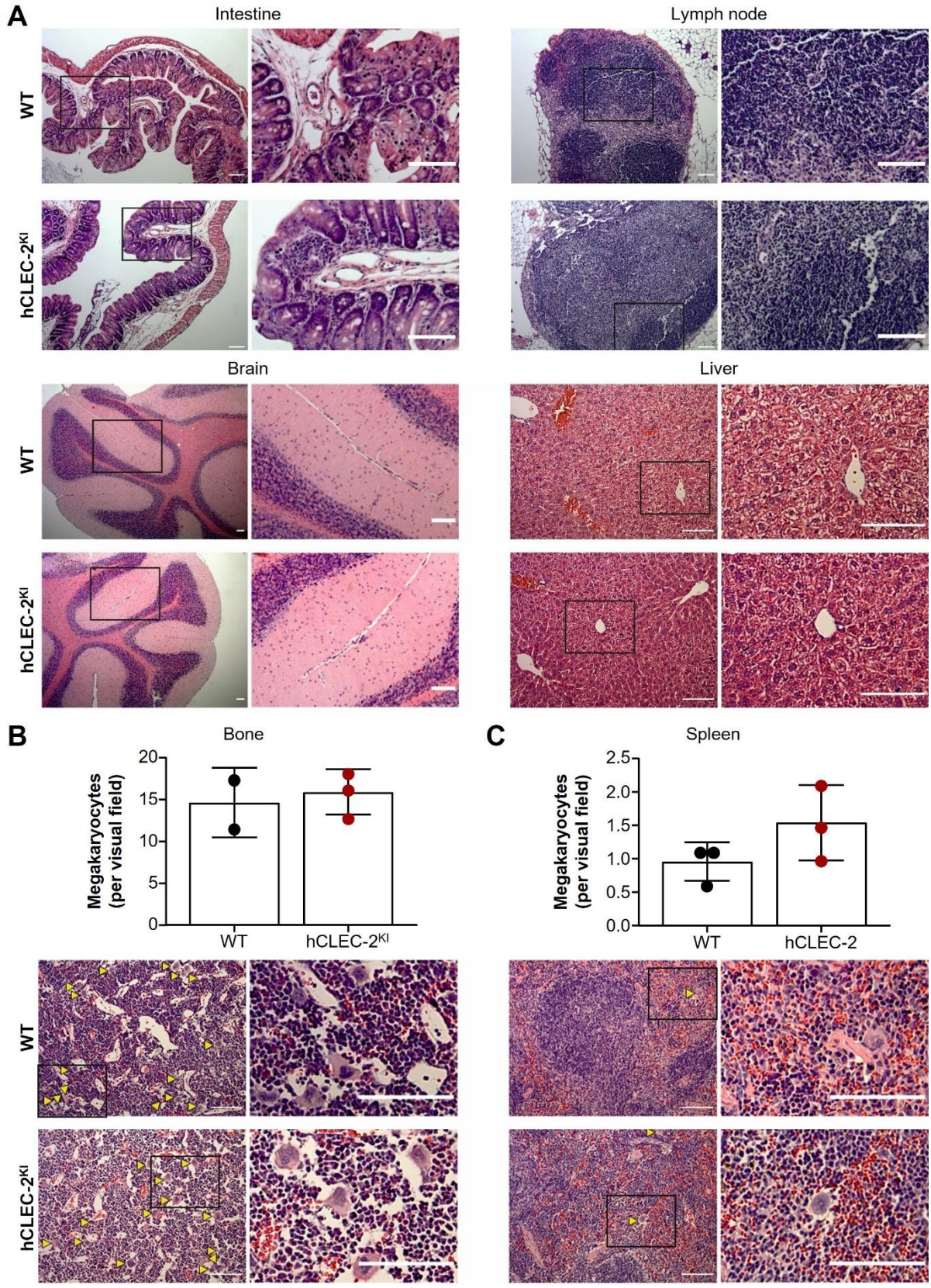

3.2.3 CLEC-2 expression

Surface expression of platelet CLEC-2 is reportedly up to 20-fold higher on murine compared to human platelets however, a smaller difference in expression has also been suggested between the two species.[16,47,49] We therefore compared CLEC-2 surface expression between WT, hCLEC-2^{KI} heterozygous, hCLEC-2^{KI} and human platelets (Figure 3.9A). As expected, WT mice did not express hCLEC-2 and hCLEC-2^{KI} mice did not express murine CLEC-2, whereas heterozygotes expressed both. hCLEC-2^{KI} platelets expressed almost 2 times more hCLEC-2 relative to human platelets based on relative mean fluorescent intensity of AYP1-FITC binding. When the difference in human and mouse platelet size is considered the difference in hCLEC-2 surface expression is 2.5-fold greater in hCLEC-2^{KI} mouse platelets compared to human. This is assuming mouse platelets having a surface area of 75% that of human platelets based on calculations by Jeremy Pike (2019).[185] We also compared the total expression of CLEC-2 on platelets by Western blotting of platelet lysates (Figure 3.9 B-C). As with surface expression, heterozygous mice expressed both human and murine CLEC-2 whereas hCLEC-2^{KI} and WT mice expressed either respectively. Human platelets also had higher total CLEC-2 compared to hCLEC-2^{KI} platelets. Furthermore, it appears that hCLEC-2 and humanised mouse CLEC-2 have a slight difference in their molecular weight (Figure 3.9C).

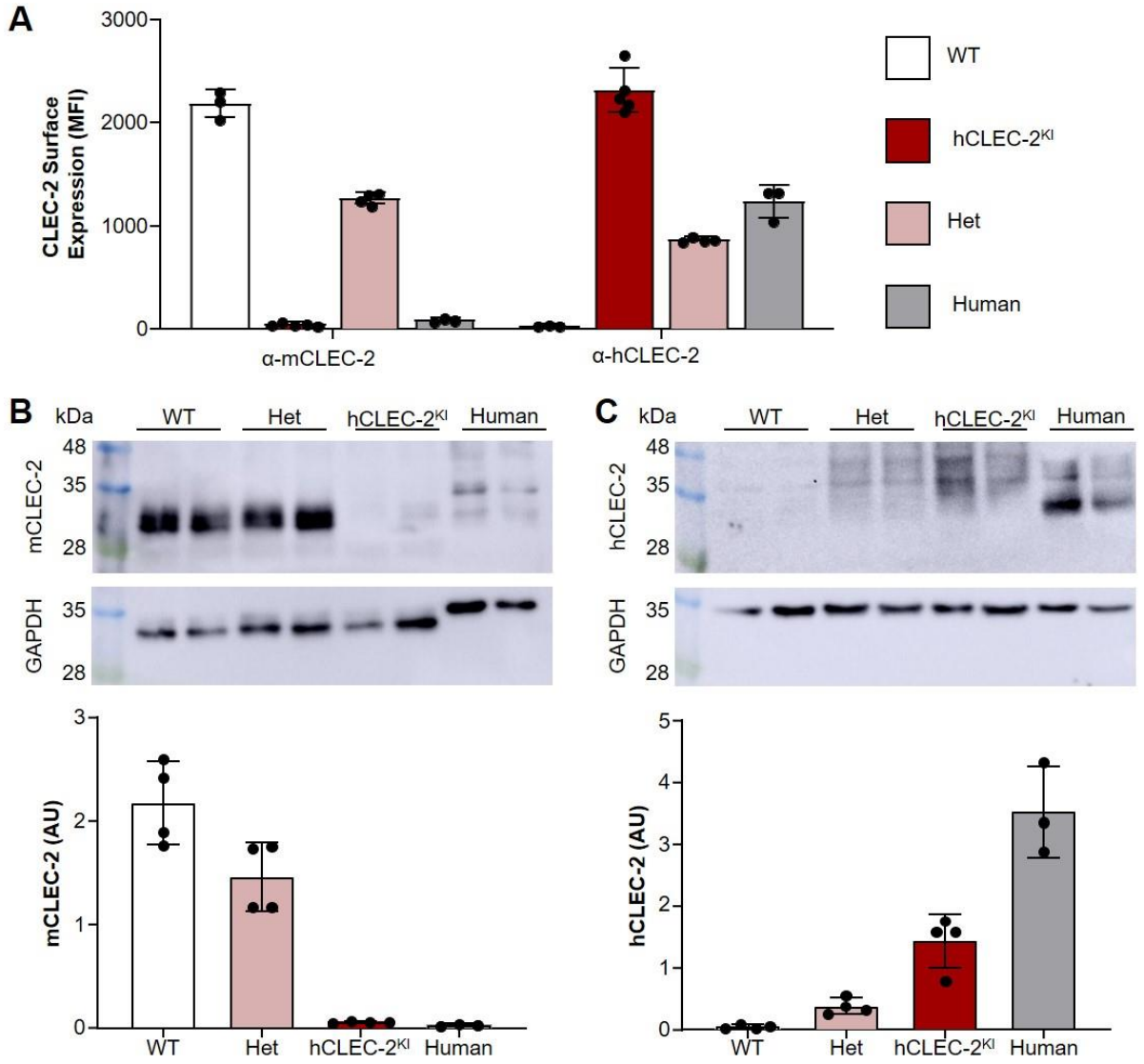

Figure 3.9 hCLEC-2^{KI} mice only express hCLEC-2 on their platelets.
CLEC-2 surface and total expression were determined by flow cytometry and Western blotting respectively and compared between WT, hCLEC-2^{KI} and hCLEC-2^{KI} heterozygous platelets and human platelets. (A) Platelet surface expression of mouse and human CLEC-2 was measured by flow cytometry in anti-coagulated blood using saturating concentrations of INU1 and AYP1-FITC conjugated antibodies respectively. (B) Expression of mCLEC-2 in platelet lysates was determined by Western Blot using 5 µg/ml INU2. Quantification shows that hCLEC-2^{KI} platelets do not express mCLEC-2. (C) Expression of hCLEC-2 in platelet lysates was determined by Western Blot using 1 µg/ml AYP2. Quantification showed that total CLEC-2 expression was higher in human than hCLEC-2^{KI} platelets. Blots are representative of 3 individual experiments.15 µl of platelet lysate (1 x 10^6 platelets/µl) and 5 µl Laemmli buffer were run per sample. Quantification was carried out using ImageJ and normalised to GAPDH. Each symbol represents one individual with n = 3-4 per group. MFI, mean fluorescence intensity; Het, heterozygous; GAPDH, Glyceraldehyde 3-phosphate dehydrogenase; AU, arbitrary units.

3.2.4 Platelet function is normal in hCLEC-2^{KI} mice

After confirming the expression of hCLEC-2 on hCLEC-2^{KI} platelets, we sought to determine if platelet function was normal in comparison to WT mice. We did this by investigating platelet receptor surface expression as well as platelet activation, aggregation and spreading responses to both agonists of CLEC-2 and other platelet activation receptors.

3.2.4.1 Platelet receptor surface expression and activation is normal in hCLEC-2^{KI} mice

Surface expression of platelet GPCR, integrin and ITAM receptors were analysed in hCLEC-2^{KI} platelets and compared to WT (Table 3.3). For all receptors tested surface expression was comparable between hCLEC-2^{KI} and WT platelets. We next investigated platelet activation in hCLEC-2^{KI} mice by measuring integrin activation and P-selectin exposure by flow cytometry (Figure 3.10). No differences were observed between hCLEC-2^{KI} and WT platelets for the GPCR agonists ADP, U46619 or thrombin or the GPVI agonist CRP in terms of either integrin activation (Figure 3.10A) or degranulation (Figure 3.10B). Furthermore, no difference was observed for the CLEC-2 agonist rhodocytin, whereas the anti-hCLEC-2 IgG AYP1 activated hCLEC-2^{KI} but not WT platelets. Together this suggests that platelet activation, including via CLEC-2, is normal in hCLEC-2^{KI} platelets. In addition, it shows that AYP1 is able to activate hCLEC-2^{KI} platelets and to a greater extent than INU1 with WT platelets.

Table 3.3 Normal surface expression of platelet receptors in hCLEC-2^{KI} mice

	WT	hCLEC-2^{KI}	Mann-Whitney
α-GPIbα	5608 (863)	5559 (288)	P > 0.05
α-GPVI	1702 (1453)	1959 (1901)	P > 0.05
α-GPV	4333 (232)	4165 (227)	P > 0.05
α-GPIbβ	7768 (764)	7922 (535)	P > 0.05
α-GPIX	8293 (385)	7997 (570)	P > 0.05
α-αIIbβ3	9341 (633)	9470 (740)	P > 0.05
α-β3	4647 (346)	4578 (878)	P > 0.05
α-α5	633 (104)	705 (92)	P > 0.05
α-α2	991 (118)	960 (129)	P > 0.05

Platelet surface receptor expression was measured by flow cytometry using FITC-conjugated antibodies against the receptors listed. Data is show as median with the interquartile range in brackets, n = 4. Data was analysed using a Mann-Whitney test and is representative of 3 independent experiments.

Figure 3.10 (below) Platelet activation is normal in hCLEC-2^{KI} mice.
Platelet activation in anti-coagulated whole blood was compared between WT and hCLEC-2^{KI} platelets by flow cytometry using the agonists and concentrations stated in the figure. Platelet activation was determined using saturating concentrations of JON/A-PE (integrin activation) and anti-P-selectin-FITC (degranulation). (A) Platelet integrin activation was compared between WT and hCLEC-2^{KI} mice with no differences observed aside from hCLEC-2 specific activation by AYP1. (B) Platelet granule secretion was unaltered in hCLEC-2^{KI} compared to WT mice following platelet activation whereas AYP1 caused hCLEC-2 specific granule secretion. Data were analysed by two-way ANOVA followed by a Sidak's multiple comparison test. ****, P < 0.001. Each symbol represents one individual and results are representative of three independent experiments. n = 4 for WT and 7 for hCLEC-2^{KI} mice. MFI, mean fluorescence intensity; Rest, resting; ADP, adenosine diphosphate; RC, rhodocytin; CRP, collagen-related peptide; PE, phycoerythrin; FITC, fluorescein isothiocyanate.

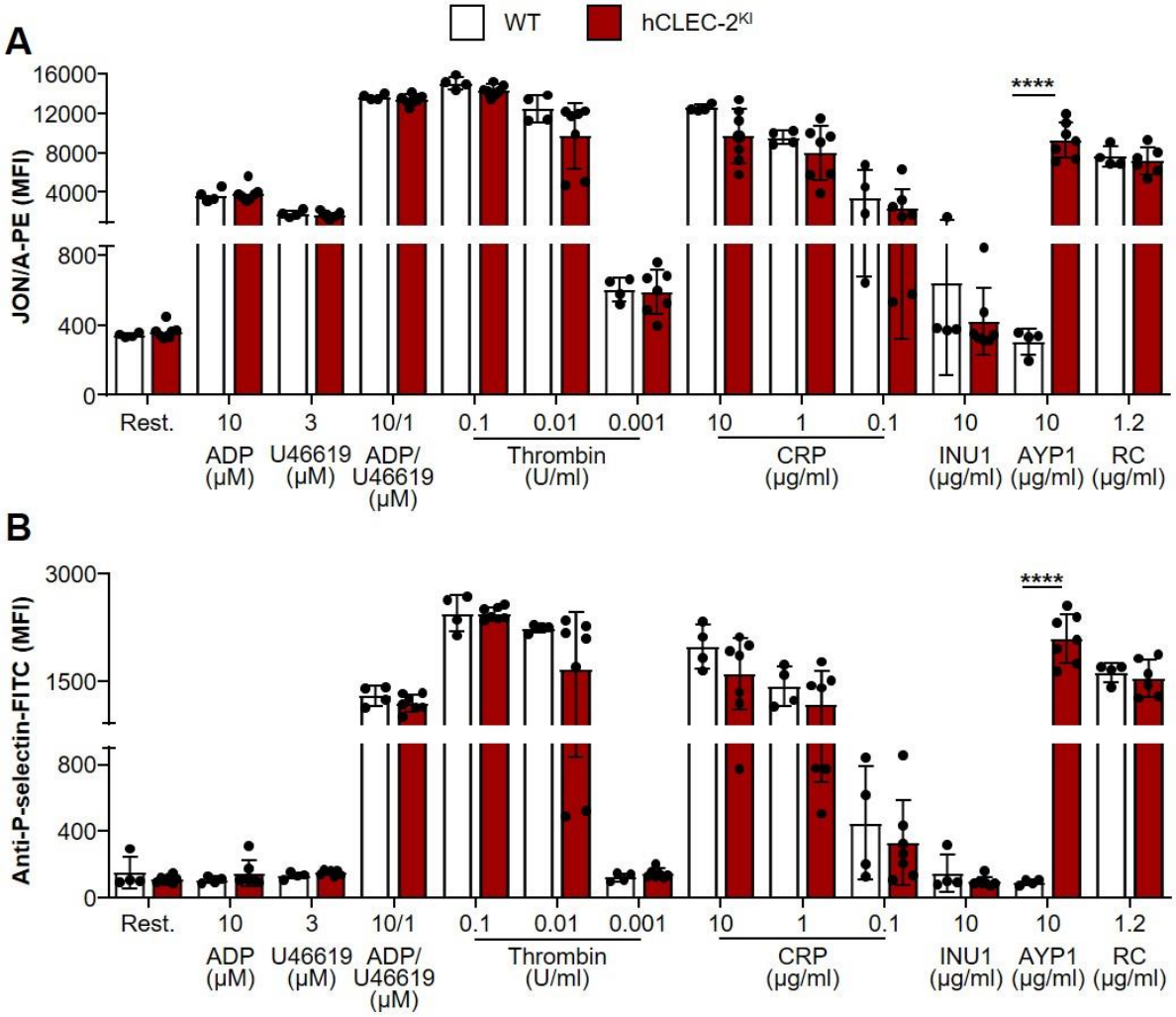

3.2.4.2 Platelet aggregation is normal in hCLEC-2KI mice

Platelet aggregation in response to GPCR, GPVI and CLEC-2 agonists was also investigated in washed platelets or PRP in the case of ADP. In agreement with the platelet activation results (Figure 3.10), no differences were observed for the GPCR agonists thrombin and ADP or the GPVI agonist collagen between hCLEC-2^{KI} and WT mice at any concentration tested (Figure 3.11 and data not shown). Aggregation in response to the CLEC-2 mAbs INU1 and AYP1 was also investigated. As expected, the anti-human antibody AYP1 caused aggregation of hCLEC-2^{KI} but not WT platelets and the anti-mouse antibody INU1 of WT but not hCLEC-2^{KI} platelets (Figure 3.12 A-B). Both antibodies induced a delayed aggregation response in hCLEC-2^{KI} heterozygous platelets in accordance with the lower level of either human or murine CLEC-2

expressed compared to hCLEC-2^{KI} or WT mice respectively (Figure 3.12 A-B). In addition, rhodocytin-induced aggregation was delayed in hCLEC-2^{KI} mice compared to WT. However, the lag phase was even more pronounced when human platelets were stimulated with rhodocytin, suggesting this is a species difference rather than a problem with CLEC-2 mediated aggregation in hCLEC-2^{KI} platelets (Figure 3.12C). Together this adds further evidence that platelet activation and function is normal in hCLEC-2^{KI} mice

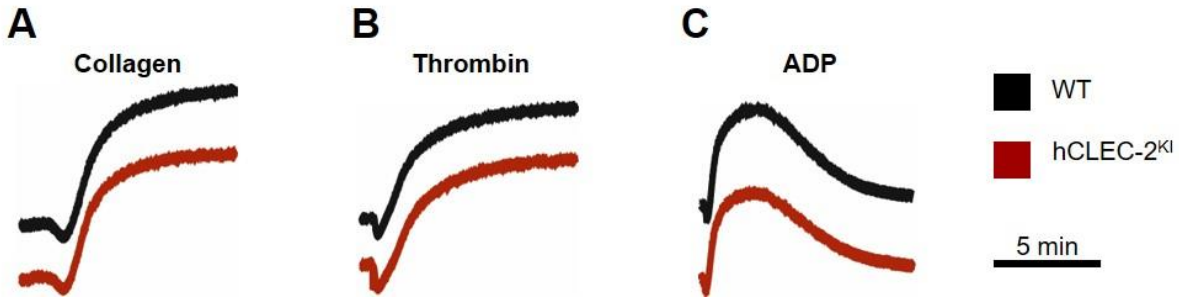

Figure 3.11 GPCR and GPVI induced platelet aggregation is normal in hCLEC-2^{KI} mice. Light transmission aggregometry was carried out under stirring conditions at 37°C with aggregation measured for 10 min. (A) Representative traces for aggregation induced by 5 µg/ml collagen in washed platelets. (B) Representative traces for aggregation induced by 0.01 U/ml thrombin in washed platelets. (C) Representative traces for aggregation induced by 5 µM ADP in PRP. Traces are representative of at least 3 mice.

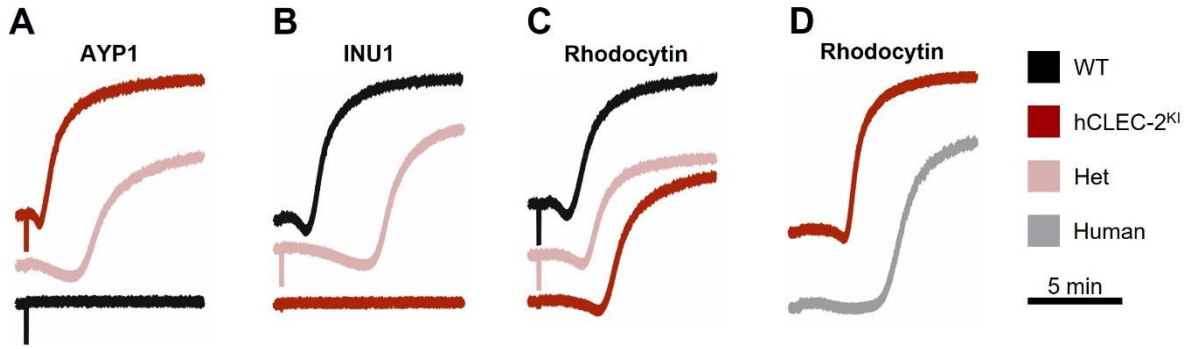

Figure 3.12 CLEC-2 induced platelet aggregation is normal in hCLEC-2^{KI} mice. Light transmission aggregometry was carried out in washed platelets under stirring conditions at 37°C with aggregation measured for 10 min. (A) Representative traces for aggregation induced by 10 µg/ml AYP1. (B) Representative traces for aggregation induced by 10 µg/ml INU1. (C) Representative traces for aggregation induced by 0.24 µg/ml rhodocytin. (D) Representative traces for aggregation induced by 0.24 µg/ml rhodocytin in human and hCLEC-2^{KI} platelets. Traces are representative of at least 3 mice or humans.

3.2.4.3 Platelet spreading of hCLEC-2^{KI} platelets

In order to further examine the function of hCLEC-2^{KI} platelets we investigated their ability to spread on fibrinogen, CRP and recombinant mouse podoplanin. On both fibrinogen and CRP spreading of hCLEC-2^{KI} platelets was comparable to WT with the majority of platelets being fully spread on fibrinogen and forming lamellipodia on CRP (Figure 3.13 A-B). However, on mouse podoplanin platelet spreading was reduced in hCLEC-2^{KI} mice, although no unspread platelets were observed (Figure 3.13 C). hCLEC-2^{KI} mice had a greater percentage of platelets forming filopodia and fewer forming both filopodia and lamellipodia or being fully spread compared to WT mice. We also tested spreading on recombinant human podoplanin, however, few platelets adhered and those that did were unspread (data not shown).

Figure 3.13 (below) Platelet spreading is unaltered on fibrinogen and CRP but reduced on mouse podoplanin in hCLEC-2^{KI} mice.
Washed platelets were incubated on glass coverslips coated with fibrinogen, CRP or mouse podoplanin at 37°C and the extent of platelet spreading was determined by differential interference contrast microscopy. (A) Thrombin (0.01 U/ml) stimulated platelet spreading after 30 min on 100 µg/ml human fibrinogen was comparable between hCLEC-2^{KI} and WT mice, P = 0.63. (B) Platelet spreading after 30 min on 10 µg/ml CRP was comparable between WT and hCLEC-2^{KI} mice, P = 0.99. (C) Platelet spreading after 60 min on 10 µg/ml recombinant mouse podoplanin-FC was reduced in hCLEC-2^{KI} mice compared to WT. The percentage of platelets with filopodia was greater in hCLEC-2^{KI} mice, (P = 0.0006) and fewer platelets formed both filopodia and lamellipodia (P = 0.0188). No unspread platelets were observed. Analysis was by two-way ANOVA with Sidak's multiple comparison test. Data represents 3 mice per genotype and is representative of at least 2 independent experiments. *** P < 0.001, * P < 0.05.

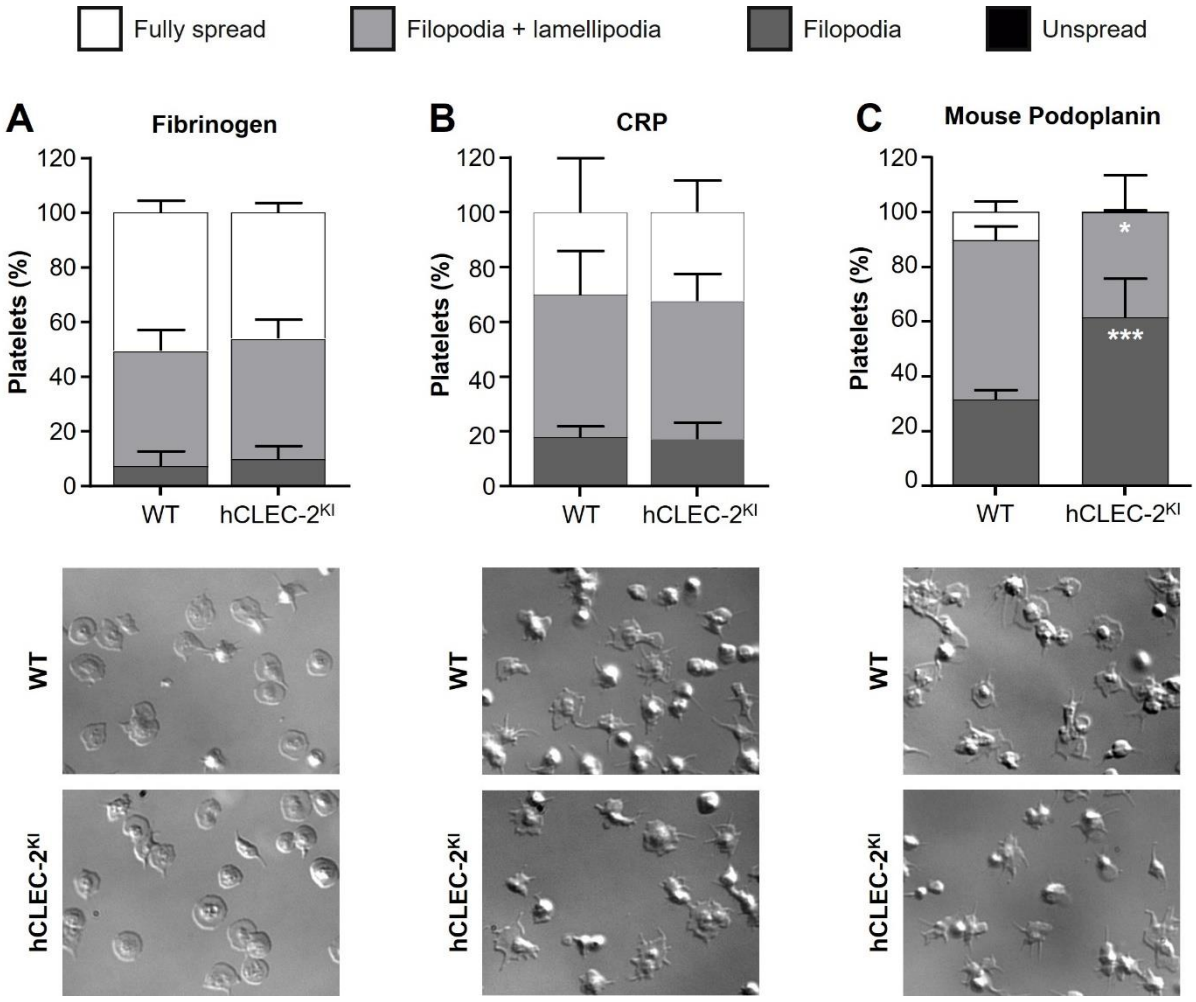

3.2.5 Arterial thrombus formation is altered *in vitro* in hCLEC-2^{KI} mice

3.2.5.1 Reduced thrombus surface coverage at 1000 s^{-1}

We observed that thrombus formation on collagen at a shear rate of 1000 s^{-1} was reduced in hCLEC-2^{KI} mice and therefore sought to compare this to the thrombus instability seen in CLEC-2 immunodepleted and *Clec1b*$^{fl/flPF4Cre+}$ knockout mice.[7,25] In hCLEC-2^{KI} mice, thrombus surface coverage was reduced compared to WT controls and a similar reduction was also observed in *Clec1b*$^{fl/flPF4Cre+}$ mice compared to Cre negative controls (Figure 3.14A). However, *Clec1b*$^{fl/flPF4Cre+}$ mice also had a decreased thrombus volume whereas hCLEC-2^{KI} mice did not (Figure 3.14B). Furthermore, thrombi from hCLEC-2^{KI} mice were stable in comparison to those from the *Clec1b*$^{fl/flPF4Cre+}$ knockout mice in which platelets and small aggregates detached

throughout the experiment. In fact, hCLEC-2^{KI} thrombi appeared to be denser and more contracted by eye compared to both WT and *Clec1b*$^{fl/flPF4Cre+}$ knockout mice (Figure 3.14C).

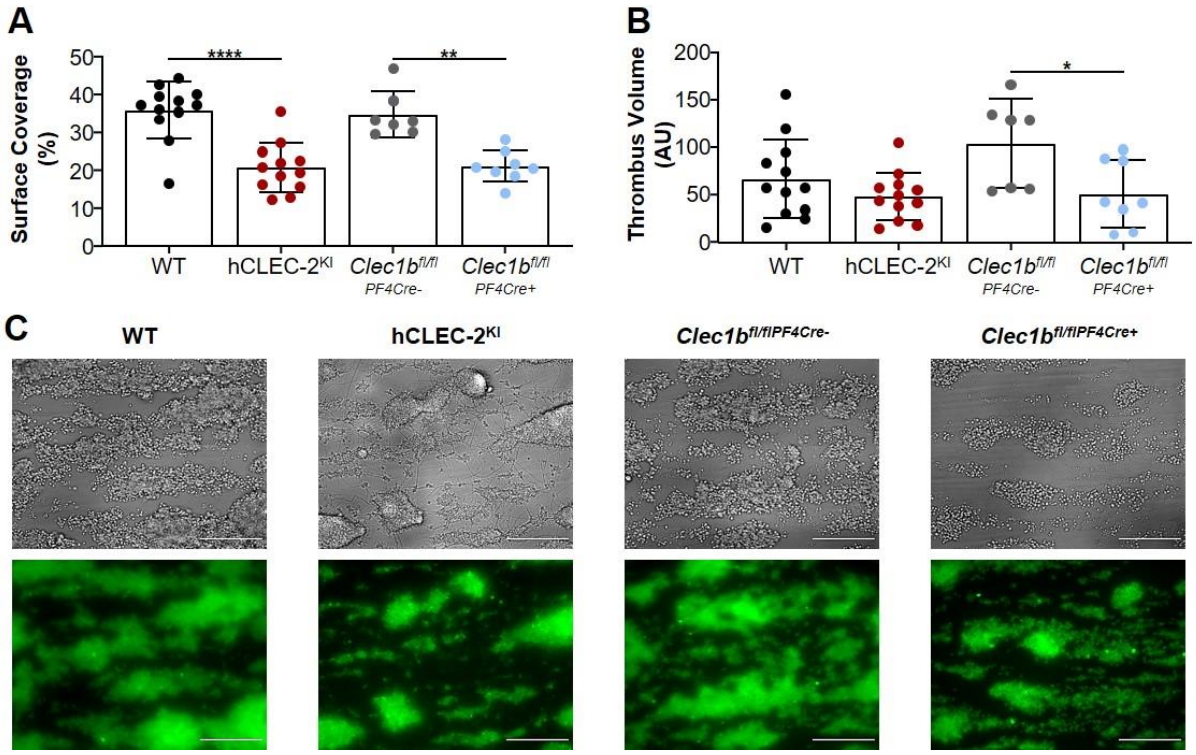

Figure 3.14 hCLEC-2^{KI} thrombi have a reduced surface coverage but not thrombus stability on collagen at 1000 s^{-1}.
Anti-coagulated whole blood was perfused over collagen for 4 min followed by 4 min washing with Tyrode's buffer at a shear rate of 1000 s^{-1} and thrombus surface coverage and thrombus volume (integrated density) were determined. (A) Percent thrombus surface coverage is reduced in both hCLEC-2^{KI} ($P < 0.0001$) and *Clec1b*$^{fl/flPF4Cre+}$ ($P = 0.0011$) mice compared to their respective controls. (B) Thrombus volume is reduced in *Clec1b*$^{fl/flPF4Cre+}$ ($P = 0.043$) but not hCLEC-2^{KI} mice ($P = 0.61$) compared to their respective controls. (C) Representative brightfield and fluorescent images from WT, hCLEC-2^{KI}, *Clec1b*$^{fl/flPF4Cre-}$ and *Clec1b*$^{fl/flPF4Cre+}$ mice. Data were analysed by one-way ANOVA and Tukey's test for multiple comparisons. Each symbol represents one mouse, n = 7-12 mice. **** $P < 0.0001$, ** $P < 0.01$, * $P < 0.05$. Scale bars represent 50 µm.

3.2.5.2 The effect on thrombus formation in hCLEC-2^{KI} mice is dependent on shear rate

As thrombus surface coverage was reduced on collagen at a shear rate of 1000 s^{-1}, we investigated if this also occurred at higher arterial shear rates. At an intermediate shear rate of 1200 s^{-1} both surface coverage and thrombus volume were comparable between WT and hCLEC-2^{KI} mice (Figure 3.15 A-C). However, hCLEC-2^{KI} thrombi still had a denser, more contracted appearance that was similar, if less pronounced, to that seen at 1000 s^{-1} (Figure

3.14C and Figure 3.15C). At a higher shear rate of 1700 s^{-1} both surface coverage and thrombus volume were increased in hCLEC-2^{KI} mice (Figure 3.15 D-F). These results, together with those at 1000 s^{-1}, suggest that there are shear dependent differences in thrombus formation between hCLEC-2^{KI} and WT mice.

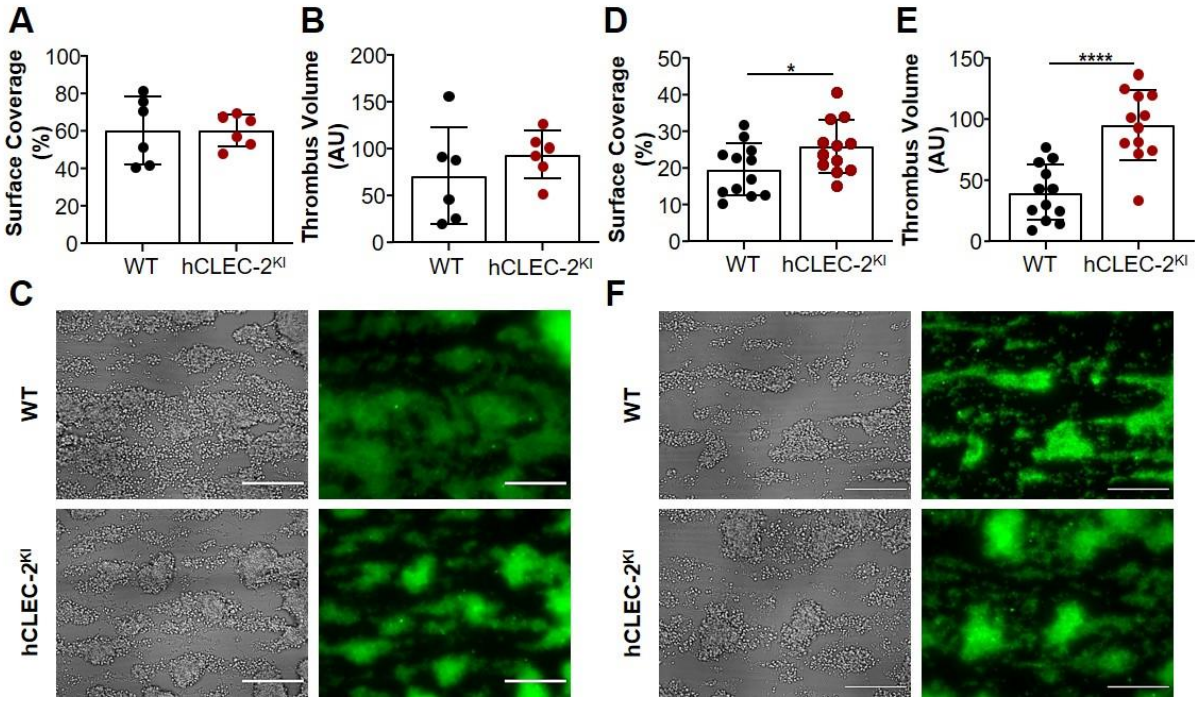

Figure 3.15 Arterial shear rates have different effects on thrombus formation on collagen in hCLEC-2^{KI} and WT mice.
Anti-coagulated whole blood was perfused over collagen for 4 min followed by 4 min washing with Tyrode's buffer at shear rates of either 1200 s^{-1} or 1700 s^{-1} and thrombus surface coverage and thrombus volume (integrated density) were determined. (A) Thrombus surface coverage at 1200 s^{-1} in WT and hCLEC-2^{KI} mice, P = 0.99. (B) Thrombus volume at 1200 s^{-1} in hCLEC-2^{KI} and WT mice, P = 0.37. (C) Representative brightfield and fluorescent images of thrombi from WT and hCLEC-2^{KI} mice formed of collagen at a shear rate of 1200 s^{-1}. n = 6. (D) Thrombus surface coverage at 1700 s^{-1} in hCLEC-2^{KI} mice compared to WT, P = 0.044. (E) Thrombus volume at 1700 s^{-1} in hCLEC-2^{KI} mice compared to WT, P < 0.0001. (F) Representative brightfield and fluorescent images of thrombi from WT and hCLEC-2^{KI} mice formed of collagen at a shear rate of 1700 s^{-1}. n = 12. Data were analysed using unpaired t-tests, **** P < 0.0001, * P < 0.05. Each symbol represents one mouse. Scale bars represent 50 µm.

3.2.5.3 Thrombus formation appears to be unaltered at venous shear in hCLEC-2^{KI} mice

We next investigated whether the differences in thrombus formation observed in hCLEC-2^{KI} mice at arterial shear rates on collagen also occurred at a venous shear rate of 150 s^{-1}. Preliminary results showed no difference in either surface coverage or thrombus volume

between hCLEC-2^{KI} and WT mice (Figure 3.16 A-C). Furthermore, the differences in thrombus appearance observed at arterial shear rates were not seen to the same extent (Figure 3.16C). These results suggest that differences in thrombus formation in hCLEC-2^{KI} mice may be confined to arterial shear rates, although further experiments will be needed to confirm this.

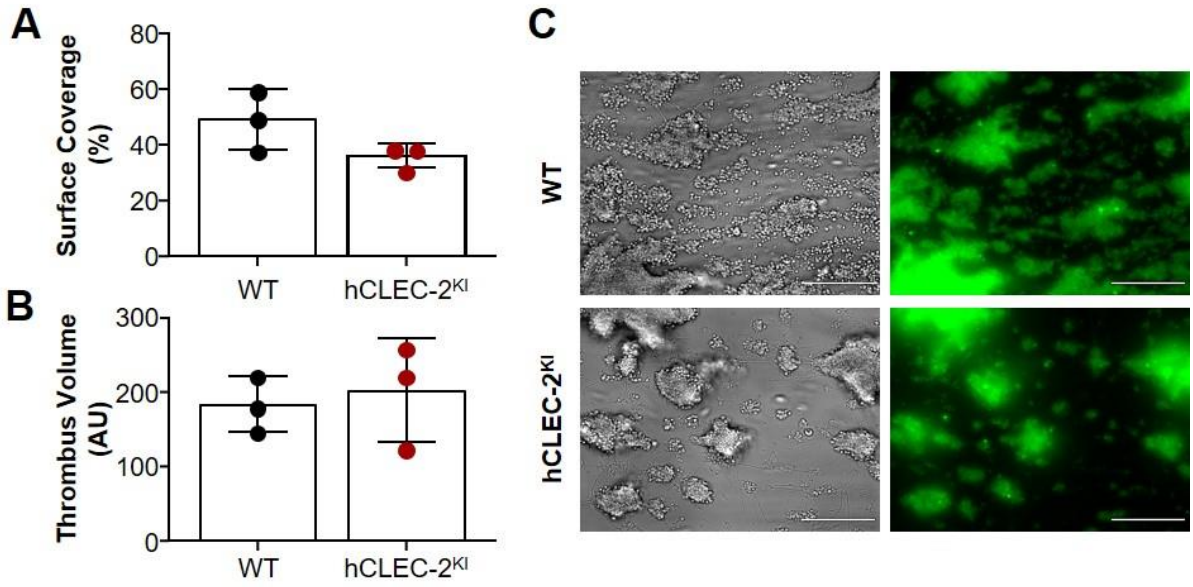

Figure 3.16 hCLEC-2^{KI} thrombus formation is unaltered at venous shear.
Anti-coagulated whole blood from WT or hCLEC-2^{KI} mice was perfused over collagen at a shear rate of 150 s^{-1} for 4 min followed by washing with Tyrode's buffer for a further 4 min and thrombus surface coverage and volume (integrated density) were measured. (A) Thrombus surface coverage at 150 s^{-1} in WT and hCLEC-2^{KI} mice, P = 0.12. (B) Thrombus volume at 150 s^{-1} is in hCLEC-2^{KI} and WT mice, P = 0.70. (C) Representative brightfield and fluorescent images of thrombi from WT and hCLEC-2^{KI} mice formed of collagen at a shear rate of 150 s^{-1}. Data were analysed using unpaired t-tests. Each symbol represents one mouse, n =3. Scale bars represent 50 µm.

3.2.5.4 GPIb binding to vWF is unaltered in hCLEC-2^{KI} mice

GPIb binding to vWF is responsible for initial platelet attachment to the ECM during thrombus formation at high shear rates.[19] Therefore, as hCLEC-2^{KI} mice exhibited greater thrombus formation at higher shear rates compared to WT mice, we sought to investigate if this was due to a difference in platelet binding to vWF. Under flow conditions there was no difference in platelet adhesion to vWF between WT and hCLEC-2^{KI} mice (Figure 3.17), suggesting that GPIb

binding to vWF does not account for the difference in thrombus formation on collagen observed at arterial flow rates in hCLEC-2^{KI} mice.

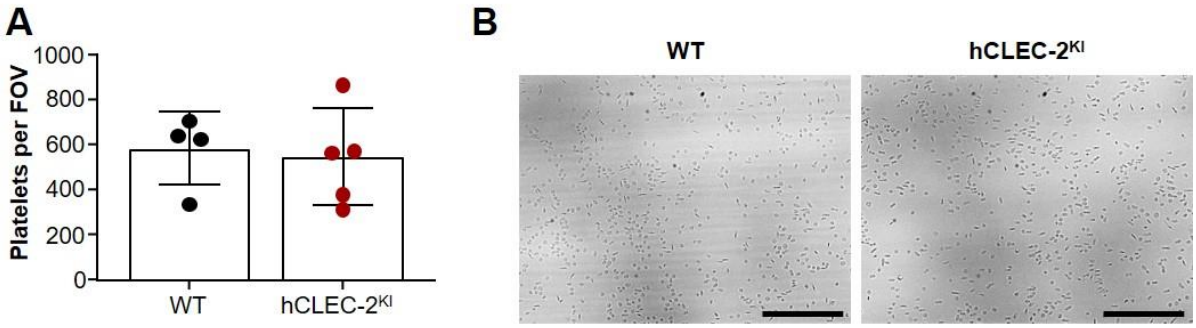

Figure 3.17 Platelet adhesion to vWF under flow at 1700 s^{-1} is normal in hCLEC-2^{KI} mice.
vWF from WT mouse plasma was allowed to adhere to rabbit-anti-human vWF antibody coated slides prior to perfusion of anti-coagulated mouse blood at 1700 s^{-1} for 10 min. The number of adherent platelets was then determined (A) No difference in the number of adherent platelets was observed between WT and hCLEC-2^{KI} mice, unpaired t-test P = 0.79. (B) Representative brightfield images of platelets adhering to vWF in WT and hCLEC-2^{KI} mice. Scale bars represent 50 µm and each symbol represent one mouse, n = 4-5. FOV, field of view.

3.3 Generation and characterisation of the novel anti-hCLEC-2 antibody HEL1

3.3.1 Generation

To further characterise the hCLEC-2^{KI} mice as a model in which hCLEC-2 specific therapeutics could be tested, we generated an anti-hCLEC-2 mAb that could be used in addition to the existing antibody AYP1. To do this we used AYP1 to immunoprecipitate hCLEC-2 from human platelet lysates using protein G Sepharose beads. These were then used to immunise Wistar rats. Splenoctyes were isolated from the rats and fused with Ag14 myeloma cells and resulting hybridomas were screened for anti-hCLEC-2 antibody production. During the initial screening hybridomas from each rat were found to secrete antibodies binding to platelets however, following subcloning only subclones from two antibodies bound to platelets. Of these, one was found to bind to a surface receptor other than CLEC-2 (data not shown) and the other, clone 22H12, bound to hCLEC-2 and was further characterised. 22H12 had three positive subclones, two polyclonal and one monoclonal, with similar binding to hCLEC-2 in flow cytometry,

therefore, the monoclonal subclone was purified and further characterised. This new anti-hCLEC-2 monoclonal antibody was named HEL1.

3.3.2 Characterisation

3.3.2.1 HEL1 is specific to hCLEC-2

The specificity of HEL1 to hCLEC-2 was determined by Western Blot, immuno-precipitation and flow cytometry (Figure 3.18). HEL1 was able to detect a protein between 32 and 40 kDa in hCLEC-2^{KI} platelets and a doublet of 30 and 40 kDa in human platelets (Figure 3.18A). This is consistent with the known molecular weight of CLEC-2 with multiple bands observed due to differential glycosylation.[38,40] It is also consistent with our previous results suggesting that hCLEC-2^{KI} mouse and human CLEC-2 have different apparent molecular weights (Figure 3.9). HEL1 can also immuno-precipitate hCLEC-2 as detected using AYP1 by Western Blotting (Figure 3.18B). Furthermore, HEL1 could be detected on the surface of hCLEC-2^{KI} but not WT platelets by anti-rat IgG-FITC binding in flow cytometry (Figure 3.18C). In addition, using clone supernatant HEL1 could be shown to bind to human platelets and not to *Clec1b*$^{fl/flPF4Cre+}$ knockout platelets (data not shown). Overall, these results show that HEL1 binds specifically to hCLEC-2 and not to mCLEC-2.

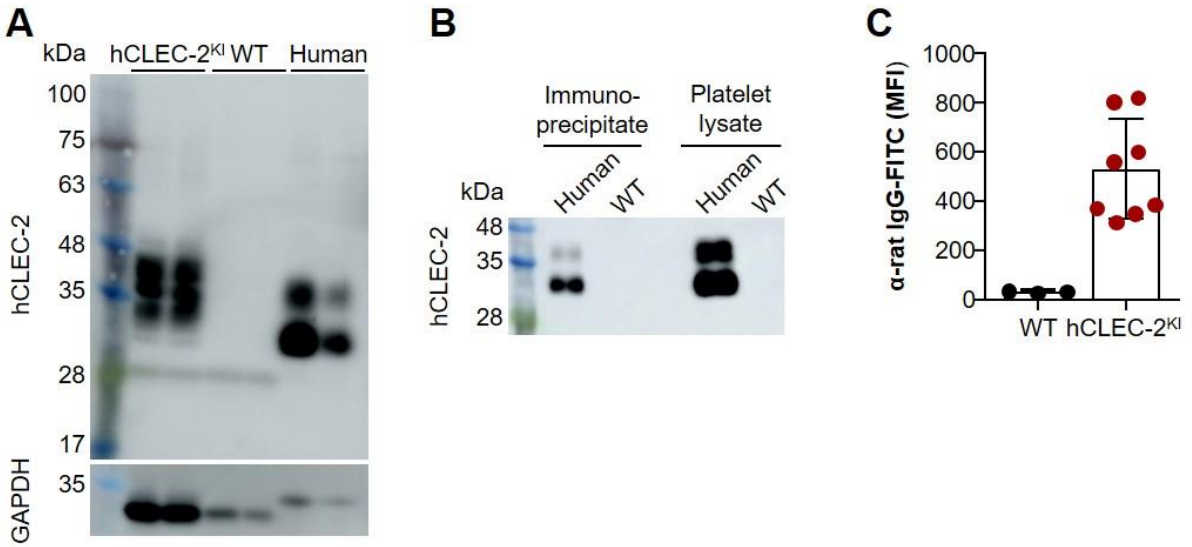

Figure 3.18 HEL1 is specific to hCLEC-2.

The specificity of HEL1 to hCLEC-2 was determined by using the antibody in Western blotting, immuno-precipitation and flow cytometry. (A) 5 µg/ml HEL1 specifically detects hCLEC-2 in hCLEC-2^{KI} mouse and human platelet lysates by Western Blotting but not in WT platelets under non-reducing conditions. n = 2. (B) 5 µg HEL1 can immuno-precipitate hCLEC-2 from human platelet lysates. AYP1 (1 µg/ml) was used to detect immuno-precipitated hCLEC-2 by Western Blot. Experiment performed by Jana Kaczmarzyk. Blot is representative of two independent experiments. (C) HEL1 binds to hCLEC-2^{KI} but not WT platelets as determined by anti-rat IgG-FITC binding to platelets incubated with 10 µg/ml HEL1 by flow cytometry. Each symbol represents one mouse, n = 3 for WT and 8 for hCLEC-2^{KI}. GAPDH, Glyceraldehyde 3-phosphate dehydrogenase; kDa, kilodaltons; MFI, mean fluorescence intensity; FITC, fluorescein isothiocyanate.

3.3.2.2 HEL1 binds to a different epitope on hCLEC-2 to AYP1

To investigate whether HEL1 and AYP1 bind to the same epitope on hCLEC-2 competitive binding experiment were performed using FITC- and un-conjugated antibodies. Detection of hCLEC-2 using AYP1-FITC following AYP1, but not HEL1, pre-incubation was reduced and detection by HEL1-FITC was reduced following HEL1, but not AYP1, pre-incubation (Figure 3.19A). This suggests that HEL1 and AYP1 bind to different sites on hCLEC-2 as both antibodies are able to bind at the same time without a reduction in MFI. We next sought to determine whether HEL1 would also activate platelets, despite not binding to the same site as AYP1 which acts at the rhodocytin and podoplanin binding site of hCLEC-2.[40,57] HEL1 IgG induced aggregation of hCLEC-2^{KI} platelets at all concentrations tested, however, lower concentrations had a longer lag period than higher concentrations (Figure 3.19B and data not shown). We next investigated whether HEL1-Fab fragments could block hCLEC-2^{KI} platelet aggregation induced by CLEC-2 agonists. Rhodocytin and AYP1 IgG induced aggregation was unaffected by HEL1-Fab pre-incubation, whereas HEL1 IgG induced aggregation was blocked (Figure 3.19B). These results suggest that HEL1 and AYP1 bind to different sites on hCLEC-2 and that CLEC-2 dimerisation by IgG antibodies is sufficient for platelet activation, independent of binding to the active site.

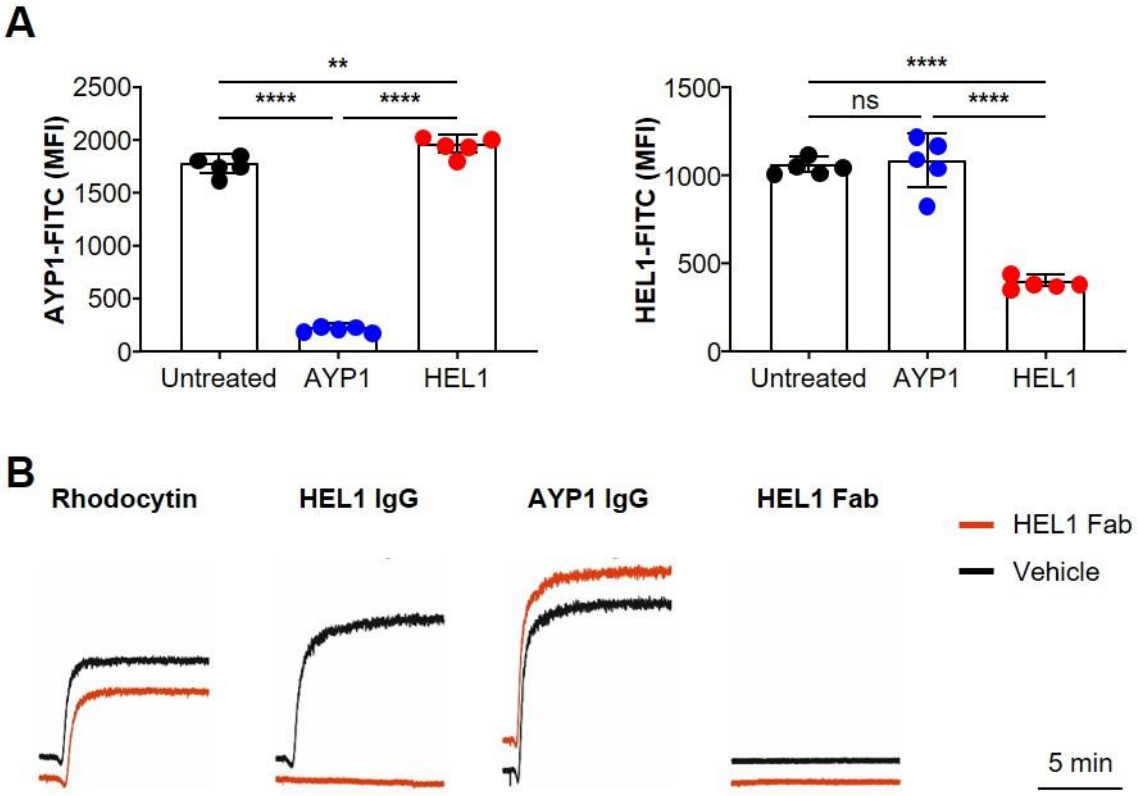

Figure 3.19 HEL1 binds to a different epitope on hCLEC-2 to AYP1 but still activates hCLEC-2^{KI} platelets.
Binding of HEL1 and AYP1 to hCLEC-2^{KI} platelets was determined by flow cytometry using a competitive binding assay and the effect of their different binding sites was assessed by light transmission aggregometry in washed platelets. (A) Binding of HEL1 and AYP1 (10 µg/ml) to hCLEC-2^{KI} platelets was detected using either the same or the opposite FITC-conjugated antibody. AYP1-FITC binding was only blocked following pre-incubation with AYP1 and HEL1-FITC binding with HEL1. Pre-incubating with one anti-hCLEC-2 antibody and detecting with the other had no effect. Data were analysed by one-way ANOVA followed by Tukey's multiple comparisons test. (B) Light transmission aggregometry under stirring conditions at 37°C was measured over 10 min. hCLEC-2^{KI} washed platelets were pre-incubated with HEL-1 Fab (10 µg/ml) and activated with rhodocytin (0.24 µg/ml), AYP1 IgG (10 µg/ml) or HEL1 IgG (10 µg/ml). HEL1 Fab (10 µg/ml) itself does not induce platelet aggregation. Experiments were performed by David Stegner. ****, $P < 0.001$ **, $P < 0.01$. Each symbol represents one mouse. MFI, mean fluorescence intensity; FITC, fluorescein isothiocyanate.

3.4 Regulation of hCLEC-2

Mouse CLEC-2 can be immunodepleted using the antibody INU1, however, it is unknown whether the same is true for hCLEC-2.[25] As immunodepletion cannot be achieved *in vitro* hCLEC-2^{KI} mice are the first model in which depletion of hCLEC-2 can be tested.[81] We therefore, sought to investigate the effect of *in vivo* administration of either AYP1 or HEL1 on

hCLEC-2 expression and the effect of immunodepletion on haemostasis and thrombosis using *in vivo* models.

3.4.1 Intravenous administration of AYP1 is lethal in hCLEC-2^{KI} mice

We began by testing AYP1 by intravenous (i.v.) injection of 10 µg of IgG antibody. In hCLEC-2^{KI} and heterozygous mice this resulted in laboured breathing and the death of two out of the four hCLEC-2^{KI} mice within 20 min of injection. A third hCLEC-2^{KI} mouse died following anaesthesia and bleeding for the 30 min time point. By this time the breathing of most hCLEC-2^{KI} heterozygous mice had returned to normal. Platelet count and CLEC-2 surface expression were determined by flow cytometry for the surviving mice and lungs, spleens, livers and brains were removed from the mice that died as well as untreated hCLEC-2^{KI} mice and WT mice treated with either INU1 or AYP1.

3.4.1.1 AYP1 can deplete hCLEC-2 in hCLEC-2^{KI} heterozygotes

AYP1 could be detected on the surface of platelets either pre-incubated with the antibody *in vitro* or following i.v. administration from hCLEC-2^{KI} and heterozygous mice, but not WT, for up to 24 h (Figure 3.20A). AYP1 administration lead to transient thrombocytopenia lasting up to 4 days in hCLEC-2^{KI} heterozygotes and surviving hCLEC-2^{KI} mice, consistent with INU1 administration in WT mice (Figure 3.20B).[25] Furthermore, AYP1 could deplete hCLEC-2 for up to 7 days, with little effect on mCLEC-2 in hCLEC-2 heterozygous mice (Figure 3.20 C-D). Together this suggests that AYP1, like INU1, can deplete CLEC-2 by binding to the receptor on platelets. However, at least with intravenous administration, lethality is observed in hCLEC-2^{KI} mice, likely due to the action of the antibody on hCLEC-2 as no adverse effects were observed in AYP1 treated WT mice. We hypothesise this was due to AYP1-induced platelet activation leading to microthrombus formation which then became trapped in the lungs. This would account for the laboured breathing observed in hCLEC-2^{KI} and heterozygous mice.

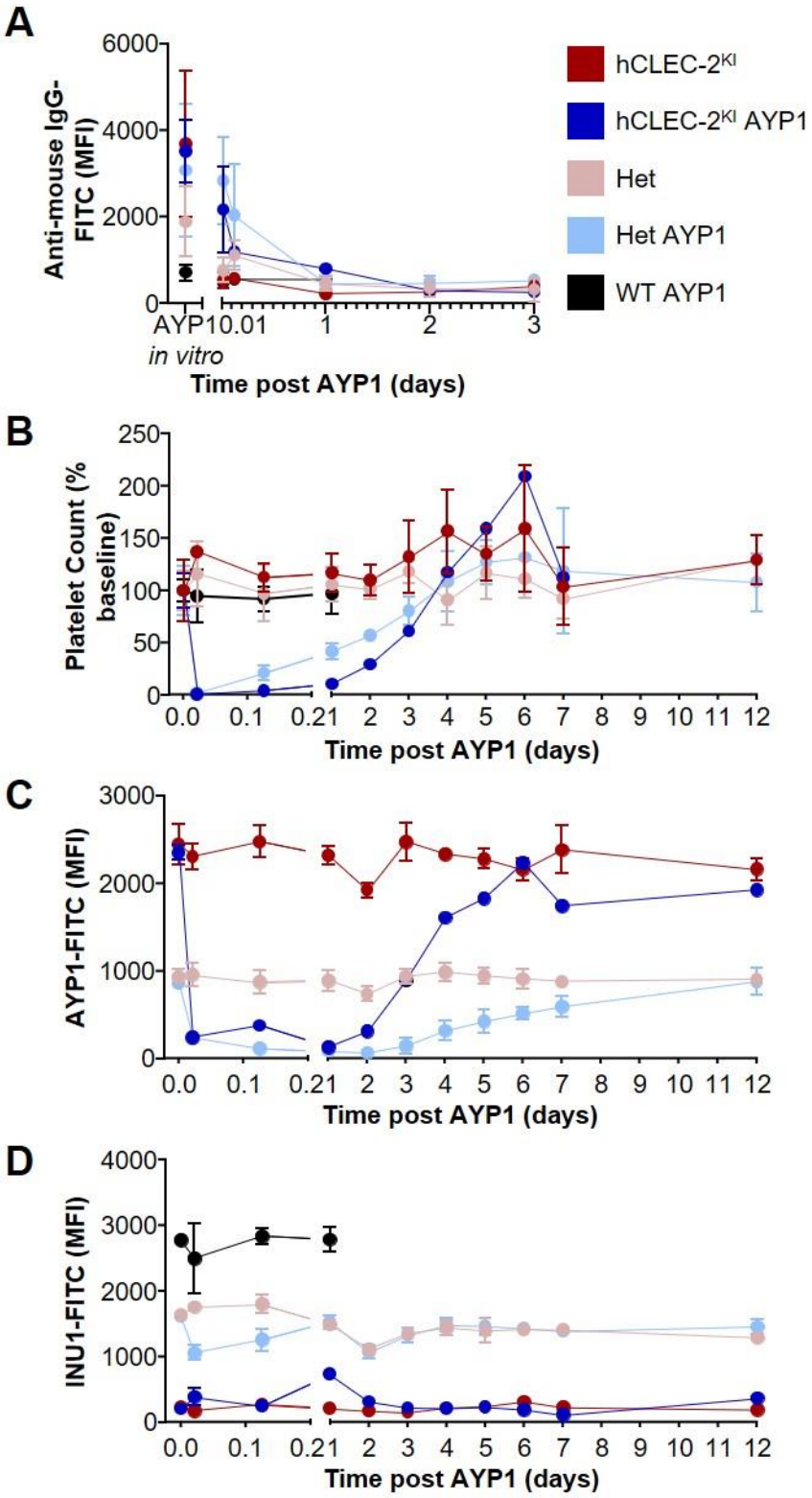

Figure 3.20 Intravenous administration of 10 µg AYP1 is lethal in hCLEC-2^{KI} mice but can deplete hCLEC-2 in heterozygotes.
AYP1 IgG (10 µg) was administered intravenously and the effect on platelet count and CLEC-2 surface expression were determined by flow cytometry at the indicated time points. (A) AYP1 could be detected on the platelet surface using an anti-mouse IgG antibody after both *in vitro*

incubation (10 µg/ml) and up to 24 h after i.v. administration of 10 µg in surviving hCLEC-2^{KI} and hCLEC-2^{KI} heterozygous mice but not WT. (B) Platelet count was determined using saturating concentrations of p0p6-FITC and JON6-PE conjugated antibodies. AYP1 administration leads to transient thrombocytopenia in hCLEC-2^{KI} and heterozygous mice but not WT. Platelet count is shown as the percentage of the pre-AYP1 counts. (C) Surface expression of hCLEC-2 was determined using AYP1-FITC. (D) Surface expression of mouse CLEC-2 was determined using INU1-FITC. Each data point is representative of 4 mice aside from the hCLEC-2^{KI} AYP1 group where n = 2 at 30 min and 1 thereafter due to the lethal effect of the antibody. MFI, mean fluorescence intensity; FITC, fluorescein isothiocyanate; Het, heterozygous.

3.4.1.2 Intravenous AYP1 administration causes microthrombi to become trapped in the lungs in hCLEC-2^{KI} mice

To investigate whether AYP1-induced platelet activation leading to the formation of microthrombi accounted for the lethality seen in AYP1 treated hCLEC-2^{KI} mice we first stained lung sections with H&E (Figure 3.21). This showed that oedema was present in the lungs of AYP1 treated hCLEC-2^{KI} but not in untreated mice. Furthermore, this was not observed in the lungs of either INU1 or AYP1 treated WT mice, further suggesting that the adverse effects of intravenous AYP1 are specific to its action on hCLEC-2.

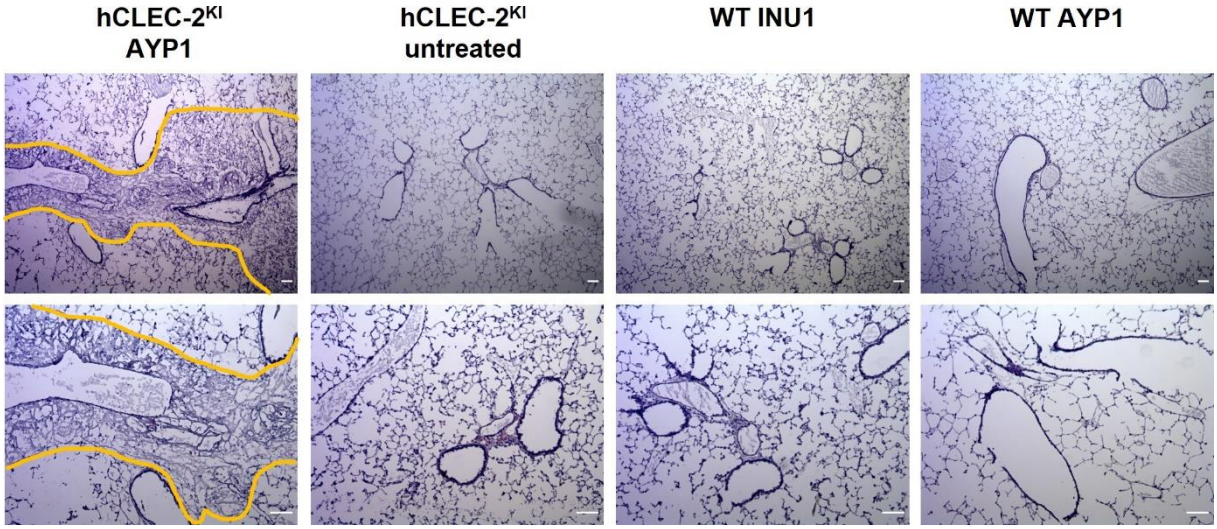

Figure 3.21 Intravenous AYP1 administration results in lung oedema in hCLEC-2^{KI} mice.
Lung cryosections stained with H&E showed that oedema (yellow outline) occurred after AYP1 administration (10 µg) in hCLEC-2^{KI} mice that died within 30 min of injection. This was not observed in untreated hCLEC-2^{KI} mice or WT mice treated with 10 µg of either INU1 or AYP1 and culled after 30 min. n = 3. Scale bars represent 100 µm.

We next investigated whether microthrombi become trapped in the lungs of hCLEC-2^{KI} mice following i.v. AYP1 administration by immunofluorescence staining. Platelet aggregates were observed in the lungs of AYP1 treated hCLEC-2^{KI} and INU1 treated WT mice, although quantification showed a non-significant trend for lower platelet surface coverage in INU1 treated WT mice (Figure 3.22). No aggregates were observed in AYP1 treated WT or untreated hCLEC-2^{KI} mice. This suggests that both AYP1 and INU1 induce microthrombus formation *in vivo* but this occurs to a greater extent with AYP1 accounting for the associated lethality.

We also investigated whether microthrombi could be observed in other organs as has been seen following INU1-Fab administration which is also lethal.[186] Therefore, brain, liver and spleen sections were stained with H&E. No thrombi or other abnormalities were observed in any organ following either AYP1 or INU1 administration (Figure 3.23). This, together with our other findings, suggests that i.v. AYP1 administration induces platelet aggregate formation and that these aggregates become trapped in the lungs but not in other vascular beds. Intravenous administration of 100 µg HEL1, on the other hand, was not lethal in hCLEC-2^{KI} mice (data not shown).

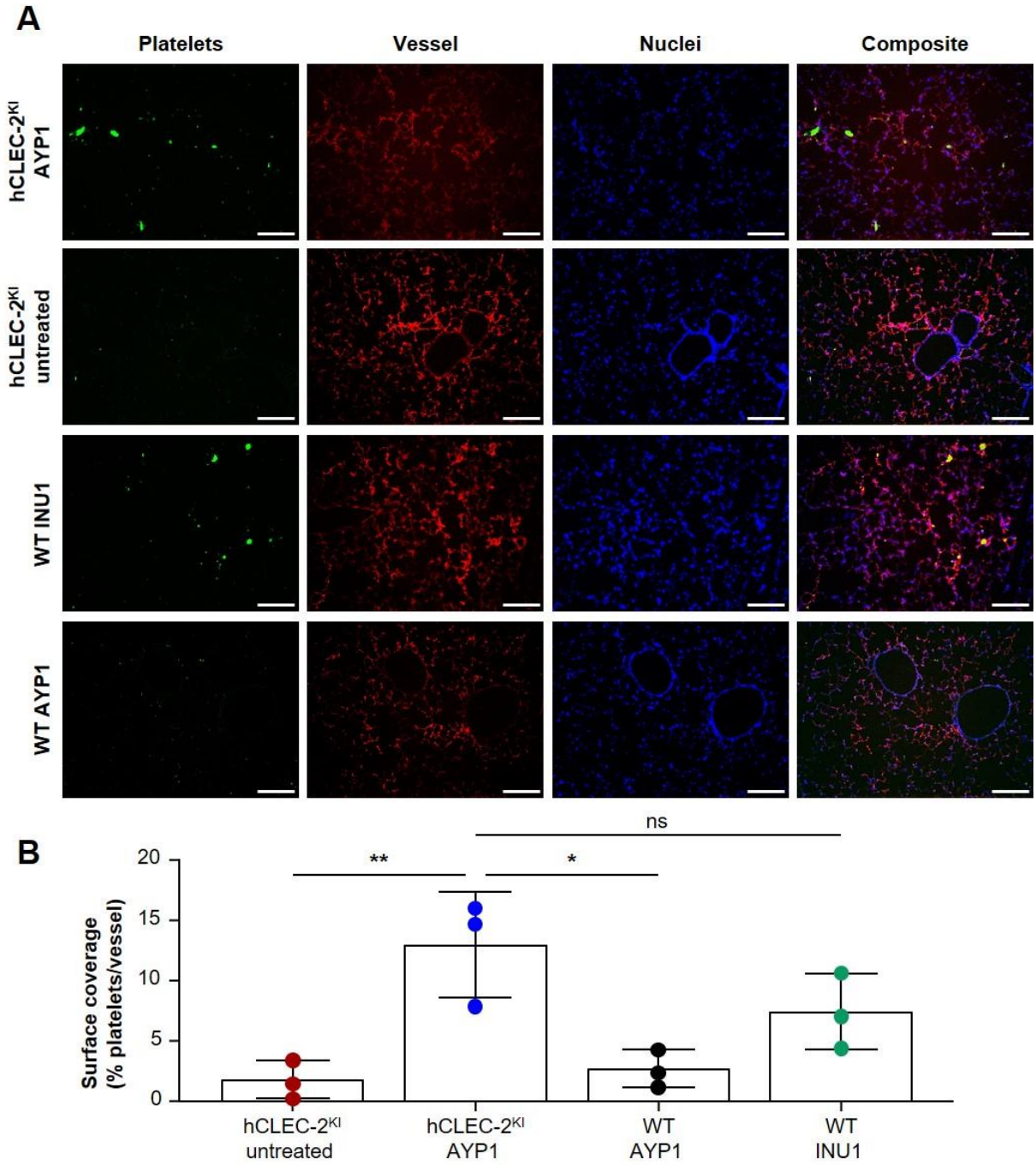

Figure 3.22 Intravenous AYP1 administration causes platelet aggregates to become trapped in the lungs of hCLEC-2^{KI} mice.

Lung cyrosections were stained and analysed following i.v. administration of 10 µg AYP1 or INU1 IgG to determine if platelet aggregates could be observed. (A) Platelets (green), vessels (red) and nuclei (blue) were stained in lungs sections using 10 µg/ml p0p6-A488, 10 µg/ml CD104-A647 and DAPI respectively. Platelet aggregates were observed in AYP1 treated hCLEC-2^{KI} and INU1 treated WT mice. Scale bars represent 200 µm. (B) Quantification of platelet surface coverage as a percentage of vessel surface coverage was greater in AYP1 treated hCLEC-2^{KI} than either untreated or AYP1 treated WT mice, P = 0.0068 and 0.011 respectively. No difference in surface coverage was observed between AYP1 treated hCLEC-2^{KI} and INU1 treated WT mice, P = 0.18. Data were analysed by one-way ANOVA followed by

Tukey's test for multiple comparisons. Each symbol represents one mouse and data is representative of n = 3. * P < 0.05, ** P < 0.01. ns, not significant

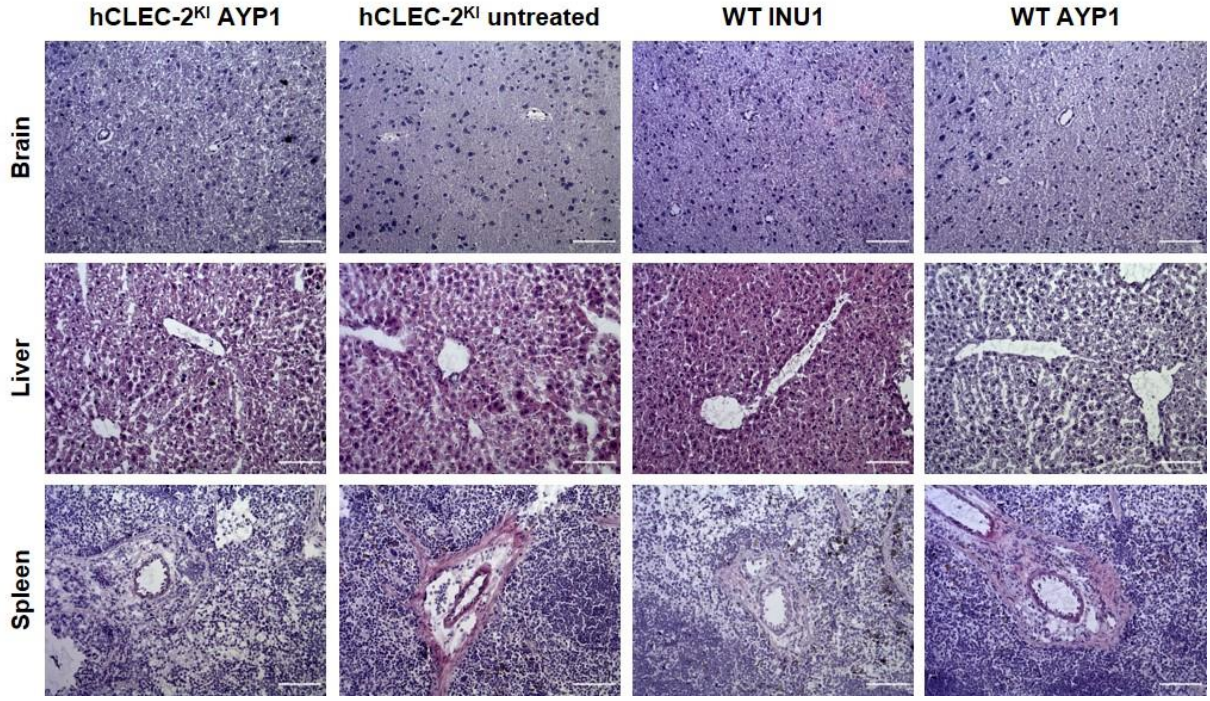

Figure 3.23 Intravenous AYP1 administration does not cause microthrombi to become trapped in brains, livers or spleens.
Brain, liver and spleen cyrosections were stained with H&E following i.v. administration of 10 µg AYP1 or INU1 IgG to determine if microthrombi could be observed. n = 3. Scale bars represent 100 µm.

3.4.2 Intraperitoneal injection of either HEL1 or AYP1 depletes hCLEC-2

Intraperitoneal (i.p.) antibody administration is likely to result in slower entry into the circulation than i.v. and therefore antibody-induced platelet aggregation should be reduced. Therefore, we injected AYP1 intraperitoneally, initially as two low dose injections 30 min apart of 2 and 8 µg. As this did not cause adverse effects, we then tried three injections, totalling 110 µg, over a period of 3 hours with an initial injection of 10 µg followed by two 50 µg injections after 30 min and 3 h. (data not shown). This also did not result in lethality, as observed with i.v. injection, and therefore we could investigate and compare the effects of HEL1, AYP1 and INU1 on CLEC-2 depletion following i.p. administration.

Intraperitoneal injection of HEL1 or AYP1 in hCLEC-2^{KI} and of INU1 in WT mice lead to a transient thrombocytopenia lasting for up to 4 days (Figure 3.24A). Both HEL1 and AYP1 depleted CLEC-2 for 11 days with levels returning to normal after 24 and 18 days respectively (Figure 3.24B). This is in contrast to INU1 induced CLEC-2 depletion in WT mice which lasts for 7 days, with normal expression returning by day 14 after administration, in agreement with previous findings from our group (Figure 3.24C).[25] All three antibodies could be detected on platelets for only up to 24 h and not after platelet count had returned to baseline levels, therefore the observed receptor depletion is not a result of injected antibody blocking the CLEC-2 binding site (Figure 3.24 D-E). These results show that hCLEC-2 can be immunodepleted and that this is prolonged compared to depletion of mCLEC-2 with INU1.

Immunodepletion of hCLEC-2 was also confirmed by Western Blot to investigate whether both surface and intracellular CLEC-2 were depleted (Figure 3.25). For both AYP1 and HEL1 induced depletion, CLEC-2 was absent from platelet lysates for at least 10 days, with a slight increase at day 15 post-injection. CLEC-2 levels then returned to normal between 20 and 25 days after injection. These data suggest that CLEC-2 is depleted both from the platelet surface and intracellularly and due to the length of depletion new platelets are produced which lack CLEC-2.

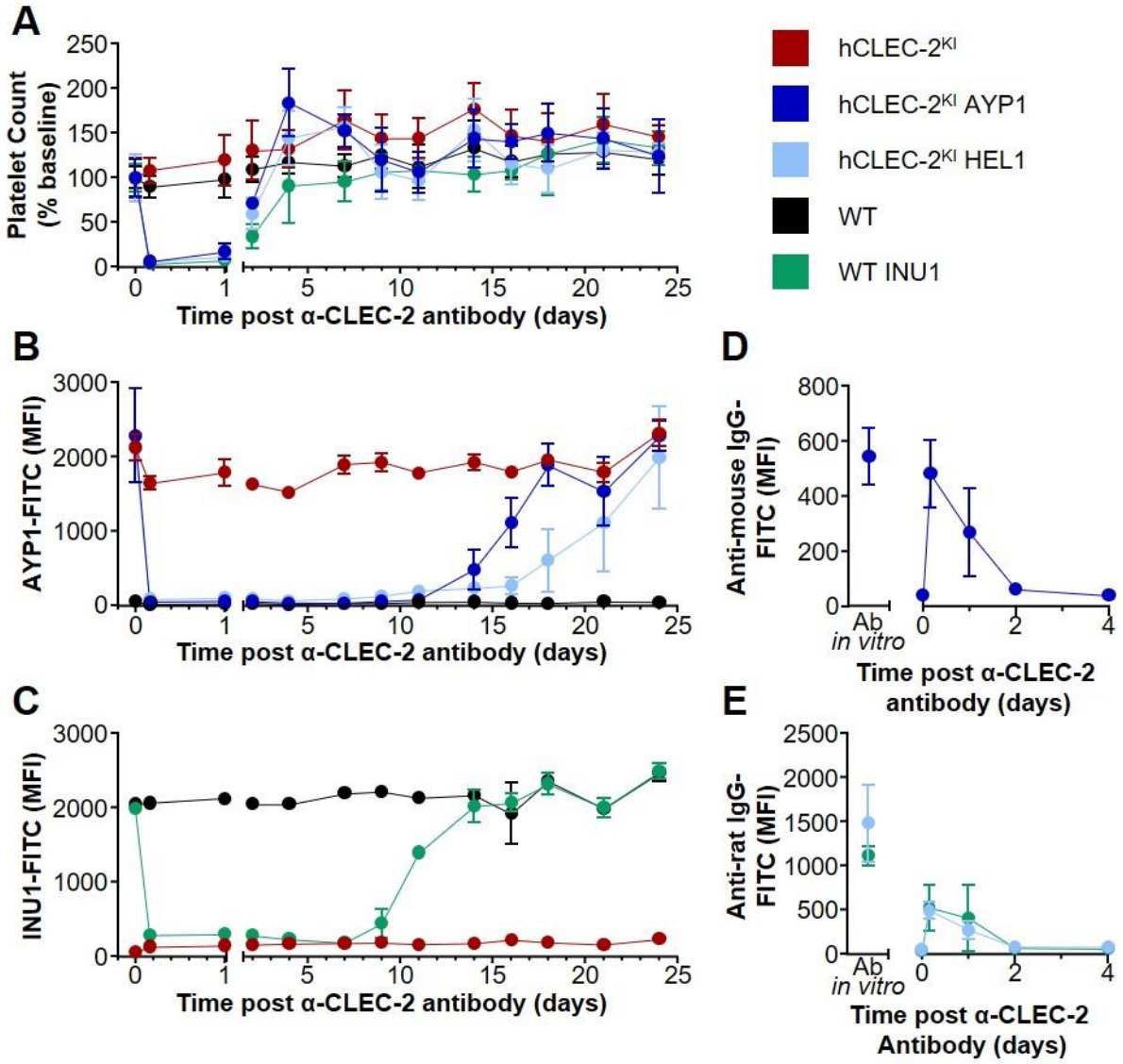

Figure 3.24 HEL1 and AYP1 can deplete hCLEC-2 from the platelet surface.
100 µg HEL1, AYP1 or INU1 were administered i.p. and the effect on platelet count and CLEC-2 surface expression were determined by flow cytometry. (A) Platelet count determined by flow cytometry using saturating concentrations of p0p6-FITC and JON6-PE conjugated antibodies and shown as the percentage of the baseline count. Thrombocytopenia was observed with all antibodies for up to 4 days (B) hCLEC-2 surface expression following depletion by either HEL1 or AYP1 and untreated controls was determined using AYP1-FITC. (C) mCLEC-2 surface expression following depletion by INU1 and untreated controls was determined using INU1-FITC. (D) AYP1 IgG binding to platelets *in vitro* and after i.p. administration was determined using an anti-mouse IgG-FITC antibody. (E) HEL1 and INU1 IgG binding to platelets *in vitro* and after i.p. administration was determined using an anti-rat IgG-FITC antibody. A minimum of 5 mice were tested per group and results are representative of at least two independent

experiments. FITC, fluorescein isothiocyanate; MFI, mean fluorescence intensity. Experiments were performed in collaboration with David Stegner

.

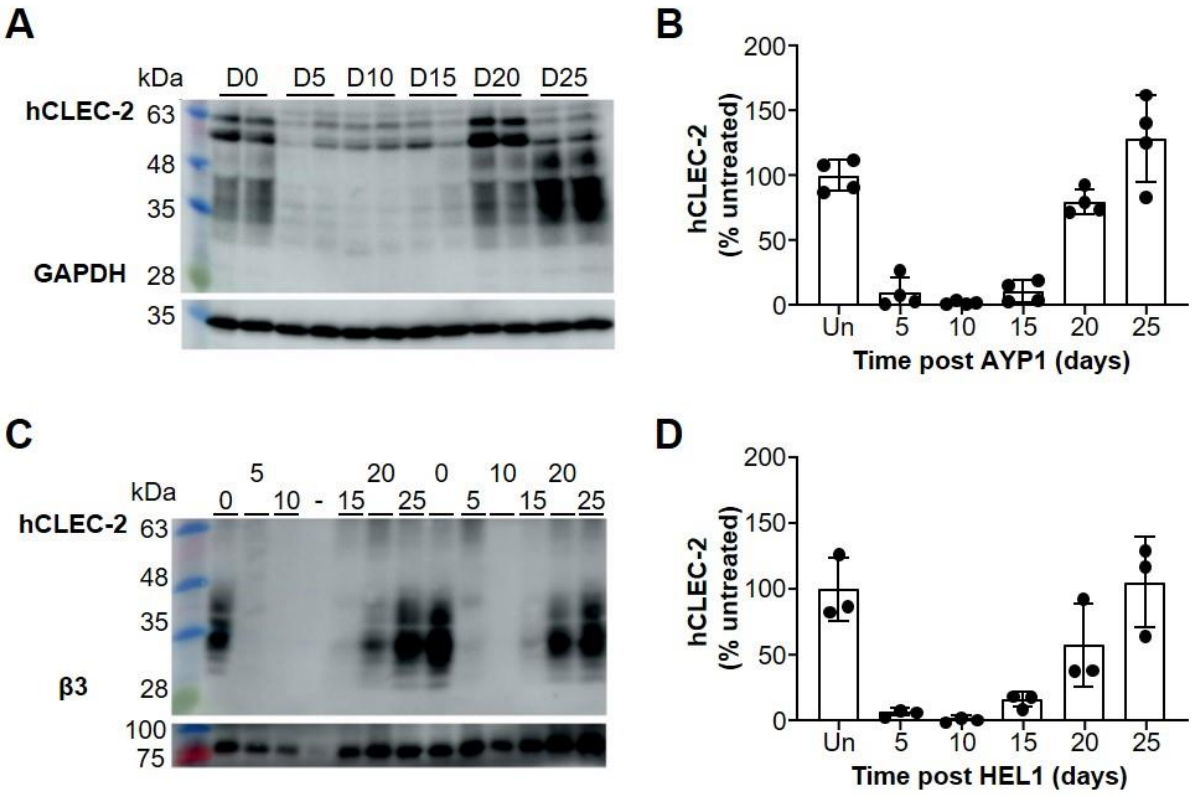

Figure 3.25 HEL1 and AYP1 deplete both surface and intracellular hCLEC-2.
100 µg HEL1 or AYP1 were administered intraperitoneally and the effect on CLEC-2 expression were determined by western blot using platelet lysates at the indicated time points. (A) Representative Western Blot of platelet lysates from AYP1 injected hCLEC-2^{KI} mice at 5 day intervals using 1 µg/ml AYP2. (B) Quantification of hCLEC-2 Western Blots from AYP1 injected hCLEC-2^{KI} mice show receptor depletion up to 15 days post injection. Data is shown as the percentage of hCLEC-2 compared to untreated mice and normalised to the loading control GAPDH. (C) hCLEC-2 Western Blot of platelet lysates from HEL1 injected hCLEC-2^{KI} mice at 5 day intervals using 5 µg/ml HEL1. "-" indicates an empty lane. (D) Quantification of hCLEC-2 Western Blots from HEL1 injected hCLEC-2^{KI} mice show receptor depletion up to 15 days post injection. Data is shown as the percentage of hCLEC-2 compared to untreated mice and normalised to the loading control β3 integrin. The HEL1 Western Blot, but not the analysis, was performed by Juliana Goldmann. GAPDH, Glyceraldehyde 3-phosphate dehydrogenase.

3.4.3 Flow adhesion

3.4.3.1 Depletion of hCLEC-2 appears to reduce thrombus formation on collagen

The effects of hCLEC-2 depletion on *in vitro* thrombus formation were investigated using a flow adhesion assay on collagen at a shear rate of 1000 s^{-1}. In preliminary experiments both surface coverage and thrombus volume showed a trend towards being reduced following

immunodepletion by AYP1 (Figure 3.26). However, statistical analysis could not be carried out due to the low number of animals in the depleted group, as a result of CLEC-2 levels beginning to return to normal in one of the mice. In agreement with results described previously hCLEC-2^{KI} mice formed thrombi that appeared denser and more contracted than in WT mice (Figure 3.14C and Figure 3.26C), whereas thrombi from AYP1 immunodepleted hCLEC-2^{KI} mice appeared much smaller and flatter than in both WT and hCLEC-2^{KI} untreated mice (Figure 3.26C). This is consistent with results from INU1 depleted WT mice.[25]

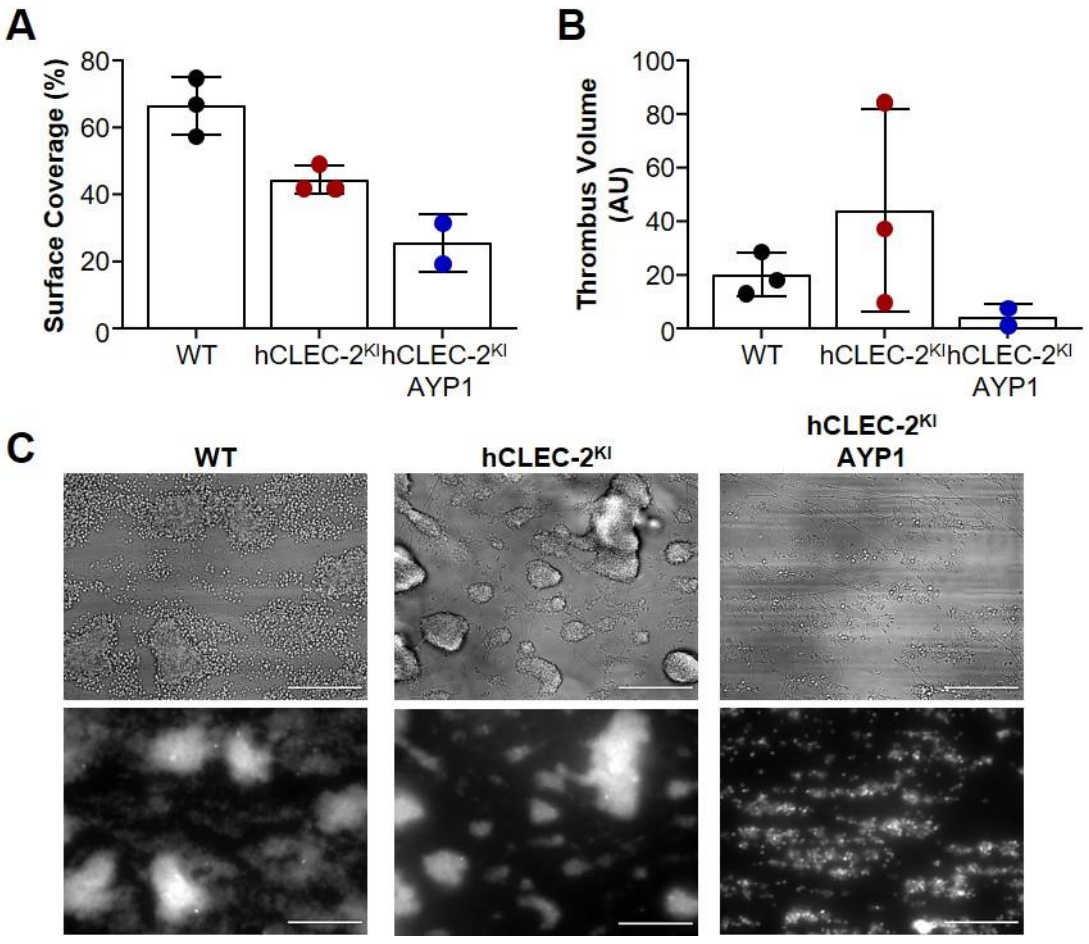

Figure 3.26 Reduced thrombus surface coverage in immunodepleted hCLEC-2^{KI} mice. Thrombus formation was assessed following perfusion of anti-coagulated whole blood over collagen for 4 min followed by 4 min of washing with Tyrode's buffer at a shear rate of 1000 s^{-1}. Experiments were carried out on day 10 after i.p. AYP1 (100 µg) administration to assess the effect of CLEC-2 depletion on thrombus surface coverage and volume (integrated density). (A) Percent thrombus surface coverage in WT, hCLEC-2^{KI} and hCLEC-2^{KI} AYP1-depleted mice. (B) Thrombus volume in WT, hCLEC-2^{KI} and hCLEC-2 depleted mice. (C) Representative brightfield and fluorescent images from WT, hCLEC-2^{KI}, and AYP1 depleted hCLEC-2^{KI} mice. Each symbol represents one mouse, n = 2-3. One mouse was excluded from

the hCLEC-2^{KI} AYP1 group as CLEC-2 had begun to return, as determined by flow cytometry (data not shown). Data is shown as mean ± standard deviation. Scale bars represent 50 µm.

3.4.3.2 Thrombus formation in both hCLEC-2^{KI} and hCLEC-2^{KI} depleted mice is comparable to WT in the absence of blood plasma

As thrombus formation appeared to be altered in hCLEC-2^{KI} and hCLEC-2 depleted mice compared to WT (Figures 3.14, 3.15 and 3.26) we hypothesised this could be due to a difference in the proposed intravascular CLEC-2 ligand for mouse and human CLEC-2. Therefore, we carried out an *in vitro* thrombus formation assay using reconstituted blood that lacks plasma from WT, hCLEC-2^{KI} and AYP1-depleted hCLEC-2^{KI} mice. No difference in thrombus surface coverage or volume were observed in either hCLEC-2^{KI} or AYP1 treated hCLEC-2^{KI} mice compared to WT (Figure 3.27). Furthermore, differences in thrombus appearance were also reduced between the three groups (Figure 3.27C). However, thrombi from WT, and particularly from hCLEC-2^{KI}, mice appeared less stable than those formed from whole blood whereas thrombi from depleted mice, although still unstable, appeared to be formed of more adherent platelets than those from whole blood at the same shear rate (Figure 3.14 and Figure 3.26). This suggests that a factor within the plasma accounts for the differences in thrombus formation in hCLEC-2^{KI} and depleted mice compared to WT.

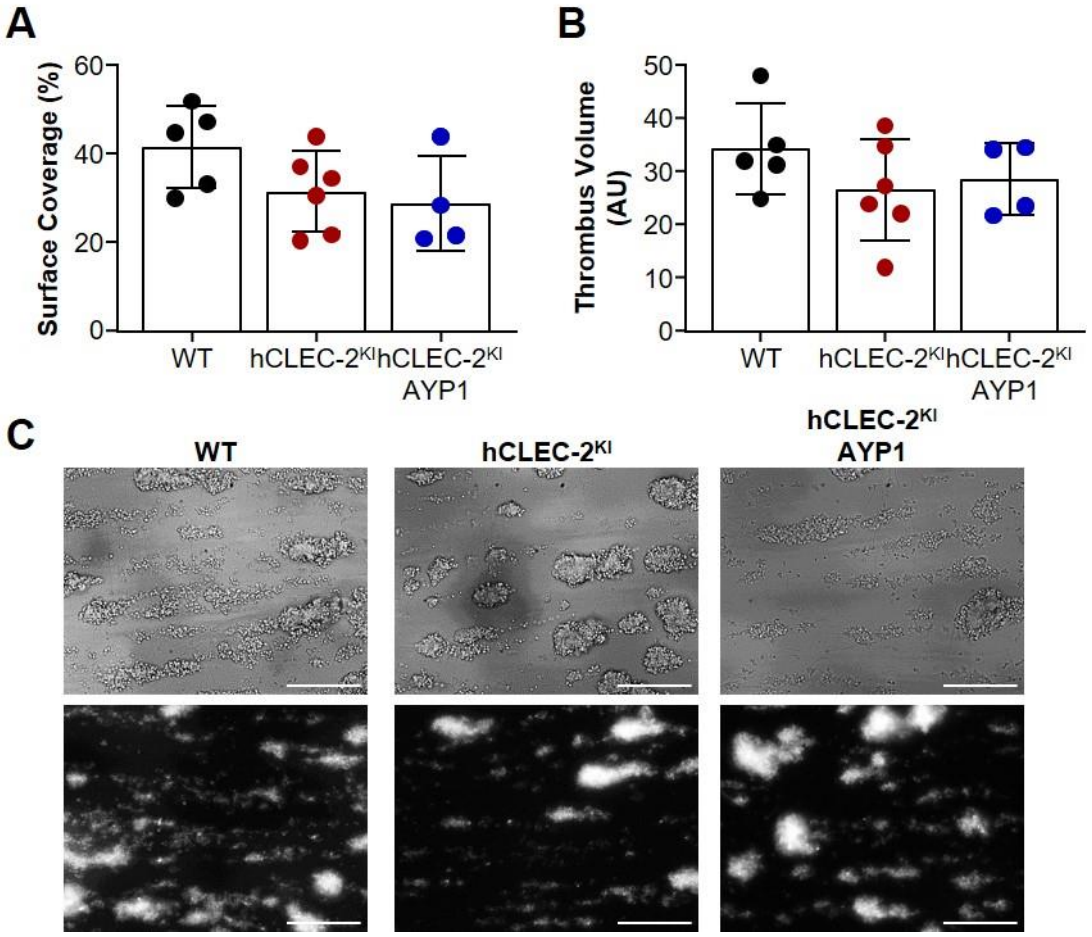

Figure 3.27 Thrombus formation in hCLEC-2^{KI} and depleted mice is comparable to WT in the absence of plasma.
Thrombus formation was assessed following perfusion of washed platelets reconstituted with red blood cells, fibrinogen and calcium over collagen at a shear rate of 1000 s^{-1} on day 9 after i.p. AYP1 (100 µg) administration. The effect of CLEC-2 depletion on thrombus formation in the absence of plasma was assessed by comparison of thrombus surface coverage and volume (integrated density). (A) Percent thrombus surface coverage in WT, hCLEC-2^{KI} and hCLEC-2^{KI} AYP1-depleted mice, P = 0.14. (B) Thrombus volume in WT, hCLEC-2^{KI} and hCLEC-2^{KI} depleted mice, P = 0.34. (C) Representative brightfield and fluorescent images from WT, hCLEC-2^{KI}, and AYP1 depleted hCLEC-2^{KI} mice. Data is shown as mean ± standard deviation and was analysed by one-way ANOVA. Each symbol represents one mouse, n = 4-6. Two mice were excluded from the hCLEC-2^{KI} AYP1 group as CLEC-2 had begun to return, as determined by flow cytometry (data not shown). Scale bars represent 50 µm.

3.4.4 Depletion of hCLEC-2 has no effect on haemostasis or arterial thrombosis in *in vivo* models

3.4.4.1 Depletion of hCLEC-2 has no effect in a tail bleeding haemostasis model

Depletion of mCLEC-2 by INU1 has a minor effect on haemostasis as seen using the filter paper tail bleeding assay.[25,73] We therefore, investigated the effect of hCLEC-2 depletion in

this model. No significant differences were observed between either hCLEC-2^{KI} depleted and untreated mice or hCLEC-2^{KI} and WT mice (Figure 3.28). However, two hCLEC-2^{KI} mice failed to stop bleeding within the 20 min of the experiment whereas this did not occur for any WT or hCLEC-2^{KI} depleted mice. This suggests that hCLEC-2 has only a minor role in haemostasis.

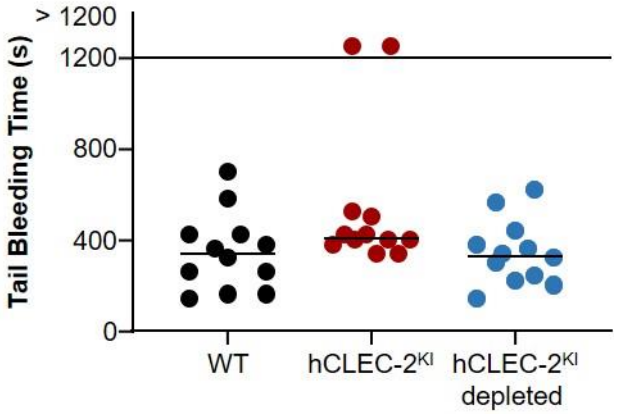

Figure 3.28 Tail bleeding is unaltered in hCLEC-2 depleted mice.
The filter paper tail bleeding assay following excision of the tail tip of anaesthetised mice was used as a measure of haemostasis. Administration of 100 µg AYP1 i.p. to deplete CLEC-2 in hCLEC-2^{KI} mice was compared to WT and untreated hCLEC-2^{KI} controls. The assay was run until either bleeding ceased or 1200 s had passed. No differences in tail bleeding time were observed P > 0.05, Fisher exact test. Horizontal lines represent median time to bleeding cessation and each symbol represents one mouse, n = 12.

3.4.4.2 Depletion of hCLEC-2 had no effect on thrombosis induced by mechanical injury to the abdominal aorta

Thrombus formation following mechanical injury of the aorta has previously been shown not to be affected by the absence of CLEC-2 using *Clec1b*$^{fl/flPF4Cre+}$ conditional knockout mice.[74] Similar results have also been shown following CLEC-2 depletion by INU1 (May, unpublished data). We therefore, investigated whether or not depletion of hCLEC-2 had an effect on vessel occlusion in this model. hCLEC-2^{KI} depleted mice had comparable occlusion times to untreated mice with one depleted mouse and 3 untreated mice failing to occlude during the first 30 min following vessel injury. This is in contrast to the WT mice in which all vessels occluded. This trend suggests that hCLEC-2^{KI} mice may have a reduced ability to form occlusive thrombi. This experiment was performed by Sarah Beck

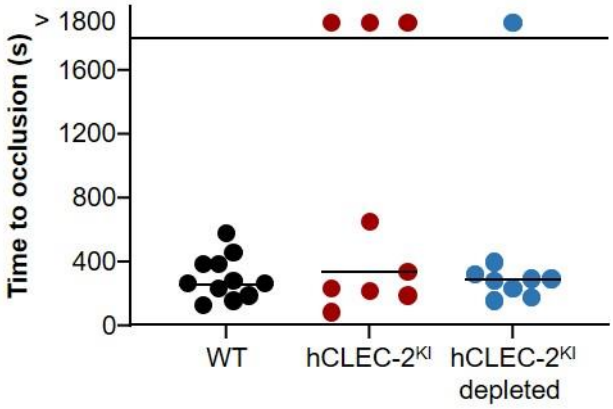

Figure 3.29 Occlusion time following mechanical injury to the abdominal aorta is unaffected by depletion of hCLEC-2.
In vivo thrombus formation in hCLEC-2^{KI} and depleted mice (100 µg HEL1 i.p.) was compared to WT mice in the mechanical injury of the abdominal aorta thrombosis model. Injury was caused by compression of the aorta using forceps and the time to vessel occlusion was determined using a Doppler ultrasonic flow probe. No difference in occlusion time was observed P > 0.05, Fisher exact test. Horizontal lines represent the median time to vessel occlusion and each symbol represents one mouse, n = 9-11 mice. Experiment performed by Sarah Beck.

3.4.4.3 hCLEC-2^{KI} mice have reduced vessel occlusion following $FeCl_3$ induced thrombosis

Depletion of mouse CLEC-2 by INU1 prevents occlusive thrombus formation following $FeCl_3$ injury to the mesenteric arterioles.[25] We therefore investigated whether depletion of hCLEC-2 in hCLEC-2^{KI} mice had a similar effect. Although no significant differences in the time to the appearance of the first thrombi were observed in either depleted or untreated hCLEC-2^{KI} mice there was a trend for increased appearance time in the hCLEC-2^{KI} depleted mice (Figure 3.30 A & C). However, occlusion time was increased in untreated hCLEC-2^{KI} mice, with 56% of the vessels failing to occlude compared to none in the WT group, whereas, in the hCLEC-2^{KI} depleted group 21% of vessels failed to occlude (Figure 3.30B-C). Together this data, along with that from the mechanical injury experiment, suggests that depletion of hCLEC-2 does not have an effect on arterial thrombosis *in vivo* however, as hCLEC-2^{KI} mice have reduced occlusive thrombus formation compared to WT the exact nature of the effect of receptor depletion is difficult to conclude. This experiment was performed by Sarah Beck.

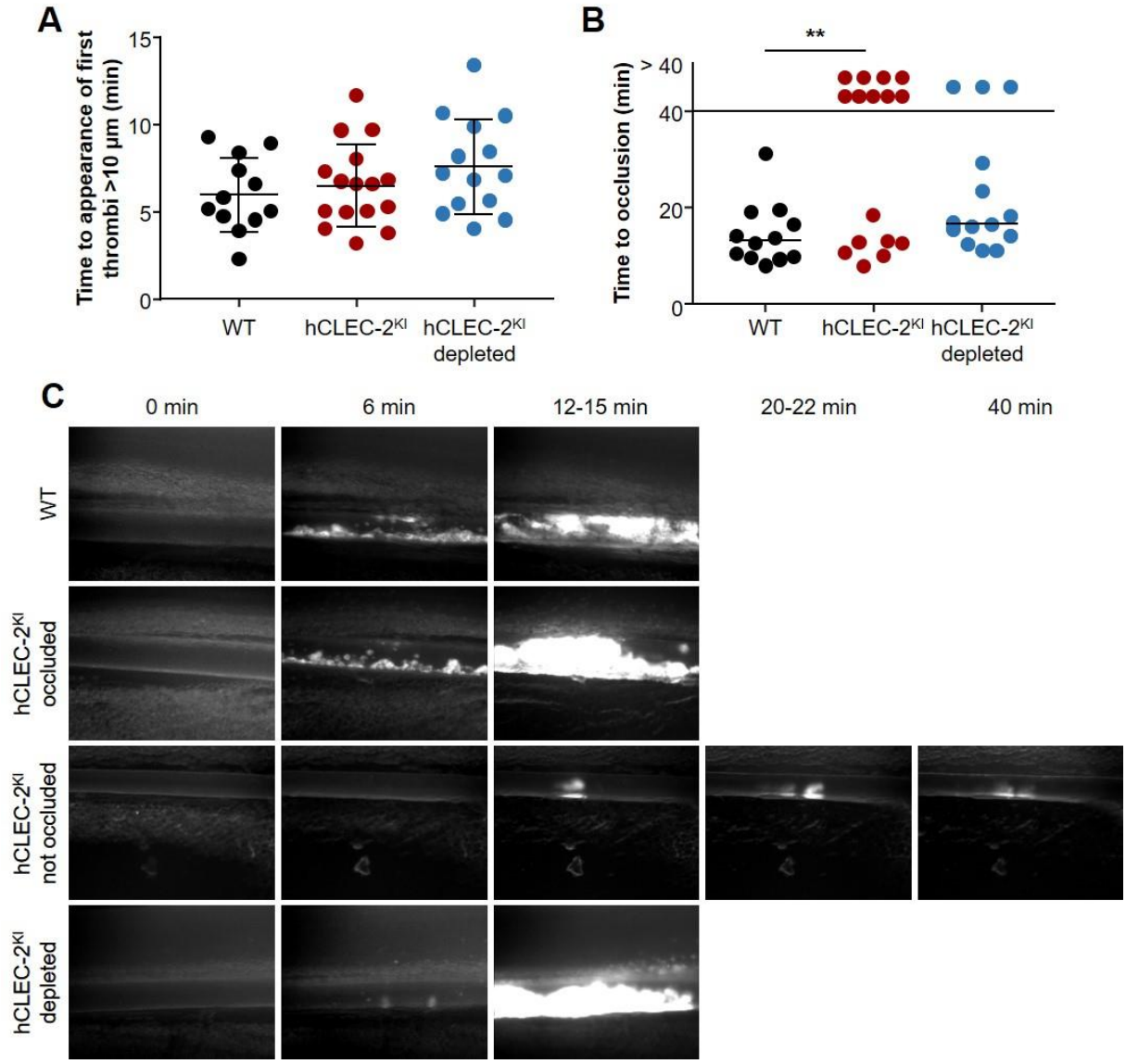

Figure 3.30 Vessel occlusion is reduced in hCLEC-2^{KI} mice following $FeCl_3$-induced injury.

In vivo thrombus formation in hCLEC-2^{KI} and depleted mice (100 µg HEL1 i.p.) was compared to WT mice following $FeCl_3$-induced injury of mesenteric arterioles. The time to the appearance of the first thrombi and the occlusion time (cessation of blood flow) were determined using intravital microscopy. (A) Time taken for the appearance of the first thrombi following $FeCl_3$-induced injury, one-way ANOVA, P = 0.073. Data is shown as mean ± standard deviation. (B) Time to vessel occlusion. hCLEC-2^{KI} mice had increased vessel occlusion times compared to WT mice, Fisher exact test P = 0.0028. Occlusion times in hCLEC-2 depleted mice were not statistically different to either WT or untreated hCLEC-2^{KI} mice, Fisher exact test P = 0.22 and 0.072 respectively. Horizontal lines represent the median. (C) Representative images of mesenteric vessels following $FeCl_3$-induced injury for each group at the times indicated after injury from n = 5-7 mice per group. Representative images of both occluded and non-occluded hCLEC-2^{KI} vessels are shown. Each symbol represents 1 vessel and up to 3 vessels per mouse were injured. **, P < 0.01. Experiment performed by Sarah Beck.

3.4.5 AYP1 Fab functions differently *in vitro* and *ex vivo*

As AYP1 IgG induces platelet activation and causes transient thrombocytopenia its potential as a therapeutic antibody is reduced. We therefore, sought to investigate the effect of AYP1 Fab fragments, firstly *in vitro* and then *ex vivo* in hCLEC-2^{KI} mice.

AYP1-Fab has previously been shown to block podoplanin and rhodocytin induced platelet activation in human platelets.[40] We therefore, tested its effect in hCLEC-2^{KI} platelets to see if it was comparable to human. *In vitro* AYP1-Fab bound to hCLEC-2^{KI} platelets as shown by reduced AYP1-FITC binding and increased anti-mouse IgG-FITC binding compared to untreated platelets from the same mice (Figure 3.31 A-B). We next investigated the effect of AYP1-Fab pre-incubation on platelet activation by measuring integrin activation and granule secretion. AYP1-Fab unexpectedly reduced GPVI-mediated platelet activation by CRP, as well as blocking both rhodocytin and AYP1 IgG-induced activation as expected (Figure 3.31 C-D). Therefore, AYP1-Fab is able to bind to and to block CLEC-2-induced platelet activation in hCLEC-2^{KI} platelets as it can in human platelets.[40]

As AYP1-Fab inhibited CLEC-2-mediated platelet activation *in vitro* in hCLEC-2^{KI} platelets we next investigated its effect 30 min after intravenous administration. Concentrations of 10, 50 and 100 µg per mouse were tested but only results for 100 µg are shown as AYP1-Fab could not be detected on platelets at the lower concentrations. None of the concentrations tested were lethal as has been found for INU1-Fab in WT mice (Nieswandt *et al*., unpublished) and AYP1-IgG in hCLEC-2^{KI} mice. AYP1-Fab bound to hCLEC-2^{KI} platelets *in vivo* as shown by reduced AYP1-FITC binding and increased anti-mouse IgG-FITC binding compared to untreated control mice (Figure 3.32 A-B). Unlike AYP1-IgG the fab fragment did not induce thrombocytopenia (Figure 3.32C). However, *in vivo* administration also had no effect on platelet activation induced by either CRP, rhodocytin or AYP1-IgG (Figure 3.32 D-E). However, rhodocytin induced platelet aggregation was slightly delayed in the AYP1-Fab treated mice,

although both CRP and AYP1-IgG induced aggregation were comparable to control mice (Figure 3.32F).

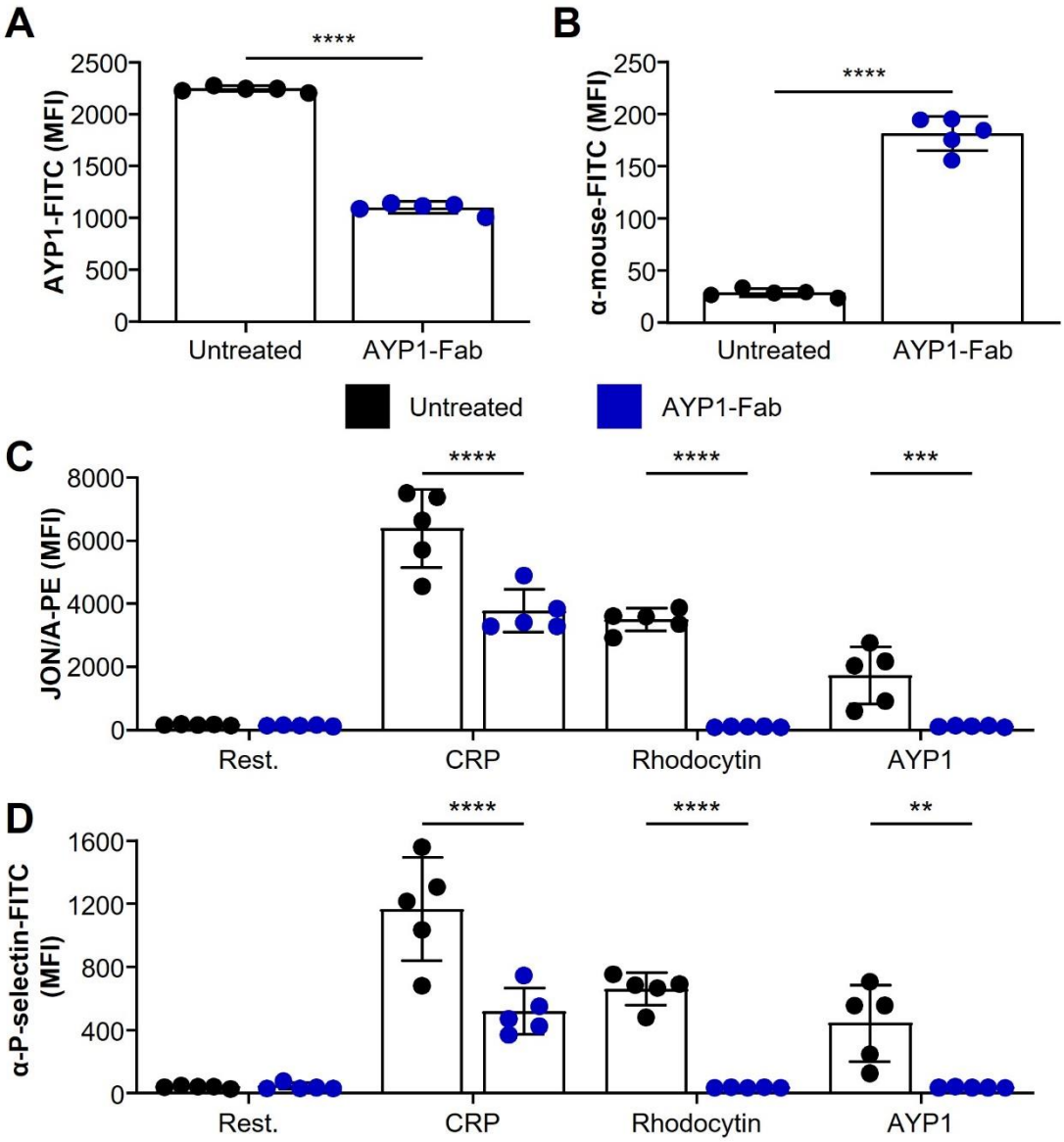

Figure 3.31 *In vitro* AYP1-Fab binds to hCLEC-2^{KI} platelets and blocks CLEC-2 induced platelet activation.
Anti-coagulated whole blood was incubated with 10 µg/ml AYP1-Fab and the effect on platelet activation was determined by flow cytometry using saturating concentrations of JON/A-PE (integrin activation) and anti-P-selectin-FITC (degranulation). (A) Pre-incubation of hCLEC-2^{KI} blood with 10 µg/ml AYP1-Fab reduces AYP1-FITC binding, paired t-test, $P < 0.0001$. (B) AYP1-Fab binds to hCLEC-2^{KI} platelets as shown by increased anti-mouse FITC binding compared to untreated controls, paired t-test, $P < 0.0001$. (C) Effect of pre-incubation with AYP1-Fab on integrin activation induced by CRP (1 µg/ml), rhodocytin (1.2 µg/ml) or AYP1 IgG (10 µg/ml). Data were analysed by a two-way ANOVA followed by Sidak's multiple comparisons test, $P < 0.0001$ for CRP, $P < 0.0001$ for rhodocytin and $P = 0.0010$ for AYP1 IgG. (D) Effect of pre-incubation with AYP1-Fab on granule release induced by CRP, rhodocytin or AYP1 IgG. Data were analysed by a two-way ANOVA followed by Sidak's

multiple comparisons test, P < 0.0001 for CRP, P < 0.0001 for rhodocytin and P = 0.0013 for AYP1 IgG. Each symbol represents one animal, n = 5. ** P < 0.01, *** P < 0.001 and **** P < 0.0001. MFI, mean fluorescence intensity; Rest, resting; PE, phycoerythrin; FITC, fluorescein isothiocyanate.

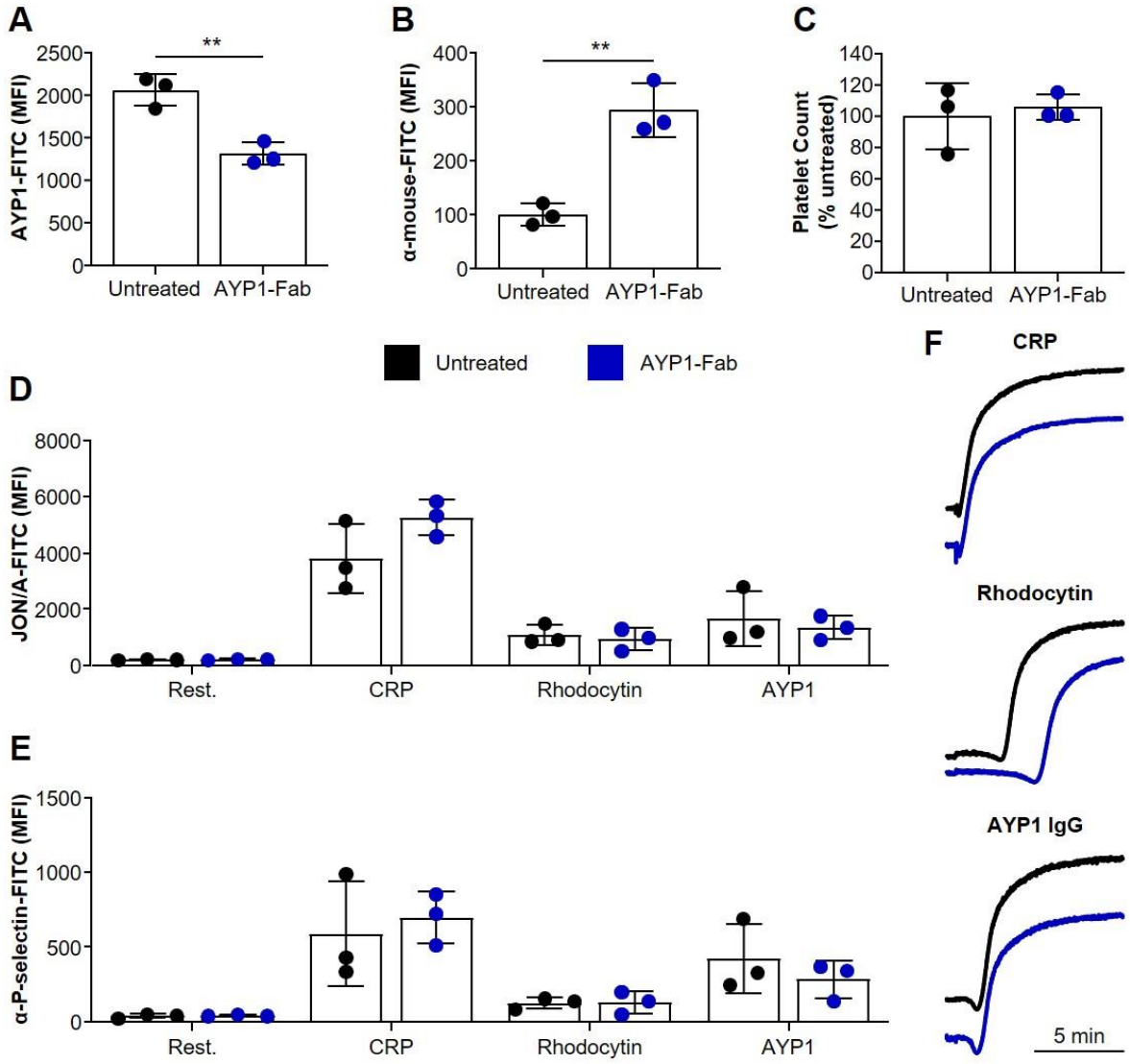

Figure 3.32 *Ex vivo* AYP1-Fab has no effect on CLEC-2-induced platelet activation although it binds to hCLEC-2^{KI} platelets.

100 µg AYP1-Fab was administered i.v. and its effects on platelet count and activation were determined by flow cytometry using saturating concentrations of JON/A-PE (integrin activation) and anti-P-selectin-FITC (degranulation). Platelet aggregation was also determined by light transmission aggregometry. (A) AYP1-FITC binding to platelets from AYP1-Fab and untreated mice show that AYP1-Fab binds to the platelet surface, unpaired t-test, P = 0.0050. (B) Anti-mouse-IgG-FITC binding to platelets from AYP1-Fab and untreated mice show that AYP1-Fab binds to the platelet surface, unpaired t-test, P = 0.0033. (C) Platelet count determined using saturating concentrations of p0p6-FITC and JON6-PE conjugated antibodies in AYP1-Fab and untreated mice, unpaired t-test P = 0.68. (D) Integrin activation induced by CRP (1 µg/ml), rhodocytin (1.2 µg/ml) or AYP1 IgG (10 µg/ml), two-way ANOVA P = 0.10. (E) Granule secretion, as shown by P-selectin exposure, induced by CRP, rhodocytin or AYP1 IgG, two-way ANOVA P = 0.10. (F) Light transmission aggregometry of washed platelets stimulated with

CRP (1 µg/ml), rhodocytin (1.2 µg/ml) or AYP1 IgG (10 µg/ml) following i.v. AYP1-Fab. Aggregation was measured for 10 min at 37°C under stirring conditions. Each symbol represents one animal, n = 3. ** P < 0.01. MFI, mean fluorescence intensity; Rest, resting; PE, phycoerythrin; FITC, fluorescein isothiocyanate.

3.5 Blockade of hCLEC-2 *in vitro* had no effect on thrombus formation

Despite AYP1 having been tested *in vitro* in human platelets it had never been tested in flow adhesion thrombus formation assays. We therefore, investigated whether either AYP1-F(ab')$_2$ or Fab fragments reduced thrombus formation as we had observed following *in vivo* administration of AYP1-IgG in hCLEC-2^{KI} mice (Figure 3.26). Antibody fragments were used as IgG antibodies can activate human platelets via their Fc portion and the FcγRIIA receptor. Incubating blood from healthy donors with either AYP1-F(ab')$_2$ or Fab fragments had no effect on thrombus formation on collagen at a shear rate of 1000 s^{-1} (Figure 3.33). Although aggregates could sometimes be observed flowing through the chamber within the blood following AYP1-F(ab')$_2$ pre-treatment suggesting it might activate the platelets, this was not observed in PBS control or Fab treated blood. We next investigated whether pre-incubation of healthy donor blood with recombinant hCLEC-2 (hFC-hCLEC-2) had an effect on thrombus formation under the same conditions. We hypothesised that recombinant hCLEC-2 could bind to the postulated plasma borne CLEC-2 ligand and therefore block its binding to CLEC-2 on activated platelets under flow. However, no effect on thrombus formation was observed following pre-incubation of donor blood with recombinant hCLEC-2 (Figure 3.34). Together these data suggest that blockade of hCLEC-2 or its postulated ligand has no effect on thrombus formation *in vitro* in human blood.

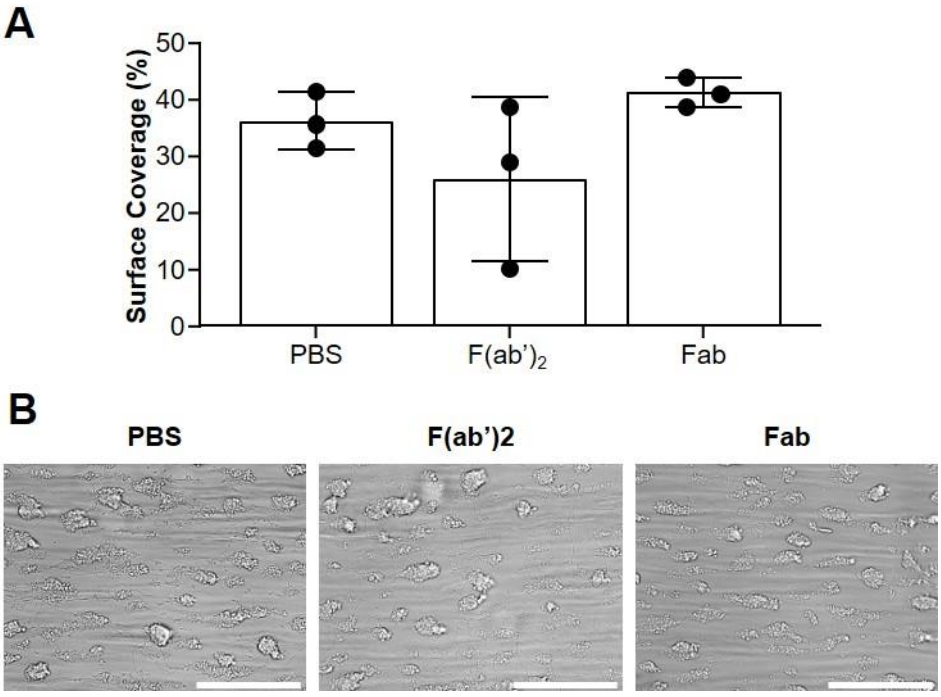

Figure 3.33 AYP1-F(ab')$_2$ or Fab fragments have no effect on thrombus formation in human blood.
Anti-coagulated whole blood from healthy donors was pre-incubated with 10 µg/ml AYP1-F(ab')$_2$ or Fab fragments and perfused over collagen for 4 min followed by 4 min washing with Tyrode's buffer at a shear rate of 1000 s^{-1}. Thrombus surface coverage was then determined. (A) Percent thrombus surface coverage following PBS control, AYP1-F(ab')$_2$ or AYP1-Fab pre-incubation., one-way ANOVA, P = 0.17. (B) Representative brightfield images of thrombi following PBS, AYP1-F(ab')$_2$ or AYP1-Fab treatment. Scale bars represent 50 µm. Each symbol represents one donor, n =3.

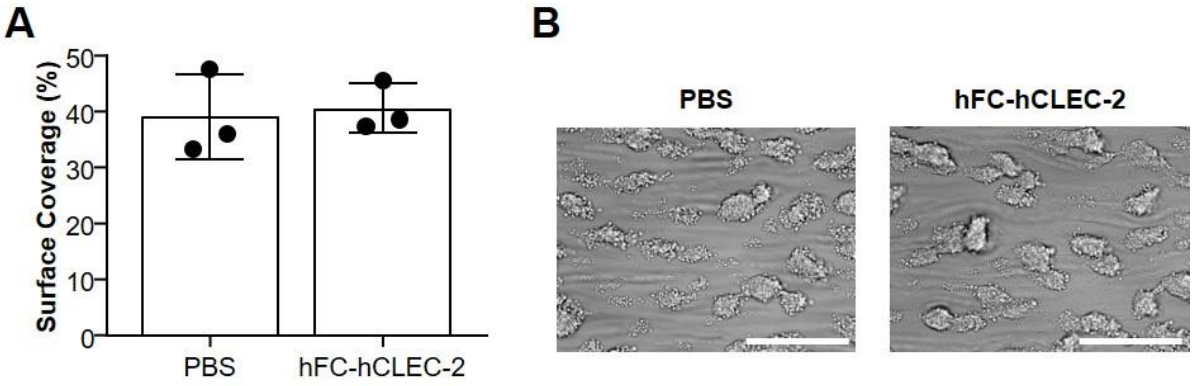

Figure 3.34 Recombinant hCLEC-2 has no effect on thrombus formation in human blood.
Anti-coagulated whole blood from healthy donors was pre-incubated with 52 µg/ml hFC-hCLEC-2 recombinant protein or PBS and perfused over collagen for 4 min followed by 4 min washing with Tyrode's buffer at a shear rate of 1000 s^{-1}. Thrombus surface coverage was then determined. (A) Percent thrombus surface coverage following PBS control or hFC-hCLEC-2 pre-incubation, paired t-test, P = 0.56. (B) Representative brightfield images of thrombi

following PBS, or hFC-hCLEC-2 treatment. Scale bars represent 50 µm. Each symbol represents one donor, n =3.

3.6 Btk inhibitors

PRN1008 (rilzabrutinib) is a third-generation Btk inhibitor currently undergoing clinical trials and PRN473 is a pre-clinical Btk inhibitor with a similar mechanism of action. First and second generation Btk inhibitors have been previously shown to selectively block CLEC-2-induced platelet activation but so far no third-generation inhibitors have been investigated.[65] Here we have investigated the effect of PRN1008 and PRN473 on platelet activation induced by rhodocytin *in vitro* in mouse platelets as well as PRN473 *in vivo* using a specially formulated diet. We then investigated the effect of this diet on Btk inhibition in a model of *Salmonella*-induced thrombosis in which CLEC-2 and podoplanin are known to be key contributors.[59]

3.6.1 *In vitro* effect of PRN1008 and PRN473 on mouse platelet activation via CLEC-2

3.6.1.1 PRN1008 inhibits CLEC-2-induced platelet aggregation only when secondary mediators are inhibited

Initially, we investigated the effect of increasing concentrations of PRN1008 on rhodocytin-induced platelet aggregation. Concentrations of 2 to 20 µM had little effect on platelet aggregation with only a slight decrease in maximal aggregation observed at 20 µM and small increases in lag time observed for each PRN1008 concentration tested (Figure 3.35, data not shown for lower concentrations). We therefore inhibited secondary mediators of platelet activation using 10 µM each of indomethacin and cangrelor to investigate whether their contributions to platelet activation masked the effect of PRN1008 on CLEC-2. Secondary mediator inhibition itself reduced platelet aggregation in response to rhodocytin but the addition of PRN1008 abolished the aggregation response altogether (Figure 3.35).

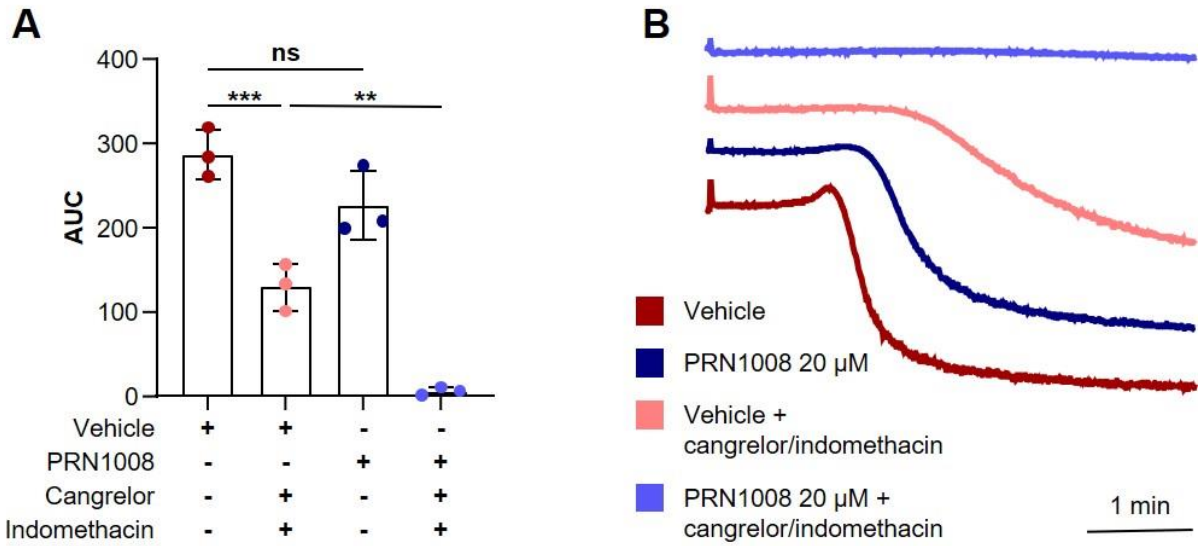

Figure 3.35 PRN1008 blocks rhodocytin-induced platelet aggregation in the absence of secondary mediators in mouse washed platelets.
Light transmission aggregometry of washed platelets under stirring conditions at 37°C was used to determine the effect of 1 h pre-incubation of 20 µM PRN1008 on CLEC-2 mediated platelet activation by 100 nM rhodocytin with or without secondary mediator inhibition by cangrelor and indomethacin (10 µM). Aggregation was measured for 5 min (A) Area under the curve analysis of platelet aggregation induced by rhodocytin following 1 h incubation with PRN1008 or DMSO vehicle with or without inhibition of secondary mediators. PRN1008 alone does not inhibit rhodocytin induced aggregation (P = 0.12) only in the absence of secondary mediators (P = 0.0034 compared to inhibited vehicle). Secondary mediator inhibition itself also reduced aggregation (P = 0.0007). Data was analysed by one-way ANOVA followed by Tukey's multiple comparison test. (B) Representative aggregation traces following rhodocytin stimulation of platelets in the presence of absence of secondary mediators. Each symbol represents one mouse, n = 3. ** P < 0.01, *** P < 0.001. AUC, area under the curve.

As secondary mediator inhibition in addition to 20 µM PRN1008 abolished rhodocytin-induced platelet aggregation, we carried out a dose-response experiment at lower PRN1008 concentrations to find the lowest concentration that blocked aggregation. 0.5 and 2 µM reduced and abolished aggregation respectively in response to rhodocytin in the presence of secondary mediator inhibitors (Figure 3.36). These concentrations also had a non-significant trend for a reduction in aggregation without secondary mediator inhibition as well as for increasing lag time under both conditions (Figure 3.36). These data suggest 2 µM PRN1008 can efficiently inhibit rhodocytin-induced platelet aggregation in mice and that much lower concentrations are needed to block aggregation in the presence of secondary mediator inhibitors.

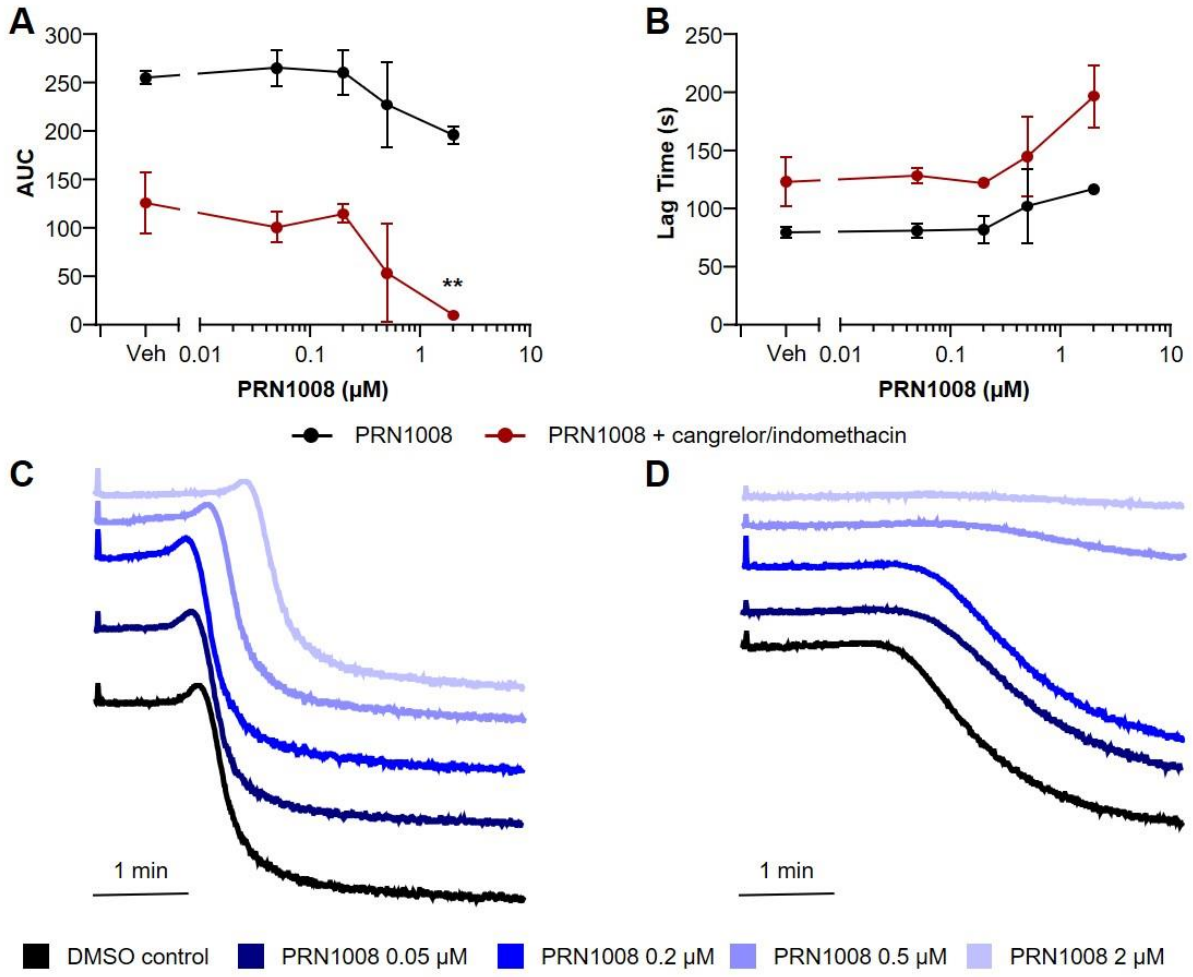

Figure 3.36 2 μM PRN1008 prevents platelet aggregation induced by rhodocytin in the presence of secondary mediator inhibitors in mouse washed platelets.
Light transmission aggregometry of washed platelets under stirring conditions at 37°C was used to generate dose response curves to increasing concentrations of PRN1008 on CLEC-2 mediated platelet activation by 100 nM rhodocytin with or without secondary mediator inhibition by cangrelor and indomethacin (10 μM). PRN1008 was incubated in washed platelets for 1 h at concentrations of 0.05, 0.2, 0.5 and 2 μM before aggregation was induced. Aggregation was measured for 5 min. (A) Area under the curve analysis of platelet aggregation induced by rhodocytin in PRN1008 or DMSO vehicle treated platelets with or without the secondary mediator inhibitors cangrelor and indomethacin. Data was analysed by one-way ANOVA followed by Dunnett's multiple comparison test, $P > 0.05$ for PRN1008 without secondary mediator inhibition. In the presence of secondary mediator inhibitors 2 μM PRN1008 inhibited platelet aggregation compared to vehicle, $P = 0.0078$. No significant reduction in aggregation was seen at any other PRN1008 concentration, $P > 0.05$. (B) Analysis of lag time to the start of aggregation. No differences were observed at any PRN1008 concentration in either the presence or absence of secondary meditators, $P = 0.095$ and 0.056 respectively, one-way ANOVA. (C) Representative aggregation traces following rhodocytin stimulation of platelets pre-incubated with increasing concentrations of PRN1008 without additional inhibition of secondary mediators. (D) Representative aggregation traces following rhodocytin stimulation of platelets pre-incubated with increasing concentrations of PRN1008 and inhibition of secondary mediators. $n = 3$. ** $P < 0.01$. AUC, area under the curve.

3.6.1.2 PRN1008 and PRN473 reduce Btk and PLCγ2 tyrosine phosphorylation

We next investigated whether 2 µM of either PRN1008 or PRN473 block phosphorylation of Btk and the downstream mediator of CLEC-2 signalling, PLCγ2, following CLEC-2 activation by rhodocytin (Figure 3.37). Both inhibitors reduced phosphorylation of Btk at tyrosine 223 in the presence and absence of secondary mediators (Figure 3.37 A-B). Furthermore, PLCγ2 phosphorylation at tyrosine 1217 was also reduced by both PRN1008 and plus secondary mediator inhibition (Figure 3.37 A & C). No other effects on tyrosine phosphorylation were observed when blotting for total tyrosine phosphorylation (Figure 3.37). These results, and those from the aggregation experiments, suggest that although both Btk inhibitors can reduce phosphorylation of Btk and PLCγ2 in the presence of secondary mediators, this is not enough to block rhodocytin-induced platelet aggregation.

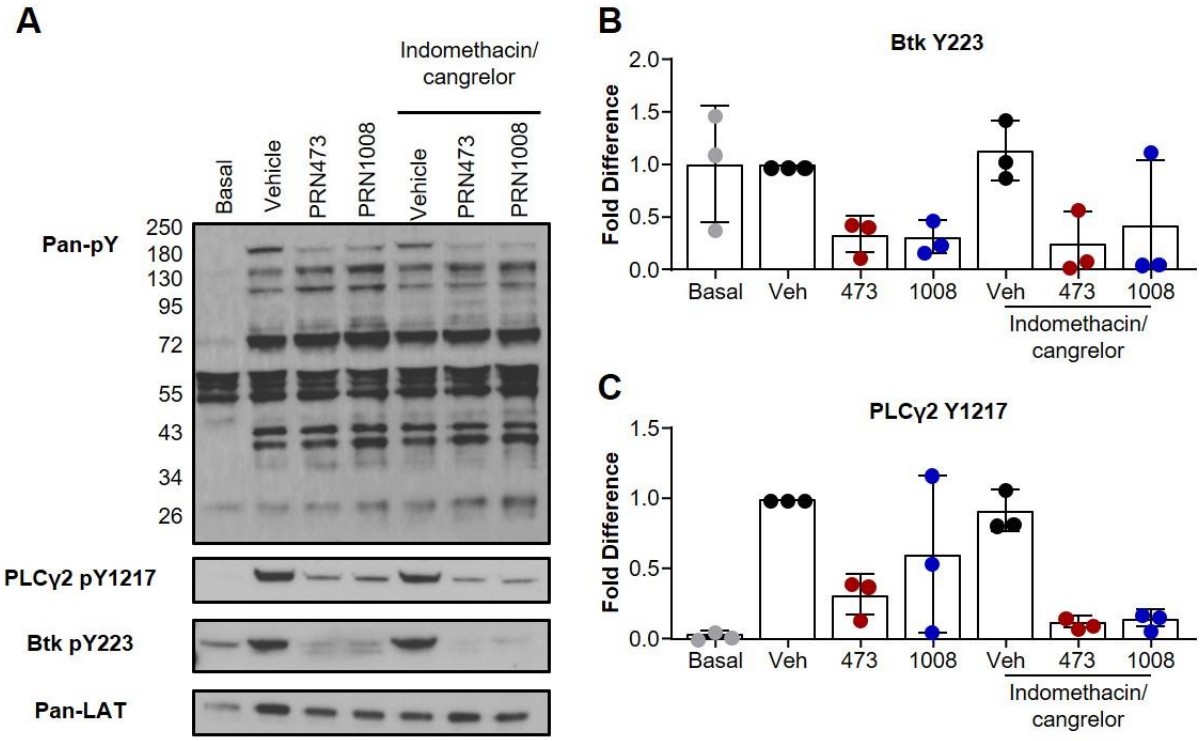

Figure 3.37 PRN1008 and PRN473 reduce phosphorylation of Btk and PLCγ2 in both the presence and absence of secondary mediators in mice.
The effect of PRN473 and PRN1008 on pan tyrosine phosphorylation (4G10) as well as phosphorylation of PLCγ2 Y1217 and Btk Y223 following stimulation of washed platelets with 100 nM rhodocytin was determined by Western blotting. The effect of Btk inhibition on tyrosine phosphorylation was also compared in the presence and absence of the secondary mediator inhibitors cangrelor and indomethacin (10 µM). Platelets were stimulated for 3 min at 37°C

under stirring conditions and were pre-treated with 9 µM eptifibatide to prevent aggregation. (A) Representative western blots of total, PLCγ2 1217 and Btk 223 tyrosine phosphorylation under basal conditions and following platelet stimulation with rhodocytin in the presence of DMSO vehicle, 2 µM PRN473 or 2 µM PRN1008 with and without secondary mediator inhibition. (B) Quantification of Btk Y223 phosphorylation normalised to the LAT loading control and shown as fold difference compared to vehicle in the presence of secondary mediators. (C) Quantification of PLCγ2 Y1218 phosphorylation normalised to the LAT loading control and shown as fold difference compared to vehicle in the presence of secondary mediators. Each symbol represents one mouse, n =3. Data are shown as mean ± standard deviation. pY, tyrosine phosphorylation; veh, vehicle.

3.6.2 *Ex vivo* effect of a PRN473 diet on platelet activation

To test the effects of Btk inhibition *in vivo*, a diet formulated to contain 6.66 g/kg PRN473 was used. Mice were fed this diet or a control diet for 7 days and the effect of the Btk inhibitor on platelet activation was investigated at days 5 and 7. Importantly, neither diet had a negative effect on bodyweight over the 7-day period (Figure 3.38). Platelet activation, as determined by integrin activation and granule secretion, was reduced in response to rhodocytin at both a low and high concentration after 5 and 7 days on the inhibitor diet. However, this reduction in CLEC-2 mediated activation was greater after 7 days (Figure 3.39). A slight decrease in GPCR-mediated granule secretion induced by PAR4 peptide was observed on day 5 and a slight increase in integrin activation on day 7 (Figure 3.39 B-C). GPVI-mediated platelet activation was also reduced after both 5 and 7 days on the PRN473 diet (data not shown and Smith *et al*., unpublished).

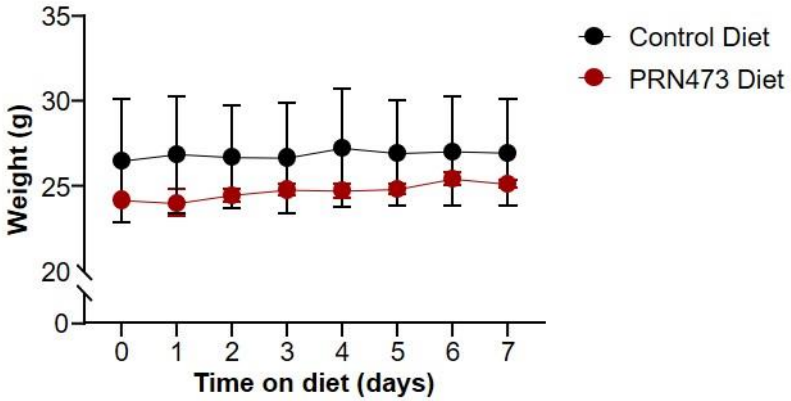

Figure 3.38 PRN473 diet has no effect on bodyweight.

WT mice were fed a diet containing 6.66 g/kg PRN473 or a control diet for 7 days and bodyweight was recorded daily. No changes in bodyweight were observed with either diet, two-way ANOVA, P = 0.99. n = 3. Data are shown as mean ± standard deviation.

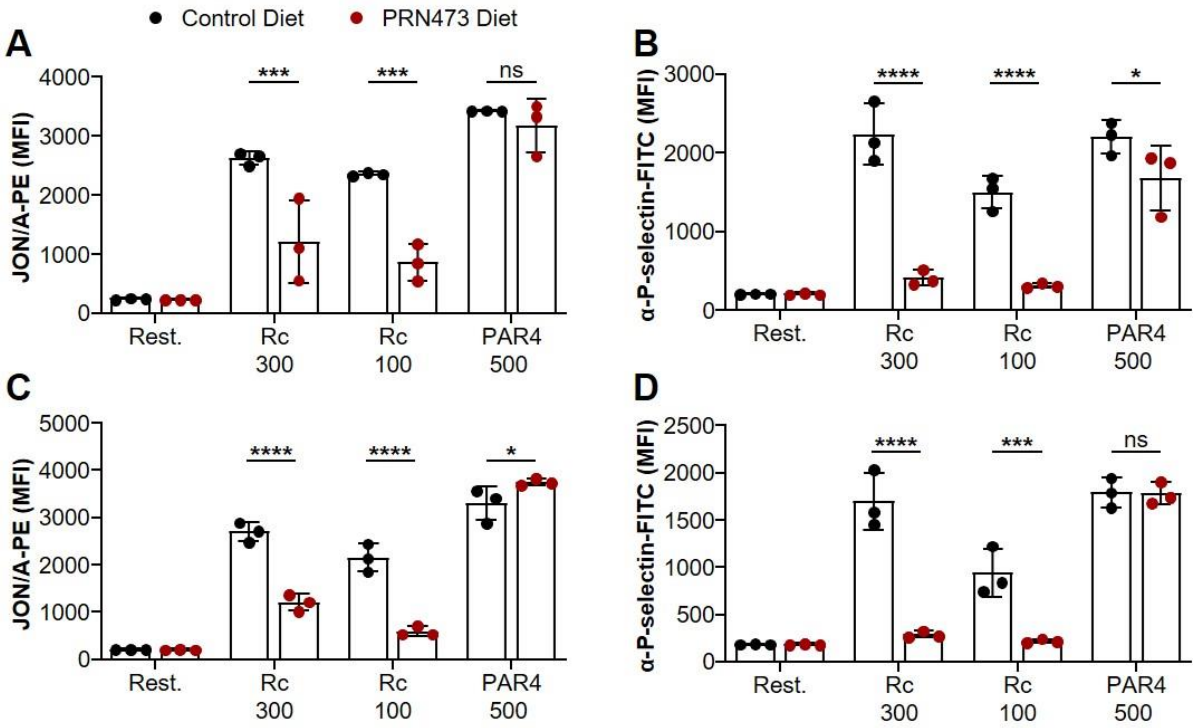

Figure 3.39 PRN473 diet reduces CLEC-2 mediated platelet activation.
Mice were feed on a PRN473 (6.66 g/kg) containing or control diet for seven days and the effect of the Btk inhibitor on rhodocytin (100 or 300 nM) and PAR4 peptide (500 nM) induced platelet activation at days five and seven was determined using saturating concentrations of JON/A-PE (integrin activation) and anti-P-selectin-FITC (degranulation). (A) Integrin activation after 5 days on the PRN473 diet, P = 0.0002 and 0.0001 for 300 and 100 nm rhodocytin respectively and P = 0.80 for PAR4 peptide. (B) Granule secretion after 5 days on the PRN473 diet. P < 0.0001 at both concentrations of rhodocytin and P = 0.046 for PAR4 peptide. (C) Integrin activation after 7 days on the PRN473 diet. P < 0.0001 at both concentrations of rhodocytin and P = 0.040 for PAR4 peptide. (D) Granule secretion after 7 days on the PRN473 diet, P < 0.0001 and P = 0.0002 for 300 and 100 nM rhodocytin respectively and P > 0.99 for PAR4 peptide. Data were analysed by one-way ANOVA followed by Sidak's multiple comparison test. * P < 0.05, *** P < 0.001 and **** P < 0.0001. Each symbol represents one mouse, n = 3. MFI, mean fluorescence intensity; Rest, resting; PE, phycoerythrin; FITC, fluorescein isothiocyanate; Rc, rhodocytin; PAR4, PAR4 peptide; ns, not significant.

3.6.3 PRN473 in a *Salmonella typhimurium* infection induced thrombosis model

As the PRN473 diet inhibited CLEC-2-mediated platelet activation *ex vivo*, we next investigated whether Btk inhibition had an effect on thrombosis caused by STm infection. After 7 days on the PRN473 or a control diet mice were injected intraperitoneally with attenuated

STm and livers were removed at the peak of thrombus formation 7 days after infection.[59] Liver sections were then analysed and thrombus size as well as podoplanin and P-selectin expression were calculated.

Liver sections were stained with either H&E or by immunofluorescence and the large portal vein vessels were analysed to determine the percentage of each vessel containing thrombi. By H&E staining there was no difference in relative thrombus area between control and PRN473 treated mice (Figure 3.40). Similar results were found with immunofluorescent staining although a trend for an increased thrombus size was observed in mice on the PRN473 diet (Figure 3.41 A and E). However, the number of thrombi in large vessels was more comparable between the control and PRN473 groups (Figure 3.41 B and E). We also investigated the upregulation of podoplanin in blood vessels of the liver following STm infection. Podoplanin expression was similar between the control and PRN473 treated mice however, there was a trend for fewer vessels expressing podoplanin also containing thrombi in the PRN473 treated group (Figure 3.41 C-E).

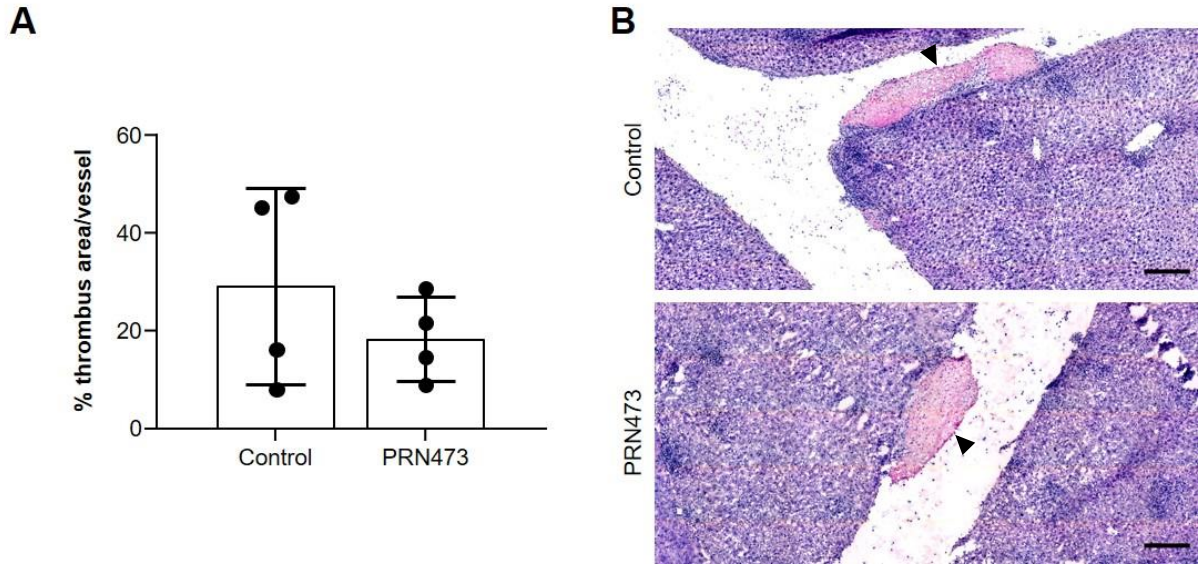

Figure 3.40 Btk inhibition by PRN473 has no effect on thrombus size in the liver following STm infection.
WT mice were fed on a diet containing 6.66 g/kg PRN473 or a control diet for seven days then infected i.p. with attenuated *Salmonella typhimurium*, after a further 7 days on the Btk inhibitor diet livers were removed from the mice and cryosections were stained with H&E. Whole liver sections were then imaged by tile scanning using a slide scanner and thrombus area was

determined. (A) The size of thrombi in the large portal vein vessels of the liver was determined relative to the vessel size from whole H&E stained cryosections. Large vessels were considered as those with an area greater than 200,000 AU. There was no difference between control and PRN473 treated mice, unpaired t-test, P = 0.36. Each symbol represents one mouse. (B) Representative H&E images of thrombi in the portal vein from mice on either a control or a PRN473 diet. Black arrow heads indicate thrombi. Scale bars represent 200 µm. n = 4.

P-selectin expression was investigated as a measure of platelet, endothelial cell and immune cell activation. P-selectin was expressed on the inside of blood vessels as well as both in and around thrombi. Staining around the edges of thrombi and in other areas of the liver coincided with areas with a high number of nuclei suggestive of infiltrating immune cells (Figure 3.42A). Although the percentage area of P-selectin expression did not differ significantly between mice on the control and PRN473 diet, there was a trend for increased expression in the PRN473 treated group (Figure 3.42B). However, the intensity of P-selectin staining in thrombi did not differ between mice treated with either PRN473 or control (Figure 3.42C).

Overall, these results suggest that inhibition of Btk by PRN473 has no effect on STm-induced thrombosis despite inhibition of CLEC-2-mediated platelet activation *ex vivo*. There were no differences in either thrombus size or number in the livers of control or PRN473 treated mice. There was also no difference in upregulation of the CLEC-2 ligand podoplanin either in or around blood vessels between the two groups, although in PRN473 treated mice there was a trend for fewer of these vessels containing thrombi consistent with Btk inhibition reducing platelet activation mediated by podoplanin and CLEC-2. Furthermore, platelet and endothelial activation, measured by P-selectin expression, was comparable between control and PRN473 treated mice, although a trend for increased expression existed in mice on the PRN473 diet, most likely from increased endothelial P-selectin expression.

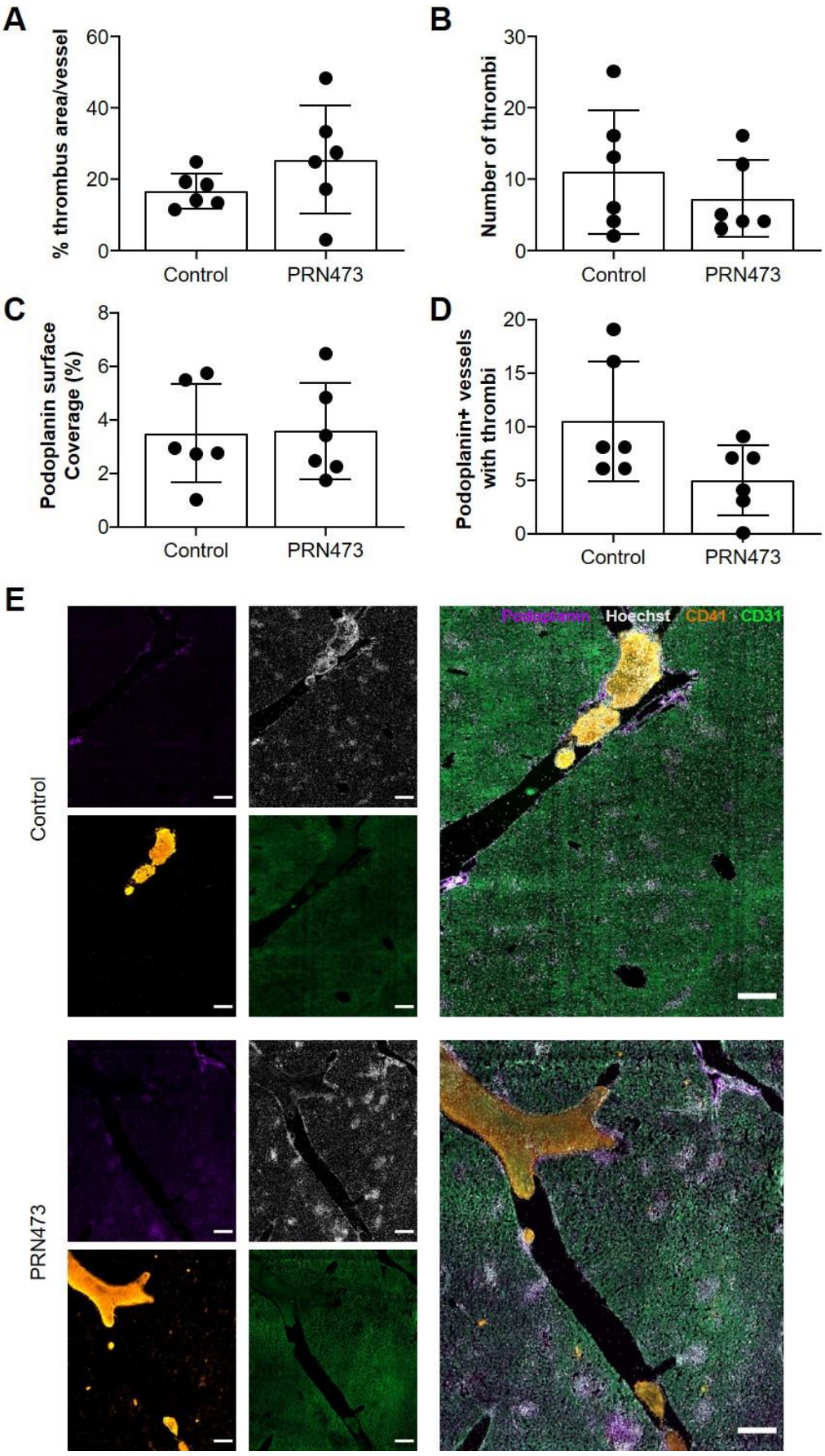
A
% thrombus area/vessel
60
40
20
0
Control
PRN473
B
Number of thrombi
30
20
10
0
Control
PRN473
C
Podoplanin surface Coverage (%)
8
6
4
2
0
Control
PRN473
D
Podoplanin+ vessels with thrombi
20
15
10
5
0
Control
PRN473
E
Control
PRN473
Podoplanin
Hoechst
CD41
CD31

Figure 3.41 Btk inhibition by PRN473 had no effect on thrombus size or podoplanin expression in the liver following STm infection.
WT mice were fed on a diet containing 6.66 g/kg PRN473 or a control diet for seven days then infected i.p. with attenuated *Salmonella typhimurium*, after a further 7 days on the Btk inhibitor diet livers were removed from the mice and cryosections were stained for podoplanin, platelets (CD41), vessels (CD31) and nuclei (Hoechst). Whole liver sections were then imaged by tile scanning using a slide scanner and thrombus area, number and podoplanin coverage were determined. (A) The size of thrombi in the large portal vein vessels of the liver was determined relative to the vessel size, P = 0.26 between PRN473 and control treated mice. (B) The number of thrombi in large portal vein vessels was compared between the control and PRN473 groups, P = 0.40. (C) Total podoplanin surface coverage was determined from 5 representative fields of view per liver section. P = 0.94 between PRN473 and control treated mice. (D) The total number of blood vessels that had upregulated podoplanin expression and contained thrombi was compared between the control and PRN473 groups, P = 0.064. (E) Representative images of liver sections stained for podoplanin (magenta), nuclei (white), platelets (orange) and vessels (green). Large vessels were considered as those with an area greater than 200,000 AU. Scale bars represent 200 µm and each symbol represents one mouse, n = 5-6. Data were analysed from tile scans of organ sections using unpaired t-tests.

Figure 3.42 (below) P-selectin expression in liver sections following STm infection.
WT mice were fed on a diet containing 6.66 g/kg PRN473 or a control diet for seven days then infected i.p. with attenuated *Salmonella typhimurium*, after a further 7 days on the Btk inhibitor diet livers were removed from the mice and cryosections were stained for P-selectin, platelets (CD41), vessels (CD31) and nuclei (Hoechst). Whole liver sections were then imaged by tile scanning using a slide scanner and total P-selectin surface coverage and thrombus P-selectin fluorescent intensity were determined. (A) Representative images from liver sections stained for P-selectin (magenta), nuclei (white), platelets (orange) and blood vessels (green). Individual images for each channel are shown on the left and composite images on the right. Scale bars represent 200 µm. (B) P-selectin expression was analysed by determining the percentage area of P-selectin staining in 5 representative fields of view per organ for each mouse, P = 0.060. (C) P-selectin-A647 intensity of thrombi in large vessels, determined as those with an area of greater than 200,000 AU, P = 0.66. Data was analysed using an unpaired t-test. Each symbol represents one mouse, n = 3-4.

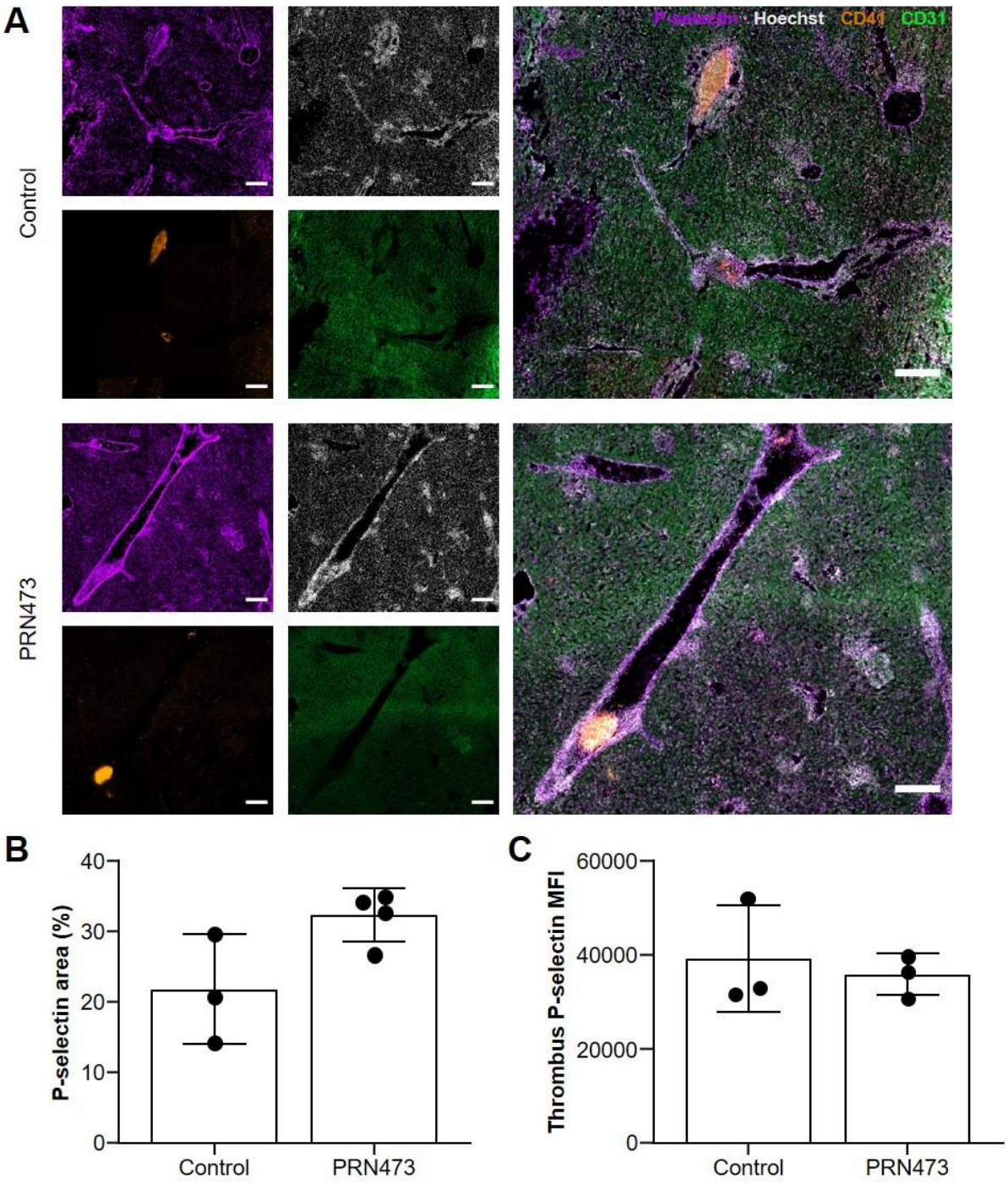
A
Control
PRN473
P-selectin
Hoechst
CD41
CD31
B
P-selectin area (%)
40
30
20
10
0
Control
PRN473
C
Thrombus P-selectin MFI
60000
40000
20000
0
Control
PRN473

4. Discussion

4.1 The role of mouse CLEC-2 in thrombus stability

A role for CLEC-2 in thrombus stability has been proposed several times based on both *in vitro* and *in vivo* experiments in CLEC-2 deficient mice.[7,25,74] However, the exact nature and mechanism of this role have not been elucidated. We therefore, investigated the effect of perfusion of blocking antibody fragments against CLEC-2 over preformed thrombi and compared it to anti-GPVI blocking antibody fragments and Syk inhibition. For these experiments we used a model of the thrombus shell where there is a lesser contribution of coagulation and fibrin to thrombus stability.[23,28]

In our initial experiments flow was discontinuous as perfusion was stopped in order to change syringes between blood, Tyrode's buffer and antibody perfusion. Under these conditions no effect of blocking either GPVI or CLEC-2 were seen (data not shown). However, while these experiments were being conducted Ahmed *et al*. published findings that GPVI had a role in thrombus stability using human blood under continuous flow.[34] Therefore, we set up a continuous flow system using y-shaped tubing and two pumps to investigate whether a similar role of GPVI in thrombus stability exists in mice and whether, under these conditions, the role of CLEC-2 in thrombus stability could be studied.

At arterial shear rates of either 1000 or 1700 s^{-1} perfusion of the Syk inhibitor BI-1002494 over preformed thrombi decreased their stability resulting in increased surface coverage compared to control treated thrombi but no difference in thrombus volume (Figure 3.1). It is possible that the apparent lack of effect of BI-1002494 on thrombus volume is the result of platelets disaggregating but not being washed away by the flow. As Syk inhibition can prevent platelet activation by both GPVI and CLEC-2 the effect of BI-1002494 is likely to be via inhibition of one or both of these signalling pathways.[184] We therefore investigated the contributions of the two receptors to thrombus stability individually. The GPVI blocking antibody fragment JAQ1

reduced thrombus stability only at the higher shear rate whereas the CLEC-2 blocking antibody fragment INU1 only reduced thrombus stability at the lower shear rate (Figures 3.2 and 3.3). The different results under continuous and discontinuous flow could be explained by the build-up of secondary mediators in the periods of stasis under discontinuous flow. During these periods, secondary mediators such as ADP and TxA_2 would no longer be washed away and could therefore accumulate in the thrombi, contributing to further platelet activation and thereby increasing thrombus stability, a process that normally only occurs in the thrombus core.[23,28] Therefore, our initial experiments more closely modelled the outer core, rather than the thrombus shell, where stability and platelet density are greater.[28]

A role for Syk in human thrombus stability has been described previously.[187] Perfusion of blood treated with the Syk inhibitor PRT060318 over untreated thrombi decreased thrombus volume, both compared to initial thrombus size, and in comparison to control treated blood.[187] Effects of Syk inhibition on initial thrombus formation have been attributed to GPVI whereas effects on thrombus stability are less clear but could also be mediated by GPVI in light of the recent findings on its role in stability.[34,187] In our experiments we used the Syk inhibitor BI-1002492 which has been shown to block both GPVI and CLEC-2-induced platelet activation in mice.[184] We found a small decrease in stability of mouse thrombi, although this appeared to be less pronounced to that seen for human thrombi using PRT060318.[187] Although results with PRT060318 on mouse thrombi were similar to those with BI-1002492 (data not shown), suggesting that the use of a different inhibitor does not account for the reduced effect on stability. However, this could instead be the result of the different methods used, as PRT060318 was perfused over preformed thrombi in blood and therefore prevents further thrombus formation as well as causing thrombus disaggregation or it could be due to a species difference.[187]

The role of GPVI in thrombus stability has been shown to be shear dependent, with a greater effect of ACT017 at higher shear rates in humans.[34] We therefore tested two arterial shear

rates and in agreement with the findings on human thrombi only found an effect of JAQ1-Fab on thrombus stability at the higher of the two. However, the effect we observed was minor, and unlike Ahmed *et al*. we could not analyse the difference between the number of thrombi disaggregating as mouse thrombi appear to be less stable than human in general.[34] This has been observed by our groups and was also recently published by Janus-Bell *et al*.[37] This study also suggested that GPVI did not have a role in thrombus stability in mice as perfusion of blood from GPVI knockouts over preformed WT thrombi did not lead to a reduction in thrombus size compared to perfusion of control blood.[37] However, they did not investigate whether perfusion of GPVI inhibitors over preformed mouse thrombi had an effect as their main measure of stability, thrombus disaggregation, could not be determined.[37] While our results agree that mouse thrombi disaggregate even in the absence of inhibitors, we found that JAQ1-Fab perfusion further disaggregated thrombi (Figure 3.2). The role of GPVI in thrombus stability has previously been suggested to be via its interaction with fibrinogen.[34,37] This would account for the absence of an effect on thrombus stability in GPVI knockout mice as mouse GPVI does not interact with fibrinogen.[37] Further evidence includes the lack of effect of ACT017, known to block the GPVI-fibrinogen interaction, in thrombus stability in humanised GPVI mice.[34] However, this does not exclude an additional role of GPVI in mouse thrombus stability via an interaction other than with fibrinogen.

CLEC-2 has been proposed to have a role in thrombus stability via an interaction with an unknown intravascular ligand following observations of unstable thrombus formation in CLEC-2 deficient mice.[7,25] However, this role has not been further investigated. Here we aimed to block CLEC-2 after thrombus formation to investigate if this would decrease stability. We found a much smaller effect on thrombus stability after perfusion of INU1-Fab than in previous *in vitro* and *in vivo* experiments using CLEC-2 deficient mice.[7,25] However, we allowed thrombi to form in the presence of CLEC-2, unlike in previous experiments, and therefore effects on thrombus stability could be separated from those on thrombus formation, which could account for the

greater loss of stability in CLEC-2 deficient mice. It has been previously shown that the role of CLEC-2 in thrombus stability is mediated via its role as an adhesion receptor and not due to CLEC-2-induced platelet activation.[74] Therefore, it is possible that the limited effect of INU1-Fab was due to at least some of the CLEC-2 receptors already being occupied. We have shown that Fab fragments can penetrate the outer layers of a thrombus when perfused after formation using Dylight 488 conjugated p0p6-Fab (data not shown) and therefore it is unlikely that the results seen with INU1-Fab are due to a failure of the Fab fragments to penetrate the thrombus.

Overall, we have found GPVI and CLEC-2 to have minor roles in mouse thrombus stability at lower and higher arterial shear rates respectively, with inhibition of Syk, which reduces platelet activation by both GPVI and CLEC-2, reducing thrombus stability at both shear rates. This suggests there could be shear dependent contributions of both GPVI and CLEC-2 in thrombus stability although to a lesser extent than GPVI in human thrombi and in mice deficient in CLEC-2.[7,25,34]

4.2 hCLEC-2 can compensate for mCLEC-2 during development and in platelet activation

Previous knockout or genetically modified CLEC-2 mouse lines have been characterised by developmental defects resulting in lethality, as have mice deficient in podoplanin and the downstream mediators of CLEC-2 signalling Syk, SLP-76 or PLCγ2.[5-7,70-74] These mice have a defect in the separation of blood and lymphatic vessels that results in a disorganised vasculature with blood-filling of the lymphatic system.[7,70] Lymphatic drainage is also defective and brain haemorrhage, as well as respiratory defects, have been observed in these mice.[5-7] These defects not only occur following constitutive CLEC-2 deficiency but also following conditional knockout of CLEC-2 in the platelet and megakaryocyte lineage, although in these mice lethality, as well as blood-filling of the lymphatic vessels, are reduced.[5,72,73] Furthermore,

lethality also occurred in CLEC-2 Y7A knockin signalling null mice, which in addition to the lymphatic defect observed in mice deficient in mediators of CLEC-2 signalling, suggests it is platelet activation via CLEC-2 that is needed for vessel separation in development.[5,6,71,74]

As a result of these findings in other mouse lines in which CLEC-2 has been genetically modified, it was possible that lymphatic defects would also be observed in hCLEC-2^{KI} mice. This could have occurred if hCLEC-2 could not bind to mouse podoplanin or if this interaction did not result in sufficient platelet activation. However, the reduced separation defect observed in conditional CLEC-2 knockout mice (*Clec1b*$^{fl/flPF4Cre+}$ and *Clec1b*$^{fl/fl}$*GPIbα-Cre* mice) suggests that activation of a small number of residual receptors is sufficient to prevent lethality, if not to completely prevent blood-filling of the lymphatic vessels.[5] Therefore, our initial characterisation of the hCLEC-2^{KI} mice was focussed on the separation of blood and lymphatic vessels.

Pups born to heterozygous hCLEC-2^{KI} parents showed a Mendelian ratio between WT, heterozygous and hCLEC-2^{KI} at the time of weaning suggesting that there was no embryonic or neonatal lethality associated with replacing mCLEC-2 with hCLEC-2 (Table 3.1). However, conditional CLEC-2 knockout mice are also born at Mendelian ratio but still have defective blood and lymphatic vessel separation.[5,72] We therefore, investigated platelet count and other blood parameters as well as the heart rate and blood pressure of hCLEC-2^{KI} compared to WT controls that could give an indication of blood-filled lymphatic vessels. Circulating platelet count is reduced in both *Clec1b*$^{fl/flPF4Cre+}$ and *Clec1b*$^{fl/fl}$*GPIbα-Cre* conditional CLEC-2 knockout mice and Y7A mutant mice as a result of a portion of the blood being in lymphatic vessels.[5,72-74] However, we observed no differences in platelet count between WT and hCLEC-2^{KI} mice (Figure 3.5), although for both genotypes platelet counts were higher in male than female mice which has previously been reported.[188] In addition, altered immune cell counts could indicate infection and a decrease in red blood cell count, as well as in haemoglobin or haematocrit, could indicate a portion of the blood is not circulating and could therefore have leaked into lymphatic vessels, as shown previously in CLEC-2 knockout mice.[45] However, no differences

in these parameters were observed in hCLEC-2^{KI} mice (Table 3.2), neither were differences in blood pressure or heart rate which could have indicated a reduced volume of circulating blood (Figure 3.6). These results differ from those of CLEC-2 knockout mice and therefore suggest that hCLEC-2^{KI} mice do not have defective blood and lymph vessel separation.[5,45,72]

To further confirm the lack of a lymphatic vessel separation defect as well as to compare organ morphology between hCLEC-2^{KI} and WT mice we imaged intestines and stained organ sections from these mice. The disorganised nature of the vasculature as well as the increase in blood due to leakage into the lymphatic vessels can be observed in the intestines of conditional CLEC-2 knockout and Y7A mice.[5,72-74] We therefore, imaged intestines from hCLEC-2^{KI} mice and compared them to both WT and *Clec1b*$^{fl/fl;PF4Cre+}$ mice (Figure 3.7). hCLEC-2^{KI} mice were comparable to WT whereas *Clec1b*$^{fl/fl;PF4Cre+}$ mice had a more disorganised vasculature and increased visible blood. This is consistent with previous observations in *Clec1b*$^{fl/fl;PF4Cre+}$ mice and further suggests hCLEC-2^{KI} do not have a defect in vessel separation.[5,73] In addition, intestine morphology appeared normal in hCLEC-2^{KI} mice as did those of lymph nodes, brains, livers, spleens and bones (Figure 3.8) suggesting there are no developmental defects in hCLEC-2^{KI} mice.

Together, these data show that hCLEC-2^{KI} mice do not have defective separation of blood and lymphatic vessels during development. They further suggest that human CLEC-2 can compensate for the lack of mouse CLEC-2 during development and that the CLEC-2 signalling and platelet activation required to separate blood and lymphatic vessels during development are unaffected in hCLEC-2^{KI} mice.[70,76] This is perhaps unsurprising when the sequence homology between human and mouse CLEC-2, including conservation of the ligand binding domain, cytoplasmic tail, hemITAM motif and the glycosylation sites required for translocation to the cell surface, is considered.[43] These similarities would suggest that CLEC-2 surface expression and signalling would be unaffected in the presence of human rather than mouse CLEC-2.

To confirm that CLEC-2 expression and platelet function were indeed normal in hCLEC-2^{KI} mice, we investigated the surface expression of platelet receptors as well as platelet activation and aggregation responses to GPCR, GPVI and CLEC-2 platelet agonists. CLEC-2 expression has been previously determined by flow cytometry and proteomics in both human and mouse platelets, with similar copy numbers having been observed using the two methods, indicating a 20-fold difference in CLEC-2 expression between human and mouse platelets.[40,47-49] However, we found that relative CLEC-2 expression between hCLEC-2^{KI} and human platelets had only an approximately 2.5-fold difference (Figure 3.9A). It is possible that differences in methodology account for the greater difference in murine CLEC-2 observed in previous flow cytometry experiments in which expression was quantified using beads with a known capacity for IgG binding.[40,49] In contrast, we determined relative CLEC-2 expression based on the MFI of AYP1-FITC binding. In previous experiments it was not possible to determine CLEC-2 expression on human and murine platelets using the same antibody due to their high specificity. However, this was made possible using hCLEC-2^{KI} mice as a measure of CLEC-2 expression on murine platelets. Furthermore, previous CLEC-2 surface expression levels in humans and mice originate from two separate experiments using different calibration beads, which could limit comparisons between the two.[40,49]

In contrast to our results on CLEC-2 expression by flow cytometry, quantification of CLEC-2 in platelet lysates by Western Blotting suggested am approximately 2-fold higher expression of CLEC-2 in human rather than hCLEC-2^{KI} mice (Figure 3.9 B-C). This could suggest that in human platelets CLEC-2 is predominantly intracellular however, it could be possible that upon platelet activation it translocates to the cell surface. This has previously been suggested in mouse platelets where CLEC-2 surface expression was increased on activated compared to resting platelets. It was further suggested that some CLEC-2 could be stored in alpha granules as there was less increase in CLEC-2 surface expression in Nbeal2 knockout mice which lack this granule type.[189] However, it is not known if this also occurs in human platelets. We also

observed that CLEC-2 from human and hCLEC-2^{KI} platelets appear to have different molecular weights. This was observed using three anti-hCLEC-2 antibodies: AYP2, HEL1 and AYP1 (Figure 3.9C, Figure 3.18A and data not shown, respectively) suggesting it is independent of the antibody used. Using AYP2 both forms of hCLEC-2 are apparent as a doublet of approximately 32 and 40 kDa in human platelets, consistent with previous reports,[40] and 40 and 45 kDa in hCLEC-2^{KI} platelets. In contrast murine CLEC-2 was apparent as a singlet of approximately 32 kDa, consistent with previous findings.[25] In human platelet lysates the 32 kDa band was dominant with lower expression of the 40 kDa band which is similar to result reported by Suzuki-Inoue *et al*.[38] However, in hCLEC-2^{KI} platelets both bands have a similar expression. The doublet observed in human platelets has been attributed to differential glycosylation and it is possible this also accounts for the higher molecular weight of CLEC-2 from hCLEC-2^{KI} platelets.[38]

In spite of the higher molecular mass of CLEC-2 in hCLEC-2^{KI} mice, platelet function was largely normal in response to both CLEC-2 and other agonists. Surface expression of all platelet receptors tested were comparable to WT mice (Table 3.3) as were platelet activation and aggregation induced by GPCR and GPVI agonists (Figure 3.10 and Figure 3.11). This was as expected as even CLEC-2 deficient mice have no defects in platelet receptor expression or platelet activation other than for CLEC-2.[7,25,73] In contrast, no difference in platelet activation induced by rhodocytin was observed compared to WT platelets (Figure 3.10). Furthermore, although there was an increase in lag time following rhodocytin-induced platelet aggregation in both hCLEC-2^{KI} and heterozygous mice, maximal aggregation was comparable to that of WT mice (Figure 3.12C). In addition, lag time was increased to a greater extent in human platelets stimulated with rhodocytin, suggesting this is due to a species difference rather than a defect in CLEC-2-induced platelet activation in hCLEC-2^{KI} mice. hCLEC-2^{KI} platelets are also activated by AYP1 and to a far greater extent than WT platelets in response to INU1 (Figure 3.10). However, in aggregation experiments AYP1 and INU1 induced aggregation to a similar

extent in hCLEC-2^{KI} and WT platelets respectively, although with INU1 a greater lag time was observed, particularly in heterozygous mice (Figure 3.12 A-B). Together this suggests that hCLEC-2^{KI} platelets have normal activation responses, including to CLEC-2 agonists.

To further investigate platelet function in hCLEC-2^{KI} mice we compared spreading on fibrinogen, CRP and mouse podoplanin with WT platelets. No spreading defects were expected on fibrinogen or CRP as CLEC-2 deficient platelets still spread on ECM components including the GPVI agonist collagen and no other platelet defects were so far observed in hCLEC-2^{KI} mice.[7] Consistent with this, spreading was comparable between WT and hCLEC-2^{KI} platelets on both fibrinogen and CRP (Figure 3.13 A-B). However, spreading was reduced on mouse podoplanin; although platelets still became activated and formed both filopodia and lamellipodia there were few fully spread platelets in contrast to WT mice (Figure 3.13C). However, no unspread platelets were observed. It has previously been shown that human platelets can form small aggregates on recombinant mouse podoplanin under flow although to a lesser extent than mouse platelets.[190] It has also been suggested that differences in platelet adhesion to human podoplanin in humans and mice could be due to a difference in affinity of mouse CLEC-2 for human podoplanin.[190,191] This could also explain the reduced spreading of hCLEC-2^{KI} platelets on mouse podoplanin. However, the extent of hCLEC-2^{KI} platelet activation appears to be sufficient for separation of blood and lymphatic vessels during development as no defect was observed. We also attempted to investigate the spreading of hCLEC-2^{KI} platelets on recombinant human podoplanin, but few platelets adhered and none spread (data not shown). This could be because platelet binding to recombinant human podoplanin is much lower than to podoplanin on LECs, most likely as a result of reduced podoplanin mobility preventing cluster formation and therefore platelet activation.[69,191] Furthermore, hCLEC-2 and human podoplanin have 3 orders of magnitude lower affinity compared to mCLEC-2 and mouse podoplanin which could further explain the spreading

results on podoplanin as it is possible that the CLEC-2 podoplanin interaction is less important in humans than mice.[190,192]

Overall, these results suggest that platelet function is normal in hCLEC-2^{KI} mice in terms of both receptor expression and activation. Furthermore, they suggest that although the interaction between hCLEC-2 and mouse podoplanin may be reduced compared with mCLEC-2, it is still sufficient for blood and lymphatic vessel separation during development. This is because such defects were not observed in hCLEC-2^{KI} to any extent, unlike in constitutive and conditional CLEC-2 knockout mice. As a result, hCLEC-2^{KI} mice could be a suitable model in which anti-hCLEC-2 agents can be tested as results would not be affected by either defective vessel development or abnormal platelet function.

4.3 Anti-hCLEC-2 antibodies activate CLEC-2 independently of their binding site

We generated the anti-human CLEC-2 antibody HEL1 to use in addition to AYP1 to test hCLEC-2^{KI} mice as a model in which potential drugs targeting hCLEC-2 could be tested *in vivo*. HEL1 is specific to hCLEC-2 and can bind to it in flow cytometry, Western blotting and immunoprecipitation (Figure 3.18 and Figure 3.19). During the characterisation of HEL1 it became apparent that it had a different binding site to AYP1 on hCLEC-2 with a competitive binding experiment showing that both antibodies could bind at the same time (Figure 3.19A). Although this was most likely due to chance, it is possible that the different binding site is the result of the way in which the rats were immunised. As AYP1 was used to immunoprecipitate CLEC-2 from human platelet lysates the rats may not have been able to produce antibodies against this site as AYP1 could have remained bound. As a result of the different binding site, HEL1 Fab fragments do not block rhodocytin-induced platelet activation, something previously reported for AYP1 (Figure 3.19B).[40] Despite binding to different sites both HEL1 and AYP1 can activate hCLEC-2^{KI} platelets (Figure 3.12 and Figure 3.19B). Activation of human platelets by antibodies is complicated by the presence of the FcγRIIA receptor which can be activated by

the Fc portion of IgG antibodies and is not present in mice.[138] Therefore activation of hCLEC-2 has not previously been shown for AYP1, although crosslinking AYP1-Fab with an anti-mouse $F(ab')_2$ fragment can induce platelet activation.[40] However, even if the FcγRIIA receptor is blocked using IV.3 a goat anti-hCLEC-2 antibody has been shown to activate human platelets resulting in CLEC-2 phosphorylation.[38] This suggests that CLEC-2 dimerisation by anti-hCLEC-2 antibodies is sufficient to cause platelet aggregation and that this is independent of the antibody binding site.

4.4 hCLEC-2 can be immunodepleted

It was previously not possible to investigate whether hCLEC-2 could be immunodepleted as this cannot be easily achieved *in vitro*, with experiments investigating the regulation of human CLEC-2 concluding that it was not regulated.[40,81] Furthermore, unlike for GPVI, no patients have been identified with CLEC-2 depletion due to autoantibodies.[193] Therefore, hCLEC-2^{KI} mice provide the first possibility to investigate antibody-mediated depletion of CLEC-2 from platelets.[16] On the other hand, immunodepletion of mouse CLEC-2 has been known about for over a decade and has been a useful model to investigate the role of CLEC-2 in thrombosis.[25,73] We used AYP1 and HEL1 to investigate whether hCLEC-2 could be depleted from hCLEC-2^{KI} platelets and compared this to depletion of mCLEC-2 by INU1.

Unexpectedly i.v. administration of AYP1 at a low dose of 10 µg was lethal with 3 out of the 4 mice injected dying within 30 min. All hCLEC-2^{KI} and heterozygous mice exhibited laboured breathing, although in most of those that survived this had returned to normal after 30 min. This was the result of microthrombi becoming trapped in the vascular bed of the lungs and also resulted in oedema (Figure 3.21 and Figure 3.22). Microthrombi were also observed in the lungs of WT mice treated with INU1, although these were smaller than in AYP1 treated hCLEC-2^{KI} mice. Thrombi were not observed in any other organ (Figure 3.23). It has been previously hypothesised that INU1 induced platelet aggregation, and therefore microthrombus

formation, upon *in vivo* administration is responsible for the associated thrombocytopenia due to microthrombi becoming trapped in the lungs or being cleared by the spleen.[81] When platelet activation was not inhibited microthrombi became trapped in the lung vasculature whereas in the absence of platelet integrin activation no aggregates formed and platelets were instead observed in the spleen.[81,186] This suggests that platelets become activated by antibody administration, aggregate and become trapped in the capillaries of the first vascular bed they encounter. The greater effect of AYP1 administration compared to INU1 could be due to faster and/or greater platelet activation, something we observed both by flow cytometry and platelet aggregation (Figure 3.10 and Figure 3.12). This could account for there being more or larger thrombi in the lungs of AYP1 treated hCLEC-2^{KI}, mice which would result in the more severe effect on breathing.

The experiments with i.v. administered AYP1 also showed that hCLEC-2 could be depleted from platelets in the surviving hCLEC-2^{KI} and heterozygotes and that this was accompanied with transient thrombocytopenia as with INU1 in WT mice (Figure 3.20B).[73] This was in spite of the dose of AYP1 being approximately 6 to 8-fold lower than that used by May *et al*., although a similar effect on platelet count was observed with the same dose of INU1 (data not shown).[25] Furthermore, results from heterozygous hCLEC-2^{KI} mice show that only hCLEC-2 is depleted from the platelets, although there is a slight drop in mCLEC-2 expression over the first 4 h, it returns to normal one day after administration and occurs at a time when the platelet count is severely reduced (Figure 3.20 C-D). This could suggest that human and mouse CLEC-2 do not form dimers in hCLEC-2^{KI} heterozygotes, if they did then a decrease in mCLEC-2 expression would be observed as both receptors in a dimer would be depleted. However, as CLEC-2 has been proposed to be both a monomer and a dimer under basal conditions, while dimers are needed only for activation,[7,67] the minimal reduction in mCLEC-2 expression is likely to be the result of AYP1 only dimerising hCLEC-2 receptors due to its high specificity.

We confirmed the initial results that hCLEC-2 could be immunodepleted from i.v. administration of AYP1 by i.p. injection. With this route of administration there would be slower entry of AYP1 into the circulation and therefore it is likely that fewer or smaller aggregates would form and be cleared without severe adverse effects. This would likely also result in initial thrombocytopenia preventing further aggregate formation. Indeed, i.p. injection of AYP1 was well tolerated in hCLEC-2^{KI} mice which appeared comparable to both INU1 and HEL1 treated mice in terms of their breathing, even at a 10-fold higher concentration compared to the i.v. dose. Administration of either AYP1 or HEL1 resulted in transient thrombocytopenia comparable to INU1 in WT mice (Figure 3.24).[25] This lasted for 3 to 4 days before the platelet count returned to baseline levels.

All three antibodies could only be detected on the platelet surface for up to 24 h after administration suggesting that the decrease in CLEC-2 surface expression was not the result of the injected antibody blocking the CLEC-2 binding site (Figure 3.24 D-E). Complete CLEC-2 depletion lasted for 11 days with both HEL1 and AYP1 administration, with levels returning to baseline after an average of 24 and 18 days respectively, whereas INU1-induced depletion lasted for 7 days and returned to normal by 14 days post antibody administration (Figure 3.2 B-C). hCLEC-2 was not only depleted from the platelet surface but also intracellularly with no CLEC-2 being detectable for 10 days following both AYP1 and HEL1 administration and levels returning to normal between 20 and 25 days (Figure 3.25). This is in line with previous findings with INU1, aside from the length of CLEC-2 depletion.[25,81] The longer depletion time of hCLEC-2 compared to mouse could be the result of a species difference or it is also possible that INU1-induced CLEC-2 depletion is unique. To elucidate this, the effect of other anti-mouse CLEC-2 antibodies on receptor expression would need to be investigated and compared to INU1. It is possible that INU1 is the exception due to the unusual findings using INU1-Fab fragments which cause widespread thrombosis upon *in vivo* administration and also deplete CLEC-2.[25,186] To fully understand the difference between depletion of mouse and human

CLEC-2 the mechanism would have to be investigated and compared to that of INU1. For both human and mouse CLEC-2, depletion lasts longer than the platelet lifespan suggesting that the antibodies can bind to megakaryocytes as well as platelets. This has previously been shown for INU1 both *in vitro* and *in vivo*.[81] It has also been shown that INU1-induced depletion occurs by SFK-mediated receptor internalisation and degradation and not by shedding, in both platelets and megakaryocytes.[73] It is possible this mechanism also occurs for human CLEC-2, particularly as no evidence of human CLEC-2 shedding has been observed.[40] However, this study also suggested that CLEC-2 was not regulated whereas we have shown this is not the case, at least in hCLEC-2^{KI} mice.[40]

It is unlikely that a whole antibody would make a good anti-platelet drug due to platelet activation induced by the Fc portion via FcγRIIA, which is present in human but not mouse platelets.[138] Furthermore, with CLEC-2, antibodies appear to be able to activate platelets independently of FcγRIIA and the transient thrombocytopenia that occurs concurrently with receptor depletion could also be a problem therapeutically and could cause an initial increase in bleeding risk.[25,38,81] In mice this has been shown to also occur with Fab fragments of INU1 although further studies have shown that thrombocytopenia can be uncoupled from receptor immunodepletion as these are Syk and SFK mediated respectively.[25,81] We therefore investigated the effect of AYP1-Fab *in vivo*. Initial *in vitro* experiments with hCLEC-2^{KI} platelets were comparable to those previously conducted in human platelets.[40] AYP1-Fab was found to bind to hCLEC-2^{KI} platelets and blocked both rhodocytin and AYP1-IgG induced platelet activation (Figure 3.31). Unexpectedly, CRP-induced activation was also reduced. This could suggest that there is a global reduction in platelet activation or a hemITAM specific reduction but the effect of AYP1-Fab on other mediators of platelet activation would need to be investigated. *In vivo* administration was not lethal, as with INU1-Fab,[186] and did not cause either thrombocytopenia or CLEC-2 depletion (Figure 3.32 A-C), consistent with AYP1-Fab not activating platelets.[25,40] However, no effect on CLEC-2, or GPVI, mediated platelet activation

was observed (Figure 3.32 D-F). Although rhodocytin-induced platelet activation was also low in untreated hCLEC-2^{KI} mice by flow cytometry following *in vivo* administration of AYP1-Fab, only a minor effect was observed on rhodocytin-mediated aggregation where there was full activation of platelets from untreated mice. Maximum aggregation was comparable, but there was a slight increase in lag time between untreated and AYP1-Fab treated mice. Together this suggests that AYP1-Fab has little effect *in vivo* which could be the result of a rapid clearance rate, often observed with Fab fragments,[113,115] as the difference in AYP1- and anti-mouse-FITC binding between untreated and Fab treated mice was reduced compared to *in vitro* incubation.

Overall, our results show that hCLEC-2 can be immunodepleted, although over a longer time period to INU1-induced depletion of mCLEC-2, whereas thrombocytopenia is comparable. Furthermore, i.v. AYP1 but not HEL1 or INU1 is lethal due to microthrombi becoming trapped in the lungs, although this is also seen to a lesser extent with INU1. On the other hand, unlike with INU1, AYP1-Fab does not appear to be lethal or to deplete hCLEC-2 or induce thrombocytopenia. However, it only has a minor effect on CLEC-2 signalling when administered *in vivo*. Together, these results suggest that although both human and mouse CLEC-2 can be immunodepleted, differences exist either between the two species or between the antibodies themselves. Experiments investigating the mechanism of hCLEC-2 depletion as well as with other anti-mouse CLEC-2 antibodies would need to be carried out to further elucidate this.

4.5 Arterial thrombus formation differs between WT, hCLEC-2^{KI} and humans

The role of CLEC-2 in thrombus formation and stability has been extensively investigated in mice but not in humans. We therefore aimed to use hCLEC-2^{KI} mice to elucidate the role of human CLEC-2 in both *in vitro* and *in vivo* thrombosis models as well as blocking CLEC-2 in human blood and investigating the effect on *in vitro* thrombus formation.

In vitro thrombus formation on collagen differed between hCLEC-2^{KI} and WT mice and was dependent on the shear rate with no difference being observed at venous shear in our preliminary experiments (Figure 3.16), only at certain arterial shear rates. Although the experiments at venous shear would need to be repeated to increase the n number and confirm these results. At 1000 s^{-1} hCLEC-2^{KI} had a reduced thrombus surface coverage compared to WT and this reduction was to a similar degree as in *Clec1b*$^{fl/fl;PF4Cre+}$ knockout mice (Figure 3.14). Our results with *Clec1b*$^{fl/fl;PF4Cre+}$ knockout mice are consistent with those previously published in that both thrombus surface coverage and volume are reduced and, although the initial attachment of platelets to the collagen is unaffected, stable thrombi do not form.[7,25] However, this was not the case for the hCLEC-2^{KI} mice in which the thrombi appeared more dense and contracted compared to those from WT mice and in which there was no reduction in thrombus volume. Therefore, the altered thrombus formation in hCLEC-2^{KI} mice is not due to deficient CLEC-2 signalling or adherence which is consistent with our results on platelet function in these mice. We also compared thrombus formation at higher arterial shear rates. At 1200 s^{-1}, both surface coverage and thrombus volume were comparable between WT and hCLEC-2^{KI} mice and in both groups these values were increased compared to those at 1000 s^{-1} (Figure 3.15 A-C). On the other hand, at 1700 s^{-1} hCLEC-2^{KI} mice had both a greater surface coverage and thrombus volume than WT mice (Figure 3.15 D-F).

The differences observed between hCLEC-2^{KI} and WT mice are not likely to be the result of altered GPIb-vWF binding, which mediates platelet tethering at higher shear rates, as platelet attachment to vWF under flow conditions was comparable (Figure 3.17).[19] On the other hand, under non-anticoagulated conditions, and therefore in the presence of high levels of thrombin and fibrin, no difference in surface coverage was observed between WT and hCLEC-2^{KI} mice (data not shown). The results on GPIb-vWF binding and in non-anticoagulated blood are consistent with those in *Clec1b*$^{fl/fl;Pf4Cre+}$ knockout and INU1-depleted mice.[25,73] However, in CLEC-2 deficient mice thrombus stability is reduced, whereas thrombi from hCLEC-2^{KI} mice

appeared to be denser and more contracted than those of WT mice. This could suggest that, while in CLEC-2 deficient mice the presence of thrombin and other secondary mediators of platelet activation overcome the requirement of CLEC-2 in thrombus stability, in hCLEC-2^{KI} mice these secondary mediators are less important for thrombus stability and their presence rather increases the stability of WT thrombi.[25] This could also explain the comparable thrombus formation between WT and hCLEC-2^{KI} mice in preliminary experiments at venous shear (Figure 3.16) as thrombi were larger and flow rate was lower which could allow a greater build-up of secondary mediators within the thrombi and therefore greater platelet activation compared to higher shear rates.[23,28] It could also be possible that thrombi from hCLEC-2^{KI} mice appeared more stable, and at some shear rates larger, than those from WT mice due to increased affinity for the proposed intravascular ligand as a result of human platelets having a lower CLEC-2 expression than hCLEC-2^{KI} or WT mouse platelets (Figure 3.9).[40,47-49] Although this is not the case for podoplanin as hCLEC-2 has a lower affinity than mCLEC-2 for their respective podoplanin.[190,192]

On the other hand, hCLEC-2^{KI} depleted mice had comparable thrombus formation to that reported for WT CLEC-2 depleted mice in our preliminary experiments, although more mice would need to be tested to confirm this. In both CLEC-2 depleted WT and hCLEC-2^{KI} mice initial attachment of platelets to collagen was unaffected however, stable thrombi did not then form as platelets or small aggregates only formed unstable interactions with the collagen adherent platelets (Figure 3.26).[25] These results are also consistent with those from *Clec1b*$^{fl/fl;Pf4Cre+}$ knockout mice where there is also a decrease in thrombus stability, although perhaps to a lesser extent than seen following antibody depletion (Figure 3.14).[7] It has previously been suggested that antibody-induced receptor depletion has other biological effects that then increase the defect in thrombus formation, which could explain this slight discrepancy.[7] However, these results were not seen when the same assay was carried out with washed platelets reconstituted with red blood cells, Ca^{2+} and fibrinogen (Figure 3.27). In

this experiment thrombus surface coverage and volume were comparable between WT, hCLEC-2^{KI} and hCLEC-2^{KI} depleted mice, although thrombi from WT and particularly hCLEC-2^{KI} mice appeared less stable than thrombi formed from whole blood. The main difference between these two assays is the absence of plasma in the reconstituted blood. This suggests that a factor in the plasma could account for the differences in thrombus formation seen between WT, hCLEC-2^{KI} and hCLEC-2^{KI} depleted mice when whole blood is perfused over collagen. A potential explanation for this could be a difference in the proposed intravascular CLEC-2 ligand between human and mouse CLEC-2, either in the ligand itself or in the affinity of its interaction with CLEC-2 from the two species.

Previous studies have suggested the presence of an intravascular ligand for CLEC-2 based on the findings of reduced thrombus formation and stability observed in CLEC-2 deficient mice, however it is yet to be identified.[7,25,73,74] So far it has been suggested that the potential ligand is present either in the plasma or on activated platelets.[7,25] However, the suggested role of this postulated ligand in thrombosis differs between studies with both May *et al*. and Suzuki-Inoue *et al*. suggesting its role is via signalling and platelet activation as co-infusion of secondary mediators rescues the defect in thrombus formation observed in CLEC-2 deficient mice, whereas Haining *et al*, have suggested it is via adhesion rather than signalling as no effect on thrombus formation was observed in CLEC-2 Y7A knockin signalling null mice.[7,25,74] As CLEC-2 signalling was absent in both studies suggesting its role is via platelet activation, it is therefore possible that a role in platelet adhesion also contributed to the defects in thrombus formation and stability seen.[7,25] Our experiments were also conducted in the absence of CLEC-2 and therefore the effect on thrombus formation could also have been the result of CLEC-2 either acting as an activation or an adhesion receptor or both. However, they do suggest that there might be a ligand for both human and mouse CLEC-2 in the plasma and that in hCLEC-2^{KI} mice the interaction with this ligand could result in more stable thrombi than in WT mice, potentially due to increased affinity.

We next aimed to investigate whether the *in vitro* effect of hCLEC-2 depletion on thrombus formation and the differences between WT and hCLEC-2^{KI} mice could also be observed *in vivo* and whether or not they had an effect on haemostasis. No difference in tail bleeding time was observed between either WT, hCLEC-2^{KI} or hCLEC-2^{KI} depleted mice (Figure 3.28). The results for the CLEC-2 depleted mice are in contrast to initial results from INU1 depleted WT mice in which two thirds of mice either failed to stop bleeding during the experiment or had an increased bleeding time compared to WT.[25] However, they were similar to results with CLEC-2 knockout chimeric mice and *Clec1b*$^{fl/fl\ PF4Cre}$ mice which did not differ significantly from WT, although in both cases there was a trend for increased bleeding.[7,73] The reason for this difference between CLEC-2 depleted and knockout has been suggested as INU1 having additional effects *in vivo* that then further inhibit thrombus formation.[7] These results also add further evidence that CLEC-2 only has a minor role in haemostasis.

Following mechanical injury to the abdominal aorta occlusion time did not differ significantly between WT, hCLEC-2^{KI} and hCLEC-2^{KI} depleted mice (Figure 3.29). However, 33% of hCLEC-2^{KI} mice and 11% of depleted did not achieve vessel occlusion whereas this was the case for all WT mice. The results from the CLEC-2 depleted mice are comparable to those from CLEC-2 deficient WT mice in which there was only a trend for increased occlusion time and all vessels occluded (May, unpublished). However, they differ slightly from those with *Clec1b*$^{fl/flPF4Cre+}$ knockout mice, in which 40% of mice did not exhibit vessel occlusion.[74] On the other hand, hCLEC-2^{KI} mice had a trend for increased occlusion time compared to WT mice which was more comparable to previous results with *Clec1b*$^{fl/flPF4Cre+}$ knockout mice.[74]

We also found similar results following $FeCl_3$-induced injury to the mesenteric arterioles with hCLEC-2^{KI} mice having a longer occlusion time than WT and CLEC-2 depleted mice being more similar to WT (Figure 3.30). However, the time to the appearance of the fist thrombi did not differ between the three groups and is therefore comparable to previous experiments in which, despite differences in occlusion time, the appearance of the first thrombi is comparable

between WT and CLEC-2 deficient mice.[25,73,74] While the defect in occlusion time in hCLEC-2^{KI} depleted mice is less pronounced than in initial experiments using INU1 to deplete CLEC-2 by May *et al*.,[25] it is more comparable to results from *Clec1b*$^{fl/flPF4Cre+}$ knockout mice in which 13%[74] or 23%[73] of vessels failed to occlude. This could suggest that the failure of any vessels to occlude in INU1 treated mice could be due to additional effects of the antibody, as previously suggested.[7,25]

The unexpected vessel occlusion defect observed in untreated hCLEC-2^{KI} mice could further suggest a difference in ligand between mouse and human CLEC-2. The shear rate in mouse mesenteric arteries is between 1200 and 1700 s^{-1} however, at these shear rates *in vitro* thrombosis in hCLEC-2^{KI} mice was either comparable or increased compared to WT mice (Figure 3.15).[194] This could therefore suggests that the difference in ligand is not the same as the plasma ligand we have suggested is responsible for the differences observed in thrombus formation in whole and reconstituted blood, as this appeared to cause increased thrombus stability. It could however be possible that a further ligand for hCLEC-2 exists *in vivo*, outside of the blood and therefore potentially on endothelial cells. This could explain the difference in thrombus formation between *in vitro* flow adhesion and *in vivo* thrombosis models as more stable thrombi form from hCLEC-2^{KI} blood due to the presence of a pro-thrombotic plasma borne ligand that is not counteracted by an anti-thrombotic ligand. Whereas in mice either this ligand is not involved in thrombosis or mCLEC-2 on activated platelets has a lower affinity for it than hCLEC-2. As a result, *in vivo*, hCLEC-2^{KI} mice might form less stable thrombi due to anti-thrombotic effect of this ligand, which prevents vessel occlusion. It is possible that these two ligands exist to regulate platelet activation by CLEC-2 and therefore prevent unnecessary activation or limit it to prevent vessel occlusion. This could be instead of receptor shedding, as previously suggested for the ITAM receptor GPVI, but not for CLEC-2.[16,40] Although this theory could explain our results it is purely speculative and further experiments would be needed to

either confirm or disprove it. These could include *in vitro* flow adhesion experiments in the presence of resting or activated endothelial cells with either whole or reconstituted blood.

The effects of blocking CLEC-2-mediated platelet activation have not previously been investigated on thrombus formation in human blood. We therefore used *in vitro* thrombosis assays, similar to those used for mice, to investigate the effect of AYP1-F(ab')$_2$ and Fab fragments on human thrombus formation on collagen. Neither F(ab')$_2$ or Fab fragments of AYP1 had any effect on thrombus formation or stability (Figure 3.33). However, there was a slight decrease in thrombus surface coverage with AYP1-F(ab')$_2$ fragments which could be the result of platelet activation and subsequent aggregate formation either during pre-incubation with the blood or once perfusion began. This would explain why aggregates could be seen in the blood flow with F(ab')$_2$, but not Fab fragments, as it could induce receptor dimerisation as previously observed using a CLEC-2 IgG antibody in the presence of a FcγRIIa inhibitor or following cross-linking of Fab fragments.[38,40] These results differ from those using mice as they suggest that CLEC-2 does not play a role in thrombosis in humans.[7,25,73,74] However, experiments suggesting CLEC-2 has a role in thrombus formation or stability in mice have been carried out in CLEC-2 deficient mice and therefore no interaction of CLEC-2 with its proposed intravascular ligand could occur.[7,25,73,74] On the other hand, in our experiment with human blood, CLEC-2 was still present and only the podoplanin/rhodocytin binding sites were blocked.[40] As these ligands are not present in the vasculature it is unlikely that blocking this binding site on CLEC-2 will have an effect on thrombosis therefore, we also pre-incubated human blood with recombinant hCLEC-2 that would be able to bind to any potential CLEC-2 ligands and prevent or reduce their interaction with platelet CLEC-2. However, we again did not observe any effect on thrombosis (Figure 3.34). This could suggest that, unlike mCLEC-2, hCLEC-2 does not have a role in arterial thrombus formation or stability, which would be consistent with the lower expression level of CLEC-2 on human platelets compared to mouse (Figure 3.9).[40,47-49] It is, however, possible that the conditions used were not representative of

those human platelets would normally be exposed to as we used a shear rate of 1000 s^{-1} which, although standard for mice, is higher than any physiological shear rate in humans which normally do not exceed a maximum of 500 s^{-1}.[194] As a result, it is possible that the mechanism of thrombosis in our experiments also did not represent that at physiological shear rates which could explain the lack of effect of blocking CLEC-2 activation or ligand interactions. As a result, further experiments should be carried out at lower, more physiological, shear rates and the effect of other CLEC-2 inhibitors should be investigated, for example HEL1-Fab fragments or Btk inhibitors that can both specifically inhibit CLEC-2 activation independently of the podoplanin/rhodocytin binding site.[65]

Overall, these results suggest that there could be differences between the role of CLEC-2 in thrombosis in humans and mice, potentially due to different ligands or to different affinities for the proposed intravascular ligand. To truly elucidate these differences, the intravascular ligand or ligands would need to be identified. However, although the presence of such a ligand was suggested over a decade ago few advances have been made in identifying it.[7,25] As a result of this the use of hCLEC-2^{KI} mice to test potential anti-thrombotic therapeutics is limited, at least in terms of arterial thrombosis. However, we have still determined proof of principle for their use in this regard using HEL1 or AYP1 to immunodeplete CLEC-2 as our results are comparable to those using CLEC-2 deficient WT mice as in both cases no ligand is able to bind to CLEC-2. Furthermore, as with humanised GPVI mice, hCLEC-2^{KI} mice could still be useful in determining the bleeding risk associated with potential therapeutics as haemostasis was unaltered compared to WT mice.[140]

4.6 CLEC-2 inhibition by the Btk inhibitors PRN1008 and PRN473

The first and second generation Btk inhibitors ibrutinib and acalabrutinib have been found to inhibit CLEC-2 mediated platelet activation in both humans and mice. The third generation Btk inhibitor PRN1008 and the preclinical inhibitor PRN473 have not previously been investigated

for their inhibitory effect on mouse platelets. However, recent findings have shown that they block rhodocytin-induced platelet aggregation (Smith *et al*., unpublished).

We initially investigated the effect of PRN1008 on rhodocytin-induced platelet activation at similar concentrations to those used to test ibrutinib but, even at the highest concentration of 20 µM, only a slight increase in lag time was observed whereas a similar concentration of ibrutinib abrogated aggregation (Figure 3.35).[65] As it was possible platelet activation by secondary mediators masked the effect of PRN1008, we investigated whether it inhibited rhodocytin-induced activation in the presence of the secondary mediator inhibitors indomethacin and cangrelor. Under these conditions, PRN1008 completely blocked CLEC-2 mediated platelet aggregation however, aggregation in vehicle treated platelets was also reduced highlighting the role of secondary mediators in platelet activation (Figure 3.35). A dose-response experiment identified 2 µM as the lowest concentration of PRN1008 to completely inhibit rhodocytin-induced platelet activation in the absence of secondary mediators. However, it should be noted that 0.5 µM almost completely blocked aggregation in 2 out of the 3 mice tested and a concentration of 1 µM was not tested (Figure 3.36). Without secondary mediator inhibition 2 µM PRN1008 slightly, but not significantly, increased the lag time following rhodocytin stimulation whereas a similar concentration of ibrutinib resulted in a much longer lag.[65] 2 µM of PRN1008 or PRN473 have also been found to inhibit rhodocytin induced aggregation of human platelets (Smith *et al*., unpublished).

In contrast to the aggregation results, both PRN1008 and PRN473 appear to reduce Btk and PLCγ2 tyrosine phosphorylation both in the presence and absence of secondary mediators (Figure 3.37). Although for PLCγ2 the effect on phosphorylation was greater when secondary mediators were inhibited. Furthermore, no other effects on tyrosine phosphorylation were observed using 4G10 suggesting that PRN1008 and PRN473 could have fewer off target effects than earlier generation Btk inhibitors.[65] However, individual phosphorylation blots for other tyrosine kinases would need to be carried out to confirm this. As eptifibatide was used to

prevent platelet aggregation in these experiments, it is possible that the reduced platelet activation, and therefore reduced secondary mediator release, accounts for PRN1008 and PRN473 reducing Btk phosphorylation without further secondary mediator inhibition.

Overall, these results suggest that the third generation Btk inhibitors PRN1008 and PRN473 can inhibit CLEC-2 mediated mouse platelet aggregation by inhibiting CLEC-2 signalling at a similar concentration to human platelets. However, in mice this is only achieved by the additional inhibition of secondary mediators. Nicolson *et al*, have previously shown that a higher concentration of ibrutinib is needed to prevent rhodocytin-induced platelet aggregation in mice than humans.[65] However, even a higher concentration of PRN1008 does not overcome the activatory effects of secondary mediators. The most likely explanation for this is the requirement of ADP and TxA_2 for positive feedback in human CLEC-2 mediated platelet activation whereas this has less of a role in mouse platelets.[62,65] In addition, the difference between ibrutinib and PRN1008 could be due to the off target effects of the former and the higher selectivity of the later.[65,146]

4.7 Effect of Btk inhibition on *Salmonella*-induced thrombosis

The interaction between CLEC-2 and podoplanin has been shown to mediate STm infection-induced thrombosis in mice, with Btk inhibitors being suggested as a potential therapeutic agent for preventing platelet activation via CLEC-2 in this disease, as well as other types of immuno-thrombosis and thrombo-inflammation.[11,59,65,87] We therefore investigated the effect of inhibiting Btk prior to and during STm infection. Btk was inhibited using a specially formulated diet containing the third-generation inhibitor PRN473. This method of inhibitor administration was chosen as mice were sacrificed 7 days after STm infection meaning that, unlike in previous experiments modelling DVT, repeat injections of inhibitor would be over a much longer time period.[65] Initial assessment of the diet showed that after 7 days it had no negative effect on bodyweight, comparable to the control diet, suggesting that mice ate a normal amount and

there were no adverse effects (Figure 3.38). The effect of PRN473 on platelet activation was also tested on days 5 and 7 after the introduction of the diet. On both days CLEC-2 mediated platelet activation was reduced whereas there was little effect on activation via PAR4 (Figure 3.39). GPVI-mediated platelet activation by CRP was also inhibited after 7 days on the PRN473 diet (Smith *et al*., unpublished). This is consistent with previous findings in which higher concentrations of inhibitor were needed to block CLEC-2 induced platelet activation in mice, compared to humans in which low doses of inhibitor selectively block CLEC-2, whereas higher doses are needed to block GPVI-mediated platelet activation.[87]

CLEC-2 and its ligand podoplanin have been implemented in both thrombo-inflammatory and immuno-thrombotic diseases, such as in DVT and *Salmonella* infection-induced thrombosis respectively. Btk-mediated inhibition of CLEC-2 signalling has been suggested as a potential therapeutic for such diseases although to date this has not been extensively investigated.[11,106] Previous research from Nicolson *et al.* has shown little effect of ibrutinib in a model of DVT and therefore we rather investigated the effect of PRN473 in STm infection induced thrombosis.[65] In this model podoplanin is upregulated due to accumulation of leukocytes and macrophages as a result of infection, as well as being expressed in the sub-endothelium on stromal cells which is exposed due to endothelial damage. As a result, platelets become activated via the interaction of podoplanin with CLEC-2 and thrombi form and are anchored to the sub-endothelium via platelet interaction with podoplanin.[59] In mice deficient in either CLEC-2 (*Clec1b*$^{fl/fl;Pf4Cre+}$) or podoplanin (*Pdpn*$^{fl/fl;Vav1\text{-}iCre+}$) thrombosis was reduced and therefore we investigated whether PRN473 mediated inhibition of CLEC-2 would have a similar effect.[59] Mice were fed with the PRN473 diet for 7 days prior to STm infection and for the following 7 days until they were sacrificed and the livers removed. We found no apparent difference in thrombus area in the large vessels of the liver in PRN473 treated compared to control treated mice, although PRN473-treated mice had a trend for larger thrombi than controls even though the number of thrombi was comparable (Figure 3.40 and 3.41).

Our results are similar to those with ibrutinib in an inferior vena cava stenosis model of DVT in which, although thrombosis is prevented in mice deficient in CLEC-2, ibrutinib treatment had only a trend for decreasing thrombosis and in those mice that still had thrombi, the size was comparable to the controls.[65,86] Even though we observed a slight trend for increased thrombus size, whereas in the DVT model there was a trend for a reduction in thrombosis, both studies suggest that inhibition of Btk does not have the expected effect on CLEC-2 mediated thrombosis based on *in vitro* experiments with Btk inhibitors and previous experiments with *Clec1b*$^{fl/fl;Pf4Cre+}$ knockout mice in these models.[59,65,86] The reason for the lack of effect of ibrutinib in the DVT model was suggested to be a result of incomplete CLEC-2 inhibition throughout the entire duration of the experiment.[65] However, Btk occupancy in the spleens of PRN473 treated mice was 98.3 ± 3.2% after 14 days on the diet (Smith *et al*., unpublished). Therefore, this could suggest that inhibition of Btk does not prevent the interaction between CLEC-2 and podoplanin. Although podoplanin expression was not reduced, either in our experiments, or following STm infection in CLEC-2 *Clec1b*$^{fl/fl;Pf4Cre+}$ mice,[59] we observed a trend for fewer thrombi being in podoplanin positive vessels (Figure 3.41) suggesting there might be reduced, but not complete inhibition, of platelet activation by the interaction of podoplanin with CLEC-2. P-selectin staining also suggests that there is still platelet activation (Figure 3.42).

The lack of effect of PRN473 on thrombosis following STm infection could also be the result of several other factors. For example, even in *Clec1b*$^{fl/fl;Pf4Cre+}$ knockout mice there was still residual thrombus formation.[59] This suggests that there may be a mechanism in addition to platelet activation by podoplanin via CLEC-2 that contributes to thrombosis. This residual thrombosis was not due to the presence of GPVI as it still occurred in CLEC-2/GPVI double deficient mice and no effect on thrombosis was observed in *Gp6*$^{-/-}$ knockout mice.[59] This also suggests that PRN473 inhibiting both CLEC-2 and GPVI mediated platelet activation would not have additional effects on thrombosis in this model. It has been suggested instead that the mechanism of residual thrombosis could be mediated by TLR4 or as a result of CLEC-2

activation being the final step in the pathway resulting in some thrombus formation prior to this.[59] However, unless this alternate mechanism of thrombosis was exacerbated in the presence of PRN473 this is unlikely to explain the thrombosis in the Btk inhibitor group. On the other hand, it is possible that the role of CLEC-2 in thrombosis following STm infection is not via activation or signalling but instead via CLEC-2 functioning as an adhesion receptor. This has previously been shown using CLEC-2 Y7A knockin mice, in which CLEC-2 is present but cannot signal, in arterial thrombosis.[74] CLEC-2 Y7A knockin mice exhibit no defects in thrombus formation or stability, unlike CLEC-2 depleted of knockout mice.[7,25,73,74] Therefore, it is possible that blocking CLEC-2 signalling using a Btk inhibitor does not inhibit the role of CLEC-2 in immuno-thrombosis as the receptor itself is still present.

Btk itself has several roles within the immune system that could be affected by PRN473. These include in the maturation and function of B cells and therefore antibody production in the adaptive immune response as well as in the innate immune response via its expression on immune cells such as monocytes, macrophages and neutrophils.[145,146] It is possible Btk inhibition could have a favourable effect in infection by preventing excessive inflammation or immune responses however, these responses are also crucial for resolution of infections.[11,147] Therefore, it is possible that inhibiting Btk could lead to worse outcomes following infection, particularly when inhibition is prior to infection as evidenced by recurrent infections in XLA patients and high rates of infection in patients treated with ibrutinib.[11,150,151,195] Although the role of Btk in antibody production could worsen the effects of STm infection, this is unlikely to have an effect on thrombosis as Rag1 knockout mice, which do not have either mature T or B cells, have comparable thrombosis to WT mice.[59] Furthermore, there was a comparable lymphocyte count between PRN473 and control treated mice following STm infection (data not shown, Smith *et al*., unpublished).

Btk also has a role in the immune response mediated by TLR4 and TLR2 activation and its inhibition can lead to inhibition of NFκB signalling and therefore IL-1β production as well as

inhibition of TNF production.[146,147,196] This has also been shown in XLA patients, whose peripheral blood mononuclear cells produce less IL-1β and TNF in response to TLR4 or TLR2 stimulation than those from control donors.[147] TLR4 has previously been shown to mediate the innate immune response to STm infection in mice, with mice lacking this receptor having no inflammatory lesions or thrombi following infection and reduced leukocyte accumulation resulting in reduced podoplanin expression in the liver.[59] As a result it is possible than Btk inhibition by PRN473 could have inhibited TLR4 signalling and reduced the immune and inflammatory response to infection as well as podoplanin expression and thrombosis. However, this was not the case suggesting that PRN473 does not inhibit signalling via TLR4, at least at the concentration used. Furthermore, Btk inhibition with PRN473 had no effect on survival as all mice in this grouped survived suggesting it had little effect on the immune response to STm infection. This is further supported by there being similar white blood cell and lymphocyte counts in PRN473 and control treated mice (data not shown, Smith *et al*., unpublished). It is possible that the hypothesised lack of effect of PRN473 on the immune response following STm infection is due to differences in the function of Btk in humans and mice as evidenced by the difference in effect of Btk deficiency in XLA patients and mice.[150-152] Furthermore, Btk inhibition has been shown to have beneficial effects following COVID-19 infection suggesting that such inhibition has an effect of immune modulation.[197,198]

Overall, these results suggest that inhibition of Btk by PRN473 has little effect on STm infection induced thrombosis in agreement with previous results for ibrutinib in DVT.[65] However, unlike the DVT experiments, we have shown that there is high Btk occupancy with the PRN473 diet excluding incomplete inhibition as a reason for the lack of effect on thrombosis. This suggests that Btk inhibitors may not have therapeutic potential in infection-induced thrombosis although it is possible they could have beneficial effects on the immune response, rather than on platelet activation. For example, Btk inhibition during COVID-19 infection results in reduced pulmonary injury and disease severity, likely due to immune modulation.[87,197,198] However, in terms of

CLEC-2-mediated thrombosis, potential therapeutics inhibiting the binding of CLEC-2 to podoplanin would need to be investigated to determine whether CLEC-2 acts as an adhesion receptor in such diseases and whether this would be a suitable therapeutic approach for preventing immuno-thrombosis.

4.8 Comparison of human and mouse CLEC-2

The research forming this thesis has highlighted several similarities and differences between human and mouse CLEC-2. Particularly the differences are important to take into consideration when comparing experiments conducted in mice with the role of hCLEC-2, especially when they involve potential therapeutics that may have different functions in mice and humans.

The main similarity was the ability of hCLEC-2 to compensate for mCLEC-2 during development. hCLEC-2^{KI} mice did not have any signs of a blood and lymphatic vessel separation defect which suggests that hCLEC-2 can interact with mouse podoplanin and was in contrast to previous genetically modified CLEC-2 mouse models.[5-7,72-74] Furthermore, hCLEC-2 was also able to compensate for mCLEC-2 in *in vitro* platelet function. These results were in spite of reduced spreading of hCLEC-2^{KI} platelets on mouse podoplanin, although platelets were still activated, just not fully. It is possible that this only occurred *in vitro* due to reduced podoplanin mobility and therefore reduced CLEC-2 clustering and activation.[69,191] However, it appears that this reduced level of activation was sufficient for separation of blood and lymphatic vessels.

A further similarity is that both human and mouse CLEC-2 can be immunodepleted. Previously it was only known that mCLEC-2 could be depleted using the mAb INU1 however, using the hCLEC-2^{KI} mice we have shown that both HEL1 and AYP1 can deplete hCLEC-2.[25] Furthermore, in both species immunodepletion had no more than a minor effect on haemostasis, suggesting CLEC-2 may not be a key contributor to this process in either species.[25,73] As well as similar effects on thrombosis both *in vitro* and *in vivo* that, along with

the haemostasis results, were also comparable to CLEC-2 knockout mice.[7,25,73,74] However, although immunodepletion of either mouse of human CLEC-2 resulted in comparable thrombocytopenia, hCLEC-2 was depleted over a much longer time frame than mCLEC-2. This could be due to a species difference, but it is also possible that immunodepletion by INU1 is unique and further experiments would be needed to compare the mechanisms of depletion by all three antibodies, as well as to investigate the effect of other anti-mouse CLEC-2 antibodies.

In contrast, we found many more potential differences between human and mouse CLEC-2. Some of which add to or confirm previous results. For example, a difference in the copy number and expression of CLEC-2 has been proposed between human and mouse platelets.[40,47-49] We confirmed that there was a difference but in contrast to previous reports CLEC-2 surface expression on mouse platelets was only 2.5-fold higher than human, rather than up to 20-fold.[40,47-49] It is important to take this difference into consideration when comparing humans and mice as it could suggest CLEC-2 has a less important role in humans. Furthermore, when comparing hCLEC-2^{KI} with humans it is possible that the increased expression of hCLEC-2 results in greater CLEC-2 signalling in hCLEC-2^{KI} mice.

A further difference between human and mouse CLEC-2 confirming previous results, was in regard to CLEC-2 inhibition by the Btk inhibitor PRN1008. As with ibrutinib and acalabrutinib rhodocytin-induced platelet aggregation was inhibited at lower concentrations of PRN1008 in human platelets compared to mouse (Smith *et al*., unpublished).[65] This was previously suggested to be a result of the dependence of hCLEC-2 signalling on positive feedback from secondary mediators whereas this is less critical in mice.[65] In line with this, PRN1008 inhibited rhodocytin-induced platelet aggregation in mice at a similar concentration to human only in when secondary mediators were inhibited. This difference is CLEC-2 signalling between humans and mice is important to take into consideration when comparing the function of CLEC-2 between the two species as it means different inhibitor concentrations are needed and could

also result in different outcomes depending on the conditions of the experiments, for example, washed platelets compared to PRP or whole blood.

Perhaps the biggest difference our data has suggested between human and mouse CLEC-2 was in their role in thrombosis. While mCLEC-2 has been shown to contribute to thrombosis, particularly thrombus stability, for over 10 years, the role of hCLEC-2 had not been well studied.[7,25] Here, we found that hCLEC-2 does not appear to have a role in arterial thrombosis, in contrast to mouse CLEC-2. Although as previously discussed, there are several limitations to our experiments that could account for the lack of effect. Furthermore, we have also shown only a minor role of CLEC-2 in thrombus stability in mice which could suggest that previous experiments using CLEC-2 deficient mice have overestimated the contribution of CLEC-2 to thrombus stability whereas no indication of such a role was observed with human blood. Further differences in thrombosis were also observed with hCLEC-2^{KI} mice, which appeared to have more stable thrombi *in vitro* and less stable thrombi *in vivo* compared to WT mice. These differences were only observed at arterial shear rates and with anti-coagulated blood whereas no difference was observed at venous shear, in the presence of thrombin and fibrin (non-anti-coagulated blood) or in the absence of plasma (reconstituted blood). Together these results could suggest that the differences in thrombus formation and stability are due to a difference in platelet activation, most likely higher activation in hCLEC-2^{KI} mice, and are dependent on an unknown plasma factor that appears to have a higher affinity for hCLEC-2. Differences *in vivo* further suggest the presence of an anti-thrombotic CLEC-2 ligand that interacts with human, but not mouse, CLEC-2 or has a lower affinity for mCLEC-2. However, the presence of this ligand or ligands remains to be conclusively determined.

Overall, these differences limit the extrapolation of results from experiments using mice to humans, particularly in terms of arterial thrombosis. They also limit the use of hCLEC-2^{KI} mice in testing potential therapeutics targeting hCLEC-2 in *in vivo* arterial thrombosis models. However, it is possible that these mice could still be used to determine the bleeding risk

associated with such agents as haemostasis was not altered between hCLEC-2^{KI} and WT mice. Furthermore, as hCLEC-2 can interact with mouse podoplanin it is possible hCLEC-2^{KI} mice will be of greater benefit to test therapeutics in the settings of immuno-thrombosis, thrombo-inflammation and cancer, although this remains to be determined.

4.9 Concluding remarks

The results presented here show for the first time that a humanised CLEC-2 mouse model is both viable and can be used to test human specific agents targeting CLEC-2, particularly in terms of their effect on haemostasis. Furthermore, they have highlighted potential differences between human and mouse CLEC-2 in thrombosis and could provide a valuable tool to investigate these further. Although these differences limit the use of hCLEC-2^{KI} mice to test potential anti-thrombotic drugs in arterial thrombosis models, the conserved interaction between hCLEC-2 and mouse podoplanin suggests they could instead be useful in models of immuno-thrombosis, thrombo-inflammation and cancer where the role of CLEC-2 is mediated by podoplanin.

We have further shown for the first time that anti-hCLEC-2 antibodies can induce hCLEC-2 activation and immunodepletion independently of their binding site using AYP1 and the novel antibody HEL1. This suggests that CLEC-2 dimerisation is enough to induce platelet activation, which is an important consideration if mAb would be used to target CLEC-2 therapeutically. Particularly as we have shown that i.v. administration of AYP1 is lethal due to micro-thrombi becoming trapped in the lungs. As a result, Fab fragments would be more beneficial however, when we tested AYP1 Fab fragments in hCLEC-2^{KI} mice they had little effect on blocking platelet activation and they also had no apparent effect on thrombosis in human blood. These results, together with those on INU1-Fab, which causes widespread thrombosis,[186] could limit the translation of anti-CLEC-2 mAbs to humans as a therapeutic strategy.

In addition, we tested the use of a Btk inhibitor to prevent thrombosis in a *Salmonella*-infection model known to be mediated by the interaction of CLEC-2 and podoplanin. However, as with ibrutinib in a model of DVT, no effect of Btk inhibition was seen. Although it is possible that the role of CLEC-2 is via adhesion rather than activation in immuno-thrombosis. If this is the case then Btk inhibitors would not be beneficial therapeutically for these diseases, although inhibition of platelet adhesion via CLEC-2 could still prove beneficial as could the immune-modulatory effects of Btk inhibition.

In conclusion, the results presented here suggest that CLEC-2 may not be the promising anti-thrombotic target it has previously been suggested to be. This is particularly true in terms of arterial thrombosis where a role for CLEC-2 in mice has so far not been translated to humans. CLEC-2 could however still be a potential therapeutic target in cancer, thrombo-inflammation or immuno-thrombosis. Although CLEC-2 inhibitors with greater function *in vivo* would need to be developed and a greater understanding of whether CLEC-2 is acting as an adhesion or an activation receptor in these diseases would be needed.

5. References

1. Schmitt A, Guichard J, Massé J-M*, et al.* Of mice and men: Comparison of the ultrastructure of megakaryocytes and platelets. *Experimental Hematology*. 2001;29(11):1295-1302.
2. White JG. Chapter 7 - Platelet Structure. In: Michelson AD, ed. Platelets (Third Edition): Academic Press; 2013:117-144.
3. Vos T, Lim SS, Abbafati C*, et al.* Global burden of 369 diseases and injuries in 204 countries and territories, 1990-2019: a systematic analysis for the Global Burden of Disease Study 2019. *The Lancet*. 2020;396(10258):1204-1222.
4. Metharom P, Berndt MC, Baker RI*, et al.* Current State and Novel Approaches of Antiplatelet Therapy. *Arteriosclerosis, Thrombosis, and Vascular Biology*. 2015;35(6):1327-1338.
5. Finney BA, Schweighoffer E, Navarro-Nunez L*, et al.* CLEC-2 and Syk in the megakaryocytic/platelet lineage are essential for development. *Blood*. 2012;119(7):1747-1756.
6. Bertozzi CC, Schmaier AA, Mericko P*, et al.* Platelets regulate lymphatic vascular development through CLEC-2–SLP-76 signaling. *Blood*. 2010;116(4):661-670.
7. Suzuki-Inoue K, Inoue O, Ding G*, et al.* Essential in vivo roles of the C-type lectin receptor CLEC-2: embryonic/neonatal lethality of CLEC-2-deficient mice by blood/lymphatic misconnections and impaired thrombus formation of CLEC-2-deficient platelets. *Journal of Biological Chemistry*. 2010;285(32):24494-24507.
8. Nurden AT, Nurden P, Sanchez M*, et al.* Platelets and wound healing. *Frontiers in Bioscience*. 2008;13:3532-3548.
9. Thomas MR, Storey RF. The role of platelets in inflammation. *Thromb Haemost*. 2015;114(3):449-458.
10. Stoll G, Kleinschnitz C, Nieswandt B. Combating innate inflammation: a new paradigm for acute treatment of stroke? *Annals of the New York Academy of Sciences*. 2010;1207:149-154.
11. Beristain-Covarrubias N, Perez-Toledo M, Thomas MR*, et al.* Understanding Infection-Induced Thrombosis: Lessons Learned From Animal Models. *Frontiers in Immunology*. 2019;10:2569.
12. Mezouar S, Frère C, Darbousset R*, et al.* Role of platelets in cancer and cancer-associated thrombosis: Experimental and clinical evidences. *Thrombosis Research*. 2016;139:65-76.
13. Stegner D, Nieswandt B. Platelet receptor signaling in thrombus formation. *Journal of Molecular Medicine*. 2011;89(2):109-121.
14. Offermanns S. Activation of Platelet Function Through G Protein–Coupled Receptors. *Circulation Research*. 2006;99(12):1293-1304.
15. Patrono C, Rocca B. Aspirin: Promise and Resistance in the New Millennium. *Arteriosclerosis, Thrombosis, and Vascular Biology*. 2008;28(3):s25-s32.
16. Rayes J, Watson SP, Nieswandt B. Functional significance of the platelet immune receptors GPVI and CLEC-2. *Journal of Clinical Investigation*. 2019;129(1):12-23.
17. Nieswandt B, Pleines I, Bender M. Platelet adhesion and activation mechanisms in arterial thrombosis and ischaemic stroke. *Journal of Thrombosis and Haemostasis*. 2011;9(s1):92-104.
18. Nieswandt B, Kleinschnitz C, Stoll G. Ischaemic stroke: a thrombo-inflammatory disease? *The Journal of Physiology*. 2011;589(17):4115-4123.
19. Savage B, Almus-Jacobs F, Ruggeri ZM. Specific Synergy of Multiple Substrate-Receptor Interactions in Platelet Thrombus Formation under Flow. *Cell*. 1998;94(5):657-666.
20. Nieswandt B, Watson SP. Platelet-collagen interaction: is GPVI the central receptor? *Blood*. 2003;102(2):449-461.

21. Nieswandt B, Brakebusch C, Bergmeier W*, et al.* Glycoprotein VI but not alpha2beta1 integrin is essential for platelet interaction with collagen. *The EMBO Journal*. 2001;20(9):2120-2130.
22. Grüner S, Prostredna M, Schulte V*, et al.* Multiple integrin-ligand interactions synergize in shear-resistant platelet adhesion at sites of arterial injury in vivo. *Blood*. 2003;102(12):4021-4027.
23. Stalker TJ, Traxler EA, Wu J*, et al.* Hierarchical organization in the hemostatic response and its relationship to the platelet-signaling network. *Blood*. 2013;121(10):1875-1885.
24. Undas A, Ariëns RAS. Fibrin Clot Structure and Function. *Arteriosclerosis, Thrombosis, and Vascular Biology*. 2011;31(12):e88-e99.
25. May F, Hagedorn I, Pleines I*, et al.* CLEC-2 is an essential platelet-activating receptor in hemostasis and thrombosis. *Blood*. 2009;114(16):3464-3472.
26. Hughes CE, Navarro-Núñez L, Finney BA*, et al.* CLEC-2 is not required for platelet aggregation at arteriolar shear. *Journal of thrombosis and haemostasis : JTH*. 2010;8(10):2328-2332.
27. Brass LF, Wannemacher KM, Ma P*, et al.* Regulating thrombus growth and stability to achieve an optimal response to injury. *Journal of thrombosis and haemostasis : JTH*. 2011;9 Suppl 1(Suppl 1):66-75.
28. Welsh JD, Stalker TJ, Voronov R*, et al.* A systems approach to hemostasis: 1. The interdependence of thrombus architecture and agonist movements in the gaps between platelets. *Blood*. 2014;124(11):1808-1815.
29. Gorog DA, Fayad ZA, Fuster V. Arterial Thrombus Stability: Does It Matter and Can We Detect It? *Journal of the American College of Cardiology*. 2017;70(16):2036-2047.
30. Signarvic RS, Cierniewska A, Stalker TJ*, et al.* RGS/Gi2alpha interactions modulate platelet accumulation and thrombus formation at sites of vascular injury. *Blood*. 2010;116(26):6092-6100.
31. Speich HE, Bhal V, Houser KH*, et al.* Signaling via P2Y12 may be critical for early stabilization of platelet aggregates. *J Cardiovasc Pharmacol*. 2014;63(6):520-527.
32. Goto S, Tamura N, Ishida H. Ability of anti-glycoprotein IIb/IIIa agents to dissolve platelet thrombi formed on a collagen surface under blood flow conditions. *Journal of the American College of Cardiology*. 2004;44(2):316-323.
33. Le Behot A, Gauberti M, Martinez De Lizarrondo S*, et al.* GpIbα-VWF blockade restores vessel patency by dissolving platelet aggregates formed under very high shear rate in mice. *Blood*. 2014;123(21):3354-3363.
34. Ahmed MU, Kaneva V, Loyau S*, et al.* Pharmacological Blockade of Glycoprotein VI Promotes Thrombus Disaggregation in the Absence of Thrombin. *Arterioscler Thromb Vasc Biol*. 2020;40(9):2127-2142.
35. Ahmed MU, Receveur N, Janus-Bell E*, et al.* Respective roles of Glycoprotein VI and FcγRIIA in the regulation of αIIbβ3-mediated platelet activation to fibrinogen, thrombus buildup, and stability. *Research and practice in thrombosis and haemostasis*. 2021;5(5):e12551-e12551.
36. Mangin P, Onselaer M-B, Receveur N*, et al.* Immobilized fibrinogen activates human platelets through glycoprotein VI. *Haematologica*. 2018;103(5):898-907.
37. Janus-Bell E, Ahmed MU, Receveur N*, et al.* Differential Role of Glycoprotein VI in Mouse and Human Thrombus Progression and Stability. *Thromb Haemost*. 2021;121(04):543-546.
38. Suzuki-Inoue K, Fuller GLJ, García An*, et al.* A novel Syk-dependent mechanism of platelet activation by the C-type lectin receptor CLEC-2. *Blood*. 2006;107(2):542-549.
39. Colonna M, Samaridis J, Angman L. Molecular characterization of two novel C-type lectin-like receptors, one of which is selectively expressed in human dendritic cells. *European Journal of Immunology*. 2000;30(2):697-704.
40. Gitz E, Pollitt AY, Gitz-Francois JJ*, et al.* CLEC-2 expression is maintained on activated platelets and on platelet microparticles. *Blood*. 2014;124(14):2262-2270.

41. Zelensky AN, Gready JE. The C-type lectin-like domain superfamily. *The FEBS Journal*. 2005;272(24):6179-6217.
42. Watson AA, Brown J, Harlos K*, et al.* The Crystal Structure and Mutational Binding Analysis of the Extracellular Domain of the Platelet-activating Receptor CLEC-2*. *Journal of Biological Chemistry*. 2007;282(5):3165-3172.
43. Wang L, Ren S, Zhu H*, et al.* Structural and functional conservation of CLEC-2 with the species-specific regulation of transcript expression in evolution. *Glycoconjugate Journal*. 2012;29(5):335-345.
44. Chaipan C, Soilleux EJ, Simpson P*, et al.* DC-SIGN and CLEC-2 mediate human immunodeficiency virus type 1 capture by platelets. *Journal of virology*. 2006;80(18):8951-8960.
45. Tang T, Li L, Tang J*, et al.* A mouse knockout library for secreted and transmembrane proteins. *Nature Biotechnology*. 2010;28(7):749-755.
46. Senis YA, Tomlinson MG, García A*, et al.* A comprehensive proteomics and genomics analysis reveals novel transmembrane proteins in human platelets and mouse megakaryocytes including G6b-B, a novel immunoreceptor tyrosine-based inhibitory motif protein. *Molecular & cellular proteomics : MCP*. 2007;6(3):548-564.
47. Burkhart JM, Vaudel M, Gambaryan S*, et al.* The first comprehensive and quantitative analysis of human platelet protein composition allows the comparative analysis of structural and functional pathways. *Blood*. 2012;120(15):e73-82.
48. Zeiler M, Moser M, Mann M. Copy number analysis of the murine platelet proteome spanning the complete abundance range. *Molecular & cellular proteomics : MCP*. 2014;13(12):3435-3445.
49. Dunster JL, Unsworth AJ, Bye AP*, et al.* Interspecies differences in protein expression do not impact the spatiotemporal regulation of glycoprotein VI mediated activation. *Journal of Thrombosis and Haemostasis*. 2020;18(2):485-496.
50. Huang TF, Liu CZ, Yang SH. Aggretin, a novel platelet-aggregation inducer from snake (Calloselasma rhodostoma) venom, activates phospholipase C by acting as a glycoprotein Ia/IIa agonist. *The Biochemical journal*. 1995;309 (Pt 3)(Pt 3):1021-1027.
51. Shin Y, Morita T. Rhodocytin, a functional novel platelet agonist belonging to the heterodimeric C-type lectin family, induces platelet aggregation independently of glycoprotein Ib. *Biochem Biophys Res Commun*. 1998;245(3):741-745.
52. Suzuki-Inoue K, Kato Y, Inoue O*, et al.* Involvement of the Snake Toxin Receptor CLEC-2, in Podoplanin-mediated Platelet Activation, by Cancer Cells *[♦]. *Journal of Biological Chemistry*. 2007;282(36):25993-26001.
53. Breiteneder-Geleff S, Matsui K, Soleiman A*, et al.* Podoplanin, novel 43-kd membrane protein of glomerular epithelial cells, is down-regulated in puromycin nephrosis. *The American Journal of Pathology*. 1997;151(4):1141-1152.
54. Schacht V, Dadras SS, Johnson LA*, et al.* Up-Regulation of the Lymphatic Marker Podoplanin, a Mucin-Type Transmembrane Glycoprotein, in Human Squamous Cell Carcinomas and Germ Cell Tumors. *The American Journal of Pathology*. 2005;166(3):913-921.
55. Kerrigan AM, Navarro-NuÑEz L, Pyz E*, et al.* Podoplanin-expressing inflammatory macrophages activate murine platelets via CLEC-2. *Journal of Thrombosis and Haemostasis*. 2012;10(3):484-486.
56. Kato Y, Kaneko MK, Kunita A*, et al.* Molecular analysis of the pathophysiological binding of the platelet aggregation-inducing factor podoplanin to the C-type lectin-like receptor CLEC-2. *Cancer Science*. 2008;99(1):54-61.
57. Nagae M, Morita-Matsumoto K, Kato M*, et al.* A Platform of C-type Lectin-like Receptor CLEC-2 for Binding O-Glycosylated Podoplanin and Nonglycosylated Rhodocytin. *Structure*. 2014;22(12):1711-1721.
58. Bourne JH, Colicchia M, Di Y*, et al.* Heme induces human and mouse platelet activation through C-type-lectin-like receptor-2. *Haematologica*. 2020.

59. Hitchcock JR, Cook CN, Bobat S*, et al.* Inflammation drives thrombosis after Salmonella infection via CLEC-2 on platelets. *The Journal of Clinical Investigation*. 2015;125(12):4429-4446.
60. Meng D, Luo M, Liu B. The Role of CLEC-2 and Its Ligands in Thromboinflammation. *Frontiers in Immunology*. 2021;12(2221).
61. Fuller GLJ, Williams JAE, Tomlinson MG*, et al.* The C-type lectin receptors CLEC-2 and Dectin-1, but not DC-SIGN, signal via a novel YXXL-dependent signaling cascade. *The Journal of biological chemistry*. 2007;282(17):12397-12409.
62. Pollitt AY, Grygielska B, Leblond B*, et al.* Phosphorylation of CLEC-2 is dependent on lipid rafts, actin polymerization, secondary mediators, and Rac. *Blood*. 2010;115(14):2938-2946.
63. Pleines I, Elvers M, Strehl A*, et al.* Rac1 is essential for phospholipase C-gamma2 activation in platelets. *European Journal of Physiology*. 2009;457(5):1173-1185.
64. Borgognone A, Navarro-Núñez L, Correia JN*, et al.* CLEC-2-dependent activation of mouse platelets is weakly inhibited by cAMP but not by cGMP. *Journal of Thrombosis and Haemostasis*. 2014;12(4):550-559.
65. Nicolson PLR, Nock SH, Hinds J*, et al.* Low-dose Btk inhibitors selectively block platelet activation by CLEC-2. *Haematologica*. 2020;106(1):208-219.
66. Mori J, Pearce AC, Spalton JC*, et al.* G6b-B inhibits constitutive and agonist-induced signaling by glycoprotein VI and CLEC-2. *The Journal of biological chemistry*. 2008;283(51):35419-35427.
67. Hughes CE, Pollitt AY, Mori J*, et al.* CLEC-2 activates Syk through dimerization. *Blood*. 2010;115(14):2947-2955.
68. Watson AA, Eble JA, O'Callaghan CA. Crystal structure of rhodocytin, a ligand for the platelet-activating receptor CLEC-2. *Protein Science*. 2008;17(9):1611-1616.
69. Pollitt AY, Poulter NS, Gitz E*, et al.* Syk and Src family kinases regulate C-type lectin receptor 2 (CLEC-2)-mediated clustering of podoplanin and platelet adhesion to lymphatic endothelial cells. *Journal of Biological Chemistry*. 2014;289(52):35695-35710.
70. Uhrin P, Zaujec J, Breuss JM*, et al.* Novel function for blood platelets and podoplanin in developmental separation of blood and lymphatic circulation. *Blood*. 2010;115(19):3997-4005.
71. Ichise H, Ichise T, Ohtani O*, et al.* Phospholipase Cgamma2 is necessary for separation of blood and lymphatic vasculature in mice. *Development*. 2009;136(2):191-195.
72. Haining EJ, Lowe KL, Wichaiyo S*, et al.* Lymphatic blood filling in CLEC-2-deficient mouse models. *Platelets*. 2020:1-16.
73. Bender M, May F, Lorenz V*, et al.* Combined In Vivo Depletion of Glycoprotein VI and C-Type Lectin-Like Receptor 2 Severely Compromises Hemostasis and Abrogates Arterial Thrombosis in Mice. *Arteriosclerosis, Thrombosis, and Vascular Biology*. 2013;33(5):926-934.
74. Haining EJ, Cherpokova D, Wolf K*, et al.* CLEC-2 contributes to hemostasis independently of classical hemITAM signaling in mice. *Blood*. 2017;130(20):2224-2228.
75. Srinivasan RS, Dillard ME, Lagutin OV*, et al.* Lineage tracing demonstrates the venous origin of the mammalian lymphatic vasculature. *Genes Dev*. 2007;21(19):2422-2432.
76. Hess PR, Rawnsley DR, Jakus Z*, et al.* Platelets mediate lymphovenous hemostasis to maintain blood-lymphatic separation throughout life. *Journal of Clinical Investigation*. 2014;124(1):273-284.
77. Suzuki-Inoue K. Platelets and cancer-associated thrombosis: focusing on the platelet activation receptor CLEC-2 and podoplanin. *Blood*. 2019;134(22):1912-1918.
78. Suzuki-Inoue K. Roles of the CLEC-2–podoplanin interaction in tumor progression. *Platelets*. 2018;29(8):786-792.
79. Nieswandt B, Hafner M, Echtenacher B*, et al.* Lysis of tumor cells by natural killer cells in mice is impeded by platelets. *Cancer Res*. 1999;59(6):1295-1300.

80. Shirai T, Inoue O, Tamura S*, et al.* C-type lectin-like receptor 2 promotes hematogenous tumor metastasis and prothrombotic state in tumor-bearing mice. *Journal of Thrombosis and Haemostasis*. 2017;15(3):513-525.
81. Lorenz V, Stegner D, Stritt S*, et al.* Targeted downregulation of platelet CLEC-2 occurs through Syk-independent internalization. *Blood*. 2015;125(26):4069-4077.
82. Meng D, Ma X, Li H*, et al.* A Role of the Podoplanin-CLEC-2 Axis in Promoting Inflammatory Response After Ischemic Stroke in Mice. *Neurotoxicity Research*. 2021;39(2):477-488.
83. Gao C, Wang H, Wang T*, et al.* Platelet regulates neuroinflammation and restores blood–brain barrier integrity in a mouse model of traumatic brain injury. *Journal of Neurochemistry*. 2020;154(2):190-204.
84. Wu X, Zhang W, Li H*, et al.* Plasma C-type lectin-like receptor 2 as a predictor of death and vascular events in patients with acute ischemic stroke. *European Journal of Neurology*. 2019;26(10):1334-1340.
85. Guo M, Zhang H, Lv Q-W*, et al.* Higher plasma C-type lectin-like receptor 2 concentrations for prediction of higher risk of 30-day mortality in isolated severe blunt traumatic brain injury. *Clinica Chimica Acta*. 2019;496:1-6.
86. Payne H, Ponomaryov T, Watson SP*, et al.* Mice with a deficiency in CLEC-2 are protected against deep vein thrombosis. *Blood*. 2017;129(14):2013-2020.
87. Nicolson PLR, Welsh JD, Chauhan A*, et al.* A rationale for blocking thromboinflammation in COVID-19 with Btk inhibitors. *Platelets*. 2020;31(5):685-690.
88. Engelmann B, Massberg S. Thrombosis as an intravascular effector of innate immunity. *Nature Reviews Immunology*. 2013;13(1):34-45.
89. Sung P-S, Huang T-F, Hsieh S-L. Extracellular vesicles from CLEC2-activated platelets enhance dengue virus-induced lethality via CLEC5A/TLR2. *Nature Communications*. 2019;10(1):2402.
90. Bourne JH, Beristain-Covarrubias N, Zuidscherwoude M*, et al.* CLEC-2 Prevents Accumulation and Retention of Inflammatory Macrophages During Murine Peritonitis. *Frontiers in Immunology*. 2021;12(2167).
91. Rayes J, Lax S, Wichaiyo S*, et al.* The podoplanin-CLEC-2 axis inhibits inflammation in sepsis. *Nature Communications*. 2017;8(1):2239.
92. Lax S, Rayes J, Wichaiyo S*, et al.* Platelet CLEC-2 protects against lung injury via effects of its ligand podoplanin on inflammatory alveolar macrophages in the mouse. *American Journal of Physiology-Lung Cellular and Molecular Physiology*. 2017;313(6):L1016-L1029.
93. Boulaftali Y, Hess PR, Getz TM*, et al.* Platelet ITAM signaling is critical for vascular integrity in inflammation. *The Journal of Clinical Investigation*. 2013;123(2):908-916.
94. Wichaiyo S, Lax S, Montague SJ*, et al.* Platelet glycoprotein VI and C-type lectin-like receptor 2 deficiency accelerates wound healing by impairing vascular integrity in mice. *Haematologica*. 2019;104(8):1648-1660.
95. Carey J, Buchstein S, Shah S. Letter to the Editor; Septic Deep Vein Thrombosis due to Salmonella johannesburg. *Journal of Infection*. 2001;42(1):79-80.
96. Ceyhan M, Kanra G, Benderlioglu B*, et al.* Transient protein S deficiency with deep venous thrombosis during Salmonella typhimurium infection. *Archives of Disease in Childhood*. 1993;68(1):138.
97. Schifferdecker B, Merchán JA, Ahmar C*, et al.* Endovascular treatment of septic thrombophlebitis: a case report of a rare complication and review of the literature. *Vascular Medicine*. 2009;14(1):47-50.
98. Vidal S, Tremblay ML, Govoni G*, et al.* The Ity/Lsh/Bcg locus: natural resistance to infection with intracellular parasites is abrogated by disruption of the Nramp1 gene. *The Journal of experimental medicine*. 1995;182(3):655-666.
99. Mastroeni P, Skepper JN, Hormaeche CE. Effect of anti-tumor necrosis factor alpha antibodies on histopathology of primary Salmonella infections. *Infection and immunity*. 1995;63(9):3674-3682.

100. Beristain-Covarrubias N, Perez-Toledo M, Flores-Langarica A*, et al.* Salmonella-induced thrombi in mice develop asynchronously in the spleen and liver and are not effective bacterial traps. *Blood*. 2019;133(6):600-604.
101. Cunningham AF, Gaspal F, Serre K*, et al.* Salmonella Induces a Switched Antibody Response without Germinal Centers That Impedes the Extracellular Spread of Infection. *The Journal of Immunology*. 2007;178(10):6200.
102. Kak G, Raza M, Tiwari BK. Interferon-gamma (IFN-γ): Exploring its implications in infectious diseases. *BioMolecular Concepts*. 2018;9(1):64-79.
103. Lu Y-C, Yeh W-C, Ohashi PS. LPS/TLR4 signal transduction pathway. *Cytokine*. 2008;42(2):145-151.
104. Bao S, Beagley KW, France MP*, et al.* Interferon-γ plays a critical role in intestinal immunity against Salmonella typhimurium infection. *Immunology*. 2000;99(3):464-472.
105. Talbot S, Tötemeyer S, Yamamoto M*, et al.* Toll-like receptor 4 signalling through MyD88 is essential to control Salmonella enterica serovar Typhimurium infection, but not for the initiation of bacterial clearance. *Immunology*. 2009;128(4):472-483.
106. Harbi MH, Smith CW, Nicolson PLR*, et al.* Novel antiplatelet strategies targeting GPVI, CLEC-2 and tyrosine kinases. *Platelets*. 2021;32(1):29-41.
107. Jiang P, Jandrot-Perrus M. New advances in treating thrombotic diseases: GPVI as a platelet drug target. *Drug Discovery Today*. 2014;19(9):1471-1475.
108. Lu R-M, Hwang Y-C, Liu IJ*, et al.* Development of therapeutic antibodies for the treatment of diseases. *Journal of Biomedical Science*. 2020;27(1):1.
109. Kaplon H, Reichert JM. Antibodies to watch in 2019. *mAbs*. 2019;11(2):219-238.
110. Strohl WR. Current progress in innovative engineered antibodies. *Protein & cell*. 2018;9(1):86-120.
111. Padlan EA. Anatomy of the antibody molecule. *Molecular Immunology*. 1994;31(3):169-217.
112. Li Z, Krippendorff B-F, Sharma S*, et al.* Influence of molecular size on tissue distribution of antibody fragments. *mAbs*. 2016;8(1):113-119.
113. Bates A, Power CA. David vs. Goliath: The Structure, Function, and Clinical Prospects of Antibody Fragments. *Antibodies*. 2019;8(2).
114. Dreher ML, Gherardi E, Skerra A*, et al.* Colony assays for antibody fragments expressed in bacteria. *Journal of Immunological Methods*. 1991;139(2):197-205.
115. Nelson AL. Antibody fragments: hope and hype. *mAbs*. 2010;2(1):77-83.
116. Hamers-Casterman C, Atarhouch T, Muyldermans S*, et al.* Naturally occurring antibodies devoid of light chains. *Nature*. 1993;363(6428):446-448.
117. Vincke C, Muyldermans S. Introduction to Heavy Chain Antibodies and Derived Nanobodies. In: Saerens D, Muyldermans S, eds. Single Domain Antibodies: Methods and Protocols. Totowa, NJ: Humana Press; 2012:15-26.
118. Jovčevska I, Muyldermans S. The Therapeutic Potential of Nanobodies. *BioDrugs*. 2020;34(1):11-26.
119. Jones PT, Dear PH, Foote J*, et al.* Replacing the complementarity-determining regions in a human antibody with those from a mouse. *Nature*. 1986;321(6069):522-525.
120. Green LL, Hardy MC, Maynard-Currie CE*, et al.* Antigen–specific human monoclonal antibodies from mice engineered with human Ig heavy and light chain YACs. *Nature Genetics*. 1994;7(1):13-21.
121. Alfaleh MA, Alsaab HO, Mahmoud AB*, et al.* Phage Display Derived Monoclonal Antibodies: From Bench to Bedside. *Frontiers in Immunology*. 2020;11(1986).
122. McCafferty J, Griffiths AD, Winter G*, et al.* Phage antibodies: filamentous phage displaying antibody variable domains. *Nature*. 1990;348(6301):552-554.
123. Smith George P. Filamentous Fusion Phage: Novel Expression Vectors That Display Cloned Antigens on the Virion Surface. *Science*. 1985;228(4705):1315-1317.
124. Gold HK, Gimple LW, Yasuda T*, et al.* Pharmacodynamic study of F(ab')2 fragments of murine monoclonal antibody 7E3 directed against human platelet glycoprotein IIb/IIIa in

patients with unstable angina pectoris. *The Journal of Clinical Investigation*. 1990;86(2):651-659.
125. Kleiman Neal S, Ohman EM, Califf Robert M*, et al.* Profound inhibition of platelet aggregation with monoclonal antibody 7E3 Fab thrombolytic therapy. *Journal of the American College of Cardiology*. 1993;22(2):381-389.
126. Investigators TGI-A. Effect of glycoprotein IIb/IIIa receptor blocker abciximab on outcome in patients with acute coronary syndromes without early coronary revascularisation: the GUSTO IV-ACS randomised trial. *The Lancet*. 2001;357(9272):1915-1924.
127. Ciccone A, Motto C, Abraha I*, et al.* Glycoprotein IIb-IIIa inhibitors for acute ischaemic stroke. *Cochrane Database of Systematic Reviews*. 2014(3).
128. Serebruany VL, Malinin AI, Eisert RM*, et al.* Risk of bleeding complications with antiplatelet agents: Meta-analysis of 338,191 patients enrolled in 50 randomized controlled trials. *American Journal of Hematology*. 2004;75(1):40-47.
129. Kolh P, Windecker S, Alfonso F*, et al.* 2014 ESC/EACTS Guidelines on myocardial revascularization: The Task Force on Myocardial Revascularization of the European Society of Cardiology (ESC) and the European Association for Cardio-Thoracic Surgery (EACTS)Developed with the special contribution of the European Association of Percutaneous Cardiovascular Interventions (EAPCI). *European Journal of Cardio-Thoracic Surgery*. 2014;46(4):517-592.
130. Duggan S. Caplacizumab: First Global Approval. *Drugs*. 2018;78(15):1639-1642.
131. Arya M, Anvari B, Romo GM*, et al.* Ultralarge multimers of von Willebrand factor form spontaneous high-strength bonds with the platelet glycoprotein Ib-IX complex: studies using optical tweezers. *Blood*. 2002;99(11):3971-3977.
132. Lancellotti S, Basso M, De Cristofaro R. Proteolytic processing of von Willebrand factor by adamts13 and leukocyte proteases. *Mediterranean journal of hematology and infectious diseases*. 2013;5(1):e2013058-e2013058.
133. Callewaert F, Roodt J, Ulrichts H*, et al.* Evaluation of efficacy and safety of the anti-VWF Nanobody ALX-0681 in a preclinical baboon model of acquired thrombotic thrombocytopenic purpura. *Blood*. 2012;120(17):3603-3610.
134. Knoebl P, Cataland S, Peyvandi F*, et al.* Efficacy and safety of open-label caplacizumab in patients with exacerbations of acquired thrombotic thrombocytopenic purpura in the HERCULES study. *Journal of thrombosis and haemostasis : JTH*. 2020;18(2):479-484.
135. Peyvandi F, Scully M, Kremer Hovinga JA*, et al.* Caplacizumab for Acquired Thrombotic Thrombocytopenic Purpura. *New England Journal of Medicine*. 2016;374(6):511-522.
136. Scully M, Cataland SR, Peyvandi F*, et al.* Caplacizumab Treatment for Acquired Thrombotic Thrombocytopenic Purpura. *New England Journal of Medicine*. 2019;380(4):335-346.
137. Lecut C, Feeney LA, Kingsbury G*, et al.* Human platelet glycoprotein VI function is antagonized by monoclonal antibody-derived Fab fragments. *Journal of Thrombosis and Haemostasis*. 2003;1(12):2653-2662.
138. McKenzie SE, Taylor SM, Malladi P*, et al.* The Role of the Human Fc Receptor FcγRIIA in the Immune Clearance of Platelets: A Transgenic Mouse Model. *The Journal of Immunology*. 1999;162(7):4311-4318.
139. Ohlmann P, Hechler B, Ravanat C*, et al.* Ex vivo inhibition of thrombus formation by an anti-glycoprotein VI Fab fragment in non-human primates without modification of glycoprotein VI expression. *Journal of Thrombosis and Haemostasis*. 2008;6(6):1003-1011.
140. Mangin PH, Tang C, Bourdon C*, et al.* A Humanized Glycoprotein VI (GPVI) Mouse Model to Assess the Antithrombotic Efficacies of Anti-GPVI Agents. *Journal of Pharmacology and Experimental Therapeutics*. 2012;341(1):156.
141. Ukaji T, Takemoto A, Shibata H*, et al.* Novel knock-in mouse model for the evaluation of the therapeutic efficacy and toxicity of human podoplanin–targeting agents. *Cancer Science*. 2021;112(6):2299-2313.

142. Lebozec K, Jandrot-Perrus M, Avenard G*, et al.* Design, development and characterization of ACT017, a humanized Fab that blocks platelet's glycoprotein VI function without causing bleeding risks. *mAbs*. 2017;9(6):945-958.
143. Voors-Pette C, Lebozec K, Dogterom P*, et al.* Safety and Tolerability, Pharmacokinetics, and Pharmacodynamics of ACT017, an Antiplatelet GPVI (Glycoprotein VI) Fab. *Arteriosclerosis, Thrombosis, and Vascular Biology*. 2019;39(5):956-964.
144. NCT03803007 Acute Ischemic Stroke Interventional Study (ACTIMIS), Internet, 2019 (accessed 26.09.2021). Available from: https://clinicaltrials.gov/ct2/show/NCT03803007.
145. von Hundelshausen P, Siess W. Bleeding by Bruton Tyrosine Kinase-Inhibitors: Dependency on Drug Type and Disease. *Cancers*. 2021;13(5):1103.
146. Langrish CL, Bradshaw JM, Francesco MR*, et al.* Preclinical Efficacy and Anti-Inflammatory Mechanisms of Action of the Bruton Tyrosine Kinase Inhibitor Rilzabrutinib for Immune-Mediated Disease. *The Journal of Immunology*. 2021;206(7):1454.
147. Horwood NJ, Page TH, McDaid JP*, et al.* Bruton's tyrosine kinase is required for TLR2 and TLR4-induced TNF, but not IL-6, production. *Journal of Immunology*. 2006;176(6):3635-3641.
148. Doyle SL, Jefferies CA, Feighery C*, et al.* Signaling by Toll-like receptors 8 and 9 requires Bruton's tyrosine kinase. *Journal of Biological Chemistry*. 2007;282(51):36953-36960.
149. Crofford LJ, Nyhoff LE, Sheehan JH*, et al.* The role of Bruton's tyrosine kinase in autoimmunity and implications for therapy. *Expert review of clinical immunology*. 2016;12(7):763-773.
150. Conley ME, Broides A, Hernandez-Trujillo V*, et al.* Genetic analysis of patients with defects in early B-cell development. *Immunological Reviews*. 2005;203(1):216-234.
151. Mohamed AJ, Yu L, Bäckesjö C-M*, et al.* Bruton’s tyrosine kinase (Btk): function, regulation, and transformation with special emphasis on the PH domain. *Immunological Reviews*. 2009;228(1):58-73.
152. Thomas JD, Sideras P, Smith CI*, et al.* Colocalization of X-linked agammaglobulinemia and X-linked immunodeficiency genes. *Science*. 1993;261(5119):355-358.
153. Byrd JC, Brown JR, O'Brien S*, et al.* Ibrutinib versus ofatumumab in previously treated chronic lymphoid leukemia. *The New England journal of medicine*. 2014;371(3):213-223.
154. Lipsky AH, Farooqui MZH, Tian X*, et al.* Incidence and risk factors of bleeding-related adverse events in patients with chronic lymphocytic leukemia treated with ibrutinib. *Haematologica*. 2015;100(12):1571-1578.
155. Nicolson PLR, Hughes CE, Watson S*, et al.* Inhibition of Btk by Btk-specific concentrations of ibrutinib and acalabrutinib delays but does not block platelet aggregation mediated by glycoprotein VI. *Haematologica*. 2018;103(12):2097-2108.
156. Barf T, Covey T, Izumi R*, et al.* Acalabrutinib (ACP-196): A Covalent Bruton Tyrosine Kinase Inhibitor with a Differentiated Selectivity and In Vivo Potency Profile. *Journal of Pharmacology and Experimental Therapeutics*. 2017;363(2):240.
157. Tam CS, Trotman J, Opat S*, et al.* Phase 1 study of the selective BTK inhibitor zanubrutinib in B-cell malignancies and safety and efficacy evaluation in CLL. *Blood*. 2019;134(11):851-859.
158. Ghia P, Pluta A, Wach M*, et al.* ASCEND: Phase III, Randomized Trial of Acalabrutinib Versus Idelalisib Plus Rituximab or Bendamustine Plus Rituximab in Relapsed or Refractory Chronic Lymphocytic Leukemia. *Journal of Clinical Oncology*. 2020;38(25):2849-2861.
159. Byrd JC, Harrington B, O'Brien S*, et al.* Acalabrutinib (ACP-196) in Relapsed Chronic Lymphocytic Leukemia. *The New England journal of medicine*. 2016;374(4):323-332.
160. Trotman J, Opat S, Gottlieb D*, et al.* Zanubrutinib for the treatment of patients with Waldenström macroglobulinemia: 3 years of follow-up. *Blood*. 2020;136(18):2027-2037.
161. Angst D, Gessier F, Janser P*, et al.* Discovery of LOU064 (Remibrutinib), a Potent and Highly Selective Covalent Inhibitor of Bruton’s Tyrosine Kinase. *Journal of Medicinal Chemistry*. 2020;63(10):5102-5118.

162. Xing Y, Chu KA, Wadhwa J*, et al.* Preclinical Mechanisms of Topical PRN473, a Bruton Tyrosine Kinase Inhibitor, in Immune-Mediated Skin Disease Models. *Immunohorizons*. 2021;5(7):581-589.
163. Duan R, Goldmann L, Brandl R*, et al.* Effects of the Btk-Inhibitors Remibrutinib (LOU064) and Rilzabrutinib (PRN1008) With Varying Btk Selectivity Over Tec on Platelet Aggregation and in vitro Bleeding Time. *Frontiers in Cardiovascular Medicine*. 2021;8(1195).
164. Murrell DF, Patsatsi A, Stavropoulos P*, et al.* Proof of concept for the clinical effects of oral rilzabrutinib, the first Bruton tyrosine kinase inhibitor for pemphigus vulgaris: the phase II BELIEVE study. *British Journal of Dermatology*. 2021.
165. NCT03395210 a Study of PRN1008 in Adult Patients With Immune Thrombocytopenia (ITP), Internet, 2018 (accessed 23.09.2021). Available from: https://clinicaltrials.gov/ct2/show/study/NCT03395210.
166. NCT03926611 Dose-finding Study to Evaluate Efficacy and Safety of LOU064 in Patients With CSU Inadequately Controlled by H1-antihistamines, Internet, 2019 (accessed 23.09.2021). Available from: https://clinicaltrials.gov/ct2/show/NCT03926611.
167. NCT03944707 Study of Efficacy and Safety of LOU064 in Inadequately Controlled Asthma Patients, Internet, 2019 (accessed 23.09.2021). Available from: https://clinicaltrials.gov/ct2/show/study/NCT03944707.
168. NCT04035668 A Phase 2 Study to Evaluate the Safety and Efficacy of LOU064 in Patients With Moderate to Severe Sjögren's Syndrome (LOUiSSe), Internet, 2019 (accessed 23.09.2021). Available from: https://clinicaltrials.gov/ct2/show/study/NCT04035668.
169. Kuter DJ, Boccia RV, Lee E-J*, et al.* Phase I/II, Open-Label, Adaptive Study of Oral Bruton Tyrosine Kinase Inhibitor PRN1008 in Patients with Relapsed/Refractory Primary or Secondary Immune Thrombocytopenia. *Blood*. 2019;134(Supplement_1):87-87.
170. NCT04992546 a Phase 2a Study of the Safety, Tolerability, and Pharmacokinetics of Topically Administered PRN473 (SAR444727) in Patients With Mild to Moderate Atopic Dermatitis, Internet, 2021, (accessed 20.10.2021). Available from: https://clinicaltrials.gov/ct2/show/NCT04992546.
171. Bradshaw JM, McFarland JM, Paavilainen VO*, et al.* Prolonged and tunable residence time using reversible covalent kinase inhibitors. *Nature chemical biology*. 2015;11(7):525-531.
172. Smith PF, Krishnarajah J, Nunn PA*, et al.* A phase I trial of PRN1008, a novel reversible covalent inhibitor of Bruton's tyrosine kinase, in healthy volunteers. *British Journal of Clinical Pharmacology*. 2017;83(11):2367-2376.
173. Kaul M, End P, Cabanski M*, et al.* Remibrutinib (LOU064): A selective potent oral BTK inhibitor with promising clinical safety and pharmacodynamics in a randomized phase I trial. *Clinical and Translational Science*. 2021;n/a(n/a).
174. Bye AP, Unsworth AJ, Desborough MJ*, et al.* Severe platelet dysfunction in NHL patients receiving ibrutinib is absent in patients receiving acalabrutinib. *Blood Advances*. 2017;1(26):2610-2623.
175. Lee RH, Piatt R, Conley PB*, et al.* Effects of ibrutinib treatment on murine platelet function during inflammation and in primary hemostasis. *Haematologica*. 2017;102(3):e89-e92.
176. Nieswandt B, Bergmeier W, Rackebrandt K*, et al.* Identification of critical antigen-specific mechanisms in the development of immune thrombocytopenic purpura in mice. *Blood*. 2000;96(7):2520-2527.
177. Nieswandt B, Bergmeier W, Schulte V*, et al.* Expression and Function of the Mouse Collagen Receptor Glycoprotein VI Is Strictly Dependent on Its Association with the FcRγ Chain *. *Journal of Biological Chemistry*. 2000;275(31):23998-24002.
178. Bergmeier W, Schulte V, Brockhoff G*, et al.* Flow cytometric detection of activated mouse integrin αIIbβ3 with a novel monoclonal antibody. *Cytometry*. 2002;48(2):80-86.
179. Bergmeier W, Rackebrandt K, Schröder W*, et al.* Structural and functional characterization of the mouse von Willebrand factor receptor GPIb-IX with novel monoclonal antibodies. *Blood*. 2000;95(3):886-893.

180. Schindelin J, Arganda-Carreras I, Frise E*, et al.* Fiji: an open-source platform for biological-image analysis. *Nature Methods*. 2012;9(7):676-682.
181. Faul F, Erdfelder E, Lang A-G*, et al.* G*Power 3: A flexible statistical power analysis program for the social, behavioral, and biomedical sciences. *Behavior Research Methods*. 2007;39(2):175-191.
182. Thielmann I, Stegner D, Kraft P*, et al.* Redundant functions of phospholipases D1 and D2 in platelet α-granule release. *Journal of Thrombosis and Haemostasis*. 2012;10(11):2361-2372.
183. Stegner D, Thielmann I, Kraft P*, et al.* Pharmacological Inhibition of Phospholipase D Protects Mice From Occlusive Thrombus Formation and Ischemic Stroke—Brief Report. *Arteriosclerosis, Thrombosis, and Vascular Biology*. 2013;33(9):2212-2217.
184. van Eeuwijk JMM, Stegner D, Lamb DJ*, et al.* The Novel Oral Syk Inhibitor, Bl1002494, Protects Mice From Arterial Thrombosis and Thromboinflammatory Brain Infarction. *Arteriosclerosis, Thrombosis, and Vascular Biology*. 2016;36(6):1247-1253.
185. Pike JA. Platelet surface area calculations, Github, 2019 (accessed 26.11.2021). Available from https://github.com/JeremyPike/plateletCalculations/blob/master/Platlet%20surface%20area%20calculations.ipynb.
186. Lorenz V. Cellular regulation of the hemITAM-coupled platelet receptor C-type lectin-like receptor 2 (CLEC-2): In vitro and in vivo studies in mice; 2018.
187. Andre P, Morooka T, Sim D*, et al.* Critical role for Syk in responses to vascular injury. *Blood*. 2011;118(18):5000-5010.
188. McDonald TP, Jackson CW. The role of genotype, genomic imprinting, and sex hormones in platelet and megakaryocyte production. *Experimental Hematology*. 1994;22(10):959-966.
189. Deppermann C, Cherpokova D, Nurden P*, et al.* Gray platelet syndrome and defective thrombo-inflammation in Nbeal2-deficient mice. *The Journal of Clinical Investigation*. 2013;123(8):3331-3342.
190. Lombard SE, Pollitt AY, Hughes CE*, et al.* Mouse podoplanin supports adhesion and aggregation of platelets under arterial shear: A novel mechanism of haemostasis. *Platelets*. 2018;29(7):716-722.
191. Navarro-Núñez L, Pollitt AY, Lowe K*, et al.* Platelet adhesion to podoplanin under flow is mediated by the receptor CLEC-2 and stabilised by Src/Syk-dependent platelet signalling. *Thrombosis and haemostasis*. 2015;113(5):1109-1120.
192. Christou Charita M, Pearce Andrew C, Watson Aleksandra A*, et al.* Renal cells activate the platelet receptor CLEC-2 through podoplanin. *Biochemical Journal*. 2008;411(1):133-140.
193. Boylan B, Chen H, Rathore V*, et al.* Anti-GPVI-associated ITP: an acquired platelet disorder caused by autoantibody-mediated clearance of the GPVI/FcRgamma-chain complex from the human platelet surface. *Blood*. 2004;104(5):1350-1355.
194. Panteleev MA, Korin N, Reesink KD*, et al.* Wall shear rates in human and mouse arteries: Standardization of hemodynamics for in vitro blood flow assays: Communication from the ISTH SSC subcommittee on biorheology. *Journal of Thrombosis and Haemostasis*. 2021;19(2):588-595.
195. Tillman BF, Pauff JM, Satyanarayana G*, et al.* Systematic review of infectious events with the Bruton tyrosine kinase inhibitor ibrutinib in the treatment of hematologic malignancies. *European Journal of Haematology*. 2018;100(4):325-334.
196. Jefferies CA, Doyle S, Brunner C*, et al.* Bruton's tyrosine kinase is a Toll/interleukin-1 receptor domain-binding protein that participates in nuclear factor kappaB activation by Toll-like receptor 4. *Journal of Biological Chemistry*. 2003;278(28):26258-26264.
197. Benner B, Carson WE. Observations on the use of Bruton's tyrosine kinase inhibitors in SAR-CoV-2 and cancer. *Journal of Hematology & Oncology*. 2021;14(1):15.
198. Rada M, Qusairy Z, Massip-Salcedo M*, et al.* Relevance of the Bruton Tyrosine Kinase as a Target for COVID-19 Therapy. *Molecular Cancer Research*. 2021;19(4):549.

6. Appendix

6.1 Abbreviations

(hem)ITAM	(Hemi) immunoreceptor tyrosine-based activation motif
°C	Degrees Celsius
ACD	Acid citrate dextrose
ADP	Adenosine diphosphate
APS	Ammonium peroxodisulphate
ARDS	Acute respiratory distress syndrome
ATP	Adenosine triphosphate
AU	Arbitrary units
AUC	Area under the curve
bp	Base pair
BPM	Beats per minute
BSA	Bovine serum albumin
Btk	Bruton’s tyrosine kinase
Ca^{2+}	Calcium cation
CDR	Complementarity-determining regions
CLEC-2	C-type lectin-like receptor 2
COX	Cyclo-oxygenase
CRP	Collagen-related peptide
DAG	Diacylglycerol
DAPI	4’-6-Diamidino-2-phenylindole
DDM	n-dodecyl-β-D-maltoside
DIC	Differential interference contrast
DMSO	Dimethylsulfoxide
DVT	Deep vein thrombosis
ECL	Enhanced chemiluminescence
ECM	Extracellular matrix
EDTA	Ethylenediaminetetraacetic acid
EGTA	Ethylene glycol tetraacetic acid
EOS	Eosinophil

F	Factor
Fab	Fragment antigen binding
FcR	Fc receptor
FCS	Foetal Bovine Serum
$FeCl_3$	Ferric chloride
FITC	Fluorescein-isothiocyanate
GAPDH	Glyceraldehyde 3-phosphate dehydrogenase
GP	Glycoprotein
GPCR	G-protein coupled receptor
GRA	Granulocyte
GTP	Guanine triphosphate
h	Hour
H&E	Haematoxylin & Eosin
HAT	Hypoxanthine-aminopterin-thymidine
HCT	Haematocrit
HEPES	N-2-Hydroxyethylpiperazine-N'-2-ethanesulfonic acid
Het	Heterozygous
HGB	Haemoglobin
HIV	Human immunodeficiency virus
HRP	Horseradish peroxidase
i.p.	Intraperitoneal
i.v.	Intravenous
IFN	Interferon
IgG	Immunoglobulin G
IP_3	Inositol-1.4.5-trisphosphate
ITIM	Immunoreceptor tyrosine-based inhibitory motifs
ITP	Immune thrombocytopenia
kDa	Kilodalton
KI	Knockin
LAT	Linker of activated T cells
LEC	Lymphatic endothelial cells
LPS	Lipopolysaccharide
LSEC	Liver sinusoidal endothelial cells

LYM	Lymphocyte
MAb	Monoclonal antibody
MCH	Mean corpuscular haemoglobin
MCHC	Mean corpuscular haemoglobin concentration
MCV	Mean corpuscular volume
MFI	Mean fluorescence intensity
Min	Minute
mmHg	Millimetres of mercury
MON	Monocyte
MPV	Mean platelet volume
NET	Neutrophil extracellular trap
NRAMP1	Natural resistance-associated macrophage protein 1
ns	Not significant
OCT	Optimal cutting temperature
PAGE	Polyacrylamide gel electrophoresis
PAR	Protease activation receptor
PBS	Phosphate buffered saline
PE	Phycoerythrin
PEG	Polyethylene glycol
PF4	Platelet factor 4
PFA	Parafromaldehyde
PGI_2	Prostacyclin
PI3K	Phosphoinositide-3-kinase
PIP_2	Phosphatidylinositol-4,5-bisphosphate
PIP_3	phosphatidylinositol-3,4,5-trisphosphate
PLC	Phospholipase C
PLP	Periodate-lysine-paraformaldehyde
PRP	Platelet rich plasma
PS	Phosphatidylserine
PVDF	Polyvinylidene difluoride
pY	Tyrosine phosphorylation
Rac1	Ras-related C3 botulinum toxin substrate 1
RBC	Red blood cell

RC	Rhodocytin
RDW	Red cell distribution width
rpm	Rotations per minute
RT	Room temperature
rt-PA	Recombinant tissue plasminogen activator
scFv	Single chain fragment variable
SDS	Sodium dodecyl sulphate
SFK	Src family tyrosine kinase
SH	Src homology
SLP-76	SH2 domain containing leukocyte protein of 76 kDa
STm	*Salmonella typhimurium*
Syk	Spleen tyrosine kinase
TBS	Tris buffered saline
TEMED	Tetramethylethylenediamine
TF	Tissue factor
TLR	Toll-like receptor
TP	Thromboxane-prostanoid receptor
tPA	Tissue plasminogen activator
TRIS	Tris(hydroxymethyl)aminomethane
TTP	Thrombotic thrombocytopenic purpura
TxA_2	Thromboxane A_2
US FDA	United States Food and Drug Agency
UTR	Untranslated region
Veh	Vehicle
V_H	Variable heavy domain
VHH	Heavy chain variable domain
V_L	Variable light domain
vWF	Von Willebrand factor
WBC	White blood cell
WT	Wildtype
XLA	X-linked agammaglobulinaemia
Y	Tyrosine

6.2 Acknowledgements

The work presented in this thesis was performed in the Institute of Experimental Biomedicine at the University Hospital and Rudolf Virchow Center, University of Würzburg in the group of Prof. David Stegner and in the Institute of Cardiovascular Sciences at the College of Medical and Dental Sciences, University of Birmingham in the group of Prof. Steve Watson between September 2018 and November 2021. This work was funded by the European Union's Horizon 2020 research and innovation programme under the Marie Skłodowska-Curie grant agreement No 766118.

I would like to thank the following people for their help and support during my PhD:

My supervisors Prof. David Stegner and Prof. Steve Watson for the opportunity to work in their laboratories and their support, guidance and encouragement throughout my PhD. As well as for challenging me and making me a better scientist.

Prof. Bernhard Nieswandt for his valuable scientific advice and discussions.

Dr Sarah Beck for the countless times she helped me, for always being around to answer my questions and who, along with Carina and Vanessa, introduced me to platelet research.

Dr Pip Nicolson and Dr Christopher Smith for their guidance and help.

Dr Irina Pleines, Dr Julie Rayes and Dr Natalie Poulter, as well as all members of the TAPAS consortium, for their useful advice and scientific discussions.

My thesis committee members Dr Steve Thomas and Prof. Katrin Heinze for their scientific discussions and advice.

Caroline McKay for her support.

Steffi, Ewa, Juliana and Ying for all their help and technical expertise as well as Sylvie, Brigit, Daniela, Beata and Lourdes for keeping the labs running.

The animal caretakers at the Center for Experimental Molecular Medicine and Rudolf Virchow Center at the University of Würzburg and the University of Birmingham Biomedical Services Unit for all their hard work, without which our work would not be possible.

Ale, Stefano, Jana, Till, Lara and all members of the Stegner, Nieswandt and Sumara labs for the laughter and the countless hours spent together both in and out of the lab, without you my time in Germany would not have been the same.

All members of the Birmingham Platelet Group for their help and support.

All TAPAS ESRs for their collaboration and friendship, even when we could not meet in person.

My friends Alice, Ryan, Pippa, Helena and Delia for their unwavering support and for always believing in me.

My dad for his unlimited love, support and encouragement.

And finally, Chris for always being there for me and for his endless patience and encouragement, this wouldn't have been the same without you.

6.3 Publications

6.3.1 Articles

Perrella G, Montague SJ, **Brown HC**, Garcia Quintanilla L, Slater A, Stegner D, Thomas M, Heemskerk JWM, Watson SP. Role of Tyrosine Kinase Syk in Thrombus Stabilisation at High Shear. *International Journal of Molecular Sciences*. 2022; 23(1):493. https://doi.org/10.3390/ijms23010493

Bourne JH, Smith CW, Joos NJ, Di Y, **Brown HC** *et al*. CLEC-2 supports platelet aggregation in mouse but not human blood at arterial shear. *Thrombosis and Haemostasis* (Accepted)

Brown HC, Beck S, Navarro S, *et al*. Antibody-mediated depletion of human CLEC-2 in a novel humanised mouse model. *bioRxiv*. 2021:2021.2010.2003.462933. (Under revision)

Smith CW, Harbi MH, Garcia Quintanilla L, Rookes K, **Brown HC** *et al*. The Btk inhibitor AB-95-LH34 potently inhibits atherosclerotic plaque-induced thrombus formation and platelet procoagulant activity. (Under revision)

Clark JC, Morán LA, Martin EM, Wang X, Maqsood Z, **Brown HC** *et al*. Divalent ligands can function as partial agonists of CLEC-2. (In preparation)

6.3.2 Poster presentations

2021 UK Platelet Society Meeting, Keele, United Kingdom (virtual), April 2021. “A humanised CLEC-2 mouse model used to test anti-human CLEC-2 biologics in vivo shows that human CLEC-2 can be depleted”.

International Society on Thrombosis and Haemostasis Congress, Milan, Italy (virtual), July 2020. “A humanised CLEC-2 mouse model to study anti-human CLEC-2 biologics in vivo”.

International Symposium of the Graduate School of Life Science: EUREKA, Würzburg, Germany, October 2019. “A humanised CLEC-2 mouse model to study anti-human CLEC-2 biologicals in vivo”.

2019 UK Platelet Society Meeting, Cambridge, United Kingdom, September 2019. “Syk inhibition, but not blockade of the platelet receptors GPVI or CLEC-2, reduces thrombus stability”.

6.4 Curriculum Vitae

6.5 Affidavit

I hereby confirm that my thesis entitled “Investigating the role of the platelet receptor C-type lectin-like receptor 2 in models of thrombosis” is the result of my own work. I did not receive any help or support from commercial consultants. All sources and/or materials applied are listed and specified in the thesis.

Furthermore, I confirm that this thesis has not yet been submitted as part of another examination process neither in identical nor in similar form.

Place, Date Signature

Eidesstattliche Erklärung

Hiermit erkläre ich an Eides statt, die Dissertation „Untersuchungen zur Rolle des Thrombozytenrezeptors CLEC-2 (C-type lectin-like receptor 2) in Thrombosemodellen“ eigenständig, d.h. insbesondere selbstständig und ohne Hilfe eines kommerziellen Promotionsberaters, angefertigt und keine anderen als die von mir angegebenen Quellen und Hilfsmittel verwendet zu haben.

Ich erkläre außerdem, dass die Dissertation weder in gleicher noch in ähnlicher Form bereits in einem anderen Prüfungsverfahren vorgelegen hat.

Ort, Datum Unterschrift